

**OBSERVATIONAL TESTS OF THE FORMATION,
MIGRATION, AND EVOLUTION PROCESSES OF
GAS GIANT PLANETS**

by

Alessandro Sozzetti

Laurea in Physics, University of Turin, 1997

M. S. in Physics, University of Pittsburgh, 2002

Submitted to the Graduate Faculty of
the Department of Physics & Astronomy in partial fulfillment
of the requirements for the degree of

Doctor of Philosophy

University of Pittsburgh

2005

UNIVERSITY OF PITTSBURGH
DEPARTMENT OF PHYSICS & ASTRONOMY

This dissertation was presented

by

Alessandro Sozzetti

It was defended on

May 25, 2005

and approved by

David A. Turnshek, PhD, Professor, Physics & Astronomy

David W. Latham, PhD, Senior Astronomer, Smithsonian Astrophysical Observatory

Andrew J. Connolly, PhD, Assistant Professor, Physics & Astronomy

Daniel Boyanovsky, PhD, Professor, Physics & Astronomy

John D. Hillier, PhD, Associate Professor, Physics & Astronomy

Bruce W. Hapke, PhD, Professor Emeritus, Geology & Planetary Science

Dissertation Advisors: David A. Turnshek, PhD, Professor, Physics & Astronomy,

David W. Latham, PhD, Senior Astronomer, Smithsonian Astrophysical Observatory

Copyright © by Alessandro Sozzetti
2005

OBSERVATIONAL TESTS OF THE FORMATION, MIGRATION, AND EVOLUTION PROCESSES OF GAS GIANT PLANETS

Alessandro Sozzetti, PhD

University of Pittsburgh, 2005

We have conducted a set of experiments aimed at improving our knowledge of the formation, migration, and evolution processes of gas giant planets, utilizing a combination of spectroscopic, photometric, and astrometric techniques.

First, the distributions of planet masses and orbital elements, different correlations among them, and measurable differences in planetary frequency are likely to be generated by diverse planetary formation scenarios and evolution mechanisms as well as different characteristics of the parent star (binarity, spectral type, metallicity, age). We have found new evidence for a correlation between the orbital periods of extrasolar planets and the metallicity of the host stars. We have undertaken a precision radial-velocity survey of a sample of 200 metal-poor stars, to confirm or disprove the correlation, to refine our understanding of the dependence of planetary frequency on the metallicity of the host stars, and to put constraints on proposed models of giant planet formation.

Second, the internal structure and composition of the atmospheres of close-in giant planets can be better understood if measurements of their radii and actual masses are available, for a range of different planet host spectral types. We have measured the spectroscopic orbit of TrES-1, the transiting Jupiter-sized planet of a moderately bright K0V star, and by improving on the determination of the stellar parameters, we have derived accurate estimates of its radius and mass.

Finally, the actual source responsible for eccentricity excitation could be understood and the long-term dynamical evolution better characterized if coplanarity measurements

of multiple-planet orbits were to be carried out. We have quantified the ability of the Space Interferometry Mission to obtain accurate measurements of the actual masses, orbital parameters, and relative inclination angles for systems of giant planets around stars in the solar neighborhood.

We conclude describing four experiments to investigate further the transiting planet TrES-1 and its parent star. These are: 1) infrared observations of the secondary eclipse; 2) high-precision visible wavelength observations of the primary eclipse; 3) a detailed chemical abundance analysis of the host star; 4) a direct distance measurement for the system.

*He, who through vast immensity can pierce,
See worlds on worlds compose one universe,
Observe how system into system runs,
What other planets circle other suns,
What varied Being peoples every star,
May tell why Heaven has made us as we are.*

Alexander Pope
An Essay on Man, 1734

TO MY FATHER.

PREFACE

Upon my arrival at the University of Pittsburgh, in August 2000, I was firmly hoping I would be able to continue to work on the topic which had monopolized my scientific interests since the early days of my undergraduate thesis research in Italy: Extrasolar planets.

When I declared my intention to carry out planet-related thesis work at the Harvard-Smithsonian Center for Astrophysics, Dave Turnshek openly encouraged me to pursue it. I want to thank him for having always been a fervent supporter of all of my plans.

The first time I met Dave Latham, having driven for ten hours from Pittsburgh to the town of Harvard, I was terribly late for supper. I called him along the way saying I was planning to eat somewhere in Connecticut, but he replied: “No, of course you must come here to eat it all, and have some good wine!”. Dave is a superlative host. If he tells you he will be serving good wine, you can rest assured it will be a night to remember. The wine tastings he sponsors at the Center for Astrophysics have become proverbial. It’s too bad he has such a strong French bias. In all my efforts, I have not been able to move him significantly toward the Italian border!

Dave and I share many common views and have a common understanding of how many things in life work. This has obviously helped a lot in both our personal and professional interactions. But most importantly, Dave has taught me countless things. One lesson I like in particular is that one should not rush, but rather be patient, and wait until until he/she has good data, and lots of them. And, of course, Dave convinced me that I should at least be able to count up to three in Spanish: uno, dos, TrES!

Willie Torres has traveled with me each and every time I had to go to Hawaii. Without his well-trained hat, we would never have gotten such a long series of good observing nights! In addition, Willie treats HIRES as a little pet, and without somebody taking such good

care of world-class instrumentation, things would never have gone smoothly, as instead they did, all the time. He's a great scientist, an outstanding collaborator, and a good friend, and I thank him for being all that at once.

Mike Kurtz, Dimitar Sasselov, and Maciej Konacki have provided crucial advice, important information, and useful discussions many times during my stay at the Center for Astrophysics. Their help is worth more than a simple word of acknowledgment!

The Graduate Secretary Leyla Hirschfeld in Pittsburgh and the Division Administrator Leslie Feldman in Cambridge have been extremely helpful throughout my student career. Any time I called for aid, even over small, tiny issues, they always responded within the blink of an eye. I owe them many thanks.

During graduate school, it's easy to stick around with a bunch of school-mates while you're working yourself through countless nasty, and sometimes pointless!, homework exercises. Then, when you start your thesis, you end up losing track of many of them. But, with good friends you stick around also out of office hours (even when there's twelve of them a day). It was no stranger who hosted us in Denver, on our way to a conference, after a wonderful trip across the National Parks of the South-West. Kip, Ramin, Phil, Michele, Barun, thanks! Even after moving to Cambridge, any time I came back to Pittsburgh it was always great to see you again, and after greetings, the first thing to be said would be: "What do we do tonight?".

It's well known that Pre-Doctoral Fellows at the CfA are looked upon by Harvard graduate students with a slight hint of superiority complex. But many pre-docs are not only very good at what they do, they also are great human beings. My stay in Cambridge would not have been the same without a pizza + movie with Ettore, a well-made italian coffee with Peter, Paula, Antonio, and Rui, or a wine + cheese + cured meats tasting with Gabor, Luis, and Balasz.

My family has supported my choices all along. It has not been easy, I decided to undertake a career path that was fully orthogonal to theirs. But even when they had a hard time understanding the need for a certain step ("What? Why do you need a Doctorate? Isn't a Laurea enough?"), they always trusted I would do the right thing. I am sure they are both

very happy now.

Mario, Alberto, Davide: an ocean is not enough to separate very good friends. Our life-long friendship has given me invaluable strength.

Finally, thanks to Ummi Abbas for simply being the person she is. I am a most fortunate man as I will be able to tell her so for all the days to come.

This work has been supported by the University of Pittsburgh through an Andrew Mellon Pre-doctoral Fellowship and a Zaccheus Daniels Fellowship, by the Smithsonian Astrophysical Observatory through an SAO Pre-doctoral Fellowship, and by the Keck PI Data Analysis Fund (JPL 1262605).

TABLE OF CONTENTS

PREFACE	vii
1.0 INTRODUCTION	1
1.1 A Historical and Philosophical Perspective	1
1.2 Scientific Motivations	4
1.3 Chapter Summaries	7
2.0 EXTRA-SOLAR PLANETS: A REVIEW OF THEORY AND OBSER- VATION	12
2.1 Introduction	12
2.2 Emerging Statistical Properties of Planetary Systems	13
2.2.1 Sample Completeness and Detection Thresholds	14
2.2.1.1 Doppler Spectroscopy	14
2.2.1.2 Transit Photometry	17
2.2.2 Metallicity of the Host Stars	19
2.2.3 Mass, Period & Eccentricity Distributions	22
2.2.4 Correlations	25
2.2.5 Multiple Systems and Planets in Stellar Systems	30
2.2.6 Follow-up Studies	33
2.2.6.1 Astrometry	33
2.2.6.2 Spectro-Photometry in the Visible	35
2.2.6.3 Infrared Emission	36
2.2.6.4 Planet-Induced Chromospheric Activity and Radio Emission	36
2.3 Renewed Theoretical Efforts	37

2.3.1 Planet Formation	37
2.3.1.1 Core Accretion	38
2.3.1.2 Disk Instability	39
2.3.2 Migration	41
2.3.3 Dynamical Interactions	44
2.3.4 Inner Structure and Atmosphere	46
2.3.5 Long-Term Stability	49
2.3.6 Formation, Migration, and Stability of Planets in Stellar Systems . . .	51
2.4 Toward a Unified Picture	53
3.0 ON THE POSSIBLE CORRELATION BETWEEN THE ORBITAL PERIODS OF EXTRA-SOLAR PLANETS AND THE METALLICITY OF THE HOST STARS	57
3.1 Introduction	57
3.2 Stellar and Planet Sample Analysis	58
3.3 Observational Biases?	68
3.4 Discussion	70
4.0 A KECK/HIRES DOPPLER SEARCH FOR PLANETS ORBITING METAL-POOR DWARFS	74
4.1 Introduction	74
4.2 Selection Criteria of the Sample	75
4.3 Results	76
5.0 TRES-1: THE TRANSITING PLANET OF A BRIGHT K0V STAR	82
5.1 Introduction	82
5.2 Observations	83
5.3 Discussion	89
6.0 HIGH-RESOLUTION SPECTROSCOPY OF THE TRANSITING PLANET HOST STAR TRES-1	93
6.1 Introduction	93
6.2 Data Reduction and Abundance Analysis	94
6.3 Stellar Parameters	94

6.3.1 Atmospheric Parameters from Spectroscopy	95
6.3.2 T_{eff} Estimate from Photometry	96
6.3.3 Stellar Activity and Age	96
6.3.4 Stellar Mass and Radius	99
6.4 Planetary Parameters	99
6.5 Summary and Discussion	100
7.0 THE SEARCH FOR PLANETARY SYSTEMS WITH SIM	103
7.1 Introduction	103
7.2 Simulation Setup, Detection and Orbital Fitting Methods	108
7.2.1 SIM Narrow-Angle Astrometric Observing Scenario	109
7.2.2 Statistical Tools for Planet Detection	111
7.2.3 Procedure for Multiple-Planet Orbital Fits	113
7.3 Results	115
7.3.1 Detectability of Multiple-Planet Systems	115
7.3.1.1 Probabilities of Detection	116
7.3.1.2 Periodogram Analysis	124
7.3.1.3 Search for Periodicities when $T > L$	132
7.3.2 Multiple-Planet Orbits Reconstruction	138
7.3.2.1 Accuracy in Orbit and Mass Determination	138
7.3.2.2 Coplanarity Measurements	148
7.3.2.3 Combining Radial Velocity and Astrometric Data	152
7.4 Summary and Conclusions	158
8.0 SUMMARY AND FUTURE PROSPECTS	162
8.1 Summary of Results	162
8.1.1 A Test of Planet Formation and Migration Models	162
8.1.2 A Test of Evolutionary Models of Irradiated Giant Planets	163
8.1.3 A Test of Models of Dynamical Interactions in Multiple-Planet Systems	163
8.2 Further Studies of the Transiting Planet System TrES-1	164
8.2.1 Detection of Thermal Emission	165
8.2.2 An <i>HST</i> Light-Curve	167

8.2.3	Placing the Host Star in Context	169
8.2.4	Taking the Distance to the System	170
8.3	Future Tests of Planet Formation and Evolution	171
8.3.1	Discriminating Between Planet-Formation Models	171
8.3.2	Structural and Evolutionary Properties of Giant Planets	173
8.3.3	Statistical Properties and Correlations	175
8.3.4	The Hunt for Other Earths	176
BIBLIOGRAPHY	178

LIST OF TABLES

2.1	Results of the K-S and rank correlation tests on different stellar and planetary sub-samples	31
3.1	Orbital periods of extrasolar planets and metallicities of the host stars	58
3.2	Results of the K-S and rank correlation tests on different stellar subsets . . .	66
3.3	Fraction of planets below a given value of period in two metallicity bins. . . .	69
5.1	TrES-1 Parent Star	86
5.2	TrES-1 Planet	90
7.1	Parameters of planetary systems and stellar hosts	117
7.2	Results from the periodogram analysis	124
7.3	Ranges of plausible starting guesses	136
7.4	Ratios of the rms errors for various parameters	139
7.5	Power-law fit to fractional errors on various parameters	148

LIST OF FIGURES

2.1	Left: mass histogram of the planet host stellar sample. Center: the histogram of apparent visual magnitudes. Right: the histogram of nominal distance estimates. Transiting planets lying at $D > 100$ pc are not included	15
2.2	Log distribution of the radial-velocity semi-amplitudes for the sample of known extrasolar planets.	16
2.3	Metallicity distribution of the planet-host stars	20
2.4	Left: minimum mass histogram of the extrasolar planet sample. Center: the distribution of orbital periods. Right: the eccentricity distribution	22
2.5	Left: eccentricity versus orbital period for the extrasolar planet sample. Center: the mass-period diagram. Right: eccentricity versus minimum planet mass	26
2.6	Minimum mass of single planets versus mass of the host stars	27
2.7	Mass versus metallicity for the planet-host stars	28
2.8	Left: minimum planet mass against $[\text{Fe}/\text{H}]$ of the host stars. Center: the period-metallicity diagram. Right: eccentricity versus $[\text{Fe}/\text{H}]$	29
2.9	Mass ratios vs. period ratios for pairs of planets in multiple systems	32
2.10	Radius vs. mass for the sample of transiting extrasolar planets discovered to-date	47
3.1	Orbital periods vs. stellar metallicity and the period distribution for three different cases	65
3.2	Histogram of rank correlation coefficients	67
4.1	rms velocity distribution and radial velocity as a function of time for a quiet star	77

4.2	Radial velocity residuals as a function of various parameters	77
4.3	Radial velocity observations of TrES-1, overplotted with the best-fit orbit.	78
4.4	Radial velocity as a function of time for one of the variable objects in our sample.	79
4.5	Planet detection thresholds for metal-poor stars with radial velocity and as- trometry	80
5.1	Time series photometry and predicted light curves for TrES-1 in different colors	85
5.2	Radial velocity observations of TrES-1, overplotted with the best-fit orbit.	88
5.3	Radii of transiting extrasolar planets plotted against their masses	91
6.1	The TrES-1 Ca II line compared to that of an inactive star	97
6.2	The TrES-1 Lithium line compared to three syntheses	98
6.3	Radius vs. mass for the sample of transiting planets discovered to-date	101
7.1	Detection Probabilities as a function of orbital inclination i	122
7.2	Periodogram analysis for the HD 38529 system	127
7.3	Periodogram analysis for the ν And system	128
7.4	Periodogram analysis for the HD 82943 system	130
7.5	Periodogram analysis for the 55 Cnc system	131
7.6	Reduced chi-square χ^2_ν as a function of trial periods	134
7.7	55 Cnc: fractional errors for various parameters	142
7.8	HD 12661: fractional errors for various parameters	143
7.9	Iso-accuracy contours for various parameters in the $e - T$ plane	145
7.10	Iso-accuracy contours for various parameters in the $\alpha/\sigma_d - T$ plane	147
7.11	Relative inclination i_{rel} between pairs of planetary orbits	151
7.12	Iso-countours of ratios of fractional errors for various parameters	154
7.13	Ratios σ_G/σ_C as a function of i for the 55 Cnc and 47 UMa systems	156
7.14	Ratios σ_G/σ_C as a function of i for the HD 21661 and HD 38529 systems	157

1.0 INTRODUCTION

1.1 A HISTORICAL AND PHILOSOPHICAL PERSPECTIVE

At the dawn of the XXI century, both the National Aeronautics and Space Administration (NASA) and the European Space Agency (ESA) are engaged in long-term scientific programs for the exploration of our as well as other Solar Systems. Tens of groups of researchers from Universities and Astronomical Observatories around the world are today using a host of different techniques from the ground and in space in order to search for, detect, and characterize planets orbiting stars other than the Sun. The ultimate goal of this large-scale effort is the realization of an unprecedented event in the history of humanity: the discovery of life elsewhere in the Universe.

Ten years have passed since the discovery of the first extrasolar planet ([Mayor & Queloz 1995](#)). However, the debate on the plurality of worlds dates back to the first written records of Western thought, in the Greece of V century B.C., and possibly to even earlier times in other cultures. It took twenty five centuries before science could provide the first observational data to confirm the Existence Theorem. One cannot regard this but as a remarkable achievement.

In order to follow the thread to understand how did the startling idea that we might not be alone in the universe originate, and by what rationale did that revolutionary idea finally triumph, many approaches can be chosen. To begin such a history, one should adopt a flexible point of view, and examine the interplay between ideas and movements in different disciplines such as the history of science, philosophy, theology, and literature. Throughout the historical ages, the idea of isolation has been replaced by the belief that there should exist a plurality of worlds and vice-versa, following the diverse theological, philosophical, scientific, and literary conquests of a specific time. In recent years ('70-'80), theories on

biological evolution and hard-core reductionists became promoters of a diffuse skepticism (Barrow & Tipler 1986): We are likely to be the only technologically advanced civilization in the Galaxy, and our Earth is the only planet hosting life. Many, including myself, believe this is not the case, but the challenge to prove the contrary is enormous.

Men who lived before the advent of scientific thought clearly could not bring any supporting evidence, yet many of them considered as absolutely obvious the fact that we would not be alone. However, the “extra-terrestrial intelligencies” they could conceive were far from anything we would expect today, no matter how vague is the idea we might have of them at present. All primitive mythologies and cosmogonies tell of the existence of beings very different from us, both super-human and super-natural, in the sense of beings capable of overruling the Laws of Nature. There is a primarily psychological explanation for the creation of such exotic descriptions of Nature: Man has always felt the need for a superior and mysterious something or somebody who would transcend him. In the beginning it was fire, lightning, or a natural catastrophe that was interpreted as a manifestation of the wrath of the Gods. Today Unknown and Inexplicable are given infinitely superior technical, rather than moral, qualities. The new divinities do not inhabit Mount Olympus anymore, but rather live on planets around stars spread all over our Galaxy. They do not ride winged horse-drawn chariots, but rather travel using sophisticated spaceships capable of traveling through the Hyper-space, whatever that is.

The birth and evolution of scientific thought have produced through the years a net fracture with these ideas, relegating Myth, Religion, and Philosophy in a somewhat decentralized position. It may come as a surprise to most to learn that the concept of extraterrestrial intelligence among scientists did not first appear in the XX century, but that its antecedents stretch back to two of the most fertile periods of Western science: ancient Greece, where the seed of this was implanted, and the XVII and XVIII centuries, which witnessed the scientific revolution, the fruition of the marriage of experimental methods and mathematics, and – somewhat ironically – the triumph of the concept of extraterrestrial life.

It is important to recognize that most ideas undergo an evolution and a transformation to such an extent that historical antecedents often bear little resemblance to their modern counterparts. This is certainly true of the concept of extraterrestrial life. The term “ex-

traterrestrial life” is itself modern, having come into widespread use only in the XX century. The historical term out of which the extraterrestrial life debate grew is “plurality of worlds”, which first appeared in ancient Greece in the V century B.C. in the extreme form of the concept of infinite worlds, became known in the Latin West as the question of many worlds, and was translated into the Italian, English, French, and German vernaculars as “plurality of worlds”.

The plurality of worlds tradition, that encompasses a larger body of ideas than simply extraterrestrial life, has received substantial contributions by many of the famous names of the history of science, among them Democritus, Epicurus, Lucretius, Aristotle, Thomas Aquinas, William of Ockham, Giordano Bruno, Nicole Oresme, Johannes Kepler, John Wilkins, Christiaan Huygens, Immanuel Kant, Bertrand Russell, Giovanni Schiaparelli, Percival Lowell, and Enrico Fermi. These people, and many others during the period bracketed by the V century B.C. and the present time, have helped transform the concept of other worlds and extraterrestrial life from heresy to orthodoxy in Western thought.

Today, in the era of the SETI (Search for Extraterrestrial Intelligencies) Program, there exists a simple, effective tool that can be used for stimulating intellectual curiosity about the universe around us, for helping us to understand that life as we know it is the state of matter of highest complexity and organization known and the end product of a natural, cosmic evolution, and for making us realize how much we are a part of that universe. This tool is the Drake Equation ([Drake 1962](#)), which allows to compute the number of technological civilizations capable of communicating and contemporary to ours that might possibly exist in our Milky Way Galaxy. It is usually formalized as follows:

$$N_c = R_\star \times f_p \times f_e \times f_l \times f_i \times f_c \times L,$$

where N_c is the number of civilizations in our Galaxy with whom we might communicate, $R_\star = N/T$ is the rate of formation of stars in the Galaxy (N is its total stellar content, and T its age), f_p is the fraction of stars that have planetary systems, f_e is the fraction of habitable worlds, i.e. planets in a given solar system with physical conditions favorable for life to arise, f_l is the fraction of habitable planets on which life actually arises, f_i is the fraction of planets on which intelligent life arises, f_c is the fraction of intelligent species that

are interested in communicating with other civilizations, and L is the average lifetime of a civilization.

The solution to the Drake Equation is all but unique. A pessimistic view (Barrow & Tipler 1986) would have $N_c \simeq 1$, thus we would be the only communicating civilization in the whole Galaxy. The intermediate view would find $N_c \simeq 10^4 - 10^5$. The optimists agree on a value of $N_c \simeq 10^9$, so that a large fraction of the stars in our galaxy could harbor planets capable of supporting complex life forms. Clearly, such a wide range of answers limits the utility of the Drake Equation to learn anything new about intelligent life in the Universe. However, it illuminates the factors involved in such a search. The bad news is that, except N_\star for which we have a fairly good estimate, all the factors in the Drake Equation carry large uncertainties, given the paucity or complete lack of observational data, thus any conclusion cannot but be defined as highly speculative. The good news is that mankind is capable today of developing means to verify its condition. We are now close to taking a first decisive step in this direction, and finally provide a good estimate for the second factor in the equation, the fraction of stars with planets in our Galaxy f_p .

We are privileged to live at a time when an answer to the age-old question of extraterrestrial life is finally within reach. Whatever the answer turns out to be – whether life is present elsewhere or absent – our view of the world and our place within it will be dramatically affected. In the words of the philosopher Bertrand Russell, ‘There are two possibilities. Maybe we’re alone. Maybe we’re not. Both are equally frightening.’

1.2 SCIENTIFIC MOTIVATIONS

Triggered by the discovery of planets orbiting other stars, the debate on the existence of life on other planets has stepped out of the boundaries of science and has become a major topic of public debate. These discoveries, however, do not provide any compelling evidence for the existence of extraterrestrial life. The techniques utilized today to search for extrasolar planets do not have enough sensitivity to detect the presence of Earth-mass objects even around the closest stars, and in fact all sub-stellar companions discovered so far are massive, with the lighter object being of order of the mass of Neptune.

As mentioned earlier, instruments built with the technology needed to achieve the goal of Earth-size, habitable planet detection will come online before the end of this decade. According to the conventional wisdom, a habitable Earth must orbit at a distance from its star where liquid water is stable on its surface. In its classic definition (Kasting et al. 1993), the Habitable Zone around a given star has its inner boundary located at the distance from the star at which a runaway greenhouse effect is generated, which induces water loss via photolysis and hydrogen loss; the outer boundary is located at the distance from the star at which carbon dioxide clouds start increasing the planet albedo in a way to cool the surface down to the point of freezing water. According to the typical time-scales of biological evolution on Earth, a planet should be habitable for several billion years, in order to allow for the development of complex life forms and possibly intelligent life. The importance of the discovery of stars harboring planetary systems containing a habitable world is such that the search for such an object today constitutes one of the major challenges to be faced by the scientific community at the turn of the XXI century.

An analog of the Earth has not been found yet, but the substellar companions to nearby stars known today already bring a wealth of important information. The present catalog of ~ 150 extrasolar planets orbiting nearby solar-type stars constitutes the fundamental database with which to undertake the first important tests of theoretical models of planet formation and evolution. However, the confrontation between theory and observation suffers from strong biases due to small-number statistics.

For example, the present number of discoveries translates in the first actual value for the fraction of solar-type stars with planets in the solar neighborhood and, by extrapolation, in our Galaxy. Today, $f_p \simeq 6\%$ for giant planets with orbital radii < 3 AU. The evidence for a strong correlation between f_p and stellar metallicity is used as an argument in support of the core accretion models of giant planet formation, as opposed to the competing disk instability model (see Chapter 2 for a thorough discussion). However, this estimate is not very robust yet. On the theoretical side, the main uncertainties derive from our poor knowledge of the early stages of planet formation and orbital evolution. On the observational side, this is due to a strong bias towards stars more like our Sun, largely disregarding a significant range of ages, spectral types, and metallicities.

The work presented in this dissertation has been thus primarily motivated by the necessity to improve our understanding of some crucial aspects of the statistical properties of extrasolar planets, in connection with the predictions formulated by models of giant planet formation, evolution, and long-term dynamical interaction. We have undertaken a set of experiments aimed at providing answers to some outstanding questions in planetary science. We have conducted such studies utilizing a combination of spectroscopic, photometric, and astrometric planet-search techniques.

First, different correlations among planetary orbital parameters and mass, and measurable differences in planetary frequency are likely to be generated by diverse planetary formation scenarios and orbital evolution mechanisms as well as different formation and evolution processes of the parent star (binarity, spectral type, metallicity, age). In particular, a Doppler survey of a statistically significant sample of metal-poor stars (so far, largely neglected) would allow to compare the frequency of gas giant planets between samples of metal-rich and metal-poor stars in the field. This in turn would help to determine whether core accretion or disk instability is the dominant formation mechanism for gas giant planets, or to verify the existence of bimodal planet formation.

Second, the internal structure and composition of the atmospheres of close-in giant planets can be better understood if measurements of their radii and actual masses are available, for a range of different planet host spectral types. A combination of transit photometry and Doppler spectroscopy of a newly discovered planet transiting across the surface of its parent star would provide accurate estimates of the planet's mass and radius. These two critically interesting parameters can then be used for directly constraining structural models of close-in giant planets.

Third, the actual source responsible for eccentricity excitation could be understood and the long-term dynamical evolution better characterized if coplanarity measurements of multiple-planet orbits were to be carried out. High-precision astrometry of stars harboring planetary systems is the only means with which the relative inclination angle between pairs of planetary orbits can be measured. It is thus important to provide an overall assessment of the planet detection and measurement capabilities of future observatories designed to carry out high-precision astrometric measurements.

1.3 CHAPTER SUMMARIES

In **Chapter 2**, we present a critical review of the status of extrasolar planet searches. We discuss completeness and detectability thresholds of ongoing surveys. We summarize the main statistical properties of extrasolar planets, and in particular correlations among orbital parameters and masses, and between planet properties and the characteristics of the host stars. Finally, we briefly review recent theoretical efforts to bring predictions from models of planet formation, migration, and evolution in better agreement with observations. We conclude by outlining some important issues in planetary science to be addressed by both theory and observation in the near future.

This chapter constitutes an expanded version of Section 2 of a review article, with myself as the only author, which has recently been accepted for publication in PASP ([Sozzetti 2005](#)).

In **Chapter 3**, we investigate a possible correlation between the orbital periods P of the extrasolar planet sample and the metallicity $[\text{Fe}/\text{H}]$ of their parent stars. Close-in planets, on orbits of a few days, are more likely to be found around metal-rich stars. Simulations show that a weak correlation is present. This correlation becomes stronger when only single stars with one detected planet are considered. We discuss several potential sources of bias that might mimic the correlation, and find that they can be ruled out, but not with high significance. If real, the absence of very short-period planets around the stellar sample with $[\text{Fe}/\text{H}] < 0.0$ can be interpreted as evidence of a metallicity dependence of the migration rates of giant planets during formation in the protoplanetary disc. The observed P - $[\text{Fe}/\text{H}]$ correlation can be falsified or confirmed by conducting spectroscopic or astrometric surveys of metal-poor stars ($[\text{Fe}/\text{H}] < -0.5$) in the field.

This work has been published as a journal article in MNRAS, with myself as the only author ([Sozzetti 2004](#)).

In **Chapter 4**, we present results from our ongoing spectroscopic search for giant planets within 1 AU around a well-defined sample of metal-poor stars with HIRES on the Keck 1 telescope. We have achieved an rms radial velocity precision of ~ 8 m/s over a time-span of 1.5 years. The data collected so far build toward evidence of the absence of very short-

period (< 1 month) giant planets. However, about 7% of the stars in our sample exhibits velocity trends indicative of the existence of companions. We place preliminary upper limits on the detectable companion mass as a function of orbital period, and compare them with the performance of future space-borne high-precision astrometric observatories.

This work has been published as a proceedings paper, with myself as the first author, as part of an ESA-SP volume (Sozzetti et al. 2005). I am the Project PI of the Keck/HIRES doppler survey for planets orbiting metal-poor stars, and directly responsible for the acquisition of data at the telescope and their analysis to derive precise radial-velocities.

In **Chapter 5**, we report the detection of a transiting Jupiter-sized planet orbiting a relatively bright ($V = 11.79$) K0V star. We detected the transit light-curve signature in the course of the TrES multisite transiting planet survey and confirmed the planetary nature of the companion via multicolor photometry and precise radial velocity measurements. We designate the planet TrES-1. Its inferred mass is $(0.75 \pm 0.07) M_J$, its radius is $1.08_{-0.04}^{+0.18} R_J$, and its orbital period is 3.030065 ± 0.000008 days. This planet has an orbital period similar to that of HD 209458b but about twice as long as those of the OGLE transiting planets. Its mass is indistinguishable from that of HD 209458b, but its radius is significantly smaller and fits the theoretical models without the need for an additional source of heat deep in the atmosphere, as has been invoked by some investigators for HD 209458b.

In this work, which has been published as a letter in ApJ with R. Alonso as the first author (Alonso et al. 2004b), I have carried out the spectroscopic observations at the Keck 1 telescope, using the HIRES spectrograph, and successively obtained precise radial-velocity measurements and derived a high-quality spectroscopic orbit for TrES-1.

In **Chapter 6**, we report on a spectroscopic determination of the stellar parameters and chemical abundances for the parent star of the transiting planet TrES-1. Based on a detailed analysis of iron lines in our Keck and Hobby-Eberly Telescope spectra, we derive $T_{\text{eff}} = 5250 \pm 75$ K, $\log g = 4.6 \pm 0.2$, and $[\text{Fe}/\text{H}] = 0.00 \pm 0.09$. By measuring the Ca II activity indicator and by putting useful upper limits on the Li abundance, we constrain the age of TrES-1 to be 2.5 ± 1.5 Gyr. By comparing theoretical stellar evolution models with the observational parameters, we obtain $M_{\star} = 0.89 \pm 0.05 M_{\odot}$ and $R_{\star} = 0.83 \pm 0.05 R_{\odot}$.

Our improved estimates of the stellar parameters are utilized in a new analysis of the transit photometry of TrES-1 to derive a mass $M_p = (0.76 \pm 0.05) M_J$, a radius $R_p = 1.04_{-0.05}^{+0.08} R_J$, and an inclination $i = 89.5_{-1.3}^{+0.5}$ deg. The improved planetary mass and radius estimates provide the grounds for new crucial tests of theoretical models of evolution and evaporation of irradiated extrasolar giant planets.

In this work, which has been published as a letter in ApJ with myself as the first author (Sozzetti et al. 2004b), I have coordinated the effort of the whole team, and in particular directly contributed to the determination of the atmospheric parameters and age of the parent star of TrES-1.

In **Chapter 7**, we utilize (1) detailed end-to-end numerical simulations of sample narrow-angle astrometric observing campaigns with the Space Interferometry Mission (*SIM*) and the subsequent data analysis process, and (2) the set of extrasolar planetary systems discovered so far by radial velocity surveys as templates to provide meaningful estimates of the limiting capabilities of *SIM* for the detection and measurement of multiple-planet systems around solar-type stars in the solar neighborhood. We employ standard χ^2 statistics, periodograms, and Fourier analysis to evaluate *SIM*'s ability to detect multiple planetary signatures; the probability of detecting additional companions is essentially unchanged from the single-planet configurations, but after fitting and subtraction of orbits with astrometric signal-to-noise ratio $\alpha/\sigma_d \rightarrow 1$, the false detection rates can be enhanced by up to a factor of 2. The periodogram approach results in robust multiple-planet detection for systems with periods shorter than the *SIM* mission length, even at low values of α/σ_d , while the least-squares technique combined with Fourier series expansions is arguably preferable in the long-period regime. We explore the three-dimensional parameter space defined by astrometric signature, orbital period, and eccentricity to derive general conclusions on the capability of *SIM* to accurately measure the full set of orbital parameters and masses for a variety of configurations of planetary systems; the accuracy of multiple-planet orbit reconstruction and mass determination suffers a typical degradation of 30%-40% from single-planet solutions; mass and orbital inclination can be measured to better than 10% for periods as short as 0.1 yr and for α/σ_d as low as ~ 5 , while $\alpha/\sigma_d \simeq 100$ is required in order to measure with similar

accuracy systems harboring objects with periods as long as 3 times the mission duration. We gauge the potential of *SIM* for meaningful coplanarity measurements via determination of the true geometry of multiple-planet orbits. For systems with all components producing $\alpha/\sigma_d \simeq 10$ or greater, quasi-coplanarity can be reliably established with uncertainties of a few degrees, for periods in the range $0.1 \text{ yr} \leq T \leq 15 \text{ yr}$; in systems where at least one component has $\alpha/\sigma_d \rightarrow 1$, coplanarity measurements are compromised, with typical uncertainties on the mutual inclinations on the order of $30^\circ - 40^\circ$. We quantify the improvement derived in full-orbit reconstruction and planet mass determination by constraining the multiple-planet orbital fits to *SIM* observations with the nominal orbital elements obtained from the radial velocity measurements; the uncertainties on orbital elements and masses can be reduced by up to an order of magnitude, especially for long-period orbits in face-on configurations and for low-amplitude orbits seen edge-on.

In this work, which has been published in PASP with myself as the first author ([Sozzetti et al. 2003a](#)), I have lead the effort in every detail of the simulations and subsequent analysis and interpretation of the results.

In **Chapter 8**, we summarize the results of the thesis. We also discuss briefly four experiments to investigate further the transiting planet TrES-1 and its parent star, which have recently been completed, are underway, or can be carried out in the near future. These are: 1) *Spitzer Space Telescope* infrared observations of the secondary eclipse, to directly detect for the first time a planet orbiting another star, and to constrain thermal emission models of close-in giant planets; 2) *Hubble Space Telescope* visible wavelength observations of the primary eclipse, to derive an accurate estimate of the planet’s diameter by resolving the uncertainty concerning the diameter of the parent star; 3) detailed abundance analysis of the host star, to establish the presence or absence of chemical abundance anomalies with respect to the sample of stars with planets, and to place TrES-1 in the context of Galactic chemical evolution by comparison with disk or halo stars of similar metal content; 4) an accurate, direct distance measurement for the system, to derive improved constraints on the parent star’s radius, and thus further reduce the uncertainties on the estimate of the planetary radius, to help discriminate between models of irradiated giant planet interiors with and

without rocky cores. We conclude the chapter by describing additional observational tests that can be carried out in the future both from the ground and in space in order to further our understanding of giant planet formation and evolution.

2.0 EXTRA-SOLAR PLANETS: A REVIEW OF THEORY AND OBSERVATION

Alessandro Sozzetti, 2005, *Publications of the Astronomical Society of the Pacific*, in press

2.1 INTRODUCTION

The astrophysics of planetary systems is a good example of a branch of science in which theory is mostly driven by observations. Hardly any of the properties of the sample of ~ 150 extrasolar giant planets discovered to-date (Jupiters on few-days orbits, very high eccentricities, objects with masses five to ten times the mass of Jupiter) had been predicted *a priori* by theoretical models. Correlations among planetary orbital and physical parameters had not been anticipated. The dependence of the frequency and properties of planetary systems on some of the characteristics of the parent stars (mass, metallicity) had not been foreseen.

The unexpected properties of extrasolar planets have sparked new enthusiasm among theorists, who have engaged in fruitful intellectual confrontations, with the aim to move from a set of models describing separately different aspects of the physics of the formation and evolution of planetary systems to a plausible, unified theory capable of making robust and testable predictions.

By analogy, a number of new as well as old techniques of astronomy has been fueled by the new discoveries, with the twin goals to follow-up and better characterize the extrasolar planet sample and cover new areas of the discovery space. The result is an ongoing, positive, creative tension between theory and observation that will put to the test the most basic ideas of how planets form and evolve.

It is the aim of this paper to provide a critical review of the emerging statistical properties of planetary systems derived from observations, in connection with the predictions from theoretical models of giant planet formation and evolution. In Section 2.2 I summarize the results of observations of extrasolar planetary systems obtained to-date. Section 2.3 contains a review of renewed theoretical efforts on giant planet formation, migration, and post-formation physical and dynamical evolution. I conclude by highlighting a number of outstanding questions in planetary science that will need to be addressed by means of a combined effort between theory and observation.

2.2 EMERGING STATISTICAL PROPERTIES OF PLANETARY SYSTEMS

Ten years after the announcement of the first Jupiter-sized object orbiting a star other than the Sun (Mayor & Queloz 1995), the number of extrasolar planets announced has increased by a few tens per year. The startling diversity of planetary systems, when compared with the properties of our own Solar System, has, if possible, become more evident with the addition of newly discovered planets.

The vast majority of the discoveries has been made thanks to Doppler surveys of thousands of nearby sun-like stars, although in recent years new detections and follow-up studies of already known systems have been pursued utilizing a variety of other techniques.

I describe in turn the general statistical properties of the extrasolar planet sample that have been uncovered to-date. I have considered all objects with minimum projected masses $M_p \sin i < 17 M_J^1$, a slightly more relaxed version of the $13-M_J$ mass cut-off (where M_J is the mass of Jupiter) introduced by Oppenheimer et al. (2000) to formally distinguish between planets and brown dwarfs. I have excluded from the sample the unconfirmed second planet around ϵ Eri, two announced but not published planets around the giant stars HD 59686 and HD 219449 (Mitchell et al. 2003), the planets around the K-G giants HD 47536 (Setiawan et al. 2003) and HD 104985 (Sato et al. 2003), due to the very large uncertainties on the

¹Recall that the intrinsically one-dimensional Doppler measurements are degenerate in the planet mass M_p and inclination angle i .

mass of the parent star and thus on the inferred value of $M_p \sin i$, and the planetary mass object detected via a microlensing event OGLE-235/MOA-53 (Bond et al. 2004), as the characteristics of the parent star and the planet are not well established. All planet and stellar host parameters have been taken from the Extrasolar Planet Encyclopedia website (<http://www.obspm.fr/encycl/encycl.html>), and references therein, as of February 2005.

2.2.1 Sample Completeness and Detection Thresholds

What we know today about extrasolar planets is the result of the selection criteria adopted for the stellar samples targeted, which are driven by the techniques adopted in the search, and their limiting capabilities.

2.2.1.1 Doppler Spectroscopy In the three panels of Figure 2.1 I summarize some of the general features of the planet host stars. If we do not include the handful of transiting planets discovered by transit photometry (Udalski et al. 2002a, b, 2003; Alonso et al. 2004b) and confirmed by high-resolution spectroscopic measurements (Torres et al. 2004a; Bouchy et al. 2004; Moutou et al. 2004; Pont et al. 2004; Sozzetti et al. 2004b; Konacki et al. 2003, 2004, 2005), belonging to very different stellar samples, the typical planet-harboring star has an average mass $\bar{M}_* = 1.1 M_\odot$, is located at an average distance $\bar{D} = 35.6$ pc, and has an average visual magnitude $\bar{m}_v = 6.9$. This reflects the fact that the stellar reservoir utilized by Doppler surveys is constituted by bright, very nearby, solar-type stars.

The groups leading the effort in radial-velocity planet searches (Korzennik et al. 1998; Queloz et al. 2000a; Butler et al. 2001; Endl et al. 2002; Tinney et al. 2002; Perrier et al. 2003; Marcy et al. 2004a; Cochran et al. 2004) are in fact targeting from both hemispheres a global sample of ~ 2000 main-sequence and sub-giant (spectral subtype IV-V) late F, G, and early K stars, with typical selection criteria based on brightness ($m_v < 7.5 - 8$), multiplicity (no close binaries within a few arcsec), surface activity (adopting as a criterion the fractional Ca II H and K flux corrected for the photospheric flux (e.g., Noyes et al. 1984, Saar et al. 1998), typically $\log R'_{\text{HK}} \lesssim -4.5$), metallicity ($[\text{Fe}/\text{H}] \geq -0.5$), rotation ($V_{\text{rot}} \sin i < 5 - 10$ km/s), and the availability of *Hipparcos* distances ($D < 100$ pc)². Dedicated surveys of

²A comprehensive summary of the temporal evolution of the stellar database for eight large Doppler

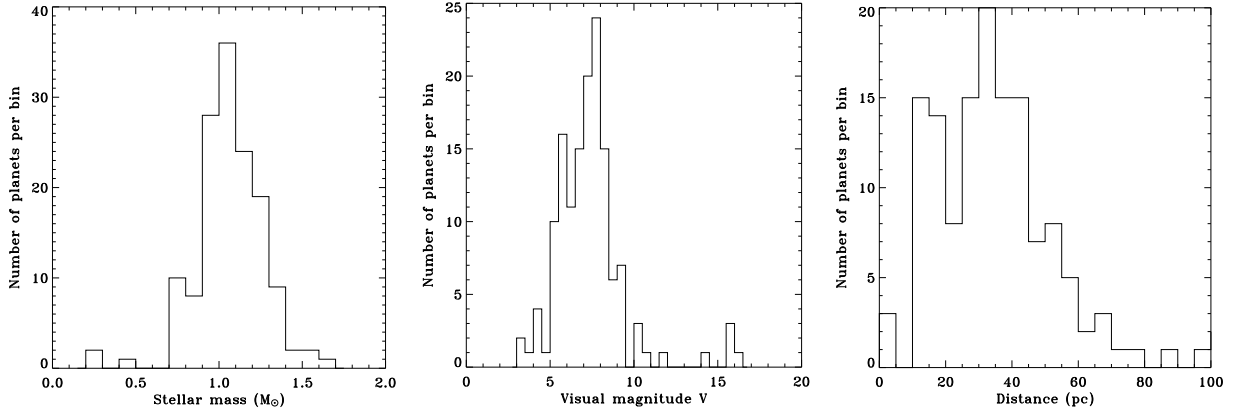


Figure 2.1 Left: mass histogram of the planet host stellar sample. Center: the histogram of apparent visual magnitudes. Right: the histogram of nominal distance estimates. Transiting planets lying at $D > 100$ pc are not included

stars in open clusters (Cochran et al. 2002), components of wide binaries (Gratton et al. 2004; Udry et al. 2004; Konacki 2005), metal-poor stars (Sozzetti et al. 2005), M dwarfs (Delfosse et al. 1998; Endl et al. 2003; Kürster et al. 2003; Kürster & Endl 2004; Bonfils et al. 2004), and K-G giants (Frink et al. 2002; Setiawan et al. 2003; Sato et al. 2003) bring the total to ~ 3000 .

For Doppler spectroscopy, the observable is the radial-velocity semi-amplitude K , which is a function of planet minimum mass $M_p \sin i$, orbital period P , eccentricity e , and stellar mass M_\star (expressed in units of solar masses M_\odot) through the following expression:

$$K = \frac{28.4}{\sqrt{1-e^2}} \left(\frac{M_p \sin i}{M_J} \right) \left(\frac{P}{1yr} \right)^{-1/3} \left(\frac{M_\star}{M_\odot} \right)^{-2/3} \text{ m/s} \quad (2.1)$$

The time coverage and achieved single-measurement precision σ_{RV} are highly variable, ranging from a few up to 17 years and from $\sigma_{RV} \simeq 10 - 15$ m/s down to $\sigma_{RV} \simeq 1 - 3$ m/s, respectively. In Figure 2.2 I show the histogram of the radial-velocity semi-amplitudes K reported for the extrasolar planet sample. As a result of variable measurement precision, time baseline, and detectability thresholds adopted by the different groups, the typical value of K is of order of at least a few tens of m/s, reflecting the fact that radial-velocity datasets still contain a significant fraction of lower precision measurements. In fact, for example, assuming $\sigma_{RV} = 3$ m/s, only $\sim 7\%$ of the detected planets induces radial-velocity variations on its parent star such that $K/\sigma_{RV} \lesssim 4 - 5$, and with one exception, they are all close-in surveys can be found in Lineweaver & Grether (2003)

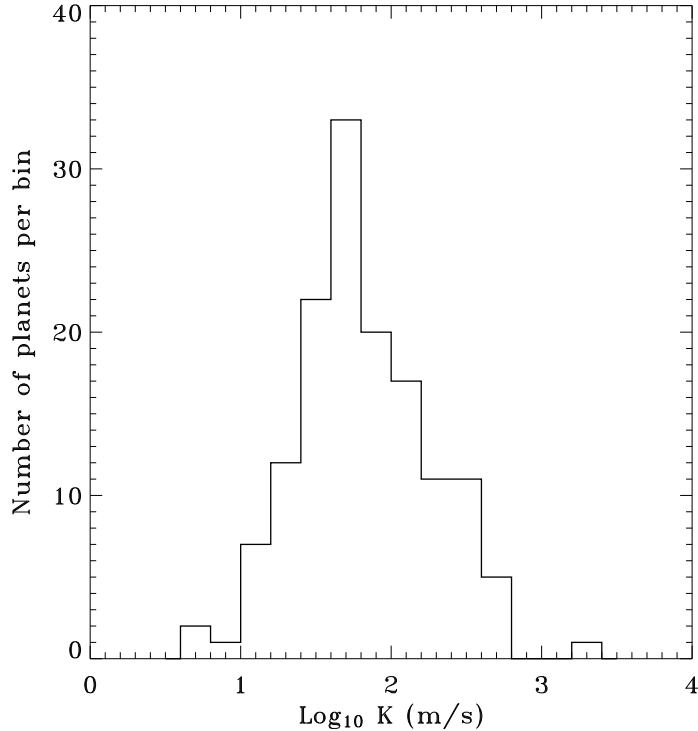


Figure 2.2 Log distribution of the radial-velocity semi-amplitudes for the sample of known exoplanets.

planets, with orbital periods not greater than several tens of days.

Statistical studies of the sensitivity of different radial-velocity surveys to planetary companions have been performed in the past by several authors (Walker et al. 1995; Cochran & Hatzes 1996; Nelson & Angel 1998; Cumming et al. 1999, 2004; Eisner & Kulkarni 2001a; Endl et al. 2002; Naef et al. 2004; Cumming 2004; Narayan et al. 2004). Such studies have utilized both numerical as well as analytical approaches to describe detection probabilities as a function of measurement errors, number and time sampling of the observations, and planet characteristics (orbital parameters, masses).

In most cases, detectability thresholds (using K/σ_{RV} as a proxy) were defined on the basis of χ^2 and Lomb-Scargle (Lomb 1976; Scargle 1982) periodogram tests. The relative roles of short and long orbital periods (compared to the time-span T of the observing campaign), high and low eccentricity, sparse and dense, even and uneven sampling have been quantified.

As a rule of thumb, assuming circular orbits, and $\sigma_{\text{RV}} = 3$ m/s, the present, robust (5σ criterion) lower limit to the detectable minimum planet mass by radial-velocity surveys of solar-like stars ($0.8 \leq M_{\star} \leq 1.2M_{\odot}$) would be of order of $0.1 M_J$, $0.5 M_J$, and $1.5 M_J$ at

0.05 AU, 1 AU, and 5 AU, respectively. Below these limits in mass, radial-velocity surveys are largely incomplete.

However, when the time-span of observations exceeds a few years, the contribution from lower-precision measurements becomes important, and direct extrapolation of the mass detection threshold to 4-5 AU is likely to be incorrect. Furthermore, even at very short periods the situation is already changing, as new instrumentation begins to attain higher-level performances, toward the 1 m/s precision.

The improved sensitivity has recently opened the door for the detection of planets close to the terrestrial planet mass regime, as confirmed by the recent discoveries of Neptune-class objects on few-day orbits (Butler et al. 2004; McArthur et al. 2004; Santos et al. 2004b). The almost simultaneous announcements have sparked a heated debate on who announced the first one first (Irion 2004).

2.2.1.2 Transit Photometry Except for HD 209458b (Charbonneau et al. 2000; Henry et al. 2000), all transiting planets have estimated distances exceeding 100 pc. This reflects the two main choices made by ground-based photometric transit surveys regarding the targeted stellar samples. About two dozen groups worldwide are now targeting hundreds of thousands of stars, trying to detect transiting Jupiter-sized planets in very close-in orbits (for a review see Horne (2004) and Charbonneau (2003), and references therein). While wide-angle transit surveys target large samples of moderately bright stars ($9 \leq m_v \leq 13$), deep galactic-plane surveys and surveys in stellar clusters focus instead on faint objects ($14 \leq m_v \leq 19.5$). As a consequence, the former primarily investigate a sphere of a few hundred pc centered on the Sun, while the typical target of the latter lies at $D > 1$ kpc.

I recall that the main observable in this case is the transit depth ΔF , where F is defined as the total observed stellar flux:

$$\Delta F = \frac{F_{no\ transit} - F_{transit}}{F_{no\ transit}} = \left(\frac{R_p}{R_\star}\right)^2 \quad (2.2)$$

Assuming the stellar radius $R_\star = 1R_\odot$, and the planet radius $R_p = 1R_J$, then $\Delta F \simeq 0.01$. The requisite photometric precision (a few times better than 1%) and phase coverage for large stellar samples are attained by most of the surveys, so completeness in the limiting

detectable mass (about $1 M_J$) is reached in most cases, in the typical period range 1-4 days. Completeness boundaries in the stellar samples targeted are however harder to assess, and useful constraints on the occurrence rate of hot Jupiters as a function of the environment and properties of the central star will be in turn difficult to establish. In fact, transit surveys are essentially magnitude-limited, thus the selection function of spectral types, ages, and metallicities is unknown (except for stars in clusters).

As recently pointed out (Moutou et al. 2004; Gaudi et al. 2005), the apparent inconsistency between the presence of a 50% of transiting objects with periods of order of 1.5 days in the OGLE surveys (Udalski et al. 2002a, b, 2003) and the fact that among the ~ 20 planets with $P \leq 5$ days detected by Doppler surveys the shortest period is rather of order of 3 days can be reconciled by observing that, once a variety of selection biases and small-number statistics are taken into account, only one in a few thousands stars is likely to harbor a transiting close-in planet on a 1.5 day period orbit. These objects are at least a few times less common than hot Jupiters with $3 \lesssim P \lesssim 10$ days, thus very close-in planets ($P < 3$ days) are not out of reach of future radial velocity surveys, such as that described by Fischer et al. (2005).

Furthermore, the lack of OGLE transiting planets with $3 \lesssim P \lesssim 10$ days, as opposed to the $\sim 50\%$ of such objects being present in the sample with $P < 10$ days detected by Doppler surveys, can also be explained in terms of selection biases such as uneven sampling and finite duration of the photometric transit campaigns (Charbonneau 2003; Gaudi et al. 2005), resulting in a strong inverse dependence of the probability of detection of transiting planets on P which significantly limits the sensitivity of transit surveys for $P \gtrsim 3.5-4$ days. Indeed, such limitations constitute the primary reason for which the number of transiting planets is not significantly larger than what is observed, as naive considerations based on the large stellar samples, achieved sensitivity, and frequency of close-in planets, would have suggested (Horne 2004).

Finally, additional complications arise due to the fact that transit searches are prone to a very high rate of false alarms. As extensively discussed by e.g, Latham (2004), Brown (2003) and Charbonneau et al. (2004), a variety of astrophysical false positives (small stars eclipsing large stars, grazing eclipsing binaries, and most importantly faint eclipsing binaries

blended with a physically associated or unassociated brighter star) can outnumber true planetary transits by well over an order of magnitude. To this end, very careful analysis of the light curves and of spectral lines profiles of the targets must be conducted (Torres et al. 2004b, 2005; Mandushev et al. 2005), in order to ascertain or rule out the existence of a blend.

2.2.2 Metallicity of the Host Stars

By looking at Figure 2.3, where I plot the metallicity distribution of stars with planets ³, one realizes immediately that the Sun, with $[\text{Fe}/\text{H}] \equiv 0.0$, falls in the low-metallicity tail. Indeed, the distribution peaks at $[\text{Fe}/\text{H}] \simeq 0.3$, showing evidence of moderate metal-enrichment with respect to the average metallicity ($[\text{Fe}/\text{H}] \simeq -0.1$) of field dwarfs in the solar neighborhood.

The possibility that super-solar metallicity could correspond to a higher likelihood of a given star to harbor a planet was investigated since the first detections by precision radial-velocity surveys (Gonzalez 1997, 1998a, 1998b; Fuhrmann et al. 1997, 1998; Laughlin & Adams 1997). A number of studies have been performed throughout these years, using increasingly larger sample sizes, employing both spectroscopic and photometric techniques for metallicity determination, and adopting control samples of field stars without detected planets (Santos et al. 2000, 2001, 2003, 2004a; Reid 2002; Laughlin 2000; Gonzalez & Laws 2000; Gonzalez et al. 2001; Israelian et al. 2001; Queloz et al. 2000a; Smith et al. 2001; Giménez 2000; Martell & Laughlin 2002; Heiter & Luck 2003; Sadakane et al. 2002; Pinsonneault et al. 2001; Murray & Chaboyer 2002; Laws et al. 2003; Fischer et al. 2003b).

The global trend is that planet-harboring stars are really more metal rich than stars without known planets. Based on observationally unbiased stellar samples, the strong dependence of planetary frequency on the host star metallicity has been clearly demonstrated by Santos et al. (2001), and confirmed by Fischer et al. (2003b) and by Santos et al. (2004a), who showed a sharp break in frequency at $[\text{Fe}/\text{H}] \simeq 0.0$, albeit in the presence of very small-number statistics at the low-metallicity end of the distribution.

The absence of short-period transiting planets in the globular cluster 47 Tucanæ is also

³Using Iron (Fe) as the reference element, then $[\text{Fe}/\text{H}] = \log[N_{\text{Fe}}/N_{\text{H}}]_{\star} - \log[N_{\text{Fe}}/N_{\text{H}}]_{\odot}$, with N_{Fe} , and N_{H} the number densities of Iron and Hydrogen in any given star (\star) and in the Sun (\odot), respectively

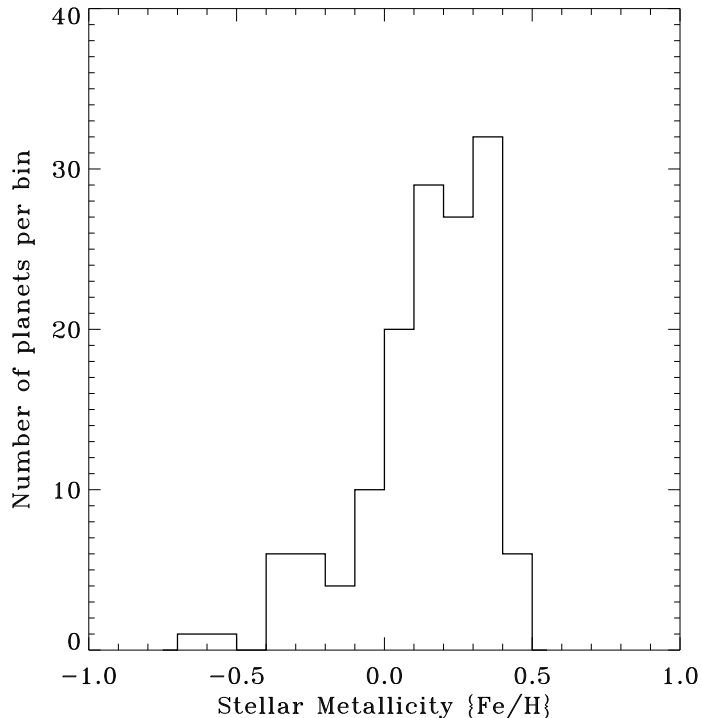


Figure 2.3 Metallicity distribution of the planet-host stars

used by Gilliland et al. (2000) and by Wel Drake et al. (2005) to argue that low-metallicity stars are less likely to harbor giant planets. The claims by these authors suffer however from some ambiguity, as in the cluster core investigated by Gilliland et al. (2000) with *HST* transit photometry crowding could play a significant role in giant planet formation, migration, and survival. The outer regions of the cluster monitored by Wel Drake et al. (2005) are less affected by crowding, however the lower occurrence rate of hot Jupiters in a metal-poor environment does not rule out the existence of a population of giant planets at wider radii⁴, and other mechanisms could be called into question to explain this result (see Section 2.3).

Many authors have debated whether the observational evidence is an indicator of primordial high metallicity in the planet host stellar sample, or if the trend with $[\text{Fe}/\text{H}]$ could be due to selection effects or pollution by ingested planetary material. The recent analyses performed by Santos et al. (2001, 2004a) and Fischer et al. (2003b) are almost conclusive

⁴Sigurdsson et al. (2003) have recently inferred a mass of a few Jupiter masses for the third, long-period component orbiting the white dwarf - pulsar system B1620-26 in the globular cluster M4, five times more metal-poor than 47 Tuc, providing the first evidence for planet formation in extremely metal-poor environments

arguments that observational selection biases do not play a major role (see Gonzalez (2003) for a thorough review of the subject of biases).

The idea of pollution is also losing credit among the scientific community, primarily based on the evidence of no correlation between $[\text{Fe}/\text{H}]$ and effective temperature T_{eff} , or convective envelope mass M_{conv} , for the planet host sample (e.g. Fischer et al. 2003b; Santos et al. 2003, 2004a, and references therein). Results on this specific issue are not conclusive yet, however. For example, Vauclair (2004) has recently pointed out how the absence of a $[\text{Fe}/\text{H}]-M_{\text{conv}}$ correlation does not automatically imply that stars with planets have not been polluted.

Furthermore, theoretical calculations (Montalbán & Rebolo 2002; Boesgaard & King 2002) suggest that detection of anomalous abundances of rare elements such as lithium (Li) or beryllium (Be) could be interpreted as evidence for accretion of planets into the atmosphere of a star. The abundances of Li isotopes in the spectral region around the 6707Å line in planet-host stars have been investigated in the recent past by several authors (Gonzalez & Laws 2000; Ryan 2000; Israelian et al. 2001, 2003, 2004; Reddy et al. 2002; Mandell et al. 2004), and similar studies have been conducted for the Be II lines at 3130Å and 3131Å. (García López & Pérez de Taoro 1998; Deliyannis et al. 2000; Santos et al. 2002, 2004c).

While evidence for Li excesses in some planet-harboring stars has been reported in the literature (Israelian et al. 2001, 2003; Laws & Gonzalez 2001), clearly suggesting that accretion of planetary material can actually take place in some stars, in general stars with planets have normal light-element abundances, typical of field stars. It thus seems unlikely that pollution effects can be responsible for the overall metallicity enhancement of the planet host stellar sample. Finally, analyses of over a dozen other elements have been carried out in the recent past (Santos et al. 2000; Gonzalez et al. 2001; Smith et al. 2001; Takeda et al. 2001; Sadakane et al. 2002; Bodaghee et al. 2003; Ecuillon et al. 2004a, b), and the general evidence is that the abundance distributions in stars with planets are the extension of the observed behavior for $[\text{Fe}/\text{H}]$, a result quantified by trends of decreasing $[X/\text{Fe}]$ with decreasing $[\text{Fe}/\text{H}]$.

As of today, the best explanation for the metallicity excess in stars with planets is that the enhanced $[\text{Fe}/\text{H}]$ is primordial in nature. I defer to Section 2.3 a discussion of what this

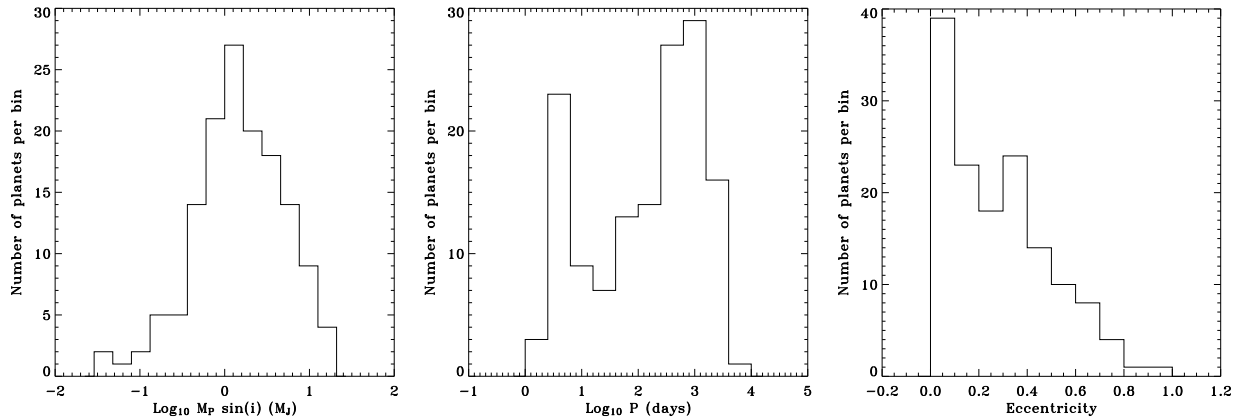


Figure 2.4 Left: minimum mass histogram of the extrasolar planet sample. Center: the distribution of orbital periods. Right: the eccentricity distribution

might imply from the point of view of theories of giant planet formation.

2.2.3 Mass, Period & Eccentricity Distributions

The extrasolar planet sample exhibits many interesting and surprising characteristics. Figure 2.4 shows the histogram distributions of $M_p \sin i$, P , and e . The three distributions have been studied intensively in recent years, and some trends observed since early works have been confirmed, while additional features have been uncovered recently due to the increased sample size.

The mass distribution (left panel of Figure 2.4) has received more attention from the community, primarily because of the intrinsic uncertainty in the actual mass values. The three main features of the distribution have been recognized and discussed by many authors (Basri & Marcy 1997; Mayor et al. 1998a, 1998b; Marcy & Butler 1998; Mazeh et al. 1998; Heacox 1999; Mazeh 1999; Halbwachs et al. 2000; Stepinski & Black 2000; Jorissen et al. 2001; Zucker & Mazeh 2001a; Mazeh & Zucker 2002; Tabachnik & Tremaine 2002; Lineweaver & Grether 2002, 2003; Marcy et al. 2004a).

First, there is a sharp cut-off above $M_p \sin i \simeq 10 M_J$. The paucity of low-mass companions to solar-type stars in the range $10M_J < M_p \sin i < 100M_J$ ⁵ is often referred to as the “brown dwarf desert”. This is considered the most compelling reason to believe that the

⁵Only a handful of spectroscopic binaries uncovered by Doppler surveys for planets have secondary masses lying in the brown-dwarf mass regime (Mazeh et al. 1996; Mayor et al. 1998a; Vogt et al. 2002; Endl et al. 2004)

formation mechanisms for giant planets and stellar companions are different.

Second, the decline of the distribution for $M_p \sin i < 1 M_J$ could be due to the fact that Doppler surveys are still incomplete below this limit at large separations (as of today, $a > 4$ AU).

Finally, the observed mass distribution can be modeled as a power-law $dN/dM \propto M^\alpha$, with a negative exponent α in the range $[-1.9, -1.0]$. Depending on the details of the analyses performed (e.g., treatment of selection effects, correlations with orbital parameters, extrapolations to small masses), the actual M_p distribution can be either logarithmically flat or it can rise toward smaller masses, with the most recent studies favoring the latter possibility.

The distributions of orbital parameters, namely period and eccentricity, have received increasing attention only at a later stage (Heacox 1999; Stepinski & Black 2000, 2001; Mayor & Udry 2000; Mazeh & Zucker 2001; Tabachnik & Tremaine 2002; Tremaine & Zakamska 2004; Udry et al. 2003; Jones 2003; Jones et al. 2003; Marcy et al. 2004a; Halbwachs et al. 2005).

The period distribution (central panel of Figure 2.4) can also be approximated by a power-law, with a negative exponent β in the range $[-1.0, -0.4]$. The decline for $P \gtrsim 3000$ days is caused by the same detection limit that applies to the mass distribution (with incompleteness dominating statistics beyond 4 AU). However, the power-law approximation holds only for $P \gtrsim 10$ days, with the 20% or so of planets on close-in orbits unaccounted for. The existence of a pile-up of planets at very short periods can be understood in terms of theories of planet formation and migration that I shall address in Section 2.3.

The mean of the eccentricity distribution of extrasolar planets is ~ 0.3 (right panel of Figure 2.4). The pile-up of planets with $e \simeq 0.0$ is explained by the presence of the very close-in objects ($P \lesssim 5 - 10$ days), for which circularization (e.g., Goldreich & Soter 1966) is almost complete. The orbits of extrasolar planets can be extremely elongated, with a maximum value of $e \simeq 0.95$ (Naef et al. 2001).

The two obvious comparisons that have been routinely performed since the first statistical studies of orbital elements and mass distributions of extrasolar planets are with the Solar System planets on the one hand, and with the database of spectroscopic binaries on the other hand.

A direct comparison of the M_p distribution between the extrasolar planet sample and our

Solar System is at best speculative, as incompleteness in the former begins to be important right below $1M_J$, i.e. exactly in the mass regime in which all Solar System planets lie. The period distribution of the Solar System giant planets is also difficult to compare with the extrasolar planet counterpart, as again Doppler surveys are only now achieving the time baseline necessary to detect Jupiter analogs. However, two main features clearly stand out, namely the presence of giant planets on very short-period orbits ($\sim 30\%$ and $\sim 15\%$ of the sample has periods less than 1% and 0.1% of Jupiter’s, respectively), and the existence of very massive planets (18% of the sample has $M_p \sin i > 5 M_J$). The two eccentricity distributions are significantly different, with $\sim 55\%$ of the extrasolar planets having e exceeding Pluto’s, the largest in our planetary system.

On the other hand, more detailed comparisons can be made between the exoplanet sample and spectroscopic binaries. Here the main results are that a) the two mass distributions are clearly separated by the “brown dwarf desert”; b) If one does not take into account the hot Jupiters with $P \lesssim 10$ days, the period distributions are very similar (but the pile-up of giant planets on few-days orbits has no counterpart among spectroscopic binaries); c) the extrasolar planet eccentricity distribution (corrected for tidal circularization) differs significantly from the one of spectroscopic binaries, the former highlighting an excess of low-eccentricity objects ($e \lesssim 0.2$) and a paucity of high-eccentricity objects ($e \gtrsim 0.5 - 0.6$) with respect to the latter (Halbwachs et al. 2005), that cannot be explained solely in terms of selection biases (e.g., the shortage of planets with very high e being due to the fact that eccentric orbits can be more easily missed by the observations). This last result is in partial disagreement with previous studies that emphasized the striking similarity between the two distributions (Stepinski & Black 2001; Mazeh & Zucker 2002), and probably due to very different selection criteria of the two samples used for the comparison by the different authors.

Estimates of planet frequency f_p around normal stars in the solar neighborhood (limited to late F, G, and early K spectral types) have been proposed by several authors, both based on the statistical occurrence of planetary systems in a given stellar sample monitored by Doppler surveys, as well as on the basis of the power-law fits to the observed properties of extrasolar planets.

When the range of masses is held fixed to that within the grasp of present-day radial-

velocity measurements and the period range to within the time-span of observations, estimates are all in fair agreement with each other (Zucker & Mazeh 2001a; Tabachnik & Tremaine 2002; Lineweaver & Grether 2003; Marcy et al. 2004b; Naef et al. 2004), with quoted values of $f_p \simeq 4\% - 5\%$ and $f_p \simeq 6\% - 9\%$ for $1M_J \leq M_p \leq 10M_J$, and $a \leq 3$ AU, and $0.5M_J \leq M_p \leq 10M_J$, and $a \leq 4$ AU, respectively. The occurrence rate of hot Jupiters ($P \leq 5 - 10$ days) is estimated to be $\sim 0.7 - 1\%$.

Using microlensing data, Gaudi et al. (2002) have instead put upper bounds to the number of giant planets orbiting M dwarfs in the Galactic bulge. They find that less than 33% of M dwarfs in the Galactic bulge have companions with mass $M_p = 1M_J$ between 1.5 and 4 AU, and less than 45% have companions with $M_p = 3M_J$ between 1 and 7 AU, while according to Snodgrass et al. (2004) the occurrence rate of Jupiter-mass planets around solar-mass stars at $a \simeq 4$ AU in the Galactic bulge is not greater than $\approx 18\%$.

Finally, Gilliland et al. (2000) used *HST* transit photometry to show that the occurrence rate of close-in planets ($P \leq 7 - 8$ days) is significantly lower in globular clusters than in the solar neighborhood, and this result has been recently confirmed for periods up to 16 days by Weldrake et al. (2005). However, when attempts are made to extrapolate f_p to encompass the Solar System properties, and beyond, somewhat arbitrary assumptions have to be made about the general properties of planetary systems, as pointed out by Beer et al. (2004). Thus, numbers reported in the literature in such cases, ranging anywhere from $f_p = 18\%$ to $f_p = 100\%$, are at best speculative.

2.2.4 Correlations

With improved statistics, in recent years a number of studies has been carried out to find evidence of correlations among orbital parameters and masses, and between planet characteristics and stellar host properties.

Figure 2.5 shows the $e - P$, $M_p \sin i - P$, and $e - M_p \sin i$ diagrams for the extrasolar planet sample. The visual impression is that all three parameters seem to be correlated. A Spearman rank-correlation test finds that the probability of the null hypothesis (no correlation) in the three cases is 1.44×10^{-10} , 3.62×10^{-11} , and 1.37×10^{-6} , respectively. Each

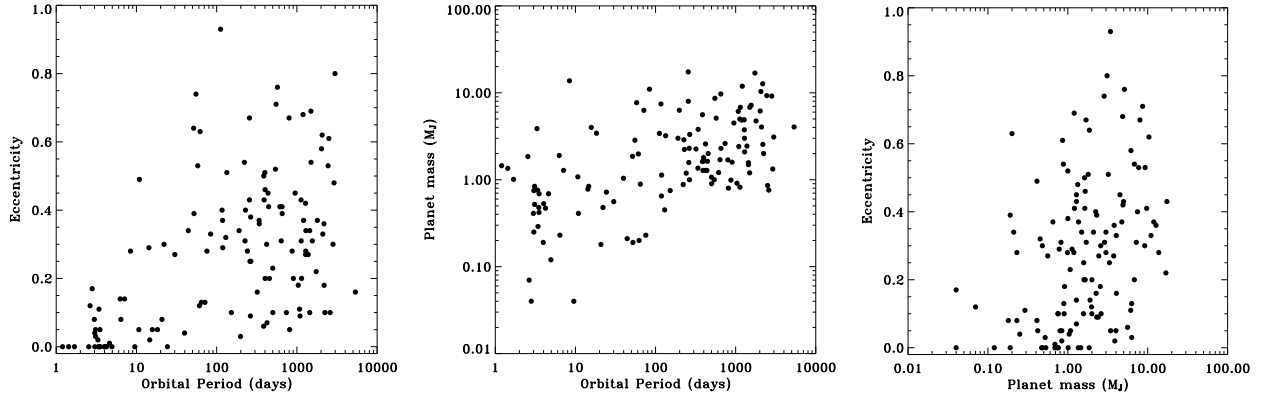


Figure 2.5 Left: eccentricity versus orbital period for the extrasolar planet sample. Center: the mass-period diagram. Right: eccentricity versus minimum planet mass

diagram deserves a separate discussion.

If we limit the sample to objects with $P > 10$ days, no $e - P$ correlation can be found. As a matter of fact, the few-days orbits of close-in planets are all likely to have been tidally circularized (Goldreich & Soter 1966). Beyond the circularization limit, extrasolar planets can be found on very eccentric orbits, regardless of the value of P .

The strong $M_p \sin i - P$ correlation can partly be explained in terms of an observational selection effect. For periods greater than several hundred days, corresponding to separations of ~ 2 AU, the sensitivity of Doppler surveys is now reaching the lower mass limit of $1 M_J$ (we recall in units of $M_p \sin i$), while for shorter periods the availability of consistent radial-velocity monitoring with precisions of 3-5 m/s allows for the detection of increasingly smaller masses. It is no surprise then that planets with minimum masses of order of the mass of Saturn and below have been found only with periods no greater than several tens of days.

However, as initially pointed out by Zucker & Mazeh (2002), Udry et al. (2002) and more recently by Eggenberger et al. (2004b), the paucity of high-mass planets on short-period orbits (the easiest to detect with the Doppler method) is real, and not due to any selection effects. The lack of massive, close-in planets deserves an explanation, which I shall address in Section 2.3.

The $e - M_p \sin i$ correlation arises, instead, as a consequence of the two main observed $e - P$ and $M_p \sin i - P$ trends. All low-mass planets are found on very short-period orbits, and their eccentricities are typically low (as pointed out for example by Udry et al. 2002).

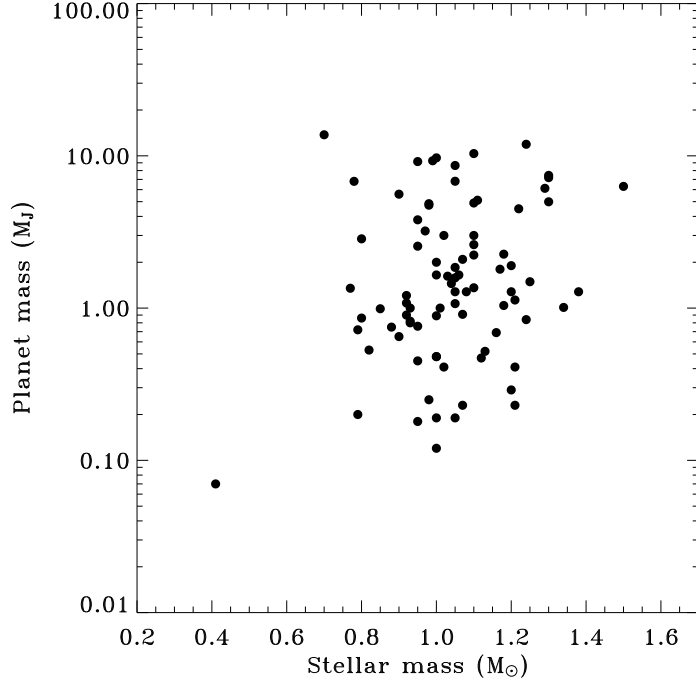


Figure 2.6 Minimum mass of single planets versus mass of the host stars

In fact, with one exception, no planet with $P < 30$ days shows $e > 0.3$. If we remove this sample from the $e - M_p \sin i$ diagram, every hint of correlation disappears, and planets can be found on orbits with a wide range of eccentricities, regardless of their mass.

The interplay between planets and their host stars at various stages of the formation and evolution processes could translate in possible correlations between the properties of the former and some of the characteristics of the latter. For example, in Figure 2.6 I show the distribution of projected masses for single planets orbiting single stars as a function of the mass of the parent star. A rank-correlation test gives a probability of no correlation of 6%, showing evidence for a marginal positive correlation.

The hint that more massive planets seem to orbit more massive parent stars might simply be due to observational selection effects. In fact, at a given period, for increasingly larger stellar masses the same radial-velocity amplitude is induced by an increasingly more massive planet, and increasingly hotter stars are at the same time more complicated targets for Doppler surveys (less, and weaker, spectral lines, jitter, and enhanced rotation being the major causes of degradation in the radial-velocity precision). The paucity of sub-Jupiter-mass planets around stars more massive than $\sim 1.2 M_\odot$ (late F, or earlier), which have not

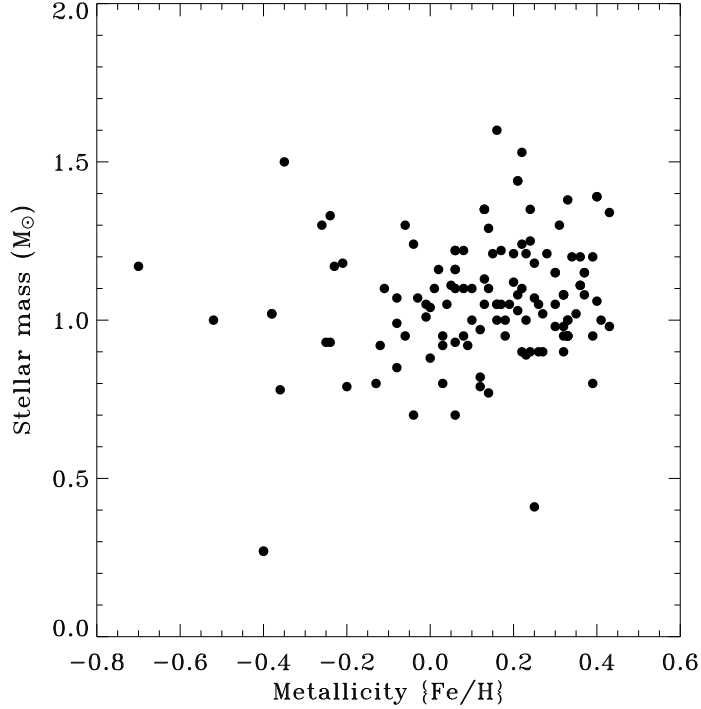


Figure 2.7 Mass versus metallicity for the planet-host stars

been considered in large numbers, should thus come as no surprise.

On the other hand, the paucity of planets orbiting late-K through early-M dwarfs ($\approx 0.4 - 0.8M_{\odot}$), and the hint for a decrease in planetary mass as we move toward smaller planet-host masses, might not be accounted for only in terms of observational biases. In fact, at lower parent star masses, the typically lower achievable radial-velocity precision (due to intrinsic radial-velocity jitter and faintness) is at least partly counterbalanced by the fact that, at a given period, a planet of the same mass will induce a larger velocity variation. For the discovery of the Neptune-mass planet orbiting the M2.5V star GJ 436, Butler et al. (2004) report typical values of $\sigma_{RV} \approx 5$ m/s, which would make objects with $M_p \sin i > 1 M_J$ detectable out to a few AU.

Although the sample size of late-K and M dwarfs monitored today is an order of magnitude smaller than that of solar-type stars, the trend appears to begin to be statistically significant. It is thus conceivable that a theoretical explanation for the paucity and smaller size of planets orbiting moderately late-type stars should be proposed. I will address this point in the next Section.

Due to the primary mass bias it is however difficult, as noted by Santos et al. (2003),

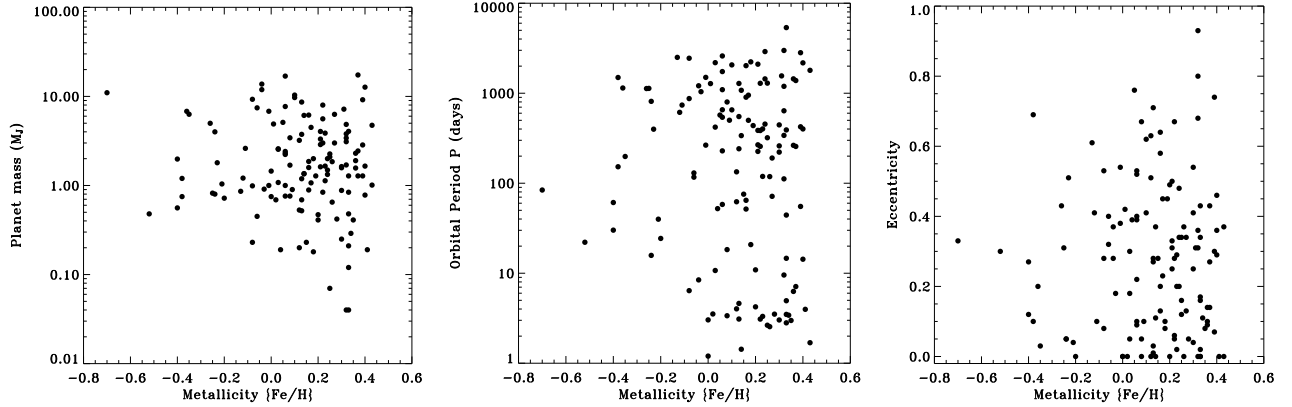


Figure 2.8 Left: minimum planet mass against $[\text{Fe}/\text{H}]$ of the host stars. Center: the period-metallicity diagram. Right: eccentricity versus $[\text{Fe}/\text{H}]$

to study the probability of planet formation as a function of M_\star solely on the basis of radial-velocity data. The adopted mass (or equivalently color, or T_{eff}) cut-offs in Doppler surveys show up when different planet-host properties are compared. In Figure 2.7 I show the distribution of masses of the planet hosts against their measured metallicity, and a marginal positive correlation can be found (probability of the null hypothesis of 10%). Santos et al. (2003) argue in fact that target lists are more likely to exclude massive metal-poor stars, or low-mass metal-rich stars. This bias does not prevent anyhow to draw conclusions on the dependence of planetary frequency on $[\text{Fe}/\text{H}]$, as discussed previously.

Several authors have searched in the past for possible correlations between stellar metallicity and planet properties. I show in the three panels of Figure 2.8 the distributions of planet masses, orbital periods, and eccentricities against $[\text{Fe}/\text{H}]$ of the planet hosts. Udry et al. (2002), Santos et al. (2001, 2003), and Fischer et al. (2002a) searched for correlations in the $M_p \sin i$ - $[\text{Fe}/\text{H}]$ diagram, but concluded no statistically significant trend can be found. A rank-correlation test on the present sample gives a probability of no correlation of 56%. No apparent correlation can be found in the e - $[\text{Fe}/\text{H}]$ diagram as well, as already pointed out by Santos et al. (2003).

The P - $[\text{Fe}/\text{H}]$ diagram deserves instead more attention. Gonzalez (1998b) and Queloz et al. (2000a) initially argued that metal-rich stars seem to possess an excess of very short-period planets with respect to other planet hosts. In later works (Santos et al. 2001, 2003; 2003 2003) no trend was found. However, after removing some potential sources of bias,

Sozzetti (2004) has shown how this trend is still present in the data, specifically when one restricts the analysis to single planets orbiting single stars. The correlation is significant at the 2-3 σ confidence level, and the latest planet announcements do not change the result: a rank correlation test on the less-biased sample of single stars orbited by only one detected planet used by Sozzetti (2004) gave a probability of no correlation 0.02.

It must be noted, however, that some bias sources, primarily small-number statistics, cannot be ruled out with high confidence. If real, the presence of a P -[Fe/H] correlation deserves an explanation, that theoretical models of formation and migration of giant planets could provide. I defer to Section 2.3 a further analysis of this point.

2.2.5 Multiple Systems and Planets in Stellar Systems

The global features of the mass and orbital parameters distributions of extrasolar planets, correlations among them, and between the former and some of the properties of the parent stars are likely to contain additional structure.

For example, as of February 2005 six planet-host stars are evolved, massive giants belonging to spectral class K-G III. They are drawn from different samples of stars (Frink et al. 2002; Setiawan et al. 2003; Sato et al. 2003) than the original F-G-K class IV-V sub-giant/dwarf stars included in the observing lists of the major Doppler surveys for planets. However, the size of the targeted sample of giants and the number of detected planets around this class of stars is small enough that no statistically meaningful study can be conducted yet.

Two other sub-samples of extrasolar planets have recently begun to reach a size large enough to favor the first explorative comparative studies. In fact, $\sim 18\%$ of the planets announced are found in multiple systems, containing up to 4 planets, while $\sim 24\%$ of the sample orbits stars that are themselves components of multiple stellar systems, and in two of the latter cases the stars harbor multiple-planet systems. Indeed, the binary fraction among stars with planets is significant (according to Patience et al. (2002) it lies between 7% and 18%, depending on different survey results), comparable to that of field G dwarfs with the same range of separations (27% according to Patience et al. (2002)).

Table 2.1 Results of the K-S and rank correlation tests on different stellar and planetary sub-samples

Sub-sample	$P_{KS}(e)$	$P_{KS}(P)$	$P_{KS}(M_p \sin i)$
(1) vs (3)	0.506	0.637	0.278
(1) vs (5)	0.710	0.809	0.497
(2) vs (4)	0.290	0.164	0.933
(2) vs (5)	0.498	0.404	0.998
(1) vs (2)	0.649	0.391	0.536
Sub-sample	$P_r(e - P)$	$P_r(e - M_p \sin i)$	$P_r(M_p \sin i - P)$
(1)	0.004	0.645	0.236
(2)	0.155	0.026	0.0001
(3)	1.098×10^{-08}	1.263×10^{-06}	2.078×10^{-11}
(4)	7.984×10^{-11}	2.936×10^{-05}	4.286×10^{-08}
(5)	2.926×10^{-10}	1.128×10^{-05}	4.724×10^{-11}

Note. — The different subsets are defined as follows: (1) planets in binaries; (2) planets in multiple-planet systems; (3) the sample with planets in binaries removed; (4) the sample with multiple-planet systems removed; (5) the sample of single planets around single stars.

A few authors have searched for differences between the distributions of orbital elements and masses of planets orbiting single and multiple stars and between those of single- and multiple-planet systems. Based on a sample of 66 planets, Zucker & Mazeh (2002) not only presented evidence for a $M_p \sin i - P$ correlation, but also for an absence of any correlation between masses and periods of planets found in stellar systems. In a more recent work, Marcy et al. (2004a) compared visually the eccentricity and mass distributions of single planets and planetary systems, and concluded that no significant difference was apparent. Using an enlarged sample of 115 planets, Eggenberger et al. (2004b) have revisited the $e - P$ and $M_p \sin i - P$ diagrams, qualitatively confirming the findings of Zucker & Mazeh (2002), and pointing at a paucity of planets on eccentric orbits around stars in stellar systems, for periods $P \lesssim 40$ days.

I have run Kolmogorov-Smirnov (K-S) and rank-order (Spearman) correlation tests to

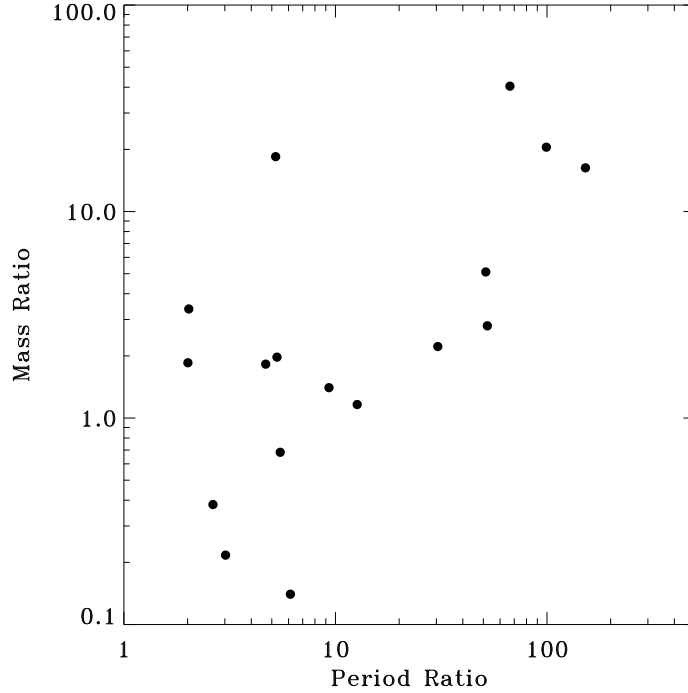


Figure 2.9 Mass ratios vs. period ratios for pairs of planets in multiple systems

search for statistically significant differences in the distributions of masses and orbital elements for planets around single and multiple stars and for single- and multiple-planet systems, and for differences in the correlations among orbital parameters and masses for the different subsets. The results are summarized in Table 2.1.

While the distributions of e , P , and $M_p \sin i$ for the different samples appear globally indistinguishable one from the other, due to high K-S probabilities of the null hypothesis, correlations among mass and orbital elements for the various subsets exhibit significantly different behaviors. In particular, planets around stars in multiple stellar systems show no signs of $e - M_p \sin i$ or $M_p \sin i - P$ correlation. This essentially confirms the findings of Eggenberger et al. (2004b) and Zucker & Mazeh (2002). Furthermore, systems of multiple planets do not show evidence of $e - P$ correlation, in contrast with the sample of single planets orbiting single and multiple stars.

Finally, Mazeh & Zucker (2003) have recently presented arguments for a correlation between mass ratios and period ratios among pairs of planets in multiple systems (assuming coplanarity). I show in Figure 2.9 the mass ratio - period ratio diagram for the sample of 13 planetary systems known to-date. A rank-correlation test gave $P_r = 0.03$. With the

addition of a few more multiple systems, and with the discovery of additional planets in already known systems, the evidence of a correlation is now somewhat weaker with respect to the Mazeh & Zucker (2003) results, but it's still present.

Possible explanations for these trends can be found in the context of theoretical models of giant planet formation, migration, and long-term dynamical stability which I will address in Section 2.3. However, as of today the sample sizes of multiple-planet systems and planets in multiple stellar systems is still small enough that general conclusions cannot be drawn.

2.2.6 Follow-up Studies

The Doppler and transit photometry techniques have so far provided the bulk of observational data from which we are learning about planets orbiting other stars. A variety of new as well as old techniques are being now utilized to perform detailed follow-up studies of known systems and to contribute to enlarge the number of discovered planets. The efforts have focused on providing better characterization of newly discovered hot Jupiters, with the exception of transit photometry, which I have addressed in Section 2.1, and astrometry, which I discuss below.

2.2.6.1 Astrometry Astronomers have long sought to find astrometric perturbations in a star's motion due to orbiting planet-sized companions. Many attempts have failed, some have produced more or less significant upper limits, a few have been successful.

The astrometric search for planets orbiting Barnard's Star (GJ 699) and Lalande 21185 (HD 95735) has spanned almost half a century. However, none of the Jupiter-sized companions on long-period orbits around Barnard's Star and Lalande 21185 announced by van de Kamp (1963, 1969a, b, 1975, 1982), Lippincott (1960a, b), Hershey & Lippincott (1982), and Gatewood (1996) was ever confirmed.

The *Hipparcos* Intermediate Astrometric Data (IAD) have been re-analyzed in recent years, in order to either detect the planet-induced stellar astrometric motion of the bright hosts or place upper limits to the magnitude of the perturbation, in the case of no detections. The *Hipparcos* IAD have been re-processed by several authors either alone, or in combina-

tion with either the spectroscopic information or with additional ground-based astrometric measurements. Initial claims of preliminary astrometric masses in the brown dwarf and stellar mass regime obtained by Mazeh et al. (1999), Zucker & Mazeh (2000), Gatewood et al. (2001), and Han et al. (2001) for over 30 candidate planets discovered by Doppler spectroscopy implied that radial-velocity surveys are strongly biased toward quasi-face-on configurations ($i < 5^\circ$). These claims have not survived detailed studies by Pourbaix (2001), Pourbaix & Arenou (2001) and Zucker & Mazeh (2001b), who showed that the conclusions are likely an artifact of the reduction procedure as applied to the *Hipparcos* data. However, in the case of non-detections, the *Hipparcos* IAD have been used successfully by Perryman et al. (1996) and Zucker & Mazeh (2001b) to confirm the sub-stellar nature of over two dozen Doppler-detected companions.

Space-borne narrow-field astrometry of the planet host star ρ^1 Cnc with the Fine Guidance Sensors (FGS) aboard *HST* has been carried out by McGrath et al. (2002, 2004). These authors failed to reveal astrometric motion induced by the $M_p \sin i = 0.88 M_J$ object on a 14.65-day orbit in the Doppler-detected multiple-planet system. With a nominal single-measurement precision of 0.5 mas, the *HST*/FGS data allow to place a firm (5σ) upper limit of $\sim 30 M_J$ on the actual mass of the companion, ruling out the preliminary *Hipparcos*-based mass estimate by Han et al. (2001).

The first undisputed astrometric mass determined for an extrasolar planet was reported by Benedict et al. (2002). The authors used *HST*/FGS measurements in combination with the available radial-velocity data to derive a perturbation size $\alpha = 250 \pm 60 \mu\text{as}$, inclination angle $i = 84^\circ \pm 6^\circ$, and actual mass $M_p = 1.89 \pm 0.34 M_J$ for the outer companion in the resonant two-planet system GJ 876. In the recent announcement (McArthur et al. 2004) of the discovery of a Neptune-sized planet on a 2.8 days orbit in the ρ^1 Cnc system (which brought the number of planets in the system to a total of four), *HST*/FGS measurements were re-analyzed to estimate, from the small arc of the orbit covered in the limited *HST* dataset, a perturbation size (1.94 ± 0.4 mas) and inclination ($53^\circ \pm 6^\circ.8$) for the outermost planet, orbiting at ~ 5.9 AU. Under the assumption of perfect coplanarity of all planets in the system, this implies an actual mass for the innermost planet of $17.7 \pm 5.57 M_\oplus$.

Currently, Benedict et al. (2003a, b, 2004) are monitoring with *HST*/FGS the stars v

And and ε Eri, and plan to combine the data with the available radial-velocity datasets and with lower-per-measurement precision ground-based astrometry. The predicted minimum perturbation sizes of the long-period (3.51 yr and 6.85 yr, respectively) planets orbiting these stars ($\alpha_{v\text{ And}} \simeq 540 \mu\text{as}$ and $\alpha_{\varepsilon\text{ Eri}} \simeq 1120 \mu\text{as}$, respectively) should be clearly detectable with *HST*/FGS, provided a sufficient time baseline for the observations.

2.2.6.2 Spectro-Photometry in the Visible High-precision photometry on stars with known planets on very short orbital periods has been performed by several groups (Charbonneau 2003, and references therein), and planetary transits have been ruled out for over a dozen hot Jupiters. As the transit probability is $P_T \simeq R_*/a \simeq 10\%$ for a planet at $a = 0.05$ AU across the disk of a Sun-like star, the null results obtained so far on the Doppler-detected planets (except for HD 209458b) is roughly consistent with the expectations, and with the assumption of a uniform distribution of orbital inclinations.

Attempts to detect planets by reflected light have been carried out in a twofold way. Charbonneau et al. (1999) and Leigh et al. (2003a) tried to detect the secondary spectrum of τ Boob directly in the optical, while Collier Cameron et al. (2002) searched v Andb, and Leigh et al. (2003b) have investigated HD 75289b. This is however a severe challenge (the ratio of the planet-to-star flux is $\sim 10^{-4} - 10^{-5}$ in the optical for orbital separations of a few milli-arseconds typical of hot Jupiters), and only upper limits on the albedo of these planets have been placed. The other possibility is to detect scattered light curves of hot Jupiters via ultra high-precision photometry. This is very difficult to attain from the ground (Kenworthy & Hinz 2003). Space-borne observatories such as *MOST* (Walker et al. 2003), *Kepler* (Jenkins & Doyle 2003), or *Corot* (Schneider et al. 1998) stand good chances to detect hot Jupiters by this effect.

Follow-up *HST* transit photometry of HD 209458b by Brown et al. (2001) and Schultz et al. (2004) has provided accurate data on transit timing that allowed them to exclude the presence of large satellites or circumplanetary rings. Even higher precision in transit timing could be achieved by future missions such as Kepler, opening the door to the tantalizing possibility of detecting additional planets in a system with masses as small as $1 M_{\oplus}$, via their gravitational interactions with the transiting planet (Miralda-Escudé 2002; Holman &

Murray 2005; Agol et al. 2005).

By means of the transmission spectroscopy technique, Charbonneau et al. (2002) detected absorption features in the spectrum of HD 209458 due to the presence of sodium in the planet’s atmosphere. Vidal-Madjar et al. (2003, 2004) showed that the upper atmosphere of the planet, mostly composed of neutral Hydrogen, also contains Oxygen and Carbon and it is evaporating in the fashion of a cometary tail. From the ground only upper limits have been placed on other atmospheric features of HD 209458b such as He I, CO (e.g., Moutou et al. 2001, 2003; Brown et al. 2002), and H α (Winn et al. 2004). However, modifications of this technique based on the Rossiter effect (Snellen 2004) could in principle provide the means for actual detections.

2.2.6.3 Infrared Emission Infrared wavelengths offer a far better (at least an order of magnitude) contrast ratio between planet and star than visible light. Lucas & Roche (2002) and Wiedemann et al. (2001) searched for H₂O and CH₄ in HD 209458b, HD 187123b, 51 Pegb, τ Boob, v Andb. Richardson et al. (2003a,b) further attempted to detect the thermal emission from HD 209458b by searching for evidence of a secondary eclipse (occultation spectroscopy), placing constraints on H₂O and CO features in the planetary atmosphere. Additional ground-based observations by Deming et al. (2005a) also failed to uncover the presence of Carbon Monoxide, but further constrained plausible models of the planetary atmosphere. However, observations with the *Spitzer Space Telescope* by Charbonneau et al. (2005) and Deming et al. (2005b) have very recently succeeded in detecting the secondary eclipse of TrES-1 and HD 209458b, respectively. The two results constitute the first direct detection of thermal emission from planets orbiting other stars. The data allow for the first time to obtain direct estimates of the planets’ effective temperature and wavelength-integrated Bond albedo, and the exact time of secondary eclipse (e.g., Charbonneau 2003) for both objects also indicates the lack of any significant orbital eccentricity.

2.2.6.4 Planet-Induced Chromospheric Activity and Radio Emission Cuntz et al. (2000) argued that planet-induced tidal and magnetic effects could show up in stellar chromospheric and coronal activity enhancement correlated with orbital phase, the hot

Jupiters being the only good candidates for detection. Saar & Cuntz (2001) searched 7 systems for enhancement of the Ca II triplet, but found none. Shkolnik et al. (2003, 2005) monitored 10 stars harboring close-in planets and detected Ca II emission in H and K in phase with the orbit of the hot Jupiter companions to HD 179949 and *v* And.

Finally, searches for cyclotron radio emission from exoplanets are almost 20 years old (Winglee et al. 1986). In fact, long-wavelength radio emission (in our Solar System gas giants arising from their polar regions) scales with planetary mass and inversely with planetary radius, and follows the rotation period (e.g., Farrell et al. 1999; Zarka et al. 2001), so that the radio power from hot Jupiters could exceed Jupiter’s by 3 orders of magnitude. Farrell et al. (2004) have placed upper limits on radio emission from τ Boob, while Bastian et al. (2000) have investigated 7 other systems. Present sensitivities (Lazio et al. 2004; Stevens 2005) are still insufficient to verify the predicted signal levels.

2.3 RENEWED THEORETICAL EFFORTS

After a decade of extrasolar giant planet discoveries, the only idea that has not yet undergone significant revision or criticism is the paradigmatic statement that planets form within gaseous disks around young T Tauri stars. Many old ideas have been revisited or revived, and a number of completely new ones has been proposed in an attempt to confront and explain the observational data on extrasolar planets. I summarize in this section the main results of serious theoretical investigations aimed at providing an overall, unified picture of how giant planets form, interact with the protoplanetary disk and amongst themselves, and evolve.

2.3.1 Planet Formation

The formation of ‘terrestrial’ planets, i.e. rocky objects with mass comparable to the mass of the Earth, is almost universally believed to occur through the slow process of coagulation of solid material through various stages – sub-micron-sized dust grains, kilometer-sized planetesimals, lunar-sized planetary embryos, and finally Earth-sized planets (for a review

see for example [Goldreich et al. 2004](#)), and I shall not discuss it in detail here. On the other hand, the formation mode for gas giant planets, with masses of the order of the mass of Jupiter, is still a matter of intense debate.

2.3.1.1 Core Accretion The core accretion mechanism for giant planet formation is historically speaking the more widely accepted and its strengths and weaknesses are best understood. Its greater success is its capability to explain in detail the global architecture of our Solar System, notably the nearly coplanar, circular orbits of the planets and the radial compositional gradient, from inner heavy elements to outer light element constituents (e.g., [Lissauer 1993](#)).

The benchmark initial condition of the core accretion model (which builds upon Kant’s (1755) initial ideas) is the so-called ‘minimum mass solar nebula’, i.e. the model of a disk obtained by considering the actual total mass contained in the planets of the Solar System plus a hydrogen and helium component reproducing the solar abundance. The resulting disk has a size of ~ 100 AU, a total mass of about $0.02 M_{\odot}$, and a surface density distribution $\Sigma(r) = 1700(r/1 \text{ AU})^{(-3/2)} \text{ g cm}^{-2}$ ([Weidenschilling 1977](#); [Hayashi 1981](#); [Hayashi et al. 1985](#); [Nakano 1987](#); [Lin & Papaloizou 1996](#)). Within the model, the radial temperature distribution is such that $T \leq 170$ K for orbital radii $r \geq 4$ AU. Beyond this ice boundary or ‘snow line’ (e.g., [Hayashi 1981](#); [Kokubo & Ida 2002](#)), the surface density of dust particles is greatly increased as ice condenses. The inner regions inside the snow line, within a few AU, are believed to be the cradle of rocky planet formation, while gas giant planet formation mainly occurs beyond the ice condensation radius.

This process encompasses the following main steps: *a*) growth of dust particles from size of order of $1\mu\text{m}$ to 1 mm and sedimentation of the dust layer onto the disk midplane (e.g., [Lissauer 1987](#); [Nakagawa et al. 1981, 1986](#)); *b*) formation and growth of solid particles from sizes of 1 mm to 1 km, either by gravitational instability ([Safronov 1969](#); [Goldreich & Ward 1973](#); [Adachi et al. 1976](#); [Coradini et al. 1981](#); [Sekiya 1983](#); [Goodman & Pindor 2000](#); [Youdin & Shu 2002](#); [Yamoto & Sekiya 2004](#); [Youdin & Chiang 2004](#); [Garaud & Lin 2004](#); [Tanga et al. 2004](#)), or by collision and coagulation ([Weidenschilling 1980, 1995](#); [Weidenschilling & Cuzzi 1993](#); [Kornet et al. 2001](#); [Wurm et al. 2001](#); [Youdin & Goodman 2005](#)); *c*)

runaway and/or oligarchic growth of planetesimals into planetary cores of order of several Earth masses (Wetherill 1990; Lissauer 1993; Goldreich et al. 2004); *d*) subsequent disk gas accretion, leading to the rapid growth of a gas giant planet (Mizuno 1980; Bodenheimer & Pollack 1986; Pollack et al. 1996; Papaloizou & Terquem 1999).

The exact mechanism driving the transition from dust particles to planetesimals, a jump of up to eight orders of magnitude in size, has been a serious problem for the core accretion mechanism right from the publication of the first versions of the model (e.g., Cuzzi et al. 1993; Sekiya 1998; Youdin & Shu 2002, and references therein; Weidenschilling 2003; Sekiya & Takeda 2003; Garaud & Lin 2004, and references therein). This issue still induces some researchers to state that the best way to explain the process is that ‘a miracle occurs’.

In recent years, the time-scales for giant planet formation by core accretion have also become a matter of concern, as the process typically requires $\sim 10^7$ years to form Jupiter at 5.2 AU (Pollack et al. 1996). As a matter of fact, current estimates of disk lifetimes for solar-type pre-main-sequence (PMS) stars are of order of a few Myr in regions of low-mass star formation (e.g., Haisch et al. 2001; Briceño et al. 2001), and even shorter in regions of high-mass star formation (e.g., Bally et al. 1998; Throop et al. 2001; Adams et al. 2004).

Furthermore, as shown in the previous Section, the high-mass tail of the mass distribution of extra-solar planets ($M_p \sin i > 5M_J$), the presence of giant planets at orbital radii well inside the snow-line, the existence of very large eccentricities, correlations among orbital parameters, and between them and some of the properties of the host stars, are all features posing quite puzzling questions to the standard version of the core accretion scenario. In the recent past significant efforts have been made to develop modifications to the standard model to make it fit the observed systems, and in the revival of alternative scenarios for giant planet formation.

2.3.1.2 Disk Instability The idea of giant planet formation directly through a local gravitational instability of the gaseous portion of a massive, self-gravitating protoplanetary disk is not new (Kuiper 1951; Cameron 1978), but it had been neglected for years due to the fact that this scenario had problems fitting the only data point available until 1995, i.e. our Solar System.

In this scenario, a thin, $0.1M_{\odot}$ disk (the high-mass tail of the mass distribution of disks around PMS stars; Beckwith & Sargent 1996) in Keplerian rotation with sound speed v_s , surface density Σ , and angular velocity Ω will become gravitationally unstable if the Toomre parameter $Q = (v_s\Omega)/(\pi G\Sigma) \simeq 1$ (Toomre 1964). Under this condition, the disk can develop nonlinear spiral density waves and fragment into one or more gravitationally bound objects, or it can evolve into a quasi-stable state in which gravitational instabilities lead to the outward transport of angular momentum.

The exact outcome depends on the rate at which the disc heats up (through the dissipation of turbulence and gravitational instabilities) and the rate at which the disc cools. Recent work suggests that fragmentation occurs in the disk if the cooling time $\tau_c \lesssim 3\Omega^{-1}$ (Gammie 2001). While pioneering work (Laughlin & Bodenheimer 1994) had shown that dense, gravitationally unstable Jupiter-mass clumps do not survive a full orbital evolution, more recent studies (Boss 1997, 1998, 2000, 2001, 2003, 2004a; Mayer et al. 2002, 2004; Rice et al. 2003a, 2003b) have shown this could actually be the case.

The disk instability mechanism has some appeal, for the following reasons. First, it easily solves the time-scale problem intrinsic to the core accretion model as, provided they can be long-lived, self-gravitating protoplanets can be produced in $\sim 10^3$ years (Boss 2000; Mayer et al. 2002), a difference of three orders of magnitude that would ensure chances of forming giant planets even in the shortest-lived protoplanetary disks. Second, it naturally explains the high-mass tail of the planet mass distribution, in particular the 20% or so of massive planets with $M_p \sin i > 5M_J$ (Boss 2001), and very recent studies suggest even the range of planetary masses $1 \lesssim M_p \lesssim 5 M_J$ can be produced by this mechanism (Mayer et al. 2004). Finally, the large spread in eccentricities for the extrasolar planet sample can also be explained by this model (Rice et al. 2003b; Mayer et al. 2004).

However, beside the debate on the actual possibility of the process to happen in the first place (e.g., Pickett et al. 2003; Mejía et al. 2005; Rafikov 2005), the main drawbacks for the disk instability mechanism are the following.

First, it still has trouble forming sub-Jupiter-mass objects (Boss 2000). Secondly, the presence of solid cores of typically 10-15 M_{\oplus} is more naturally explained within the framework of multi-stage core accretion, although it is still a matter of debate whether Jupiter actually

does have a core (Guillot et al. 1997; Guillot 1999) and also for some of the hot Jupiters, for which the inner structure can be directly probed, the presence of a core does not seem to be a requirement (Hubbard et al. 2002; Guillot & Showman 2002).

Furthermore, one of its main predictions, i.e. that planet frequency should be independent on the metallicity of the protoplanetary disk (Boss 2002), is apparently contradicted by the empirical evidence for a significantly enhanced probability of forming planets around the metal-rich stellar sample (see Section 2), although the possible flatness of f_p for $[\text{Fe}/\text{H}] \leq 0.0$ (Santos et al. 2004a) could reflect the existence of two different formation mechanisms.

Finally, the typical orbital radii of giant planets formed via disk instability are of order of at least 3-4 AU, thus the evidence for a population of gas giants orbiting with periods as short as 1.5 days is a problem for this mechanism much as it is for the competing core accretion mode.

2.3.2 Migration

The possibility of forming gas giant planets by core accretion well inside the ice condensation zone (e.g., Ward 1997; Wuchterl 1997; Bodenheimer et al. 2000; Ikoma et al. 2001) suffers from one major drawback: the disk temperature is too high, thus, in absence of icy planetesimals, the surface density of solids at orbital radii $\ll 3$ AU is too low to be able to support the growth of a rocky core of the required 15-20 M_\oplus . Recent work by Sasselov & Lecar (2000) and Jang-Condell & Sasselov (2004) suggests that the snow-line may occur closer to the central star than previously thought, thanks to its dependence on subtle temperature variations in the disk due to a variety of effects, However, Kornet et al. (2004) come to somewhat opposite conclusions. Given the present understanding of the matter, we can conclude that almost certainly $\approx 25\%$ of the present extrasolar planet sample (orbiting at $r < 0.1$ AU) would still lie too close to the parent star for the model to work.

The disk temperature also hampers the ability of forming gas giant planets inside the snow line by disk instability: the disk is simply not cool enough (and the Toomre parameter is too high) to allow for the generation of local gravitational instabilities (Mayer et al. 2004; Rafikov 2005). The conclusion one draws is thus that, regardless of how they formed, a

significant number of the giant planets detected to-date must have undergone some degree of orbital migration.

Within the context of the core accretion model, four mechanisms have been put forth to explain the presence of Jupiter-sized objects at very small orbital radii. Gravitational interactions between two giant planets may translate in ejection of one planet from the system while the other is left on a smaller orbit (Rasio & Ford 1996; Weidenschilling & Marzari 1996), but the frequency of hot Jupiters is far larger than this mechanism could produce (Ford et al. 2001a).

Resonant interactions of a planet with a disk of planetesimals inside its orbit can effectively move it inward (Murray et al. 1998), but the disk planetesimal mass required in order for the planet to spiral in to a few-days orbit is unusually large (Ford et al. 1999).

Dynamical friction between a planet and a planetesimal disk could provoke migration to very short orbital distances (Del Popolo et al. 2001, 2003; Del Popolo & Eksi 2002), without the need to invoke a suspiciously large reservoir of planetesimals. This model is appealing as it naturally reproduces the observed distribution of orbital radii in the range $0.02 \leq r \leq 0.1$ AU. However, by the time this mechanism begins to operate the gaseous portion of the disk has essentially disappeared, thus it is unlikely to play a major role in the shaping of the distribution of orbital periods of extrasolar planets if tidal interactions between the protoplanet and the surrounding gas disk are at work at much earlier times. This is indeed today the more widely accepted scenario for giant planet migration, and one of the few cases in this field in which a theoretical prediction (Goldreich & Tremaine 1979, 1980; Lin & Papaloizou 1979, 1993; Papaloizou & Lin 1984; Ward 1986) preceded the observational evidence.

Tidal interaction between a gaseous disk and an embedded planet can lead to three types of migration (Terquem 2003a, and references therein). Type I migration encompasses disk-protoplanet tidal interactions in the linear regime (e.g., Ward 1986, 1997; Terquem et al. 2000). The migration occurs primarily for low-mass solid cores (10- 15 M_{\oplus}), which move inward rapidly relative to the disk, without opening a gap. Type II migration foresees disk-protoplanet tidal interactions in the non-linear regime (e.g., Goldreich & Tremaine 1980; Lin & Papaloizou 1993). A Jovian-mass planet opens a gap around itself, gets locked into

the subsequent viscous evolution of the disk, and spirals in. In the Type III migration mode (Masset & Papaloizou 2003; Edgar & Artymowicz 2004), an intermediate-mass planet (typically of order of the mass of Saturn) can undergo a runaway migration, induced by the presence of co-orbital, co-rotation torques produced by fluid elements as they perform a horseshoe U-turn in the planet vicinity.

The three mechanisms described above are quite efficient at moving protoplanets inward. Indeed, the addition of migration effects to the standard core accretion scenario allows to explain some of the properties of the extrasolar planet sample, such as the mass-period correlation (Zucker & Mazeh 2002) and the highly non-gaussian shape of the orbital period distribution (Udry et al. 2003). In the first case, migration efficiency can be slowed down when the planet mass becomes comparable to the disk mass with which it interacts, thus reproducing the lack of high-mass planets on short-period orbits (Trilling et al. 2002). In the second case, the fact that giant planets can be found on short-period orbits in the first place does require some degree of migration to have occurred. Also note that, although the evidence is not very strong, the correlation between the orbital periods of extrasolar planets and the metallicity of the host stars (Sozzetti 2004, and references therein) could either reflect the fact that migration rates are slowed down in protoplanetary disks whose metal content is suppressed (Livio & Pringle 2003), or it might be indicative of longer timescales for giant planet formation around metal-poor stars, and thus reduced migration efficiency before the disk dissipates (Ida & Lin 2004b).

However, the scenarios for giant protoplanet migration in gaseous disks are not without problems. As a matter of fact, time-scales for migration (especially Type I and III) are very short, much shorter than typical disk and planet formation lifetimes. Furthermore, a stopping mechanism must be devised in order to prevent the migrating protoplanets from plunging into the central star, and to reproduce the observed pile-up of planets on few-days orbits. When the interaction between the disk and the planets is linear, orbital decay of cores can be stopped if the planet is on a sufficiently eccentric orbit as a result of the orbital crossing of resonances in the disk that do not overlap the orbit when the eccentricity is very small (Papaloizou & Larwood 2000). Magnetic torques encountered by the planet in a magnetized region of the disk can also significantly slow down migration (Terquem 2003b).

For a non-linear interaction, no mechanism among those proposed (Trilling et al. 1998, 2002; Lin et al. 2000, and references therein; Ivanov et al. 1999; Bryden et al. 1999; Kley 1999; Masset & Snellgrove 2001; Kuchner & Lecar 2002; Lecar & Sasselov 2003) has been shown so far to prevent orbital decay of an isolated planet in a natural way. As discussed by Terquem (2003a), the main problems are that it is unclear how to make the disk suddenly disappear, and most of the halting mechanisms cannot reproduce the distribution of close-in giant planets in the range $0.02 \leq r \leq 0.2$ AU.

Finally, migration scenarios in the context of the alternative mode of giant planet formation by disk instability are only now beginning to be taken into consideration. Given the computationally very intensive simulations needed to model the evolutionary behavior of marginally unstable, three-dimensional disks, and the complex physical processes associated, the analyses are not carried out yet for sufficiently long times to allow for an assessment of the efficiency of Type II migration (the other two types are not a matter of concern for this model, as objects formed by disk instability have typical masses of at least $1 M_J$).

Preliminary analyses (Mayer et al. 2004) suggest that migration might not be very efficient, or it might produce patterns resembling a random walk (Rice & Armitage 2003). However, dynamical relaxation of a population of massive planets formed through gravitational instabilities, assuming short time-scales for disk dissipation, could enhance migration and help to reproduce the observed orbital period distribution of extrasolar planets (Papaloizou & Terquem 2001). None the less, the studies are still falling short of being able to make predictions on the final post-formation distribution of orbital radii after disk dissipation.

2.3.3 Dynamical Interactions

In the context of the standard core accretion scenario for giant planet formation, the eccentricity distribution of extrasolar planets, whose mean is $e \simeq 0.3$ and differs from the one of the solar system planets at the 99.9% confidence level of a K-S test (Tremaine & Zakamska 2004), is hard to explain. Several attempts have been made to reconcile the standard model with observations, based on a variety of mechanisms of dynamical interactions.

Gravitational interactions between a forming planet in resonance with the surrounding

circumstellar disk can excite or damp its eccentricity (e.g., [Goldreich & Tremaine 1979, 1980](#); [Ward 1986](#); [Artymowicz 1993](#)), but a variety of complex constraints (mostly due to the nature of resonances) must operate simultaneously (e.g., [Ward & Hahn 1998, 2000](#); [Goldreich & Sari 2003](#); [Ogilvie & Lubow 2003](#)).

Close encounters between planets at the end of the formation process may lead one object to be ejected from the system, while the other is left on an highly eccentric orbit (e.g., [Rasio & Ford 1996](#); [Weidenschilling & Marzari 1996](#); [Lin & Ida 1997](#); [Ford et al. 2001a](#)). This mechanism makes clear predictions (very few Hot Jupiters, median $e = 0.6$, negative $e - M_p$ correlation) which are largely in contrast with the observations.

Dynamical interaction or dynamical friction of a migrating planet with a planetesimals disk ([Murray et al. 1998, 2002](#); [Del Popolo et al. 2001, 2003](#); [Del Popolo & Ekşi 2002](#)) could reproduce the observed spread of eccentricities, but as discussed in the previous Section these models also suffer from important shortcomings.

Resonant interactions between migrating planets can also excite eccentricities (e.g., [Yu & Tremaine 2001](#); [Lee & Peale 2002](#); [Chiang et al. 2002](#); [Terquem & Papaloizou 2002](#); [Nagasawa et al. 2003](#)), but this in the first place applies only to multiple-planet systems, and other predictions (negative $e - M_p$ correlation) are also not observed. While the migrating planets interact, resonant inclination excitation may occur as well ([Thommes & Lissauer 2003](#)), thus the multiple planet systems discovered so far with high e may also be highly non-coplanar. The observational data available to-date do not allow to test this interesting prediction.

Secular interactions with a distant companion star out of the planet's orbital plane (the so-called Kozai mechanism) could also excite a planet's eccentricity and even cause some degree of orbital migration, depending on whether such interactions take place in presence or absence of a protoplanetary disk (e.g., [Kozai 1962](#); [Holman et al. 1997](#); [Innanen et al. 1997](#); [Mazeh et al. 1997](#); [Krymowski & Mazeh 1999](#); [Ford et al. 2000](#); [Wu & Murray 2003](#); [Wu 2004](#)). In this case predictions (no $e - M_p$ correlation, high e found primarily in binary systems) are only marginally in agreement with the observations, while others (low e in multiple system that happen to be coplanar) are not supported, although values for the mutual inclination distribution of multiple-planet systems are not available yet.

Finally, [Zakamska & Tremaine \(2004\)](#) have recently suggested the possibility of the

propagation of eccentricity excitation for planets still embedded in long-lived protoplanetary disks due to encounters with passing stars, but their model does not make clear predictions on the resulting eccentricity distribution.

The alternative mode of formation by gravitational instability naturally forms Jupiter-sized objects with eccentricities of the order of those seen in the extrasolar planet sample (e.g, [Rice et al. 2003b](#); [Mayer et al. 2004](#)), although for the same reasons discussed in the previous Section no clear prediction of the final eccentricity distributions are available yet. High eccentricities could also be produced by dynamical relaxation of systems of massive planets formed via disk instability ([Papaloizou & Terquem 2001](#); [Terquem & Papaloizou 2002](#)), but even in this case studies are still at the exploratory level.

2.3.4 Inner Structure and Atmosphere

Building on the successes of the theory as applied to the stellar mass range, a variety of models describing in a consistent manner atmospheres, inner structure and evolutionary properties (mass, radius, temperature, age) of giant planets and brown dwarfs are today available. A number of quantitative predictions still awaits confirmation or confutation from observations, in particular for what concerns the non-irradiated gas giant planets.

Models of irradiated giant planets have been put to the test for the first time with the discovery of the photometric transits of HD 209458b. The main tool that is usually utilized to confront theory and observation is the mass-radius relation. In [Figure 2.10](#) I show the mass-radius diagram for all known transiting extrasolar planets as of February 2005, compared to the predictions from three models of isolated and irradiated giant planets ([Guillot 2005](#)). The case of HD 209458b clearly stands out.

All theories of irradiated giant planets ([Saumon et al. 1996](#); [Guillot et al. 1996](#); [Allard et al. 1997, 2004](#); [Seager & Sasselov 1998, 2000](#); [Burrows et al. 1997, 2000, 2003, 2004](#); [Marley et al. 1999](#); [Fortney & Hubbard 2004](#); [Hubbard et al. 2001](#); [Bodenheimer et al. 2001, 2003](#); [Guillot & Showman 2002](#); [Showman & Guillot 2002](#); [Baraffe et al. 2003](#); [Sudarsky et al. 2000, 2003](#); [Chabrier et al. 2004](#); [Cody & Sasselov 2002](#); [Barman et al. 2001](#); [Laughlin et al. 2005a](#)) have had trouble so far fitting the observed value of the radius of HD209458b, un-

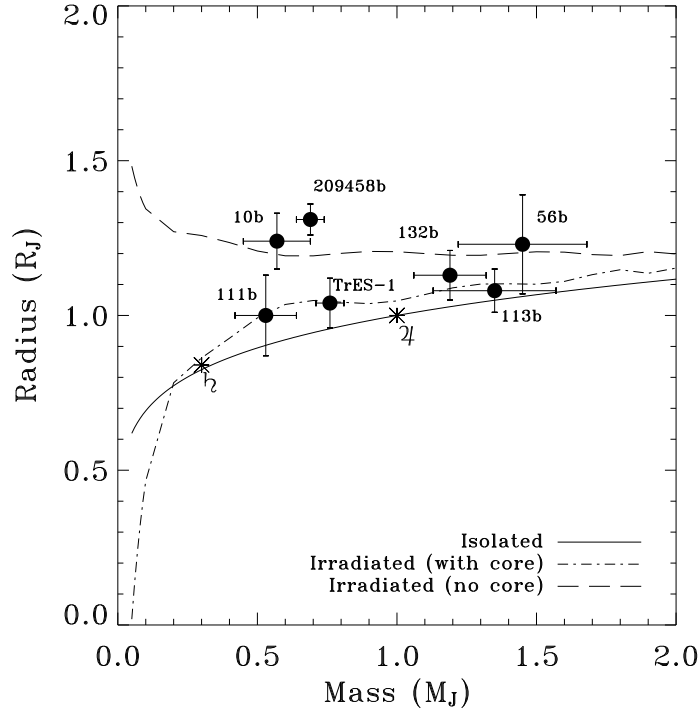


Figure 2.10 Radius vs. mass for the sample of transiting extrasolar planets discovered to-date. The values and uncertainties are taken from Brown et al. (2001) for HD 209458b, Torres et al. (2004a) for OGLE-TR-56b, Bouchy et al. (2004) for OGLE-TR-113b, Moutou et al. (2004) for OGLE-TR-132b, Pont et al. (2004) for OGLE-TR-111b, Sozzetti et al. (2004b) for TrES-1, and Konacki et al. (2005) for OGLE-TR-10b. Asterisks indicate Jupiter and Saturn. Lines of various styles represent the theoretical mass-radius relationship for an irradiated (with and without core, and with $T_{\text{eff}} = 1500$ K) and isolated giant planet at an age of ~ 3 Gyr (based on the models of Guillot 2005).

less one invokes an additional heat/power source in the core, generated for example by tidal dissipation of a nonzero orbital eccentricity induced by the gravitational perturbation of an undetected long-period companion (Bodenheimer et al. 2001, 2003; Laughlin et al. 2005a). However, the recent successful detection of thermal emission from the planet (Deming et al. 2005b), and in particular the timing of the secondary eclipse, clearly suggests the planet revolves on an orbit with no significant eccentricity, thus essentially ruling out the promising scenario suggested by Bodenheimer et al. (2001, 2003) and Laughlin et al. (2005a).

However, the other transiting planets (OGLE-TR-56b, OGLE-TR-113b, OGLE-TR-111b, OGLE-TR-132b, OGLE-TR-10b, and TrES-1) provide much better agreement between theory and observations. Apart from the ‘oddball’ HD 209458b, the main features of the theory of the internal structure of irradiated giant planets and the dependence of its main observable quantity, i.e. the radius, on stellar irradiation, mass and age seem to be, as of

today, essentially understood.

Theoretical predictions of the atmospheric composition of irradiated giant planets are more difficult to confront with observations, due to the more challenging nature of the measurements to be carried out (see Section 2.2.6.2). The predominant elements predicted are H₂, He, H₂O, Na, K, CO, and CH₄ (e.g, [Burrows 2005](#), and references therein). Furthermore, atmospheres of close-in jupiters should be mostly clear, with correspondingly low albedos ([Burrows 2005](#)). The upper limits on various elements obtained so far (Section 2.2.6.2) have failed in many cases to reach the detection limits required for testing theoretical models. When the required sensitivity has been reached, non-detections have allowed to infer the possible existence of a cloud-free atmosphere for HD 75289b ([Leigh et al. 2003b](#)), while high clouds appear to be present in the atmosphere of HD 209458b (e.g, [Richardson et al. 2003a,b](#); [Deming et al. 2005a, 2005b](#)). When detected, the low absorption feature due to Na for HD 209458b ([Charbonneau et al. 2002](#)) appears to confirm that clouds are indeed present in the planet’s atmosphere.

Spin-orbit evolution of short-period giant planets due to tidal interactions with their host stars ([Mardling & Lin 2002](#); [Ogilvie & Lin 2004](#)) could produce observable results, such as a correlation between fast stellar rotation rates and significant orbital eccentricities for planets with periods in the range 1-3 weeks ([Dobbs-Dixon et al. 2004](#)). Estimates of the time scales for spiraling into the host stars have been used by [Sasselov \(2003\)](#) to argue for the possibility of discriminating between different tidal dissipation models, but agreement on this prediction does not seem to have been reached ([Pätzold & Rauer 2002](#); [Pätzold et al. 2004](#)).

Finally, the evidence for an extended atmosphere around HD 209458b ([Vidal-Madjar et al. 2003, 2004](#)) due to evaporation effects has bolstered studies of the phenomenon of atmospheric escape from hot Jupiters, which had already been undertaken at a preliminary stage in the past ([Burrows & Lunine 1995](#)). [Lammer et al. \(2003\)](#), [Gu et al. \(2003, 2004\)](#), [Lecavelier des Etangs et al. \(2004\)](#), [Baraffe et al. \(2004\)](#), and [Grißmeier et al. \(2004\)](#) come to the similar conclusion that, under strong irradiation, hot Jupiters, depending on their mass and orbital distance, could undergo significant evaporation of their gaseous envelope, and expose their central rocky cores in a few Gyr, thus creating a new class of “hot Neptunes”.

However, independent calculations by Yelle (2004) do not seem to support the evidence for very large mass loss rates. Furthermore, it still remains to be seen whether evaporation effects can account for the sizes, masses, and ages of both the transiting hot Jupiters and the very recently announced hot Neptunes (Butler et al. 2004; McArthur et al. 2004; Santos et al. 2004b), or formation and/or migration should also be blamed.

2.3.5 Long-Term Stability

Until the discovery of the first extrasolar multiple-planet system (Butler et al. 1999), the theory of planetary orbits dynamics had had to deal with only one data point, our Solar System. The applicability of its predictive power had thus been rather limited. Now that a variety of additional systems, with a wide, and quite unexpected, range of different orbital arrangements, has been found, the field of planetary system dynamics has received revived interest.

The long-term dynamical evolution of the 13 extra-solar planetary systems known to date has been extensively investigated by theorists, utilizing both direct numerical integrations and approximate analytical approaches for the description of the N-body mutual interactions.

As opposed to our own solar system, or the three-planet system discovered by Wolszczan & Frail (1992) around the pulsar PSR 1257+12, both appearing dynamically stable over long time-scales (Laskar 1994; Gladman 1993), the dynamical evolution and long-term stability issues for the majority of the multiple-planet systems discovered by radial velocity are rather uncertain, and a variety of dynamical effects that are not seen in the context of the solar system planets (but are common instead among moon systems and Kuiper Belt objects, for example) have been uncovered.

Many studies have tried to gauge the general dynamical behavior of the extra-solar planetary systems ν Andromedæ (ν And; Laughlin & Adams 1999; Rivera & Lissauer 2000; Stepinski et al. 2000; Jiang & Ip 2001; Barnes & Quinn 2001; Chiang et al. 2001; Lissauer & Rivera 2001; Laughlin & Chambers 2001; Chiang & Murray 2002; Michtchehnko & Malhotra 2004; Barnes & Quinn 2004; Ford et al. 2005), 55 Cancri (55 Cnc; Novak et al. 2004; Ji et al. 2003; Barnes & Quinn 2004), 47 Ursæ Majoris (47 UMa; Goździewski

2002; Laughlin et al. 2002; Zhou & Sun 2003; Barnes & Quinn 2004; Ji et al. 2003), GJ 876 (Kinoshita & Nakai 2001; Laughlin & Chambers 2001; Rivera & Lissauer 2001; Ji et al. 2002; Goździewski et al. 2002; Lee & Peale 2002; Beaugé et al. 2003; Ji et al. 2003; Laughlin et al. 2005b; Beaugé & Michtchenko 2003, 2004; Lee 2004), HD 82943, HD 168443, HD 37124, HD 12661, HD 38529, HD 169830, HD 74156, HD 160691, and HD 202206 (Goździewski & Maciejewski 2001, 2003; Laughlin & Chambers 2001; Kiseleva-Eggleton et al. 2002; Goździewski 2003a, 2003b; Goździewski et al. 2003, 2005; Bois et al. 2004; Barnes & Quinn 2004; Ji et al. 2002; 2003; Ferraz-Mello et al. 2004, 2005; Goździewski & Konacki 2004; Correia et al. 2004; Zhou & Sun 2003; Lee & Peale 2003).

The following conclusions can be drawn: *a)* five of the systems belong to a class of “hierarchical” planetary systems, with widely separated orbits, in which dynamical interactions appear negligible (HD 74156, HD 37124, HD 168443, HD 38529, HD 169830); *b)* four systems (47 UMa, *v* And, HD 12661, and HD 160691) form a class of planetary systems subject to strong secular interactions; *c)* another four systems (GJ 876, HD 202206, HD 82943, and two of the planets orbiting 55 Cnc) appear to be locked in mean motion resonances, and two of them (GJ 876 and HD 202206) exhibit important variations of the orbital elements on short time-scales, comparable to the time-span of the radial-velocity monitoring.

However, the stability of the systems can be sensitive to small variations of the instantaneous orbital elements of the planetary orbits obtained from the radial velocity data and utilized as initial conditions for the numerical integrations. In particular, for the systems not to be destabilized and disrupted on very short time-scales (as short as 10^3 - 10^5 years), constraints must be placed on the maximum allowed values for the masses and on the range of allowed relative inclinations of the orbits.

Most of the time analytical calculations are performed with the coplanarity of the orbits as a working assumption. Due to the impossibility to derive independent values for the actual planet masses and relative inclination angles in multiple systems from the radial-velocity datasets, even when self-consistent dynamical fitting procedures are adopted (e.g., Laughlin & Chambers 2001; Rivera & Lissauer 2001), some degree of ambiguity cannot be removed, and general conclusions on the architecture, orbital evolution and long-term stability of the newly discovered planetary systems are thus difficult to derive.

Early attempts have also been made to verify the possibility of regions of dynamical stability inside the parent stars' Habitable Zones ⁶, where Earth-size planets may be found (Jones et al. 2001; Noble et al. 2002; Jones & Sleep 2002, 2004; Rivera & Haghighipour 2004; Goździewski 2002; Cuntz et al. 2003; Menou & Tabachnik 2003; Dvorak et al. 2003b; Atobe et al. 2004; Asghari et al. 2004; Érdi et al. 2004). However, the existence of such regions does not directly imply that rocky planets may have actually formed, in these systems, at such privileged distances, in the first place (Thébaud et al. 2002; Raymond & Barnes 2004; Barnes & Raymond 2004; Raymond et al. 2004).

2.3.6 Formation, Migration, and Stability of Planets in Stellar Systems

The presence of a nearby stellar companion can affect all stages of formation, migration, and long-term dynamical stability of planetary systems. As we have seen, it is already complicated enough to address in detail such processes when dealing with a single parent star, and the literature of models of the formation and evolution of planets in binaries is nowhere comparable in size.

Given the constraints on disk truncation for circumbinary, circumprimary, and circumsecondary disks (Artymowicz & Lubow 1994), a number of studies has focused on the formation of terrestrial planets in binary systems (Heppenheimer 1973, 1978; Whitmire et al. 1998; Marzari & Scholl 2000; Barbieri et al. 2002; Quintana et al. 2002; Moriwaki & Nakagawa 2004), while others have addressed the possibility of forming giant planets in circumstellar disks around a binary system by either core accretion or disk instability (Boss 1998; Nelson 2000; Thébaud et al. 2004; Mayer et al. 2005).

The latter are of particular interest for the possibility of a direct comparison with observations, but the overall impact of the presence of a secondary star on the efficiency of planet formation is far from being clear. For example, Boss (1998) claims planet formation by disk instability can be enhanced in the case of a secondary residing at 40 AU. Nelson (2000) and Mayer et al. (2005) come to the opposite conclusions, i.e. planet formation by

⁶The Habitable Zone of any star is defined as the range of orbital distances at which a potential water reservoir, the primary ingredient for the development of life as we know it, would be found in liquid form (e.g., Kasting et al. 1993)

both mechanisms can be strongly inhibited. The presence of giant planets around the stars γ Cep (Hatzes et al. 2003) and HD 41004A (Zucker et al. 2004), having stellar companions at ≈ 20 AU, partially contradicts the latter results.

A handful of studies has so far concentrated on giant planet migration in the presence of nearby stellar companions, and two possible scenarios have been discussed. Kley & Burkert (2000) and Kley (2000b, 2001) have studied the effect of an external companion on the migration and mass accretion rates of a giant planet embedded in a circumprimary disk, while Nelson (2003) has analyzed the evolution of giant protoplanets in circumbinary disks.

In both cases, the predictions of enhanced migration and mass accretion rates with respect to the single-star case may already find some support from the observations, given the evidence (see Section 2.2.5.2) of no $M_p - P$ correlation for the sample of planets in binaries (note however that no planet has yet been detected orbiting both components of a close binary).

A second scenario involves planet migration due to the Kozai mechanism, as discussed in the Section 2.3.3. The Kozai migration could be responsible for the large eccentricities of the planets orbiting 16 Cyg B and HD 80606 (Holman et al. 1997; Mazeh et al. 1997; Wu & Murray 2003). However, it is unclear how any of the above mechanisms could naturally explain the low eccentricities of short-period planets in binaries (see Section 2.2.5.2).

Finally, the long-term dynamical stability of planets in binary stellar systems has been investigated extensively in the past (Dvorak 1986; Inmanen et al. 1997; Holman et al. 1997; Mazeh et al. 1997; Holman & Wiegert 1999; Pilat-Lohinger & Dvorak 2002; Pilat-Lohinger et al. 2003, 2004; David et al. 2003; Dvorak et al. 2003a, 2004; Marzari et al. 2005; Musielak et al. 2005), both in the case of known systems as well as in order to predict stable orbits for hypothetical rocky planets in binary stellar systems.

The overall results are that a) the detected giant planets in binaries are likely to reside in stable orbital configurations, and b) there are margins for the presence of rocky planets in the Habitable Zone of close binaries, although the formation of terrestrial planets in such environments does not easily occur in the first place.

2.4 TOWARD A UNIFIED PICTURE

Recent work on planet formation theory has led to significant improvements and important, testable predictions.

For example, within the context of the core accretion scenario, Alibert et al. (2004, 2005) could reconcile the time-scales for the formation of giant planets with the inferred typical disk lifetimes (Haisch et al. 2001) by modeling the simultaneous formation and migration of giant planets in an evolving disk. Currie (2004) and Durisen et al. (2005) come to similar conclusions arguing for either a “migration enhanced” build-up of planetesimals in the outer regions of the protoplanetary disk, or a hybrid scenario for gas giant planet formation in which gravitational instabilities in disks produce dense rings that are conducive to accelerated growth of gas giants by core accretion. Shortened time-scales for core formation (Rafikov 2004; Goldreich et al. 2004) also contribute to alleviate the time-scale issue in the core accretion scenario.

Trilling et al. (2002) and Armitage et al. (2002) were able to qualitatively reproduce the observed semi-major axis distribution of giant planets, for $r > 0.1$ AU.

More recently, Laughlin et al. (2004a) have shown there should be a strong dependence of the frequency of giant planets on stellar mass, quantified by a significantly suppressed probability of forming giant planets around M dwarfs ($M_{\star} \leq 0.4M_{\odot}$). Similar conclusions are derived by Ida & Lin (2005), who also propose more detailed recipes for the actual planet mass distribution around stars of various masses, and find that, for example, Neptune-sized objects around M dwarfs could be relatively common. This prediction appears to have some degree of support from the observations (see Section 2.2.4), although the presently low frequency of giant planets discovered around M dwarfs might still be partly an artifact due to small-number statistics as well as to the intrinsic difficulty in obtaining precise Doppler measurements for this class of stars.

Ida & Lin (2004a) have derived a theoretical mass-period diagram that closely resembles the one of the extrasolar planet sample, and predicted a paucity of planets in the intermediate mass range $0.05 \leq M_p \leq 0.5 M_J$, for orbital distances < 3 AU.

Kornet et al. (2005) and Ida & Lin (2004b) have quantified the dependence of planetary

frequency on stellar metallicity, in qualitatively good agreement with the observed trend (Fischer et al. 2003b; Santos et al. 2004a).

As for what concerns the alternative scenario of giant planet formation by disk instability, Rice et al. (2003b) have built upon the early results by Boss (2002), and predicted a different metallicity dependence of the frequency of planets built by core accretion or disk instability. Rice et al. (2003b) and Rafikov (2005) also argue that giant planets formed by the latter mechanism should populate the high-mass tail of the planet mass distribution, and they should be preferentially found on not too close-in orbits. The very recent results by Mayer et al. (2004), however, seem to indicate the possibility that disk instability could form even sub-Jupiter-size objects.

Finally, recent provocative suggestions by Kuchner (2004) indicate that, in order to simultaneously explain the existence of extrasolar planets and our Solar System, a more critical investigation of some of the fundamental assumptions constituting the base of planet formation theories might be required, such as the dependence of the minimum-mass solar nebula surface density distribution on the disk radius or the steady-state protoplanetary accretion disk model.

As of today, no general conclusion on what is the preferred formation mode can be drawn, except that perhaps both mechanisms could operate (Beer et al. 2004).

Improvements in the understanding of the complex physical processes dominating the interaction and migration of planets in the protoplanetary disk rely upon the relaxation of some of the rather simplifying assumptions, such as linear analytical theories (Goldreich & Tremaine 1979, 1980; Lin & Papaloizou 1979, 1986a, 1986b, 1993; Papaloizou & Lin 1984; Ward 1986, 1997; Ward & Hourigan 1989; Tanaka et al. 2002; Tanaka & Ward 2004), and two-dimensional numerical models of laminar, artificially viscous α -disks (Shakura & Sunyaev 1973; Kley 1999, 2000a; Lubow et al. 1999; Bryden et al. 1999, 2000; Lin et al. 2000; Terquem et al. 2000; Nelson 2000; Snellgrove et al. 2001; Trilling et al. 1998; Papaloizou et al. 2001; Tanigawa & Watanabe 2002; Kley et al. 2004; Veras & Armitage 2004).

Three-dimensional numerical models of planet-disk and planet-planet interaction, both using nested-grid and smoothed-particle-hydrodynamics approaches (Kley 2001; D'Angelo et al. 2002, 2003; Papaloizou & Nelson 2003; Nelson & Papaloizou 2003, 2004; Papaloizou

et al. 2004; Bate et al. 2003; Winters et al. 2003; Laughlin et al. 2004b; Lufkin et al. 2004; Schäfer et al. 2004), have been developed, and the role of magneto-hydrodynamic turbulence in both type I and type II migration scenarios has been addressed.

The general picture that is beginning to unveil is that nearly all stages of planet migration are very sensitive to the initial conditions and may exhibit chaotic behavior. The most obvious implication is that the outcome of any given migration event may not be simply described in terms of a single final result, but it may require more careful modeling in terms of probabilistic distributions of possible outcomes.

A better comprehension of the dynamical interaction mechanisms responsible for the highly eccentric orbits of the extrasolar planet sample will likely arise from a refined understanding of migration-related processes. Theoretical calculations of the long-term stability of extrasolar planetary systems at large will primarily benefit from more statistically robust datasets and from the future availability of estimates of crucial parameters such as actual masses and inclination angles, and the same holds for models of inner structure, atmosphere, and evaporation for irradiated giant planets as well as for evolutionary models of widely-separated planetary-mass objects.

To summarize, observational data on extrasolar planets and their precursor disks indicate that there are numerous problems in connection with the elucidation of planetary formation and evolution processes. The observations of extrasolar planets show such striking differences in properties as compared with the Solar System that one must infer that planet formation and evolution is a very complex process.

An ideal theory of planet formation and evolution should be capable of explaining in a self-consistent way, be it deterministic or probabilistic, all the different phases discussed above. To this end, the help from future data obtained with a variety of different techniques will be crucial. Ultimately, both theory and observation will have to provide answers to a number of fundamental questions, that can be summarized as follows. (1) Where are the Earth-like planets, and what is their frequency? (2) What is the preferred mode of gas giant planet formation? (3) When, where, and for how long does migration occur? (4) What is the origin of the large planetary eccentricities? (5) Are multiple-planet orbits coplanar? (6) How many families of planetary systems can be identified from a dynamical viewpoint? (7) What

are the atmospheres, inner structure and evolutionary properties of gas giant planets? (8) Do stars with circumstellar dust disks actually shelter planets? (9) What are the actual mass and orbital elements distributions of sub-stellar companions? (10) How do planet properties and frequencies depend upon the characteristics of the parent stars (spectral type, age, metallicity, binarity/multiplicity)?

The experiments described in the next Chapters of this thesis are aimed at providing improved understanding of some of the outstanding issues in planetary science I have listed above.

ACKNOWLEDGMENTS

During the preparation of this manuscript, I have benefited from very fruitful discussion with many colleagues. I am particularly grateful to A. P. Boss, S. Casertano, D. Charbonneau, D. W. Latham, M.G. Lattanzi, G. W. Marcy, M. Mayor, D. Pourbaix, D. Queloz, D. D. Sasselov, and G. Torres for helpful comments and insights. The author acknowledges support from the Smithsonian Astrophysical Observatory through the SAO Predoctoral Fellowship program and the Keck PI Data Analysis Fund (JPL 1262605). This research has made use of NASA's Astrophysics Data System Abstract Service and of the SIMBAD database, operated at CDS, Strasbourg, France.

3.0 ON THE POSSIBLE CORRELATION BETWEEN THE ORBITAL PERIODS OF EXTRA-SOLAR PLANETS AND THE METALLICITY OF THE HOST STARS

Alessandro Sozzetti, 2004, *Monthly Notices of the Royal Astronomical Society*, **354**, 1194

3.1 INTRODUCTION

The nearby F-G-K dwarfs harbouring giant planets show evidence of moderate metal-enrichment with respect to the average metallicity of field dwarfs in the solar neighborhood. The dependence of planetary frequency on the metallicity of the host stars was investigated since the first detections by precision radial-velocity surveys (Gonzalez 1997; Laughlin & Adams 1997), and different explanations were proposed, such as enhanced giant planet formation by high stellar metallicity (Santos et al. 2000, 2001; Reid 2002), observational selection effects or pollution by ingested planetary material (Laughlin 2000; Gonzalez et al. 2001; Israelian et al. 2001; Pinsonneault et al. 2001; Murray & Chaboyer 2002). Recently, based on observationally unbiased stellar samples, the evidence for higher planetary frequency around unpolluted, primordially metal-rich stars has been clearly demonstrated by Santos et al. (2001), and confirmed by Fischer et al. (2003b) and by Santos et al. (2004a), who showed a sharp break in frequency at $[\text{Fe}/\text{H}] \simeq 0.0$. In this paper we investigate further the possible correlation between the orbital period of the extra-solar planet sample and the metallicity of the parent stars, in favor of which some authors had argued in the past (Gonzalez 1998b; Queloz et al. 2000a; Jones 2003), while others (Santos et al. 2001; Laws et al. 2003) had not found evidence of its existence.

In a recent work, Santos et al. (2003) discussed extensively possible dependencies be-

tween stellar and planetary properties. In particular, they concluded that the *metallicity* distribution of stars with very short-period planets ($P \leq 10$ days) is essentially indistinguishable from the same distribution of stars with longer period ($P > 10$ days) planets. In this paper we show instead that there appears to be some evidence for a significant difference between the *period* distributions of planets around metal-rich ($[\text{Fe}/\text{H}] \geq 0.0$) and metal-poor ($[\text{Fe}/\text{H}] < 0.0$) stars. This correlation between stellar metallicity and orbital periods is highlighted by a paucity of close-in planets (*Hot Jupiters* on circular orbits with $P \leq 5$ days) around the metal-poor stellar sample.

In Section 3.2 we present our statistical studies of the P – $[\text{Fe}/\text{H}]$ correlation for the extra-solar planet sample. In Section 3.3 we analyze possible sources of bias that might contribute to produce the observed trend. In Section 3.4 we briefly present our findings in the context of formation and, in particular, migration processes for giant planets in primordial protoplanetary discs, and discuss possible observational tests that might help disprove or verify the reality of the correlation.

3.2 STELLAR AND PLANET SAMPLE ANALYSIS

Table 3.1: Metallicities of planet-host stars and orbital periods of the planetary-mass companions utilized in the analysis. The list is sorted by increasing period of the innermost planet. The literature source used for the metallicity values is Santos et al. (2004a), except for HD 330075 (Pepe et al. 2004), BD-10 3166 (Gonzalez et al. 2001), and HD 37605 (Cochran et al. 2004).

Star	[Fe/H]	Orbital Period (days)		
		Planet 1	Planet 2	Planet 3
HD 73256	0.26	2.548
HD 83443	0.35	2.985
HD 46375	0.30	3.024
HD 179949	0.22	3.093
HD 187123	0.13	3.097

Table 3.1: (continued)

Star	[Fe/H]	Orbital Period (days) ¹		
		Planet 1	Planet 2	Planet 3
τ Boo ²	0.23	3.313		
HD 330075	0.08	3.369
BD -10 3166	0.50	3.487
HD 75289 ³	0.28	3.510
HD 209458	0.02	3.525
HD 76700	0.41	3.971
51 Peg	0.20	4.231
ν And ²	0.13	4.617	241.5	1284.0
HD 49674	0.33	4.948
HD 68988	0.24	6.276
HD 168746	-0.08	6.403
HD 217107	0.37	7.110
HD 162020	-0.04	8.428
HD 130322	0.03	10.72
HD 108147	0.20	10.90
HD 38529	0.40	14.31	2174.3	...
55 Cnc ²	0.33	14.65	44.28	5360.0
GJ 86 ²	-0.24	15.78
HD 195019 ²	0.08	18.30
HD 6434	-0.52	22.09
HD 192263	-0.20	24.35
ϱ Crb	-0.21	39.85
HD 74156	0.16	51.64	2300.0	...

²Star in a binary system (Eggenberger et al. 2004b, and references therein)

³Star in a binary system (Mugrauer et al. 2004a)

Table 3.1: (continued)

Star	[Fe/H]	Orbital Period (days) ¹		
		Planet 1	Planet 2	Planet 3
HD 168443	0.06	58.12	1739.5	...
HD 3651	0.12	62.23
HD 121504	0.16	64.60
HD 178911 ²	0.27	71.49
HD 16141	0.15	75.56
HD 114762 ²	-0.70	84.03
HD 80606 ²	0.32	111.8
70 Vir	-0.06	116.7
HD 216770	0.23	118.5
HD 52265	0.23	119.0
HD 1237	0.12	133.8
HD 37124	-0.38	152.4	1495.0	...
HD 73526	0.27	190.5
HD 82943	0.30	221.6	444.6	...
HD 169830	0.21	225.6	2102.0	...
HD 8574	0.06	228.8
HD 89744 ⁴	0.22	256.6
HD 134987	0.30	260.0
HD 12661	0.36	263.6	1444.5	...
HD 150706	-0.01	264.9
HD 40979	0.21	267.2
HD 17051	0.25	320.1
HD 142	0.14	338.0
HD 92788	0.32	340.0

⁴Star in a binary system (Wilson et al. 2001; Mugrauer et al. 2004b)

Table 3.1: (continued)

Star	[Fe/H]	Orbital Period (days) ¹		
		Planet 1	Planet 2	Planet 3
HD 28185	0.22	385.0
HD 142415	0.21	386.3
HD 177830	0.33	391.0
HD 108874	0.23	401.0
HD 4203	0.40	401.0
HD 128311	0.03	414.0
HD 27442	0.39	423.8
HD 210277	0.19	437.0
HD 19994 ²	0.24	454.0
HD 20367	0.17	500.0
HD 114783	0.09	501.0
HD 147513	0.06	540.4
HD 222582	0.05	572.0
HD 65216	-0.12	613.1
HD 160691	0.32	638.0	1300.0	...
HD 141937	0.10	653.2
HD 23079	-0.11	738.5
16 Cyg B ²	0.08	799.0
HD 4208	-0.24	812.2
HD 114386	-0.08	872.0
HD 213240	0.17	951.0
HD 10647	-0.03	1040.0
HD 10697	0.14	1078.0
47 UMa	0.06	1095.0	2594.0	...
HD 190228	-0.26	1127.0

Table 3.1: (continued)

Star	[Fe/H]	Orbital Period (days) ¹		
		Planet 1	Planet 2	Planet 3
HD 114729	-0.25	1131.5
HD 111232	-0.36	1143.0
HD 2039	0.32	1192.6
HD 136118	-0.04	1209.6
HD 50554	0.01	1279.0
HD 196050	0.22	1289.0
HD 216437	0.25	1294.0
τ^1 Gruis	0.24	1443.0
HD 106252	-0.01	1500.0
HD 23596	0.31	1558.0
14 Her	0.43	1796.4
HD 39091	0.10	2063.8
HD 72659	0.03	2185.0
HD 70642	0.18	2231.0
HD 33636	-0.08	2447.3
ε Eri	-0.13	2502.1
HD 30177	0.39	2819.7
GJ 777 A ²	0.24	2902.0

We summarize in Table 3.1 the values of orbital periods P for the sample of extra-solar planets known to-date and the metallicities [Fe/H] of their parent stars that have been utilized in our analysis. As described in the Table, orbital periods were taken from up-to-date online catalogues, while the metallicity values were collected from a variety of sources, primarily a recent paper by Santos et al. (2004a). The detailed list of literature sources used

is reported in Table 3.1, along with the relevant information about binarity. This sample of 96 stars, and 109 planets, is the result of the adoption of a few selection criteria we believe are important in order to keep the possible sources of bias at a minimum. The impact of additional potential biases, that cannot be removed by simply excluding a few objects from the analysis, will be discussed in Section 3.3. For the purpose of our study, we have excluded from the sample the following objects:

- 1) sub-stellar companions to nearby stars with minimum projected masses in the brown dwarf mass regime. Given the still uncertain and evolving definition of a giant planet, the dividing line must be set with some degree of arbitrariness, and it may ultimately turn out that brown dwarfs and planets indeed populate a common mass range and/or share a common origin. However, in our case we have used a more relaxed version of the Oppenheimer et al. (2000) theoretical Deuterium-burning threshold of $13 M_J$ (where M_J is the mass of Jupiter), that establishes both the lower limit to the mass of a brown dwarf and the upper bound to the mass of a planet (assuming solar metallicity). In particular, we have excluded objects with masses exceeding this limit by more than 25-30%, except for the case of the multiple system orbiting HD 168443, which probably shares a common origin;
- 2) six spectral class III K-G giants (HD 219449, HD 104985, HD 59686, Hip 75458, HD 47536, and γ Cep), belonging to different samples of stars with respect to the original F-G-K class IV-V subgiant/dwarf stars included in the observing lists of the major precision Doppler surveys for planets;
- 3) the unconfirmed second planet around ε Eri;
- 4) the first recently discovered planetary mass object OGLE-235/MOA-53 by means of the microlensing technique (Bond et al. 2004), as the characteristics of the parent star are not well determined;
- 5) the two strongly interacting planets orbiting the M4 dwarf GJ 876 and the planet around HD 41004 A, for which no reliable metallicity estimates have been provided yet;
- 6) the three recently announced “very” Hot Jupiters orbiting OGLE transiting candidates (e.g., Konacki et al. 2003; Bouchy et al. 2004). Indeed, for two of these objects (OGLE-TR-113 and OGLE-TR-132) Bouchy et al. (2004) have provided metallicity estimates,

but the low S/N ratios of the spectra for these stars do not allow at present such parameter to be well constrained. Furthermore, the metallicity distribution of the OGLE sample (at a typical distance of about 1.5 kpc) is unknown, and it might significantly differ from the one of the solar neighborhood sample (within 40-50 pc of the Sun) observed by current precision radial-velocity surveys. In a recent work, Nordström et al. (2004) confirmed the existence of a mild radial metallicity gradient in the disc of the Milky Way, and its evolution with time. In particular, stars younger than ~ 10 Gyr show an average metallicity gradient of ~ -0.09 dex/kpc, while the oldest stars in their sample do not show any gradient at all. On the face of it, it is then safer to exclude the OGLE transiting planets from the sample.

In Figure 3.1, left panel, we show the log-distribution of P as a function of $[\text{Fe}/\text{H}]$. According to Santos et al. (2004a), the percentage of planet host stars increases linearly with $[\text{Fe}/\text{H}]$ for metallicity values greater than solar, while it flattens out for metallicities lower than solar. We then divide the orbital period distribution into two metallicity bins ($[\text{Fe}/\text{H}] < 0.0$ and $[\text{Fe}/\text{H}] \geq 0.0$), and compare them in the histogram plot in the right panel of Figure 3.1. For reference, the full distribution of orbital periods for all metallicities is also overplotted. The most striking feature arising from the plot is the total absence of close-in planets on $P \leq 5$ days, circularized orbits around the metal-poor stellar sample. We must then ask if this effect is statistically significant. In order to do so, several tests can be conducted. We opt for a Kolmogorov-Smirnov (K-S) test, to measure to what extent the two period distributions might differ, and for a rank correlation test, to verify whether the period and metallicity distributions are actually uncorrelated.

As for the latter, we prefer to evaluate the (Spearman or Kendall) rank-order correlation coefficient rather than the classic linear (Pearson) correlation coefficient. In fact, non-parametric, rank correlation analyses are on average more robust, and the significance of a negative or positive rank-order correlation coefficient can usually be assessed (see for example Press et al. 1992).

The computation of the relevant D statistics in the K-S test gave as a result $D = 0.26$, corresponding to a probability of the two period distributions to be the same $Pr(D) \simeq 0.09$. A measure of the relevant statistics r_s for the rank-order (Spearman) correlation test gave

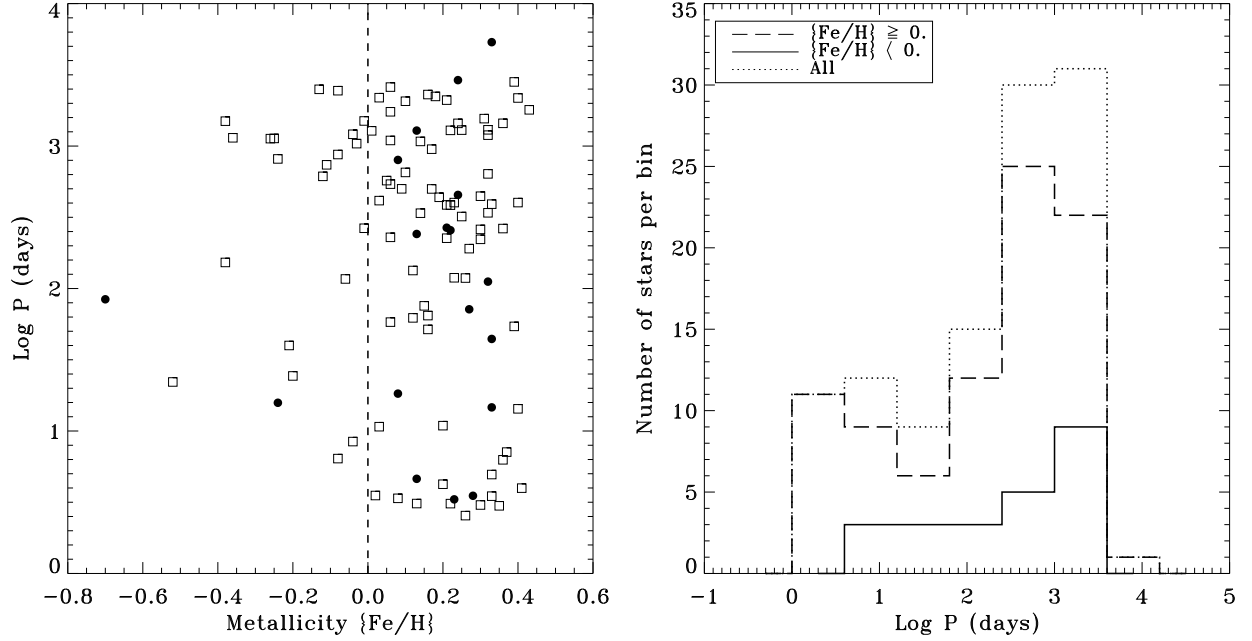


Figure 3.1 Left panel: orbital periods of extra-solar planets as a function of the metallicity of the host stars. Planets identified by filled circles are orbiting known members of binary systems. Right panel: distribution of orbital periods for the stellar sample with $[\text{Fe}/\text{H}] < 0.0$ (solid line), with $[\text{Fe}/\text{H}] \geq 0.0$ (dashed line), and for the full sample (dotted line)

$r_s = -0.14$, with a corresponding probability of the two distributions to be uncorrelated $Pr(r_s) \simeq 0.11$. There is then evidence for marginal differences in the period distributions for metal-poor and metal-rich stars, as well as a weak anti-correlation between the P and $[\text{Fe}/\text{H}]$ distributions.

To further investigate the possible existence of such effect, we have performed the same two tests on three sub-samples of the full dataset, i.e., removing stars in binary or multiple stellar systems, stars with multiple-planet systems, and both, respectively. The results are summarized in Table 3.2. As it can be seen, the K-S test is not very sensitive to different sub-samples of stars with planets, while the correlation between the P and $[\text{Fe}/\text{H}]$ distributions gets more significant, especially when only single stars orbited by a single planet are taken into account. Anyhow, the two tests are in fair agreement with each other. The lack of sensitivity of the K-S test is possibly due to an intrinsic property of the test itself. In fact, the K-S test is most sensitive around the median value of a given cumulative distribution function, and less sensitive at the extreme ends of the distribution. For this reason the test probably works best in detecting shifts in a probability distribution, which will likely affect

Table 3.2. Results of the K-S and rank correlation tests on different stellar subsets

Sub-sample	$Pr(D)$	$Pr(r_s)$	N_{rich}	N_{poor}
1	0.09	0.11	86	23
2	0.09	0.11	70	21
3	0.06	0.04	64	21
4	0.03	0.01	54	19

Note. — Results of the K-S and rank correlation tests on different stellar subsets: the full sample (1), when binaries are removed (2), when stars with multiple-planet systems are removed (3), and when both binaries and stars with planetary systems are removed (4). For completeness, we also list, for each case studied, the numbers N_{rich} and N_{poor} of planets orbiting stars in the two metallicity bins ($[\text{Fe}/\text{H}] \geq 0.0$ and $[\text{Fe}/\text{H}] < 0.0$, respectively).

its median value, while it might fail to detect spreads, that would primarily affect the tails of a probability distribution rather than its median. This is quite likely our case, as the main difference between the distributions of planet orbital periods for the metal-poor and metal-rich sample resides in the very short-period regime, i.e. at one of the tails of the distribution. Note, however, that any hint of correlation disappears if one removes from the analysis the stars harbouring the Hot Jupiters with $P \leq 5$ days. For comparison, analogous K-S and rank correlation tests were performed on the planet mass distribution split in two metallicity bins, and probabilities of the null hypotheses to be the correct ones in the ranges $0.22 \leq Pr(D) \leq 0.44$ and $0.38 \leq Pr(r_s) \leq 0.87$ were obtained, respectively. In this case, similarly to the findings of Santos et al. (2003), no significant trend was revealed.

In order to further quantify the statistical significance of the results on the P – $[\text{Fe}/\text{H}]$ correlation, we have utilized Monte Carlo simulations, in a fashion similar to the analyses undertaken by Zucker & Mazeh (2002) and Mazeh & Zucker (2003) in their works on the mass-period correlation of extra-solar planets and the possible mass ratio-period ratio correlation in multiple-planet systems. We have randomly drawn 109 pairs of points (corresponding to the present total number of planets announced, with the constraints discussed above) from the *observed* log-distributions of orbital periods of the extra-solar planet sample

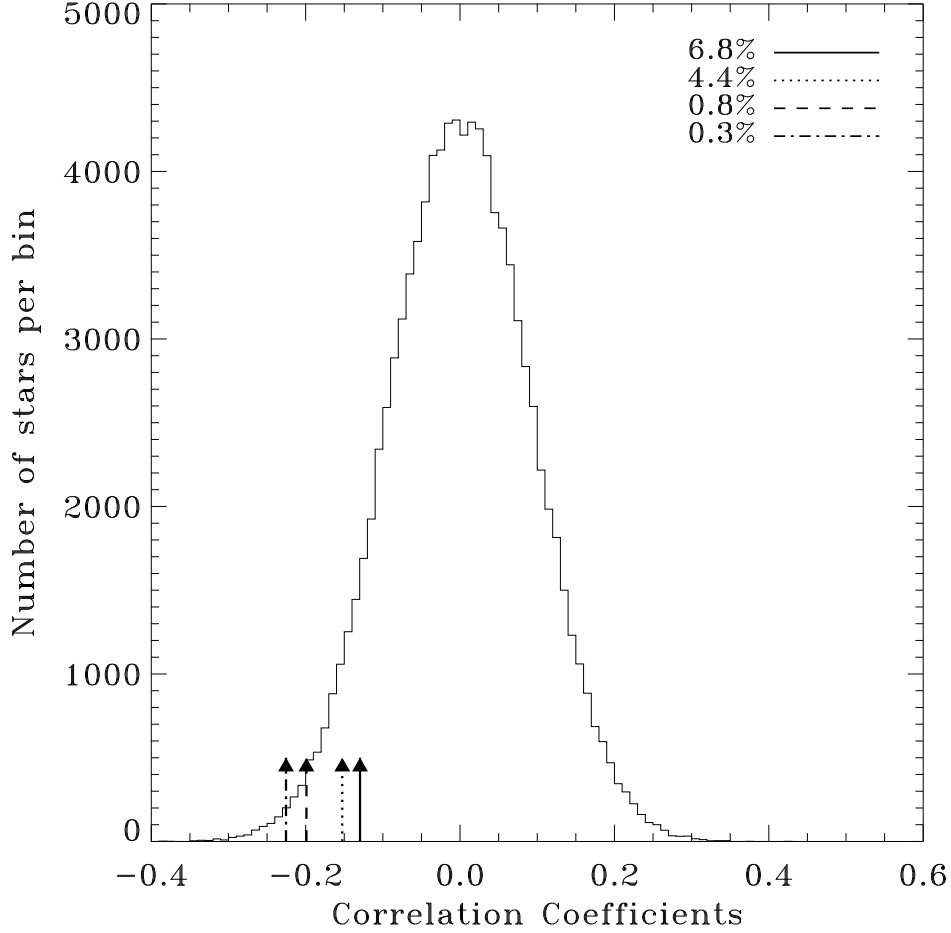


Figure 3.2 Histogram of the rank correlation coefficients calculated from 10^5 random samples drawn from the observed stellar metallicity and orbital period distributions. The observed values discussed in Section 3.2 (arrows of different styles) have between 6.8% and 0.3% chances of being consistent with no correlation

and metallicities of the host stars, and repeated the process 10^5 times, calculating the rank correlation coefficient for each simulated dataset.

In Figure 3.2 we show the histogram of the simulated values of the r_s statistics, together with the observed values we obtained for the full stellar sample and the three sub-sets defined above. As a general result, both the intrinsic probability estimates of the statistical tests and the simulations we performed agree in indicating that the null hypothesis that orbital period and metallicity distributions are uncorrelated is rejected with a confidence level in the range 93.2%-99.7%, corresponding to a 2- to 3- σ result. Indeed, the evidence for a correlation is somewhat weak, but the pile-up of very close-in planets preferably around metal-rich parent stars, if real, may have important consequences for our understanding of some crucial aspects

of the formation and migration processes of gas giant planets.

3.3 OBSERVATIONAL BIASES?

There are at least three main sources of potential observational biases in the data (see [Gonzalez 2003](#) for a thorough review of the subject): 1) there could be significant errors in the determination of the metal content of the host stars, 2) the sample of extra-solar planets around stars with $[\text{Fe}/\text{H}] < 0.0$, only 1/3 of the number of planets detected around metal-rich field dwarfs, might not be large enough for statistical analyses; and 3) metal-poor stars have weaker spectral lines with respect to solar-type dwarfs, so that they are in principle more difficult targets for high-precision radial-velocity surveys.

In the first case, all the metallicity values we utilized (see [Table 3.1](#)) have been derived by means of spectroscopic analysis methods of high-resolution, high-S/N echelle spectra. As pointed out in recent works (e.g. [Laws et al. 2003](#); [Gonzalez 2003](#), and references therein), significant systematic offsets can be found between spectroscopic and photometric $[\text{Fe}/\text{H}]$ determinations, and ultimately spectroscopic methods seem to be more reliable. With this approach, the typical uncertainties reported in abundance analyses for planet-host stars are of order of a few hundredths of a dex. Within these limits, then according to [Santos et al. \(2004a\)](#) 12 of the 14 Hot Jupiters with $P \leq 5$ days included in our sample would still orbit metal-rich stars, and the same holds for HD 330075 and BD -10 3166, according to [Pepe et al. \(2004\)](#) and [Gonzalez et al. \(2001\)](#), respectively. In conclusion, uncertainties in the $[\text{Fe}/\text{H}]$ determination can be ruled out, at least to first approximation, as possible causes of the observed correlation between extra-solar planets' orbital periods and metallicities of the parent stars. However, if the metallicities of a couple of the stars harbouring Hot Jupiters were ill-determined due for example to some unrecognized systematics and they turned out to be falling in the range $-0.2 \leq [\text{Fe}/\text{H}] \leq -0.1$, then this would significantly dilute the effect.

Secondly, due to the lower planet occurrence rate around metal-poor stars, the absence of Hot Jupiters around the metal-poor stellar sample could indicate that simply not enough objects have been observed yet in that metallicity bin. However, comparable sample sizes of

Table 3.3. Fraction of planets below a given value of period in two metallicity bins.

Period interval	[Fe/H] < 0.0	[Fe/H] ≥ 0.0
$P \leq 5$ days	0%	16% ± 4%
$P \leq 10$ days	9% ± 6%	19% ± 5%
$P \leq 15$ days	9% ± 6%	23% ± 5%
$P \leq 20$ days	13% ± 7%	24% ± 5%
$P \leq 25$ days	22% ± 8%	24% ± 5%

stars in the two metallicity bins have been monitored for several years by precision Doppler surveys (e.g. [Fischer et al. 2003b](#); [Santos et al. 2003](#)). There are 23 planets in the $[\text{Fe}/\text{H}] < 0.0$ bin, and 86 in the $[\text{Fe}/\text{H}] \geq 0.0$ bin. In the latter, 14 objects are orbiting the parent stars with $P \leq 5$ days, about $16\% \pm 4\%$ of the full sample (assuming Poisson statistics). If the occurrence rate for Hot Jupiters in the low-metallicity bin is comparable, then we should expect about 4 ± 2 planets to be orbiting with $P \leq 5$ days, but there are no detections in this period range. This is about a $2\text{-}\sigma$ deviation. As summarized in [Table 3.3](#), this difference is present up to periods of order of 20-25 days. Above this threshold, the two fractional values become the same. Furthermore if we divide the $[\text{Fe}/\text{H}] \geq 0.0$ sample in two bins, $0.0 \leq [\text{Fe}/\text{H}] \leq 0.25$ and $[\text{Fe}/\text{H}] > 0.25$, what is observed is that, for example, the occurrence rate of Hot Jupiters with $P \leq 5$ days increases by about 60% from the first to the second high-metallicity bin: there are in fact 7 such planets out of 52 ($\sim 13\% \pm 5\%$) orbiting stars with $0.0 \leq [\text{Fe}/\text{H}] \leq 0.25$, while 7 out of 34 planets ($\sim 21\% \pm 8\%$) are found on $P \leq 5$ days orbits around stars in the metallicity range $[\text{Fe}/\text{H}] > 0.25$. However, due to the limited amount of data, uncertainties are large enough that such trend is even less significant than the one observed by comparing the $[\text{Fe}/\text{H}] < 0.0$ and the $[\text{Fe}/\text{H}] \geq 0.0$ bins.

In the end, these results are further suggestive of a higher likelihood of finding giant planets on close-in orbits around increasingly more metal-rich stars. The small-number statistics argument can thus be ruled out as a major contributor to the observed P - $[\text{Fe}/\text{H}]$ correlation, but only at the $2\text{-}\sigma$ confidence level.

Finally, due to the weak spectral lines, the low-metallicity objects might have been monitored by Doppler surveys with somewhat lower velocity precision, thus a fraction of the planets might have gone undetected. [Santos et al. \(2003\)](#) and [Fischer et al. \(2003b\)](#) have

studied this possibility by calculating the median velocity error as a function of metallicity for the stars in their planet surveys, and found a velocity degradation of up to 50% for the lowest metallicity stars ($[\text{Fe}/\text{H}] \simeq -0.5$). Radial-velocity surveys currently attain typical single-measurement precisions $\sigma_{\text{RV}} \simeq 3\text{--}5$ m/s, and given the fact that the most glaring discrepancy between the orbital period distributions for planets around low- and high-metallicity is the absence of close-in planets, which would be easily detected (we recall the radial velocity amplitude $K \propto P^{-1/3}$) even with $\sigma_{\text{RV}} \simeq 5\text{--}8$ m/s, then we can conclude that also radial-velocity precision degradation for metal-poor stars is not a major cause for the observed correlation (in the long period regime the datasets typically contain observations with lower precision, say 10-15 m/s, but in this limit the two period distributions do not present any differences). However, the fine details of the observing strategies for the two stellar samples are not known exactly, and there is a non-zero chance that some bias might be introduced by human factors (e.g., less observing time spent on the metal-poor sample, more on the metal-rich sample with a higher chance of planet discovery announcements).

3.4 DISCUSSION

We have presented new intriguing evidence for a lack of planets on very short-period orbits ($P \leq 5$ days) around stars with metallicity $[\text{Fe}/\text{H}] < 0.0$, confirming early findings by Gonzalez (1998b) and Queloz et al. (2000a), and more recently by Jones (2003). As shown through statistical tests as well as Monte Carlo simulations, the $P\text{--}[\text{Fe}/\text{H}]$ correlation is moderately significant (2- to 3- σ level), and it gets stronger when only single stars orbited by single planets are considered. We have discussed a variety of possible sources of observational biases, and did not find any strong evidence of them playing a significant role in the determination of the observed correlation. However, potential biases introduced by uncertainties in the determination of the metallicities of the planet-host stars and the small-number statistics cannot be ruled out with very high confidence, thus a clear conclusion is difficult to draw at this point.

On the other hand, if this trend is real, then the paucity of short-period giant planets around metal-poor stars should be explained in principle within the scenarios of their

formation and in the context of the migration processes protoplanets are likely to undergo while embedded in the primordial protoplanetary disc. For the purpose of this analysis, we focus on the ‘cleaner’ sample of single stars orbited by single planets, which exhibits the stronger P – $[\text{Fe}/\text{H}]$ correlation, as in presence of multiple planets and/or binary stellar systems the outcome of formation and/or migration could be significantly different (e.g., [Zucker & Mazeh 2002](#), and references therein; [Mazeh & Zucker 2003](#), and references therein; [Eggenberger et al. 2004b](#), and references therein). This is however subject to change if for example a significant fraction of the present-day single-planet systems turned up to have additional long-period companions.

It is probably premature at this stage to make meaningful statements on the relative roles of the two proposed mechanisms for gas giant planet formation, i.e. core accretion (e.g., [Lissauer 1993](#); [Pollack et al. 1996](#); [Alibert et al. 2004](#)) and disc instability (e.g., [Boss 1997, 2001](#); [Mayer et al. 2002](#); [Rice & Armitage 2003](#)). As there is no reason to believe that orbital parameters distributions of giant planets formed in different ways around different stellar populations would be very similar ([Boss 2002](#)), one should in principle be able to find fossil evidence of the formation processes in such distributions. For example, the two formation mechanisms would predict quite distinct mass distributions (e.g., [Ida & Lin 2004a](#); [Rice & Armitage 2003](#)), and the dependence of planetary frequency on the metallicity of the protoplanetary disc is also expected to be rather different (e.g., [Pollack et al. 1996](#); [Boss 2002](#)). However, either because of a lack of sensitivity of present-day detection techniques at the low-mass end or in light of incompleteness of the different stellar populations targeted, no general conclusions can be drawn at present (except that maybe both mechanisms operate).

On the other hand, regardless of how giant planets formed, a significant fraction of them must have undergone some degree of orbital migration, in particular all the Hot Jupiters. Thus the observed period and eccentricity distributions of extra-solar planets, and correlations among planet orbital parameters and masses, are somewhat more likely to reflect migration-related effects, blurring the evidence in such distributions for different formation scenarios. Indeed, [Udry et al. \(2003\)](#), for example, showed that the highly non-Gaussian distribution of orbital periods is likely to be the outcome of the (Type II) migration process, and the variety of mechanisms that might trigger it, in fair agreement with theoretical pre-

dictions (see, for example, [Armitage et al. 2002](#) and references therein). Similar conclusions are also reached by [Zucker & Mazeh \(2002\)](#) to justify the evidence for a shortage of high-mass planets in short-period orbits.

The absence of planetary objects with $P \leq 5$ days around stars with $[\text{Fe}/\text{H}] < 0.0$ can also be explained within the context of migration scenarios. Again, we concentrate on models that do not consider interactions with a distant companion star or dynamical instabilities in multiple-planet systems, which might be required for explaining at most $\sim 20 - 25\%$ of the systems discovered so far (out of 108 stars with planets, 16 have a certified binary companion, 12 harbour more than one giant planet, with two of the planetary systems found orbiting one of the components of wide binary stellar systems). In the more widely accepted model of (Type II) migration in a gaseous disc, a giant planet massive enough to open a gap around itself will become locked to the disc and will ultimately share its fate (e.g., [Goldreich & Tremaine 1979](#); [Papaloizou & Lin 1984](#); [Ward 1997](#); [Trilling et al. 2002](#)). As shown by [Livio & Pringle \(2003\)](#), if disc opacity κ increases with increasing metallicity, if disc temperature T increases with increased opacity, then this leads to a higher kinematic viscosity ν , and this shortens the viscous inflow timescale τ_ν , i.e. it makes the disc evolve faster. In their work, [Livio & Pringle \(2003\)](#) assume a weak dependence of migration timescales on metallicity ($\tau_\nu \propto \nu^{-1} \propto T^{-1} \propto \kappa^{-0.34} \propto [\text{Fe}/\text{H}]^{-0.34}$), and conclude that this effect cannot account for the observed decrease in the probability of a star having giant planets in the observed range of periods as its metallicity decreases, thus a lower occurrence rate at low values of $[\text{Fe}/\text{H}]$ is indicative of lower probability of formation, not migration. However, given the uncertainties on some of the parameters describing the detailed structure of a protoplanetary disc and its evolution, and their relative dependencies, it is not inconceivable to argue for a more substantial dependence of migration rates on metallicity. Such explanation would fit the observed trend we are beginning to unveil, i.e. the much lower occurrence rate of Hot Jupiters around the metal-poor sample of stars with planets. Indeed, although not yet statistically significant, this trend seems to be present already in the metal-rich sample, with the fraction of Hot Jupiters decreasing by $\sim 60\%$ when we move from the $[\text{Fe}/\text{H}] > 0.25$ to the $0.0 \leq [\text{Fe}/\text{H}] \leq 0.25$ bin.

In conclusion, there are several ways to improve on our understanding of the complex

interplay between the observed properties of extra-solar planets (due to formation and/or migration processes) and those of the host stars.

For what concerns the possible P – $[\text{Fe}/\text{H}]$ correlation, a solid theoretical basis for its existence or absence (as pointed out by [Livio & Pringle 2003](#)) could be established if detailed high-resolution, three-dimensional, time-dependent migration computations were to be carried out, which would include a sophisticated treatment of the thermal structure of disc.

On the observational side, improvements in quantitative spectroscopic analyses due for example to better input physics (stellar atmosphere models), high-quality instrumentation, and more refined measurement and analysis software may help to further reduce the uncertainties on metallicity determination, hopefully also for stars significantly cooler or hotter, as well as more active, than our Sun. Such efforts will nevertheless have to be coupled to an enlargement of the sample-size of stars with planets. In particular, one of the most effective ways to prove or falsify the P – $[\text{Fe}/\text{H}]$ correlation and its potential consequences for orbital migration and/or giant planet formation scenarios discussed in this work would be to extend the sample size of the metal-poor population, including a statistically significant number of very metal poor ($[\text{Fe}/\text{H}] \leq -0.5$) objects. This could be achieved by combining radial-velocity (e.g., [Sozzetti et al. 2004a](#)) and high-precision astrometric searches with ground-based as well as space-borne observatories that will come on-line during the next decade or so (e.g., [Sozzetti et al. 2002](#), [Sozzetti et al. 2003a](#)).

ACKNOWLEDGMENTS

We are grateful to A. P. Boss, D. W. Latham, D. D. Sasselov and G. Torres for stimulating discussion and helpful insights. This work has greatly benefited from the comments they provided on an earlier version of this paper. We thank an anonymous referee for a careful reading of the manuscript and for very important suggestions and advice. AS acknowledges support from the Smithsonian Astrophysical Observatory (SAO) through the SAO Predoctoral Fellowship programme.

4.0 A KECK/HIRES DOPPLER SEARCH FOR PLANETS ORBITING METAL-POOR DWARFS

Alessandro Sozzetti, David W. Latham, Guillermo Torres, Robert P. Stefanik, Alan P. Boss, Bruce W. Carney, John B. Laird, 2005, *ESA-SP*, **576**, in press

4.1 INTRODUCTION

With a present-day catalogue of well over 130 extrasolar planets ¹, several important statistical properties of the sample are beginning to emerge. One of the most intriguing features unveiled so far, however, concerns the parent stars rather than the planets themselves. In particular, both the probability of a star to harbor a planet and some orbital properties of the latter appear to depend on the metallicity of the former.

The metallicity distribution of stars with planets peaks at $[\text{Fe}/\text{H}] \simeq 0.3$, showing evidence of moderate metal-enrichment with respect to the average metallicity ($[\text{Fe}/\text{H}] \simeq -0.1$) of field dwarfs in the solar neighbourhood (Santos et al. 2001; Fischer et al. 2003b; Santos et al. 2004a). The evidence for higher planetary frequency around metal-rich stars has been confirmed based on observationally unbiased stellar samples. This trend seems to agree with the predictions from theoretical models of gas giant planet formation by core accretion (Ida & Lin 2004a). However, the alternative scenario of giant planet formation by disk instability (Boss 2002) is insensitive to the primordial metallicity of the protoplanetary disk, and, although not statistically significant, the possible evidence for bi-modality of the planet frequency distribution as a function of metallicity (Santos et al. 2004a) suggests the existence of two different mechanisms for forming gas giant planets.

¹See for example <http://www.obspm.fr/encycl/encycl.html>

Furthermore, despite potential biases introduced by the small-number statistics, the orbital periods of extrasolar planets seem to correlate with the metallicity of their parent stars (Sozzetti 2004, and references therein). In particular, close-in planets, on few-day orbits, are more likely to be found around metal-rich stars. If true, the correlation could reflect a dependence of migration rates on the amount of metals present in the disk (Livio & Pringle 2003). Alternatively, it might be indicative of longer timescales for giant planet formation around metal-poor stars, and thus reduced chances for the protoplanets to undergo significant migration before the disk evaporates (Ida & Lin 2004a).

Such questions can be addressed by comparing the frequency of gas giant planets and their properties between metal-rich and metal-poor stars. However, the low-metallicity stellar sample is at present too small to test but the most outstanding differences between such hypothetical populations. It is then crucial to provide a statistically significant, unbiased sample of metal-poor stars screened for giant planets. This can be achieved by means of both Doppler (Sozzetti et al. 2004a) and astrometric (Sozzetti et al. Sozzetti et al., 2002, 2003a) surveys.

4.2 SELECTION CRITERIA OF THE SAMPLE

In this project we are using the HIRES spectrograph on the Keck 1 telescope (Vogt et al. 1994) to search for planetary companions within 1 AU orbiting a sample of 200 metal-poor dwarfs. The sample has been drawn from the Carney-Latham and Ryan samples of metal-poor, high-velocity field stars (Ryan 1989; Carney et al. 1994). The stars have been selected not to have close orbiting companions in the stellar mass regime that might hamper the formation or survival of planets (Carney et al. 2001; Latham et al. 2002).

Old stars have the advantage that they rotate slowly and have low levels of chromospheric activity. All of the stars in our sample exhibit rotational velocities $V_{\text{rot}} \leq 10$ km/s. Thus, velocity jitter due to astrophysical phenomena is not expected to be a problem for this sample. However, metal-poor stars have weak absorption lines in comparison to their solar-metallicity counterparts. The lines also grow weaker as the effective temperature rises. Furthermore, very metal-poor stars are rare, and therefore they tend to be distant and

faint. In order to characterize the behavior of the radial velocity precision as a function of stellar metallicity $[\text{Fe}/\text{H}]$, effective temperature T_{eff} , and visual magnitude V (assuming non-rotating, inactive stars), we have run simulations utilizing the CfA library of synthetic stellar spectra (Sozzetti et al. 2004a). In light of those results, we have refined our sample of 200 metal-poor dwarfs from the Carney-Latham and Ryan surveys by selecting objects in the metallicity range $-2.0 \leq [\text{Fe}/\text{H}] \leq -0.6$, and utilized the following magnitude and temperature cut-offs: $V \leq 11.5$ and $T_{\text{eff}} \leq 6250$ K.

Based on our experience with solar neighborhood G dwarfs observed with HIRES for the G Dwarf Planet Search Program (Latham 2000), we have set an initial threshold of 20 m/s precision for planet detection, and have computed the relative exposure times needed to achieve such precision, for each star in our sample.

Finally, our sample-size is large enough that a null result, i.e. no detections, would be significant. The frequency of giant planets within 1 AU around F-G-K dwarfs is $f \simeq 3\text{-}4\%$ (Santos et al. 2004a). In order for the failure to detect any planetary companions to be significant at the $3\text{-}\sigma$ level (corresponding to a probability of 0.0027), we need to survey a sample of N stars, where $(1 - f)^N = 0.0027$, which is satisfied for $N = 194 - 145$. Our sample of 200 metal-poor stars should eventually provide a robust $3\text{-}\sigma$ null result in case of no detections.

4.3 RESULTS

Our analysis pipeline encompasses the full modeling of temporal and spatial variations of the instrumental profile of the HIRES spectrograph (Valenti et al. 1995) and is conceptually similar to that described by Butler et al. (1996). This analysis technique has allowed us to significantly improve upon our initial estimates of achievable radial velocity precision. In Figure 4.1, left panel, we show the histogram of the rms velocity residuals of the first 1.5 years of precise radial velocity measurements with HIRES for about 75% of our sample. The rms velocity residuals distribution of the *full* sample (excluding variables with $\text{rms} \geq 30$ m/s) averages ~ 8 m/s. For about two dozens of the stars in our sample, in common with the G dwarf planet survey of Latham (2000), we could establish the long-term stability of

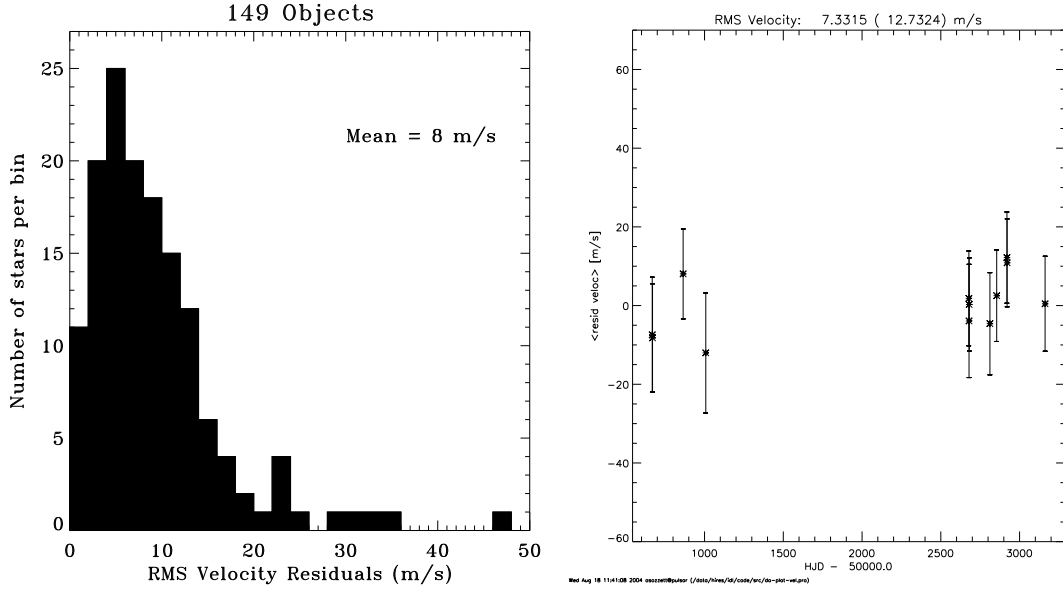


Figure 4.1 Left: rms velocity distribution for the full sample. A number of objects exhibiting significant radial velocity variations (> 50 m/s) is not shown. Right: radial velocity as a function of time for a quiet star in our sample.

the velocity zero-point over time-scales of up to seven years (Figure 4.1, right panel). This demonstrates the true radial-velocity precision we are obtaining on the sample of metal-poor stars, with a significant improvement of $\sim 60\%$ with respect to the targeted 20 m/s single-measurement precision.

The exposure times predicted by the model derived from the simulations with the CfA library of stellar spectra are determined as a function of $[\text{Fe}/\text{H}]$, T_{eff} , and V . One possible matter of concern would be the evidence of systematic trends in the rms velocity distribution

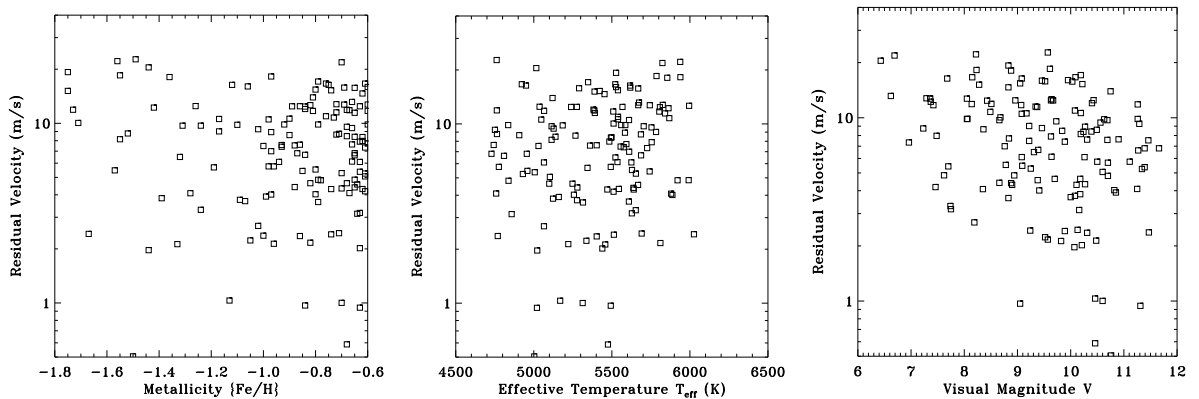


Figure 4.2 Radial velocity residuals (excluding variables) as a function of $[\text{Fe}/\text{H}]$ (left), T_{eff} (center), and V (right).

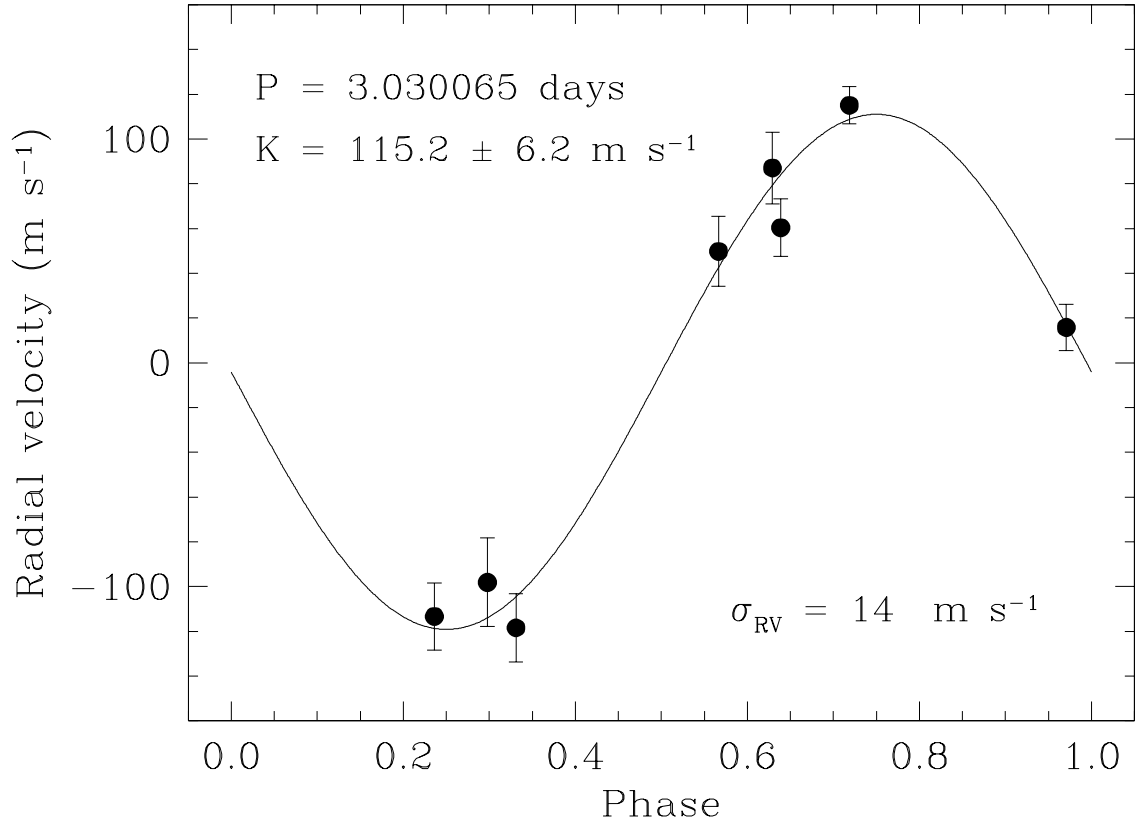


Figure 4.3 Radial velocity observations of TrES-1, overplotted with the best-fit orbit.

as a function of these three parameters. However, as shown in Figure 4.2, no clear rms velocity trends as a function of $[\text{Fe}/\text{H}]$, T_{eff} , and V are present. This gives us confidence that the model we developed for the dependence of the radial velocity precision on the above parameters is robust.

We have provided an important confirmation of our ability to derive high-precision radial velocities for stars 2 to 5 mag fainter than the typical targets in Doppler surveys of nearby stars by determining the spectroscopic orbit for the recently announced (Alonso et al. 2004b) transiting extra-solar planet TrES-1 (Figure 4.3). As recently determined by means of detailed abundance analyses (Sozzetti et al. 2004b), its parent star is a relatively cool ($T_{\text{eff}} \simeq 5250$ K), moderately faint ($V = 11.79$) solar-metallicity dwarf. The rms of the post-fit velocity residuals is ~ 14 m/s, in good agreement with the average of the internal errors. This is a remarkable result if we consider that this star is 2 mag fainter than the faintest stars with planets for which spectroscopic orbits with similar velocity precision have ever been derived.

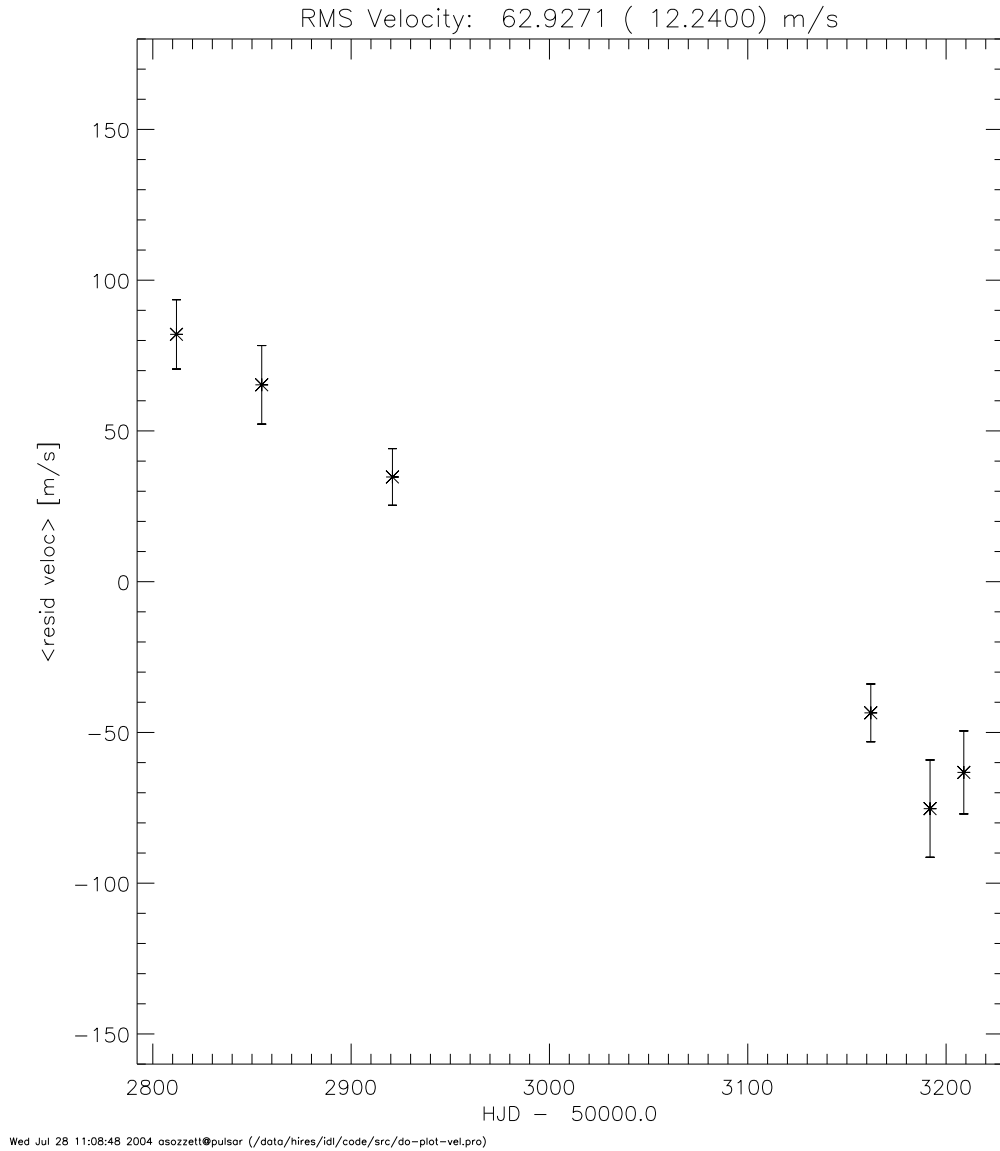


Figure 4.4 Radial velocity as a function of time for one of the variable objects in our sample.

None of the 149 metal-poor dwarfs screened for planets so far (with an average number of 5 observations per target spanning 1.5 years), exhibits short-term, low-amplitude variations. However, $\sim 7\%$ of the stars in the sample appear to be long-period candidates. In Figure 4.4 we show radial velocities as a function of time for one of the objects with a large rms velocity value. The star shown in Figure 4.4 exhibits a linear radial-velocity trend which is indicative of the existence of a companion, and thus, together with another handful of objects, will become a primary target for follow-up observations.

We have run Monte Carlo simulations to obtain a first estimate of the sensitivity of our

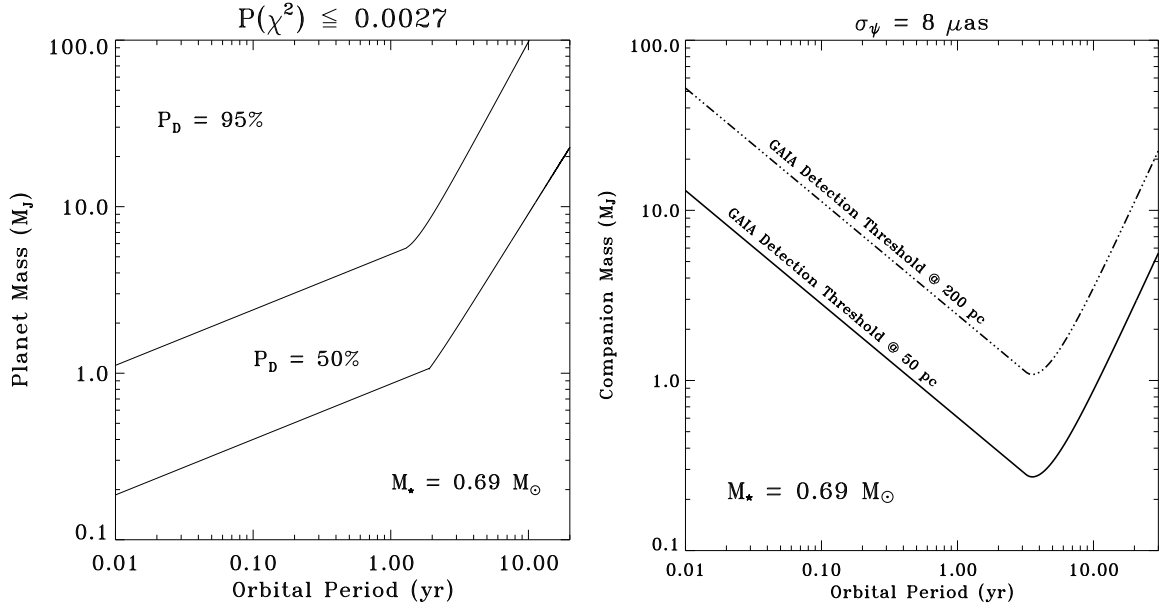


Figure 4.5 Left: detectable planet mass as a function of orbital period for the sample of 149 metal-poor stars observed so far. Right: Gaia 95% detection thresholds for bright ($V < 13$) metal-poor stars in the 50-200 pc distance range (based on the simulations of Sozzetti et al. (2003c)).

survey to planetary companions of given mass and orbital period. In Figure 4.5, left panel, we show the minimum detectable planet mass M_p as a function of orbital period P , assuming a $0.69 M_\odot$ primary (the average stellar mass of our sample) and a single-measurement precision $\sigma_{RV} = 8 \text{ m/s}$. For a typical observing strategy consisting of five observations spanning 1.5 years, the two curves identify the loci in the $M_p - P$ discovery-space diagram for 50% and 95% probability of a $3\text{-}\sigma$ detection, respectively. If present, essentially all Jupiter-sized objects on very-short periods (< 1 month) would have been detected. The data collected so far thus build toward evidence of the absence of close-in planets around metal-poor stars.

The right panel of Figure 4.5 shows the $M_p - P$ discovery space for the ESA Mission Gaia around a $0.69 M_\odot$, bright ($V < 13$) metal-poor star in the 50-200 pc distance range. A single-measurement error $\sigma_\psi = 8 \mu\text{as}$ on the one-dimensional, along-scan coordinate and a 5-yr mission lifetime are assumed. The complementarity between Doppler and astrometric measurements is clearly evident. In particular, by surveying for planets all bright metal-poor dwarfs within 150-200 pc (of order of a few thousands), Gaia will help to understand whether the lack of close-in giant planets around the old stellar population extends also to the long-period regime, thus providing a firm statistical basis in favour of the core-accretion

scenario for giant planet formation (e.g., [Ida & Lin 2004a](#)). Alternatively, the Gaia data, combined with ground-based radial-velocity monitoring, might confirm that metal-poor stars do harbor long-period giant planets (albeit at a reduced rate with respect to the metal-rich population), and thus different formation mechanisms might have to be called into play ([Boss 2002](#)) and the role of metallicity on giant planet migration rates might have to be revisited (e.g., [Sozzetti 2004](#)).

ACKNOWLEDGMENTS

A. S. gratefully acknowledges support from the Smithsonian Astrophysical Observatory through the SAO Predoctoral Fellowship program.

5.0 TRES-1: THE TRANSITING PLANET OF A BRIGHT K0V STAR

Roi Alonso, Timothy M. Brown, Guillermo Torres, David W. Latham, Alessandro Sozzetti, Georgi Mandushev, Juan A. Belmonte, David Charbonneau, Hans J. Deeg, Edward W. Dunham, Francis T. O'Donovan, Robert P. Stefanik, 2004, *The Astrophysical Journal*, **613**, L153

5.1 INTRODUCTION

Since before the discovery of the first transiting extrasolar planet ([Charbonneau et al. 2000](#); [Henry et al. 2000](#)), it has been recognized that transits provide a sensitive way to infer the existence of small bodies orbiting other stars ([Struve 1952](#)). There are now dozens of ground-based photometric searches underway that aim to detect planets of distant stars by means of their photometric signatures ([Horne 2004](#)), as well as several space projects with the same purpose ([Auvergne et al. 2003](#); [Borucki et al. 2003](#)).

Until now, the only confirmed planet detections by transits ([Konacki et al. 2003, 2004](#); [Bouchy et al. 2004](#)) have been based on the OGLE survey ([Udalski et al. 2002a, b, 2003](#)), which is performed with a telescope of 1.3m aperture. The strategy of using a moderate-aperture telescope with seeing-limited spatial resolution must be commended for its obvious successes, and moreover because the 3 OGLE planets are peculiar, having the shortest orbital periods yet known. But surveys using large telescopes suffer from the faintness of the stars with which they deal (the I magnitudes of the OGLE planet host stars range from 14.4 to 15.7). For such faint stars, the necessary follow-up observations are difficult and time-consuming, and the precision with which planetary parameters such as mass and radius can be determined is compromised.

For these reasons, we have pursued a transiting planet search organized along different lines – one that uses small-aperture, wide-field telescopes to search for transits among brighter stars. The principal challenges facing wide-field surveys such as ours are to attain adequate photometric precision in the face of spatially varying atmospheric extinction and instrumental effects. And, as in all planet-search surveys, we must implement efficient methods for rejecting the many false alarms that appear in the photometric light curves. These false alarms result almost entirely from eclipsing systems involving 2 or more stars, including grazing eclipsing binaries, small stars transiting large ones, and eclipsing binaries diluted by the light of a third star. For bright-star searches, these imposters can outnumber true planetary transits by an order of magnitude (Brown 2003). Because of the diverse nature of the false alarm sources, several kinds of follow-up observations are needed to reject them all (Alonso et al. 2004a). We report here the first transiting extrasolar planet to be detected by such a wide-field, bright-star survey. We also describe the confirmation process in some detail, as an illustration of the necessary steps in verifying that transits are caused by an object of planetary and not stellar mass.

5.2 OBSERVATIONS

Our initial photometric observations leading to the detection of a planetary transit signature were conducted using the 3 telescopes of the Trans-Atlantic Exoplanet Survey (TrES) network. These telescopes (STARE, located on Tenerife in the Canary Islands, PSST, located at Lowell Observatory, Arizona, and Sleuth, located at Mt. Palomar, California)¹ are being described individually elsewhere (Dunham et al. 2004; Brown et al. 2004). Briefly, all 3 are small-aperture (10 cm), wide-field (6°), CCD-based systems with spatial resolution of about 11 arcsec per pixel. They usually observe in red light (roughly Johnson *R* for STARE and PSST, Sloan *r* for Sleuth), and they operate in coordination, observing the same field in the sky continuously (or as nearly as possible) for typically 2-month intervals. The observing cadence at each site is roughly one image every 2 minutes, and the resulting time series are

¹See also <http://www.hao.ucar.edu/public/research/stare/stare.html> and [http://www.astro.caltech.edu/~sim\\$ftod/sleuth.html](http://www.astro.caltech.edu/~sim$ftod/sleuth.html)

later binned to 9-minute time resolution. Recent adoption of an image-subtraction algorithm (based on [Alard 2000](#)) yields photometric precision of better than 2 mmag for the brightest non-saturating stars ($R \simeq 8$), and better than 10 mmag for $R \leq 12.5$.

We designate the planet described herein as TrES-1, the first confirmed planet detected using the TrES network; we refer to the parent star by the same name, since the distinction between planet and star will be clear from context. The star’s coordinates, observed characteristics, and index numbers from various full-sky catalogs are given in [Table 5.1](#). The V and $B - V$ values come from differential photometry relative to 32 stars with B and V data in SIMBAD; R_J was obtained from observations of Landolt’s standards ([Landolt 1992](#)), and the JHK values are from the 2MASS catalog. The field containing this star was observed by 2 sites (STARE and PSST) during the summer of 2003, with STARE obtaining 49 good nights of observations and PSST 25. The Sleuth telescope was still under development at that time, and so did not observe this field.

The top panel of [Figure 5.1](#) shows the near-transit portion of the light curve of TrES-1, folded with a period of 3.030065 days. This curve is a superposition of 4 full transits and 2 partial ones, all observed with the STARE telescope. Even though the PSST telescope obtained 25 nights of good observations on the field, it observed no transits of TrES-1 in 2003. This circumstance arose because the orbital period is very nearly an integral number of days, so that for long intervals, transits can be observed only from certain longitudes on the Earth. Although data from PSST played no role in detecting the transits, its data proved essential for a correct determination of the orbital period: we rejected several candidate periods because they implied transit events that were not seen from the western US. TrES-1 is thus a graphic demonstration of the utility of a longitude-distributed network of transit-detection telescopes.

The R -band transit seen by TrES has a flat-bottomed shape, a depth of 0.023 mag, and a total duration of about 3 hr. These characteristics are consistent with expectations for a Jupiter-sized planet crossing a cool dwarf star, but both experience ([Latham 2004](#); [Charbonneau et al. 2004](#)) and theory ([Brown 2003](#)) show that they are more likely to result from an eclipsing stellar system. Multiple star systems, in which the eclipsing binary component contributes only a small fraction of the total light, are particularly insidious. Thus, TrES-1

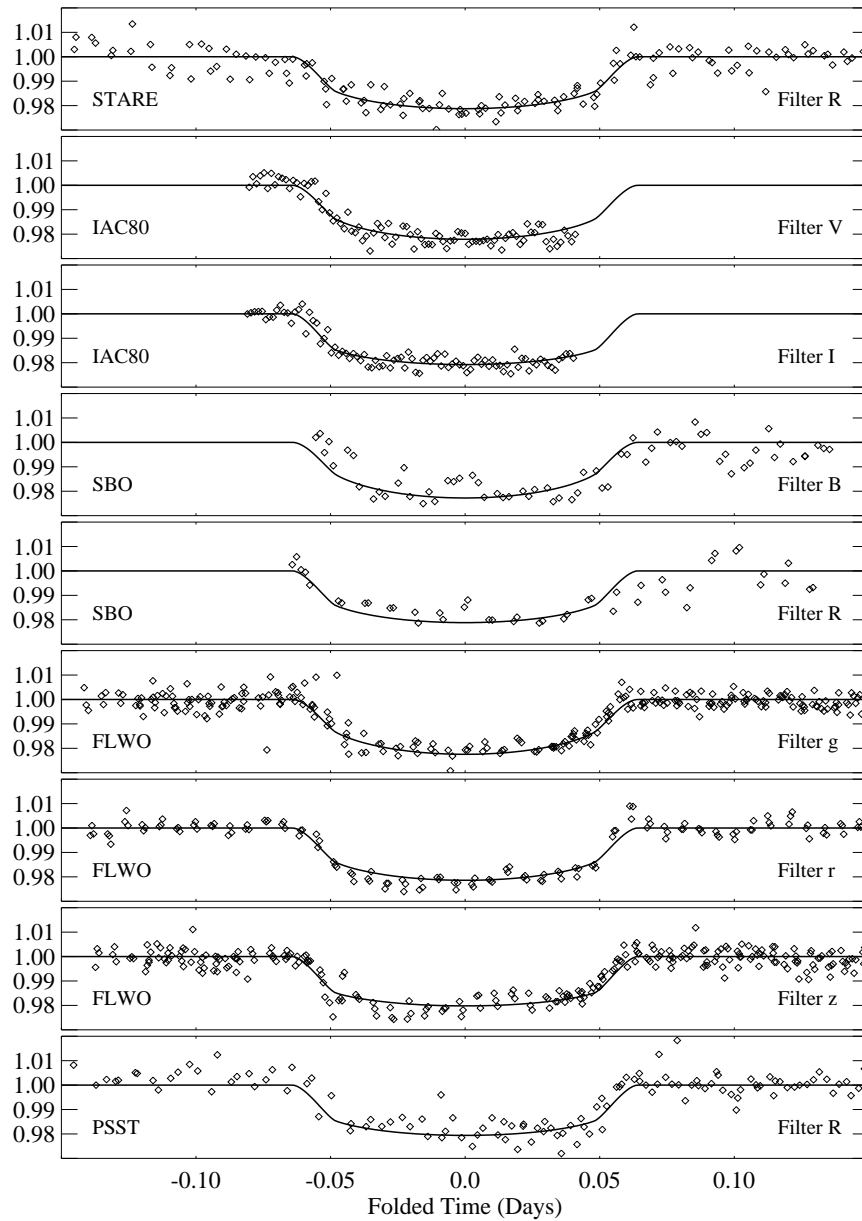


Figure 5.1 Time series photometry used in estimating the radius and inclination of TrES-1, plotted against heliocentric time modulo the orbital period from Table 5.2. The telescope and filter bandpass used are indicated on each plot. Each set of observations is overplotted with the predicted light curve for that color, given the parameters in Table 5.2.

Table 5.1. TrES-1 Parent Star

Parameter	Value
RA	19:04:09.8 (J2000)
Dec	+36:37:57 (J2000)
R	11.34
V	11.79
$B - V$	0.78
J	10.294
$J - H$	0.407
$H - K$	0.068
Spectrum	K0V
M_s	$0.88 \pm 0.07 M_\odot$
R_s	$0.85^{+0.10}_{-0.05} R_\odot$
GSC	02652-01324
2MASS	19040985+3637574

was one of 16 stars that displayed transit-like events among the 12000 stars we monitored in its surrounding field. We therefore began an extensive program of observations with larger telescopes, to determine whether the eclipses actually result from a body of planetary mass.

From Table 5.1, the $J - K$ color of 0.48 suggests a star with spectral type of late G or early K. Digitized Sky Survey images show no bright neighbors within the 20 arcsec radius of a STARE stellar image, and adaptive-optics H - and K -band imaging with the William Herschel Telescope showed no companion within 2 mag in brightness, farther than 0.3 arcsec from the primary star. With its observed V magnitude of 11.79, and ignoring interstellar extinction, the implied distance to TrES-1 is about 150 pc. Combining this distance with the USNO-B1.0 proper motion of 47 mas y^{-1} (Monet et al. 2003) gives a transverse velocity of 26 km s^{-1} , which is fairly typical for low-mass field stars in the solar neighborhood. Thus, the photometric and astrometric evidence tends to confirm that most of the detected light comes from a nearby dwarf star.

We observed the star using the CfA Digital Speedometers (Latham 1992) at 7 different epochs, giving coverage of the full orbital phase. These instruments record 4.5 nm of spectrum centered on the Mg b lines, with spectral resolution of about 8.5 km s^{-1} . For the 7 exposures spanning 60 days we determined a mean velocity of -20.52 km s^{-1} . The average internal error estimate and actual velocity rms achieved were both 0.39 km s^{-1} , suggesting

that any companion orbiting with a 3.03-day period must have a mass smaller than $5 M_{\text{Jup}}$. This conclusion is not firm, however, if there is blending light from a third component. From comparisons of our observed spectra with synthetic spectra calculated by J. Morse using Kurucz models (Morse & Kurucz, private communication), we estimate that TrES-1 has $T_{\text{eff}} = 5250 \pm 200$ K, $\log(g) = 4.5 \pm 0.5$, $v \sin i \leq 5$ km s⁻¹, and metallicity similar to that of the Sun. The slow rotation is particularly significant, for several reasons: it indicates that the star has not been spun up by tidal interactions with a massive secondary, it forecloses some blending scenarios, and it means that more precise radial velocity measurements can be obtained fairly readily.

We also obtained a moderate resolution echelle spectrum covering the entire visible wavelength range, using the Palomar 1.5m telescope. Based on the comparison of this spectrum with the spectral standards of Montes et al. (1999), we classify the star as K0V; it shows no sign of a composite spectrum nor of other peculiarities.

Many multiple-star configurations involve components with different colors, which cause the blended eclipses to have color-dependent depths. Moreover, the detailed shape of eclipse light curves provides two independent estimates of the secondary’s size, relative to that of the primary star. One of these estimates comes from the eclipse depth, and the other from the duration of the eclipse’s ingress and egress portions (Brown et al. 2001; Seager & Mallén-Ornelas 2003). Consistency between these estimates is an indication that blending with light from a third star is not important. We therefore obtained multicolor photometric observations of several transits, using larger telescopes and a variety of filters. At the IAC 80-cm telescope, we observed a partial transit (missing the egress) with Johnson *V* and *I* filters; at the University of Colorado Sommers-Bausch Observatory 61-cm telescope, we observed a full transit with Johnson *B* and *R* filters; at the CfA’s Fred L. Whipple Observatory 1.2-m telescope, we observed one full and one partial transit with Sloan *g*, *r*, and *z* filters. The PSST telescope also observed 4 transits in *R* during the 2004 season.² Figure 5.1 displays all of these observations, along with a fit to a model, which we shall discuss below. The light curves show no evidence for color dependence of the transit depth (beyond that

²The photometric and radial velocity data described in the text are available at <http://www.hao.ucar.edu/public/research/stare/data/TrES1.asc>.

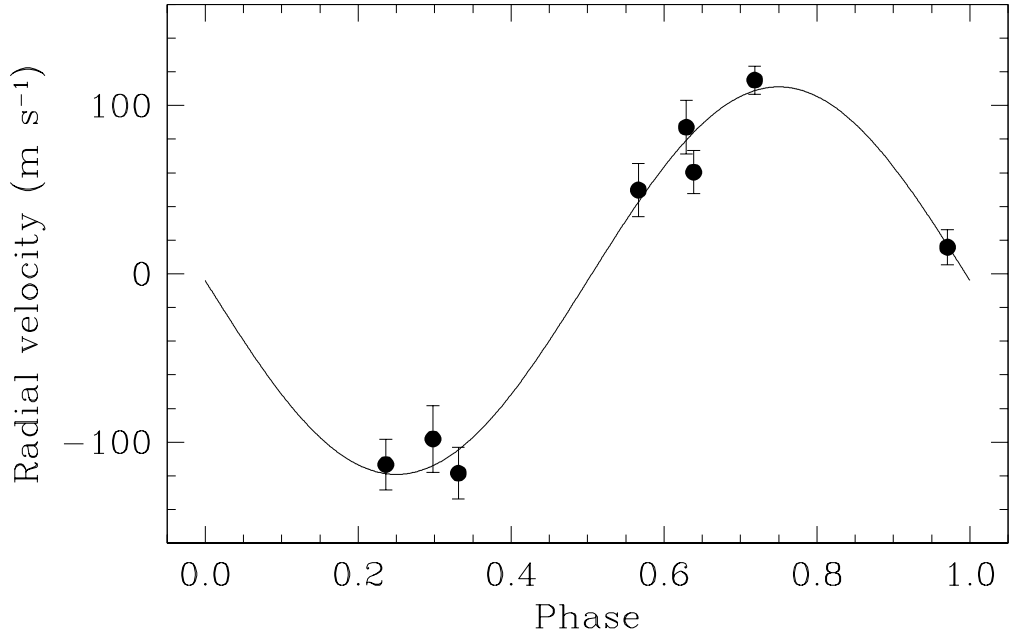


Figure 5.2 Radial velocity observations of TrES-1, overplotted with the best-fit orbit.

expected from color-dependent stellar limb darkening), and both the transit depth and the short ingress/egress times are consistent with transits by an object whose radius is a small fraction (less than about 0.15) of the primary star’s radius.

Detailed modeling of the light curves following Torres et al. (2004b) was carried out in an attempt to explain the observations as the result of blending with an eclipsing binary. We found all plausible fits to be inconsistent with constraints from the CfA spectroscopy. We conclude that TrES-1 is not significantly blended with the light of another star.

On the strength of the foregoing analysis we obtained precise radial velocity measurements using the I₂ absorption cell and HIRES spectrograph on the Keck I telescope. Eight observations were collected over a period of 18 days in July 2004, providing good coverage of critical phases. The data reduction involved modeling of the temporal and spatial variations of the instrumental profile of the spectrograph (Valenti et al. 1995), and is conceptually similar to that described by Butler et al. (1996). Internal errors were computed from the scatter of the velocities from the echelle orders containing I₂ lines, and are typically 10-15 m s⁻¹. Figure 5.2 shows the radial velocity measurements, along with a fit to a sinusoidal variation that is constrained to have the period and phase determined from the photometric data. This constrained fit matches the data well, and yields a velocity semi-amplitude of

$K = 115.2 \pm 6.2 \text{ m s}^{-1}$. The rms residual of the fit is 14 m s^{-1} , in good agreement with the average of the internal errors. Examination of the spectral line profiles in our Keck spectra by means of the bisector spans (Torres et al. 2004a) indicated no significant asymmetries and no correlation with orbital phase, once again ruling out a blend.

5.3 DISCUSSION

For purposes of an initial estimate of the planetary mass and radius, we assumed TrES-1 to have $T_{\text{eff}} = 5250\text{K}$ and solar metallicity. By comparing with the accurately-known mass and radius of α Cen B, which has a similar T_{eff} but probably higher metallicity (Eggenberger et al. 2004a), and correcting for the assumed metallicity difference of $\delta[\text{Fe}/\text{H}] = -0.2$ using evolutionary models by Girardi et al. (2000), we estimate a stellar mass $M_s = 0.88M_\odot$ and a radius $R_s = 0.85R_\odot$. We took limb darkening relations from Claret (2000) and from Claret (private communication), for models with solar metallicity, $\log(g) = 4.5$, and $T_{\text{eff}} = 5250 \text{ K}$. We assign (somewhat arbitrarily) an uncertainty of $\pm 0.07M_\odot$ to M_s . We also take $0.80R_\odot \leq R_s \leq 0.95R_\odot$, since adequate fits to the photometry cannot be obtained for stellar radii outside this range.

Using the approximate orbital period and the constraints and assumptions just described, we estimated the orbital semimajor axis a and planetary mass M_p from the observed stellar reflex velocity and Kepler’s laws. We then performed a minimum- χ^2 fit to all of the photometry (with errors estimated from the internal scatter of the input data, taken when possible from the out-of-transit data only), to obtain estimates for the planetary radius R_p and orbital inclination i , and refined estimates for the epoch of transit center T_c and for the orbital period P . Our best estimates of the planet’s orbital and physical parameters are given in Table 5.2, and the solid curves in Figures 5.1 and 5.2 show the fitted photometric and radial velocity variations overplotted on the data.

The error estimates given in Table 5.2 include errors that follow from our uncertainty in the radius and mass of the parent star (which is assumed to be a main-sequence object), as indicated in Table 5.1. These uncertainties (especially in R_s) dominate errors in the photometry as regards estimates of R_p and i . If the stellar radius and mass were known accurately,

Table 5.2. TrES-1 Planet

Parameter	Value
Orbital	
P	$3.030065 \pm 8 \times 10^{-6}$ d
T_c	2453186.8060 ± 0.0002 (HJD)
a	0.0393 ± 0.0011 AU
i	$88.5^{\circ}_{-2.2}^{+1.5}$
K	115.2 ± 6.2 m s $^{-1}$
Physical	
M_p	$0.75 \pm 0.07 M_{\text{Jup}}$
R_p	$1.08^{+0.18}_{-0.04} R_{\text{Jup}}$
R_p/R_s	$0.130^{+0.009}_{-0.003}$

the uncertainties in R_p and in i would be smaller by about a factor of 10. Contrariwise, if the star is actually a subgiant (photometric constraints notwithstanding), R_p could exceed the upper limit in Table 5.2. The error in M_p arises about equally from the radial velocity measurement precision and from our uncertainty in M_s .

The mass, orbital radius, and radiative equilibrium temperature of TrES-1 are quite similar to those of HD 209458b, yet the former planet’s radius is about 20% smaller. Indeed, as shown in Figure 5.3, the radius of TrES-1 is more similar to those of the OGLE planets, and it closely matches current models for irradiated planets without internal energy sources (Chabrier et al. 2004; Burrows et al. 2004). This discrepancy between the radii of HD 209458b and TrES-1 reinforces suspicion that HD 209458b has an anomalously large radius.

The confrontation between theory and observation for this object would be facilitated if the stellar radius and (to a lesser degree) mass could be better constrained. We are undertaking a careful study of the Keck spectra of TrES-1, and we will report improved estimates of the stellar parameters derived from them in a later paper. In the long run, however, a better approach is to obtain improved observations. With spaceborne photometry, one can achieve low enough noise to fit for both the planetary and the stellar radius (Brown et al. 2001). Though one still requires a guess for M_s , the derived planetary properties are much less sensitive to this parameter than they are to R_s . Similarly, an accurate parallax

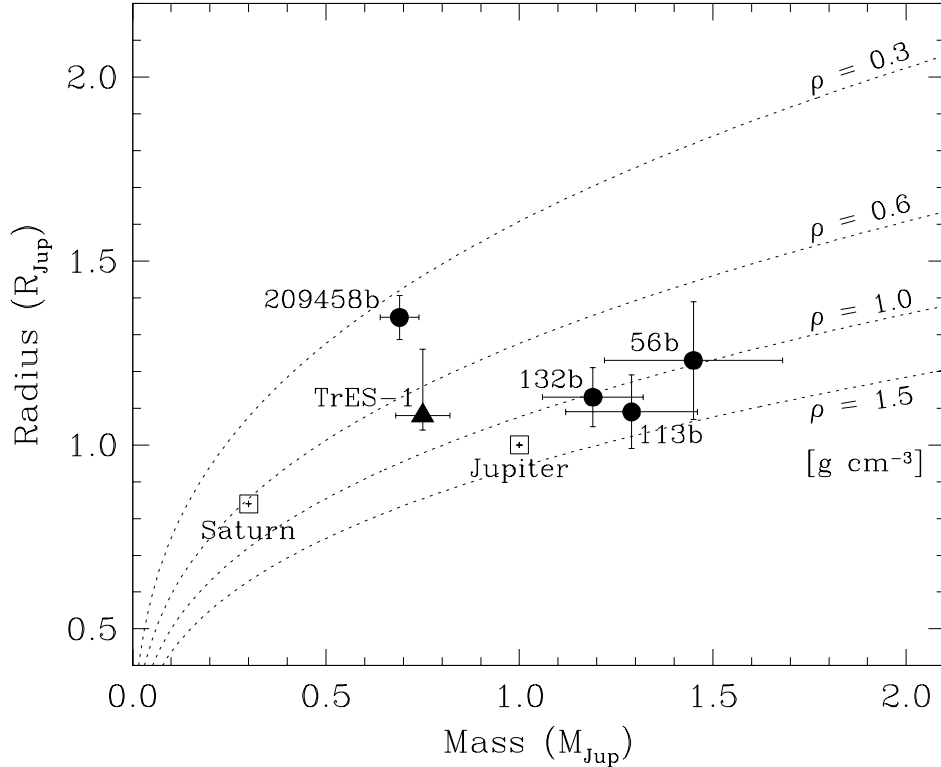


Figure 5.3 Radii of transiting extrasolar planets plotted against their masses. Dashed curves are lines of constant density. Data are from Brown et al. (2001) for HD 209458b, Torres et al. (2004a) for OGLE-TR-56, Bouchy et al. (2004) and Konacki et al. (2004) for OGLE-TR-113, Moutou et al. (2004) for OGLE-TR-132, and the present work for TrES-1.

measurement would imply a useful constraint on R_s . Thus, TrES-1 may be an attractive target for either ground- or space-based interferometric astrometry, since it is relatively bright ($K = 9.8$), and it has several neighbors of similar brightness within a radius of a few arcminutes.

ACKNOWLEDGMENTS

We thank the students and staff of many observatories for their assistance in obtaining the data needed for this study. At FLWO, we thank Perry Berlind, Mike Calkins, and Gil Esquerdo; at the Oak Ridge Observatory, Joe Caruso, Robert Davis, and Joe Zajac; at Iza?a/Tenerife, Cristina Abajas, Luis Chinarro, Cristina D?az, Sergio Fern?ndez, Santiago L?pez, and Antonio Pimienta; at SBO, Christine Predaina, Lesley Cook, Adam Ceranski, Keith Gleason, and John Stocke. We also thank A. Claret for computing limb-darkening coefficients for the Sloan filter set and J. Morse for helping with models for stellar classifica-

tion. Partial support for some of this work was provided through NASA's Kepler Project, W. Borucki, principal investigator. The IAC 80 m telescope is operated by the Instituto de Astrofísica de Canarias in its Observatorio del Teide. This publication makes use of data products from 2MASS, which is a joint project of the University of Massachusetts and the Infrared Processing and Analysis Center/California Institute of Technology, funded by the National Aeronautics and Space Administration and the National Science Foundation. Some of the data presented herein were obtained at the W. M. Keck Observatory, which is operated as a scientific partnership among the California Institute of Technology, the University of California, and the National Aeronautics and Space Administration. The Observatory was made possible by the generous financial support of the W. M. Keck Foundation.

6.0 HIGH-RESOLUTION SPECTROSCOPY OF THE TRANSITING PLANET HOST STAR TRES-1

Alessandro Sozzetti, David Yong, Guillermo Torres, David Charbonneau, David W. Latham, Carlos Allende Prieto, Timothy M. Brown, Bruce W. Carney, John B. Laird, 2004, *The Astrophysical Journal*, **616**, L167

6.1 INTRODUCTION

The discovery of an extra-solar Jupiter-sized planet transiting the disk of the K0V star TrES-1 ([Alonso et al. 2004b](#)) has marked the first success of ground-based photometric surveys targeting large areas of the sky with small-size telescopes searching for low-amplitude periodic variations in the light curves of bright stars ($V \leq 13$). In this Letter we report on a detailed spectroscopic determination of the stellar parameters and chemical abundances of iron and lithium of the transiting planet host star.

TrES-1 is only the second transiting planet orbiting a star bright enough to allow for a variety of follow-up analyses similar to those conducted for HD 209458b (see, for example, [Charbonneau 2004](#) and references therein). In particular, high-resolution, high signal-to-noise ratio spectroscopic observations of TrES-1 can be readily conducted, allowing for improved values of the effective temperature, surface gravity, and metallicity of the star. These parameters, when compared with stellar evolution models, provide the means to derive good estimates of its mass and radius. Finally, by combining spectroscopic observations with transit photometry it is possible to determine refined estimates of the mass and radius of the planet. A better knowledge of these parameters offers the tantalizing possibility for crucial tests of giant planet formation, migration, and evolution. In addition, the hypothesis

of self-enrichment due to recent ingestion of planetary material can be tested using detailed abundances of elements such as lithium.

6.2 DATA REDUCTION AND ABUNDANCE ANALYSIS

The spectroscopic observations which led to the radial-velocity confirmation of the planetary nature of the transiting object detected by the TrES (Trans-atlantic Exoplanet Survey) consortium (Alonso et al. 2004b) were performed with the HIRES spectrograph and its I₂ absorption cell on the Keck I telescope (Vogt et al. 1994). Eight star+iodine spectra and one template spectrum were collected over 18 days in July 2004. The template spectrum used here has a resolution $R \simeq 65,000$ and a signal-to-noise-ratio $S/N \simeq 80 \text{ pixel}^{-1}$. Three $R \simeq 60,000$ spectra were taken with the High Resolution Spectrograph (HRS; Tull 1998) on the Hobby-Eberly Telescope (HET) during consecutive nights in August 2004, with spectral coverage in the range 5879-7838 Å. The averaged spectrum has $S/N \simeq 120 \text{ pixel}^{-1}$. For all spectra, Thorium-Argon lamp exposures provided the wavelength calibration.

Our abundance analysis of the Keck/HIRES and HET/HRS spectra of TrES-1 was carried out under the assumption of local thermodynamic equilibrium (LTE) using a modified version of the spectral synthesis code MOOG (Snedden 1973) and a grid of Kurucz (1993) stellar atmospheres. We selected a set of 30 Fe I and 4 Fe II lines (with lower excitation potentials $0.86 \leq \chi_l \leq 5.03 \text{ eV}$ and $2.58 \leq \chi_l \leq 3.90 \text{ eV}$, respectively) from the HIRES spectrum, and used standard packages in IRAF to derive equivalent widths (EWs) for all of them. Our selection of lines and transition probabilities followed that of Lee & Carney (2002).

6.3 STELLAR PARAMETERS

Alonso et al. (2004b) report on the analysis of 7 spectra of TrES-1 taken with the CfA Digital Speedometers (Latham 1992). By comparing them with a library of synthetic spectra they derive estimates of the effective temperature, surface gravity, and metallicity as follows: $T_{\text{eff}} = 5250 \pm 200 \text{ K}$, $\log g = 4.5 \pm 0.5$, $[\text{Fe}/\text{H}] \sim 0.0$. As the authors later point out in their

discovery paper, these relatively large uncertainties have a significant impact on the final estimates of the mass and radius of the transiting planet, and ultimately on the possibility to confront theory with observation. We describe below the four-fold strategy we have devised to better constrain the stellar and consequently planetary parameters, based on a detailed analysis of our Keck and HET spectra.

6.3.1 Atmospheric Parameters from Spectroscopy

The stellar atmospheric parameters for TrES-1 were obtained using a standard technique of Fe ionization balance (see, for example, Santos et al. 2004a and references therein). The best-fit configuration of the parameters is obtained by means of an iterative procedure that encompasses the following three steps: *a*) the effective temperature is obtained by imposing that the abundances $\log \varepsilon(\text{Fe I})$ obtained from the Fe I lines be independent of the lower excitation potential χ_l (i.e., zero correlation coefficient); *b*) the microturbulent velocity ξ_t is determined so that $\log \varepsilon(\text{Fe I})$ is independent of the reduced equivalent widths EW_λ/λ ; *c*) the surface gravity is determined by forcing exact agreement between abundances derived from the Fe II and those obtained from the Fe I lines. Uncertainties in the parameters were estimated following the prescriptions of Neuforge & Magain (1997) and Gonzalez & Vanture (1998), and rounded to 25 K in T_{eff} , 0.1 dex in $\log g$, and 0.05 km s⁻¹ in ξ_t .

The final atmospheric parameters, along with the best-fit Fe I abundances, are: $T_{\text{eff}} = 5250 \pm 75$ K, $\log g = 4.6 \pm 0.2$, $\xi_t = 0.95 \pm 0.1$ km s⁻¹, and $[\text{Fe}/\text{H}] = 0.00 \pm 0.09$. Including in the analysis EWs of 11 Fe I and 4 Fe II lines measured in the region of the HRS averaged spectrum in common with the Keck template spectrum gave identical results. The good agreement between the HIRES-only and HIRES+HRS analysis suggests that significant sources of systematic errors due to different spectrographs/configurations are absent. Our spectroscopic estimates of T_{eff} , $\log g$, and $[\text{Fe}/\text{H}]$ also agree remarkably well with the numbers reported by Alonso et al. (2004b).

Finally, a possible matter of concern are systematic uncertainties inherent to the 1-D, LTE model atmospheres used in the derivation of effective temperature and metallicity for a star as cool as TrES-1. However, recent studies (Yong et al. 2004) argue that non-LTE effects

arise primarily in stars significantly cooler than TrES-1, and with metallicities significantly departing from solar (e.g., [Asplund 2003](#) and references therein).

6.3.2 T_{eff} Estimate from Photometry

There is no direct distance estimate for TrES-1, and this prevents the determination of an absolute luminosity. In addition, as the star does not show signs of evolution off the main sequence, the surface gravity constitutes a poor constraint for the models. The effective temperature and metallicity, together with an age estimate as we discuss below, are thus the only reliable metrics that can be used in the comparison with theoretical isochrones. It is then crucial to provide an independent estimate of T_{eff} for an assessment of the validity of its spectroscopic value and uncertainty.

To this end, we utilized the *BVJHK* apparent magnitudes to derive several T_{eff} estimates based on a number of empirical color-temperature calibrations from the literature. The Johnson *B* and *V* magnitudes for TrES-1 were obtained by means of differential photometry (including differential extinction) relative to a number of nearby stars (Mandushev, private communication). For the apparent luminosity in the infrared filters we relied upon the 2MASS catalog. From these values, and their relative uncertainties, we derived empirical T_{eff} estimates based on the color-temperature calibrations of Martínez-Roger et al. (1992), Alonso et al. (1996), and Ramírez & Meléndez (2004). We obtained an average value for the effective temperature of $T_{\text{eff}} = 5206 \pm 92$ K. This result is in good agreement with our own spectroscopic T_{eff} determinations reported in the previous Section, giving us confidence in the spectroscopically determined T_{eff} from Keck and HET.

6.3.3 Stellar Activity and Age

Inspection of the Ca II H and K lines in the HIRES spectra revealed a slight core reversal, indicating that TrES-1 is an active star. In Figure 6.1 we show a region of the HIRES template spectrum centered on the Ca II H line. For comparison, we have overplotted the spectrum of an old, inactive star (HIP 86830) with the same temperature from the Sozzetti et al. (2004c) sample of metal-poor stars, which has a metallicity of $[\text{Fe}/\text{H}] = -0.68$. The

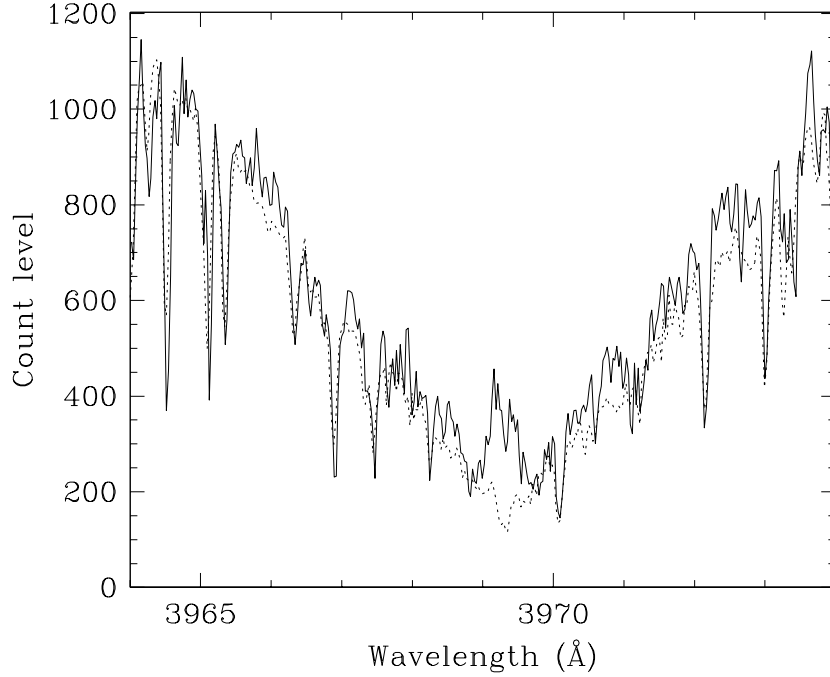


Figure 6.1 Comparison between the Ca II H line for TrES-1 (solid line) and an inactive star of the same temperature (dotted line)

emission feature is clearly evident. A possible explanation for the activity level is that the star is not very old. To provide useful constraints on its age, we have collected three different pieces of external evidence.

First, we have measured the chromospheric activity index S from the Ca H and K lines, based on the prescriptions by Duncan et al. (1991), for TrES-1 and for two Hyades stars (HD 28462 and HD 32347) of the same spectral type observed in the context of the G-dwarf Planet Search program (Latham 2000). We transformed our S values to the standard Mount Wilson S index applying the relation derived by Paulson et al. (2002). We then applied relations from Noyes et al. (1984, and references therein), to convert to the chromospheric emission ratio R'_{HK} and to derive estimates of the age t for the three stars. We obtained $\log R'_{\text{HK}} = -4.77$ for TrES-1. The activity levels for the two Hyades stars are in excellent agreement with the values reported by Paulson et al. (2002), giving us confidence that our R'_{HK} for TrES-1 is reliable. As its activity level is about half that of the two Hyades members, but higher than that reported for its very close analog α Cen B ($\log R'_{\text{HK}} = -4.92$; Chmielewski 2000), we can argue that TrES-1 is older than Hyades stars of the same spectral type, but younger than α Cen B (~ 4.2 Gyr; Henry et al. 1996). Indeed, based on the Noyes

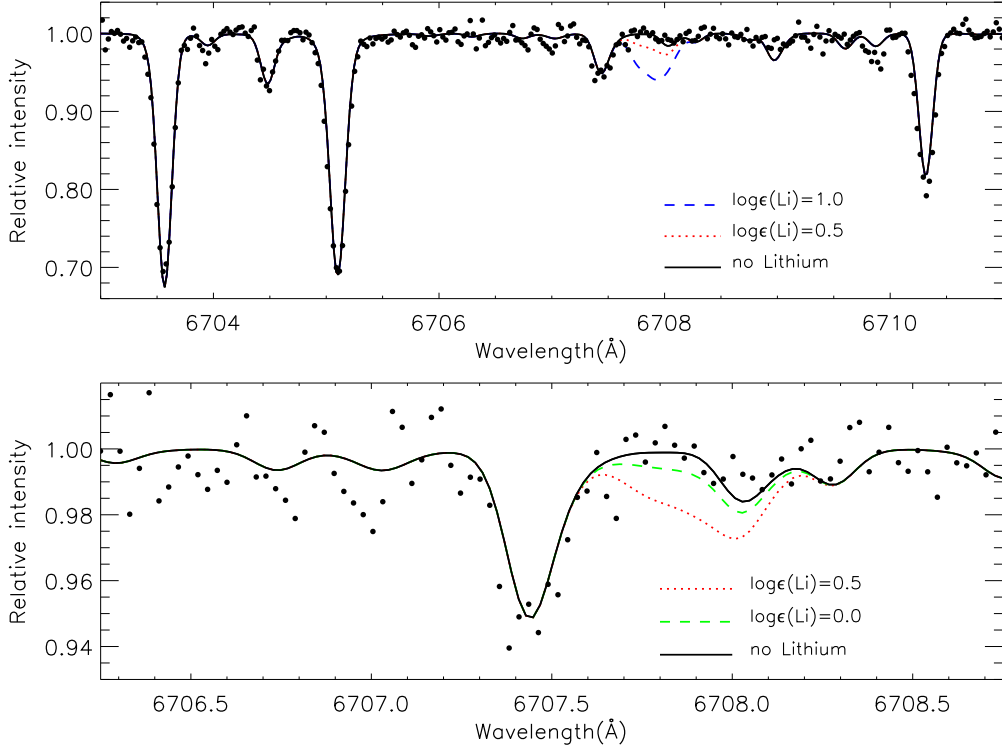


Figure 6.2 A portion (upper panel) of the HET averaged spectrum of TrES-1 containing the Li I line at 6707.8 Å (filled dots), compared to three syntheses (lines of various colors and styles), each differing only for the lithium abundance assumed. The bottom panel shows the data on an enlarged scale, so the model spectra for low Li abundance can be distinguished

et al. (1984) relations, we find an age value $t = 2.5$ Gyr. We note, however, that our measure of R'_{HK} is based on a single-epoch observation, thus additional Ca II measurements are clearly encouraged.

Secondly, following Gonzalez (1998a), using the atmospheric parameters derived from the Fe-line analysis, we synthesized a 10 Å region of the spectrum including the 6707.8 Å Li line in the HRS averaged spectrum. In Figure 6.2 we show the comparison of the spectrum of TrES-1 with three models, each differing only in the Li abundance assumed. The lithium line is not detectable by eye in the noise. We place an upper limit for the Li abundance of $\log \epsilon(\text{Li}) < 0.1$, consistent with the star being older than a Hyades star of the same temperature.

Finally, due to a fast decrease in activity levels for ages greater than ~ 1 Gyr (Pace & Pasquini 2004), at ~ 2 Gyr the emission in Ca II is down by a factor of a few with respect to the Hyades, and the value of R'_{HK} for TrES-1 is consistent with this interpretation. Our

preliminary age estimate for TrES-1 is then 2.5 ± 1.5 Gyr.

6.3.4 Stellar Mass and Radius

Using the constraints described above on T_{eff} , $[\text{Fe}/\text{H}]$, and the age of the star, we used stellar evolution models and ran Monte Carlo simulations to infer the stellar mass and radius for TrES-1 as well as their uncertainties. The simulations were repeated using two different evolutionary models: Girardi et al. (2000) and Yi et al. (2003). We obtain very good agreement in the derived parameters in both cases, to within 0.01 solar units in both mass and radius, despite slightly different assumptions in the input physics of these two sets of models. We report here the results for TrES-1 using the Girardi et al. (2000) models: $M_{\star} = 0.89 \pm 0.05 M_{\odot}$, $R_{\star} = 0.83 \pm 0.05 R_{\odot}$. These error bars include a somewhat arbitrary contribution of 0.04 added in quadrature to the formal Monte Carlo errors of 0.03 in both mass and radius, to account for unforeseen systematics in both the stellar evolution and stellar atmosphere models, as well as other physical assumptions. The uncertainties on metallicity and effective temperature contribute about equally to the errors on both mass and radius, while the age uncertainty contributes negligibly.

Finally, based on our simulations, we estimate an absolute magnitude $M_v = 5.85 \pm 0.15$, and thus place TrES-1 at a nominal distance $d \simeq 150$ pc. Its resulting galactic velocity vector is $[U, V, W] = [-15, -33, 16]$ km s⁻¹.

6.4 PLANETARY PARAMETERS

Following Alonso et al. (2004b), we utilized the revised values of M_{\star} and R_{\star} , and their uncertainties, in a new χ^2 minimization procedure of the photometric points for the model light curve as a function of R_p and i . We find $R_p = 1.04^{+0.08}_{-0.05} R_J$, and $i = 89^{\circ}.5^{+0.5}_{-1.3}$. The values and uncertainties for the primary mass, inclination, and the radial velocity semi-amplitude are then combined to give a value of the planetary mass $M_p = 0.76 \pm 0.05 M_J$. With the improved value of the stellar mass, now the dominant contribution to the planet mass uncertainty comes from the spectroscopic orbit, while the contribution due to the error

in the inclination angle is negligible.

While the revised value for M_p is essentially identical to the one reported by Alonso et al. (2004b), the planetary radius found here is slightly smaller, due to the smaller stellar radius estimate obtained in our analysis.

6.5 SUMMARY AND DISCUSSION

We have derived new values of the stellar atmospheric parameters of the transiting planet host-star TrES-1 from high-resolution, high S/N spectra. Our spectroscopic T_{eff} values are in very good agreement with empirical color-temperature calibrations and with the estimates reported by Alonso et al. (2004b). The star is a main-sequence object with a metallicity consistent with solar. The lack of detectable lithium argues both against youth and recent pollution events due to ingestion of planetary material. Its measured Ca II activity levels are further suggestive of an object with an age of a few Gyr, an intermediate value between the Hyades and α Cen B.

Based on the new constraints on atmospheric parameters and age, we have significantly improved on the determination of the stellar and planetary mass and radius. Our updated values for M_\star and R_\star are consistent with those reported by Alonso et al. (2004b), although we find a slightly smaller radius and a slightly larger mass. The most significant improvement comes at the level of the determination of R_p and M_p with our new analysis of the transit photometry. In Figure 6.3 we show masses and radii for all transiting planets known to-date, including TrES-1. Thanks to the more accurate values of the stellar parameters, the radius and mass of the planet have reduced uncertainties with respect to those reported by Alonso et al. (2004b). In particular, for very similar values of M_p , the difference between the values of R_p for HD 209458 and TrES-1, about 25%, is now significant at the $3\text{-}\sigma$ level.

The well-determined radius of TrES-1 opens the door to new important tests of theoretical evolutionary models of irradiated extrasolar giant planets (Bodenheimer et al. 2003; Burrows et al. 2004; Chabrier et al. 2004), as its parent star is about 1000 K cooler than HD 209458 and OGLE-TR-56, the other two objects that have recently been targets of extensive investigations. Its radius seems to agree better with the predictions from models that do not

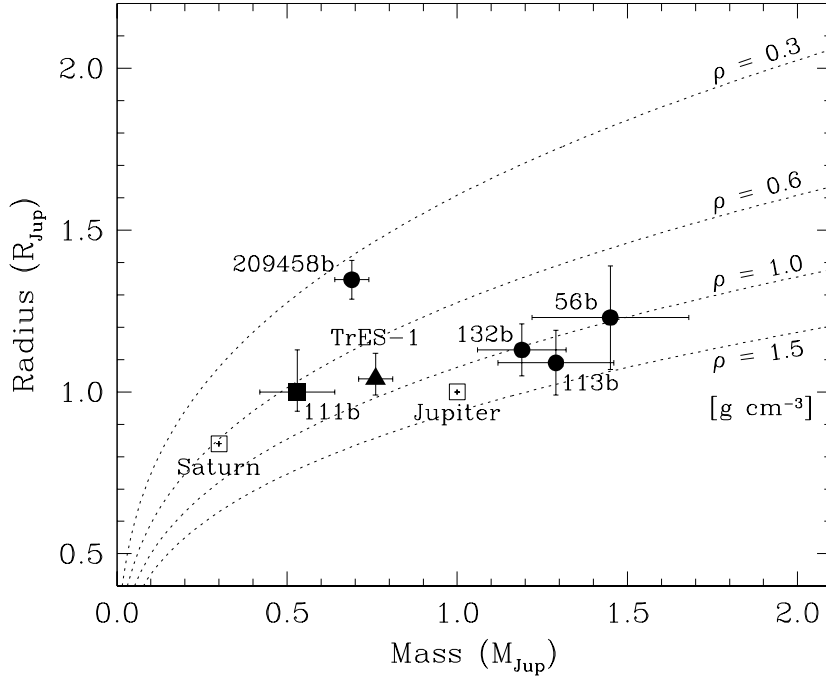


Figure 6.3 Radius vs. mass for the sample of transiting extrasolar planets discovered to-date, including TrES-1 (this work). The values and uncertainties are taken from Brown et al. (2001) for HD 209458b, Torres et al. (2004a) for OGLE-TR-56b, Bouchy et al. (2004) for OGLE-TR-113b, Moutou et al. (2004) for OGLE-TR-132b, and Pont et al. (2004) for OGLE-TR-111b.

invoke additional heat/power sources in the core (Showman & Guillot 2002; Baraffe et al. 2003), or tidal heating effects due to the gravitational perturbation of an undetected long-period companion (Bodenheimer et al. 2003). Given its orbital radius and the characteristics of the host star, its mass loss rate (Baraffe et al. 2004) is also likely to be significantly reduced with respect to those, for example, expected for OGLE-TR-56b and OGLE-TR-132b.

Additional detections of giant planets transiting relatively bright stars covering a range of spectral types are clearly necessary for a continued improvement of our understanding of the structure and evolutionary properties of this peculiar class of objects.

ACKNOWLEDGMENTS

Over the course of this investigation, we have benefited from stimulating discussions with various colleagues, in particular, G. Mandushev, R. Alonso, H. Deeg, J. Belmonte, E. Dunham, and F. O'Donovan. We are thankful to the Director of the McDonald Observatory, D. Lambert, for providing Director's discretionary time and to the HET staff, in particular

S. Odewahn, V. Riley, and M. Villareal, for their assistance. The Hobby-Eberly Telescope is operated by the McDonald Observatory on behalf of the University of Texas at Austin, Pennsylvania State University, Stanford University, Ludwig Maximilians Universität München, and Georg August Universität Göttingen. Some of the data presented herein were obtained at the W. M. Keck Observatory, which is operated as a scientific partnership among the California Institute of Technology, the University of California, and the National Aeronautics and Space Administration

7.0 THE SEARCH FOR PLANETARY SYSTEMS WITH SIM

Alessandro Sozzetti, Stefano Casertano, Robert A. Brown, Mario G. Lattanzi, 2003, *Publications of the Astronomical Society of the Pacific*, **115**, 1072

7.1 INTRODUCTION

After more than thirteen years of precise radial velocity measurements, today there is clear evidence that several nearby solar-type stars harbor candidate planetary systems, composed of two or more planets (Butler et al. 1999; Marcy et al. 2001b; Mayor et al. 2001; Jones et al. 2002; Fischer et al. 2002b; Marcy et al. 2002; Fischer et al. 2003a; Butler et al. 2003), or a planet and a probable brown dwarf (Marcy et al. 2001a; Udry et al. 2002)

The answers provided by these discoveries have presented even more challenging puzzles to theoretical models aimed at describing the formation and evolution of planetary systems. The variety of orbital arrangements in multiple-planet systems found by spectroscopy calls into question both the origin and early dynamical evolution of such systems, in terms of formation mechanisms and orbital migration scenarios, as well as their long-term dynamical evolution and stability. Early attempts have been made to connect and relate the early stages of their formation to their presently observed orbital properties. For example, the two planets orbiting the M4V star Gliese 876 appear to be locked in a 2:1 resonance, and the existence of such commensurabilities may be considered important evidence of possible inward migration for pairs of planets due to mutual interactions as well as tidal interaction with the protoplanetary disk during and shortly post-formation (Snellgrove et al. 2001; Nelson & Papaloizou 2002). Similarly, the three-planet system around the F8V star ν Andromedæ (ν And) appears to be stable over evolution timescales of order of the star's lifetime, again sug-

gesting the possibility that the system's orbits were shaped by the interaction of protoplanets with the protoplanetary disk, in the first few million years of ν And's existence (Artymowicz 2001). Furthermore, in many of the observed multiple-planet systems the eccentricities are much larger than those of the planets of our own solar system. Again, this may be explained with significant eccentricity evolution due to mutual interaction between planets as well as with the protoplanetary disk during the epoch of disk depletion (Chiang et al. 2002; Nagasawa et al. 2003). However, direct extrapolations from the early stages of their formation to the presently observed configurations of extra-solar planetary systems are still somewhat speculative. Today, in fact, there is still a lack of observational support to the theoretical models describing the early epochs of the formation of planetary systems, either because of the objective difficulty to identify good targets among very young stellar objects (often completely obscured by circumstellar material) or due to insufficient sensitivity of the present generation of ground-based and space-borne instrumentation. Thus, theorists have focused primarily on the issues of long-term stability and orbital evolution of extra-solar planetary systems, independent on the details of their formation.

Since Newton's discovery of the law of universal gravitation, the problem of predicting the orbits of the planets in our own solar system has been tackled by many giants of mathematics (Euler, Laplace, Jacobi, Lagrange, Gauss, Poincaré). By the end of the nineteenth century, it had been demonstrated that it is not possible to find an exact analytic solution describing the motion of N bodies, for $N \geq 3$, and the theory of perturbations in celestial mechanics was developed and extensively applied to many interesting cases, always within the boundaries of our solar system. During the two last decades, with the advent and exponential progress of computer technology, large-scale computations that follow the full evolution of the nine planets for a significant fraction of the lifetime of the Sun became possible. This has allowed the establishment of, for example, the long-term chaotic behavior of the orbits of planets in the solar system (Sussman & Wisdom 1992). In fact, the typical (Lyapunov) timescale for exponential divergence of two orbits in the solar system starting with slightly different initial conditions is only several million years, and soon the issue of stability only becomes a statistical question. The planetary orbits in the solar system are on the other hand stable, in the sense that the probability of ejections or close encounters during a time frame comparable

to the main-sequence lifetime of the Sun (~ 12 Gyr) is extremely low.

However, until the first multiple-planet system was announced (Butler et al. 1999), the problem of planetary orbits dynamics had in recent years been almost relegated to the level of an academic pursuit. Now that a variety of additional systems, with a wide range of different orbital arrangements, has been found, the field of planetary system dynamics has received revived interest. The long-term dynamical evolution of the 11 extra-solar planetary systems known to date has been extensively investigated by theorists, utilizing both direct numerical integrations and approximate analytical approaches for the description of the N-body mutual interactions. As opposed to our own solar system, or the three-planet system discovered by Wolszczan & Frail (1992) around the pulsar PSR 1257+12, both appearing dynamically stable over long timescales (Laskar 1994; Gladman 1993), the dynamical evolution and long-term stability issues for the majority of the multiple-planet systems discovered by radial velocity are highly uncertain. As a general result, studies specifically targeted to gauge the general dynamical behavior of extra-solar planetary systems such as ν And (Laughlin & Adams 1999; Rivera & Lissauer 2000; Stepinski et al. 2000; Jiang & Ip 2001; Barnes & Quinn 2001; Chiang et al. 2001; Lissauer & Rivera 2001; Chiang & Murray 2002), 55 Cancri (55 Cnc; Novak et al. 2004; Ji et al. 2003), 47 Ursæ Majoris (47 UMa; Goździewski 2002; Laughlin et al. 2002), Gliese 876 (Kinoshita & Nakai 2001; Laughlin & Chambers 2001; Rivera & Lissauer 2001; Ji et al. 2002; Goździewski et al. 2002; Lee & Peale 2002, 2004), HD 82943, HD 37124, HD 12661, HD 38529, and HD 160691 (Goździewski & Maciejewski 2001; Kiseleva-Eggleton et al. 2002; Goździewski & Maciejewski 2003; Goździewski & Maciejewski, 2003b), come to the same conclusion: the stability of the systems can be greatly affected by small variations of the instantaneous orbital elements of the planetary orbits obtained from the radial velocity data and utilized as initial conditions for the numerical integrations. In particular, for the systems not to be destabilized and disrupted on very short timescales (as short as 10^3 - 10^5 years), constraints must be placed on the maximum allowed values for the masses and on the range of allowed relative inclinations of the orbits. Often analytical calculations are performed with the coplanarity of the orbits as a working assumption. Early attempts have also been made to verify the possibility of regions of dynamical stability inside the parent stars' Habitable Zones (Kasting et al. 1993), where Earth-size planets may be

found (Jones et al. 2001; Noble et al. 2002; Jones & Sleep 2002, 2004; Rivera & Haghighipour 2004; Cuntz et al. 2003; Menou & Tabachnik 2003). However, the existence of such regions does not directly imply that rocky planets may have actually formed, in these systems, at such privileged distances, in the first place (Thébaud et al. 2002).

The results obtained by many of the present studies on the dynamical stability of extra-solar planetary systems contain significant ambiguities. The impossibility to draw at present more than general statistical conclusions on such issues arises partly from the intrinsically chaotic nature of N-body systems, and partly from a lack of knowledge of a few key parameters that cannot be derived by the present observational datasets, but must be *a priori* fixed throughout the analyses. As a matter of fact, in general four quantities drive the effects of the mutual perturbations in multiple-planet systems investigated by theorists: the planetary eccentricities, the orbital periods (and possible commensurabilities among them), the planet masses (usually through their ratio), and the relative inclinations of the orbital planes. The last two of these parameters cannot be determined from the intrinsically one-dimensional information extracted from stellar spectra. In fact, radial velocity measurements do not determine either the inclination i of the orbital plane with respect to the plane of the sky (and this in turn allows only for lower limits to be placed on the actual mass of each companion to the observed star) or the position angle Ω of the line of nodes in the plane of the sky (and thus relative inclination angles remain unknown): without knowledge of the full three-dimensional geometry of the systems and true mass values, general conclusions on the architecture, orbital evolution and long-term stability of the newly discovered planetary systems remain questionable.

Attempts have been made to break the $\sin i$ degeneracy and determine the true masses of planets in multiple systems utilizing self-consistent dynamical fits (Laughlin & Chambers 2001; Rivera & Lissauer 2001). Such procedures significantly improve orbital fits performed assuming independent Keplerian motions in cases such as that of Gliese 876, where mutual perturbations are relevant and the orbital elements of the planets undergo significant changes on timescales comparable to the timespan of the observations. However, these dynamical fits to the radial velocity data are not conclusive, as assumptions must still be made on the actual relative inclinations of the planets, and broad ranges of $\sin i$ provide similarly good

fits. Thus, tightly constraining planetary masses will be difficult for several years to come, if one has to rely only upon radial velocity measurements. Furthermore, different orbital configurations giving similarly good values of the reduced chi-square $\chi^2_\nu = \chi^2/\nu$ (where ν is the number of degrees of freedom) behave very differently when integrated over long timescales, and the ambiguity on the actual long-term stability of the systems cannot be removed.

In the latest years other techniques have reached the sensitivity necessary to complement spectroscopy in extra-solar planet searches. In particular, transit photometry has been successful in identifying the first gas giant planet eclipsing its parent star (Charbonneau et al. 2000; Henry et al. 2000), confirming the spectroscopic detection (Mazeh et al. 2000; Queloz et al. 2000b), and very recently in directly discovering the second transiting planet (Konacki et al. 2003). The observations of planetary transits on the disk of HD 209458 allow for a direct estimate of the planet's size and actual mass (as the inclination of the orbital plane is known, and the $\sin i$ degeneracy breaks down), thus, also thanks to the recent detection of sodium in its atmosphere (Charbonneau et al. 2002), its density can be inferred and important insights on its composition can be obtained. However, transit photometry detects only the small proportion of planets whose orbits happen to line up almost exactly with the line of sight to the star. We anticipate that future high-precision ground-based (Mariotti et al. 1998; Booth et al. 1999; Colavita et al. 1999) as well as space-borne (Danner & Unwin 1999; Perryman et al. 2001) astrometric observatories will be among the most effective techniques to remove the present ambiguities in the dynamical analysis of extra-solar planetary systems as well as provide valuable data to probe models addressing the issues of the formation of planetary systems and the actual nature of sub-stellar companions. The intrinsically two-dimensional astrometric data provide the means to directly measure the two missing parameters, i.e. the inclination angle and the line of nodes of each planetary orbit. Knowledge of the full viewing geometry of a system of planets allows then to derive meaningful estimates for the true masses of each orbiting object and the relative inclinations of the orbital planes.

In our previous work (Sozzetti et al. 2002, S02 hereafter), we addressed the issues of the detectability and measurability of single planets around single stars with the Space Interferometry Mission (SIM), with the instrument operated in narrow-angle astrometric mode. We

expressed our results as a function of both SIM mission parameters and properties of the planet (mass, orbital characteristics). In the continuation of our studies we have utilized extensive simulations of SIM observations of the present sample of extra-solar multiple-planet systems in order to draw general conclusions on the ability of SIM to discover and measure systems of planets, as well as quantify the instrument’s capability to determine the coplanarity of multiple-planet orbits. Similarly, Sozzetti et al. (2001) have recently assessed the capabilities of ESA’s Cornerstone Mission GAIA for the detection and measurement of planetary systems utilizing the ν And system as a template. Our study is different in that, addressing the entire set of presently known multiple-planet systems, it extends the analysis beyond the favorable cases (well-spaced, well-sampled orbits, high “astrometric” signal-to-noise ratios) studied by Sozzetti et al. (2001), and is specifically tailored to SIM.

This second paper is organized as follows. In the second Section we briefly describe the setup for the simulation of SIM sample narrow-angle campaigns, the statistical tools implemented for planet detection, and the algorithms for multiple orbital fits. In the third Section we present results on multiple-planet systems detection, multiple-planet orbit reconstruction, and coplanarity analyses, and compare our results to those of previous studies. Finally, in the fourth Section we summarize our results and discuss our findings in the context of the present status of planet searches.

7.2 SIMULATION SETUP, DETECTION AND ORBITAL FITTING METHODS

The code for the reproduction of sample observing campaigns with SIM operated in narrow-angle astrometric mode and the subsequent analysis of the simulated dataset has been thoroughly described in S02, where we defined detectability horizons and limits on distance for accurate orbital parameters and mass determination in the case of single planets orbiting single, nearby solar-type stars. In this Section we summarize its main features and working assumptions, and describe the modifications made in order to address the issues of multiple-planet system observations, detection, and measurement.

7.2.1 SIM Narrow-Angle Astrometric Observing Scenario

The SIM instrument (for a thorough presentation of the mission concept see for example [Danner & Unwin 1999](#)) executes pointed observations at arbitrary times and orientations of the interferometric baseline. When operating in the regime of narrow-angle astrometry, its fundamental one-dimensional measurement is the *relative* optical path-length delay:

$$\Delta d_{\star,n} = \mathbf{B} \cdot (\mathbf{S}_{\star} - \mathbf{S}_n) + \sigma_d \quad (7.1)$$

which corresponds to the instantaneous angular distance between the target and its n -th reference star, projected onto the baseline of the science interferometer, while the two guide interferometers accurately monitor changes in the satellite's attitude by acquiring fringes of two bright guide stars. In the above formula $\mathbf{B} = B\mathbf{u}_b$ is the interferometer baseline vector of length B , \mathbf{S}_{\star} and \mathbf{S}_n are the unit vectors to the target star and its n -th reference object, while σ_d is the single-measurement accuracy on each relative delay measurement.

Throughout all our simulations we have adopted the template observing scenario outlined in [S02](#): within a domain of 1° in diameter around each target we place $N_r = 3$ reference stars, and execute $N_o = 24$ full two-dimensional observations (corresponding to a total of $N_m = 144$ relative delay measurements) randomly, uniformly distributed over the nominal $L = 5$ years mission lifetime, each composed of two one-dimensional standard visits made with orthogonal orientations of the interferometer baseline vector. Since in our study we have utilized the present set of extra-solar planetary systems, orbiting very bright ($V \leq 10$ mag), nearby, solar-type stars (spectral types F-G-K, except for Gliese 876), we have utilized a structure of the standard visit which applies to bright target and reference stars ($V \leq 11$ mag), and consequently set a single-measurement error $\sigma_d = 2 \mu\text{as}$ throughout all our analysis (see [S02](#) for details on the adopted error model). This value for σ_d is in line with the presently envisaged SIM performance in its new shared-baseline configuration. ¹

The basic assumptions made in our previous work with regard to the SIM instrument and the systems to be investigated are unchanged in this study: 1) we assume perfect knowledge of the error model and attitude of the spacecraft; 2) the objects composing the local frame

¹The results presented and discussed in the following Sections can easily be rescaled to different timing and numbers of full-observations and reference stars, with the simple scaling laws already derived in [S02](#)

of reference, with respect to which observations of a given scientific target are made, are assumed astrometrically clean, i.e. sources of astrometric noise intrinsic to the source, such as flares, rotating spots, or marginally unstable circumstellar disks, have not been taken into consideration, nor have we discussed the possibility of binaries among either targets or reference stars; 3) effects on the targets' displacement due to perspective acceleration, changing parallax, or higher-order contributions from relativistic aberration and light deflection from the major solar system bodies have not been included.

We have modified the description of the target motion on the celestial sphere to allow for the presence of multiple planets. The stellar motion is described in terms of the 5 basic astrometric parameters and of the gravitational perturbations produced by the orbiting planets. The difference between the position vector to the target S_\star evaluated at time t and the same quantity S'_\star measured at time t' can then be expressed as a sum of small perturbative terms:

$$S'_\star - S_\star = dS_\star = dS_\mu + dS_\pi + \sum_{i=1}^{n_p} dS_K^i, \quad (7.2)$$

where n_p is the number of planets orbiting the target. The gravitational effects produced by the planets are assumed to be linear (i.e., as the sum of independent Keplerian motions). Such simplification (no mutual gravitational interactions between planets) has in general little impact on the significance of our analysis. In fact, assuming the orbits are coplanar, over the time-scale of SIM observations (5 years), variations of the orbital parameters due to secular as well as resonant perturbative terms can be confidently considered negligible. This assumption may not be correct only in the case of Gliese 876, where the two gas giant planets orbiting the star are locked in a 2:1 resonance, and strong mutual perturbations are already evident in the data over the timescale of the radial velocity observations (~ 13 years). We plan to study in detail in a future work the effects induced by mutual gravitational perturbations between planets on the quality of multiple-planet orbital fits that do and do not contain analytic descriptions of the resonant and/or secular perturbative nature of the systems.

7.2.2 Statistical Tools for Planet Detection

We adopt two different procedures for investigating the efficiency of SIM in detecting multiple-planet systems.

First of all, following the approach in S02, we employ a standard χ^2 test with confidence level set to 95% applied to the observation residuals. The test is performed initially against the null hypothesis that there is no planet, then after removal of the first planetary signature it is applied in succession until no further significant deviations (at the 95% confidence level) from the fitted model containing n_p planets appear in the residuals.

Secondly, we have upgraded our code to include a basic periodogram analysis in order to search for hidden periodicities in the astrometric measurements. To this aim, we have utilized the standard algorithm for the evaluation of the Lomb-Scargle normalized periodogram for the spectral analysis of unevenly sampled data (Press et al. 1992), specifically its ‘fast’ version by Press & Rybicki (1989). The traditional Lomb-Scargle formula is equivalent to performing an unweighted linear least-squares fit of a sinusoid to the data, after subtraction of the mean. For a time series of relative delays $\Delta d(t_i)$, where i takes on integer values up to the total number of measurements N_m , the normalized periodogram as a function of the test angular frequency ϑ is defined as:

$$z(\vartheta) = \frac{1}{2\sigma_d^2} \left\{ \frac{\left[\sum_{i=1}^{N_m} (\Delta d(t_i) - \overline{\Delta d}) \cos \vartheta(t_i - t_c) \right]^2}{\sum_{i=1}^{N_m} \cos^2 \vartheta(t_i - t_c)} + \frac{\left[\sum_{i=1}^{N_m} (\Delta d(t_i) - \overline{\Delta d}) \sin \vartheta(t_i - t_c) \right]^2}{\sum_{i=1}^{N_m} \sin^2 \vartheta(t_i - t_c)} \right\} \quad (7.3)$$

Here, $\overline{\Delta d}$ is the mean of the data, while t_c is given by

$$t_c = \frac{1}{2\vartheta} \arctan \left(\frac{\sum_{i=1}^{N_m} \sin 2\vartheta t_i}{\sum_{i=1}^{N_m} \cos 2\vartheta t_i} \right) \quad (7.4)$$

The normalization factor is by default taken as the variance of the sample. Because of the exploratory nature of this investigation, we assign equal weight to all observations and set $\sigma_d = 2 \mu\text{as}$, the value of the single-measurement error on relative delays as defined in the previous Section. At the moment we do not discuss the merit of other possible choices for the normalization of the periodogram (Gilliland & Baliunas 1987; Schwarzenberg-Czerny 1996).

Observation residuals are inspected successively after the single-star fit, and after removal of each planetary signature, to establish the existence or absence of further periodicities. Also in this case, the significance of the detection or non detection of a periodic signal in the residuals, i.e. the significance of a particular peak in the power spectrum $z(\vartheta)$, must be assessed. For the above choice of the normalization factor, the probability that a periodogram power z is above some value z_0 is then $P(z > z_0) = e^{-z_0}$ (Scargle 1982; Horne & Baliunas 1986), and, if M independent frequencies are scanned, the probability that none gives values larger than z_0 is $(1 - e^{-z_0})^M$. Then, the *false-alarm probability* of the null hypothesis that the data are pure noise is computed for each value of z as:

$$P(> z_0) = 1 - (1 - e^{-z_0})^M \quad (7.5)$$

This expression provides an estimate of the significance of each given peak in the spectrum that can be identified. For sufficiently high values of z_0 the false-alarm probability is very small, and this corresponds to the detection of a highly significant periodic signal.

The choice of M is critical in assessing the true significance of a given peak in the spectrum. In general, the larger the number of frequencies, the less significant is any ‘bump’ in the periodogram power. The actual value of M depends in general on the actual frequency range scanned, and on the number and clumpiness of the data points available for the investigation. For this reasons, it is difficult to derive a closed analytical form for the number of independent frequencies. For period searches between the average Nyquist period ($T_{\text{Nyq}} \simeq 2L/N_m$) and the duration of the data set a reasonable choice is $M \simeq N_m$ (Horne & Baliunas 1986). However, when sampling very short periods, in general frequencies much higher than the average Nyquist frequency are reached, then the number of independent frequencies will be higher. For any particular case, an actual value of M can be estimated by simple Monte Carlo analysis: holding fixed the number and epochs of the observations, generate synthetic datasets containing only Gaussian (normal) noise representative of the actual errors, then find the largest value of $P(> z_0)$ and fit the resulting distribution for M in Eq. 7.5. By doing so, Marcy & Benitz (1989) and Cumming et al. (1999) derive $M = 1.15N_m$ and $M = 1.175N_m$, respectively, and this may be compared with the analytic relation $M = -6.4 + 1.19N_m + 0.00098N_m^2$ by Horne & Baliunas (1986). Given the illustrative

purpose of our analysis, we rely on results from the literature and choose a typical value $M = 1.20N_m$ throughout our simulations.

7.2.3 Procedure for Multiple-Planet Orbital Fits

The iterative method for the solution of the non-linear systems of equations of condition is based on a slightly modified version of the Levenberg-Marquardt algorithm, as described in [S02](#), which ensures stability of the solution. It has been upgraded to allow for the presence of multiple, independent planetary perturbations.

The photocenter motion of the target is described by an analytical model in which the recomputed relative delay between the target and its j -th reference star ($j = 1, \dots, N_r$) is in the form:

$$\begin{aligned} \Delta d_{\star,j} = & \mathbf{B} \cdot (\mathbf{S}_{\star}(\lambda_{\star}, \beta_{\star}, \mu_{\lambda,\star}, \mu_{\beta,\star}, \pi_{\star}, \sum_{l=1}^{n_p} (X_{1,l}, X_{2,l}, X_{3,l}, X_{4,l}, e_l, T_l, \tau_l)) \\ & - \mathbf{S}_j(\lambda_j, \beta_j, \mu_{\lambda,j}, \mu_{\beta,j}, \pi_j)) \end{aligned} \quad (7.6)$$

The five astrometric parameters (two positions, two proper motion components, and parallax) of the target $(\lambda_{\star}, \beta_{\star}, \mu_{\lambda,\star}, \mu_{\beta,\star}, \pi_{\star})$ and each of the N_r local reference objects $(\lambda_j, \beta_j, \mu_{\lambda,j}, \mu_{\beta,j}, \pi_j)$ are defined in ecliptic coordinates (see [S02](#) for details), while for the seven orbital elements needed to describe the orbit of each of the n_p planets around the target we have utilized the Thiele-Innes representation, in which the semi-major axis a_l , the inclination i_l , the longitude of pericenter ω_l and the position angle of the line of nodes Ω_l of the l -th planet are combined to form the quantities:

$$\begin{aligned} X_{1,1} &= a_l(\cos \omega_l \cos \Omega_l - \sin \omega_l \sin \Omega_l \cos i_l) \\ X_{2,1} &= a_l(-\sin \omega_l \cos \Omega_l - \cos \omega_l \sin \Omega_l \cos i_l) \\ X_{3,1} &= a_l(\cos \omega_l \sin \Omega_l + \sin \omega_l \cos \Omega_l \cos i_l) \\ X_{4,1} &= a_l(-\sin \omega_l \sin \Omega_l + \cos \omega_l \cos \Omega_l \cos i_l) \end{aligned}$$

In this model, the observation equations are strictly nonlinear only in the orbital period T_l , the eccentricity e_l , and the epoch of pericenter passage τ_l . At the end of each simulation, the classic orbital parameters are recomputed from the Thiele-Innes elements (see for example

Heintz 1978). The mass $M_{p,1}$ of the l -th planet is then determined by combining the values of T_l (in years), π_* and the semi-major axis of the stellar orbit around the barycenter of the system $a_{*,1}$ (both in arcseconds), all estimated from the fit to the observed delays, and the stellar mass M_* , assumed perfectly known, in the following approximation of the mass-function formula for $M_{p,1} \ll M_*$:

$$M_{p,1} \simeq \left(\frac{a_{*,1}^3 M_*^2}{\pi_*^3 T_1^2} \right)^{1/3} \quad \text{for } l = 1, \dots, n_p \quad (7.7)$$

The multiple-orbit fitting procedure also determines the formal errors on each estimated parameter x_m as:

$$\sigma(x_m) = \sqrt{C_{mm}}, \quad (7.8)$$

where the C_{mm} 's are the diagonal elements of the covariance matrix of the fit (Press et al. 1992). In the case of the orbital parameters recomputed from the Thiele-Innes elements and the mass of each planet, formal errors are propagated utilizing the classic error propagation formula, including correlations between the measured parameters:

$$\sigma(z_k) = \sqrt{\sum_{i=1}^{m_f} \sum_{j=1}^{m_f} \frac{\partial z_k}{\partial x_i} \frac{\partial z_k}{\partial x_j} \sigma(x_i) \sigma(x_j)}, \quad (7.9)$$

where the sums are extended to the m_f fitted parameters from which the k -th recomputed quantity z_k depends.

As already highlighted in S02, convergence of the non-linear fitting procedure and quality of the orbital solutions can both be significantly affected by the choice of the starting guesses. In the studies presented here this issue has been left aside because, focusing on the set of presently known planetary systems, we have utilized as starting guesses the values of the orbital parameters for the planets in each system published in the literature. Nevertheless, whenever data will be inspected to search for planetary signatures in the absence of *a priori* information on the actual presence of planets around a given target, important questions will have to be addressed and answered, related to how and to what extent effective starting values, i.e., leading to successful orbital solutions, will be identified from the data as a function of actual instrument performances, uncertainties in the error model, and intrinsic properties of the planetary systems. To this end, realistic global search strategies will have

to be tested and double-blind test campaigns conducted. Work on these issues is in progress and will be reported in the future.

7.3 RESULTS

In addressing the problem of the detection and measurement of multiple planets with SIM, we have utilized the entire set of existing planetary systems known to date as representative test cases. The results are discussed below, as follows. First, we study SIM's efficiency in multiple-planet detection by means of a method that combines standard χ^2 statistics, periodogram analysis and Fourier series expansions. Next, we estimate SIM's ability to make accurate measurements of multiple-planet orbits and masses. Then, we gauge the boundaries of SIM's capability to determine the coplanarity of the orbits of planets in systems. Finally, we quantify how beneficial it would be to be able to combine astrometric and spectroscopic orbital elements in order to improve the accuracy in full-orbit reconstruction, planet mass determination, and coplanarity measurements. All results reported here have been obtained assuming end-of-mission analysis of the simulated datasets. We do not discuss in this paper modifications to the strategy for the analysis of SIM observations at earlier stages of the mission, when the instrument operations are still ongoing.

7.3.1 Detectability of Multiple-Planet Systems

In this Section we focus on establishing the boundaries of reliable multiple-planet system detection with SIM for a wide range of orbital arrangements, including low values of the astrometric signal-to-noise ratio α/σ_d and orbital periods exceeding the mission lifetime. To this end, we have investigated the performances of various detection methods (χ^2 test, Fourier series, periodogram analysis) in the different regimes. Our study is primarily illustrative, and clearly does not cover all possible arrangements of planetary systems, such as configurations with extreme orbital shapes and orientations, and small amplitudes of the astrometric signal (either because of small planet masses, or due to large distances).

7.3.1.1 Probabilities of Detection As discussed in S02, the easiest way to quantify SIM’s sensitivity to planetary perturbations is to parameterize it through the orbital period T and the *astrometric signal-to-noise ratio* α/σ_d , where σ_d is the single-measurement error on each relative delay measurement, while the *astrometric signature* α is the apparent amplitude of the gravitational perturbation induced on the observed star by a single companion, defined as:

$$\alpha = \frac{M_p a_p}{M_\star D}, \quad (7.10)$$

where M_p , M_\star are the masses of the planet and star respectively (in solar masses), a_p the semi-major axis of the planetary orbit (in AU), D the distance of the system from the observer (in pc). In the case of multiple, independent Keplerian perturbations, the orbital motion of the star about the barycenter will contain components reflecting the orbital periods of each of the companions, with the peak amplitude corresponding to the object with the larger value of the product $M_p \times a_p$ (for a given distance of the system and mass of the central star). It must be noted that Eq. 7.10 constitutes only an upper limit to the actual magnitude of the measured perturbation, without any projection or eccentricity effect. If the plane of a circular orbit lies in the plane of the sky, the two projections of the perturbation will be equal, with amplitudes given by Eq. 7.10. If the orbital plane is inclined with respect to the line of sight, there will always be some projection of the orbit on the plane of the sky which has the amplitude given by Eq. 7.10, but the amplitude at other positions angles will be less. If the orbit is eccentric, there could be cases where the orientation of the orbital plane with respect to the observer’s line of sight gives rise to significantly smaller apparent amplitudes than indicated in Eq. 7.10: in the worst-case scenario, when the line of apsides is aligned with the line of sight the maximum measured amplitude corresponds to the orbital semi-minor axis, which is still equal to $> 0.95 a_p$ for moderately eccentric orbits ($e < 0.3$), but can drop below $0.5 a_p$ for high eccentricities ($e > 0.8$). For very eccentric orbits, the projected amplitude of the stellar orbital motion can thus be up to a factor 2 or more smaller than the value calculated with Eq. 7.10. The variety of orbital arrangements reproduced by the set of planetary systems known to date does not present any such case, as the eccentricity of the orbits is usually moderate ($e \leq 0.55$). The only exception is HD 160691 b ($e = 0.8$), but its astrometric signature ($\alpha = 139/\sin i \mu\text{as}$) is sufficiently high not to constitute a problem in

terms of ability to detect it or to determine its orbit, even in the worst-case scenario.

Table 7.1: Parameters of planetary systems and stellar hosts

Stellar Parameters ^a	Central Star	Orbital elements ^b	Planet b	Planet c	Planet d
System: ν And					
λ (deg)	38.36	α (μas)	2.32	89.58	541.8
β (deg)	29.25	a (AU)	0.059	0.83	2.53
μ_λ (mas/yr)	-313.16	T (d)	4.6	241.5	1284.0
μ_β (mas/yr)	-277.30	e	0.012	0.28	0.27
π (mas)	74.25	τ (JD)	2450002.1	2450160.5	2450064.0
V Magnitude	4.09	ω (deg)	73.0	250.0	260.0
Spectral Type	F8V	$M_p \sin i$ (M_J)	0.69	1.89	3.75
d (pc)	13.47	Ω (deg)	$[0, \pi]$	$[0, \pi]$	$[0, \pi]$
M_\star (M_\odot)	1.3	i (deg)	$[0, \pi/2]$	$[0, \pi/2]$	$[0, \pi/2]$
System: 55 Cnc					
λ (deg)	127.79	α (μas)	7.75	4.04	1916.6
β (deg)	10.70	a (AU)	0.115	0.24	5.9
μ_λ (mas/yr)	-530.91	T (d)	14.653	44.28	5360.0
μ_β (mas/yr)	-93.54	e	0.02	0.34	0.16
π (mas)	79.81	τ (JD)	2450001.479	2450031.4	2452785.0
V Magnitude	5.95	ω (deg)	99.0	61.0	201.0
Spectral Type	G8V	$M_p \sin i$ (M_J)	0.84	0.21	4.05
d (pc)	12.53	Ω (deg)	$[0, \pi]$	$[0, \pi]$	$[0, \pi]$
M_\star (M_\odot)	0.95	i (deg)	$[0, \pi/2]$	$[0, \pi/2]$	$[0, \pi/2]$
System: HD 38529					
λ (deg)	86.23	α (μas)	1.71	805.7	...
β (deg)	-21.78	a (AU)	0.129	3.71	...
μ_λ (mas/yr)	-83.66	T (d)	14.31	2207.4	...
μ_β (mas/yr)	-139.69	e	0.28	0.33	...
π (mas)	23.58	τ (JD)	24510005.8	24510043.7	...
V Magnitude	5.95	ω (deg)	90.0	13.0	...
Spectral Type	G4IV	$M_p \sin i$ (M_J)	0.78	12.8	...
d (pc)	42.40	Ω (deg)	$[0, \pi]$	$[0, \pi]$...
M_\star (M_\odot)	1.39	i (deg)	$[0, \pi/2]$	$[0, \pi/2]$...
System: Gliese 876					
λ (deg)	339.21	α (μas)	264.4	48.5	...
β (deg)	-6.77	a (AU)	0.21	0.13	...

Table 7.1: (continued)

Stellar Parameters ^a	Central Star	Orbital elements ^b	Planet b	Planet c	Planet d
μ_λ (mas/yr)	634.86	T (d)	61.02	30.12	...
μ_β (mas/yr)	-987.72	e	0.10	0.27	...
π (mas)	213.22	τ (JD)	2450106.2	2450031.4	...
V Magnitude	10.15	ω (deg)	333.0	330.0	...
Spectral Type	M4	$M_p \sin i$ (M_J)	1.89	0.56	...
d (pc)	4.69	Ω (deg)	$[0, \pi]$	$[0, \pi]$...
M_\star (M_\odot)	0.32	i (deg)	$[0, \pi/2]$	$[0, \pi/2]$...
System: HD 168443					
λ (deg)	225.07	α (μas)	58.64	1269.5	...
β (deg)	13.33	a (AU)	0.295	2.87	...
μ_λ (mas/yr)	-99.95	T (d)	58.10	1771.5	...
μ_β (mas/yr)	-220.79	e	0.53	0.20	...
π (mas)	25.97	τ (JD)	2450047.6	2450250.0	...
V Magnitude	6.91	ω (deg)	172.9	289.0	...
Spectral Type	G5IV	$M_p \sin i$ (M_J)	7.73	17.2	...
d (pc)	38.5	Ω (deg)	$[0, \pi]$	$[0, \pi]$...
M_\star (M_\odot)	1.01	i (deg)	$[0, \pi/2]$	$[0, \pi/2]$...
System: HD 12661					
λ (deg)	37.70	α (μas)	47.43	100.4	...
β (deg)	12.26	a (AU)	0.82	2.56	...
μ_λ (mas/yr)	-161.28	T (d)	263.3	1444.5	...
μ_β (mas/yr)	-127.78	e	0.35	0.20	...
π (mas)	26.91	τ (JD)	2459943.7	2459673.9	...
V Magnitude	7.43	ω (deg)	292.6	147.0	...
Spectral Type	G6V	$M_p \sin i$ (M_J)	2.30	1.56	...
d (pc)	37.16	Ω (deg)	$[0, \pi]$	$[0, \pi]$...
M_\star (M_\odot)	1.07	i (deg)	$[0, \pi/2]$	$[0, \pi/2]$...
System: HD 160691 ^c					
λ (deg)	267.20	α (μas)	155.8	139.2	...
β (deg)	-28.87	a (AU)	1.48	2.30	...
μ_λ (mas/yr)	-20.96	T (d)	637.3	1300.0	...
μ_β (mas/yr)	-190.61	e	0.31	0.8	...
π (mas)	65.36	τ (JD)	2450959.0	2451613.0	...
V Magnitude	5.15	ω (deg)	320.0	99.0	...
Spectral Type	G3IV/V	$M_p \sin i$ (M_J)	1.74	1.0	...
d (pc)	15.30	Ω (deg)	$[0, \pi]$	$[0, \pi]$...

Table 7.1: (continued)

Stellar Parameters ^a	Central Star	Orbital elements ^b	Planet b	Planet c	Planet d
$M_\star (M_\odot)$	1.08	i (deg)	$[0, \pi/2]$	$[0, \pi/2]$...
System: 47 UMa					
λ (deg)	149.30	α (μas)	366.1	195.5	...
β (deg)	31.28	a (AU)	2.09	3.73	...
μ_λ (mas/yr)	-259.16	T (d)	1089.0	2594.0	...
μ_β (mas/yr)	188.90	e	0.06	0.10	...
π (mas)	71.02	τ (JD)	2453622.0	2451363.5	...
V Magnitude	5.03	ω (deg)	172.0	127.0	...
Spectral Type	G0V	$M_p \sin i (M_J)$	2.54	0.76	...
d (pc)	14.08	Ω (deg)	$[0, \pi]$	$[0, \pi]$...
$M_\star (M_\odot)$	1.03	i (deg)	$[0, \pi/2]$	$[0, \pi/2]$...
System: HD 82943 ^d					
λ (deg)	150.22	α (μas)	65.58	22.28	...
β (deg)	-24.79	a (AU)	1.16	0.73	...
μ_λ (mas/yr)	-58.14	T (d)	444.6	221.6	...
μ_β (mas/yr)	-164.07	e	0.41	0.54	...
π (mas)	36.42	τ (JD)	2451620.3	2451630.9	...
V Magnitude	6.54	ω (deg)	96.0	138.0	...
Spectral Type	G0	$M_p \sin i (M_J)$	1.63	0.88	...
d (pc)	27.46	Ω (deg)	$[0, \pi]$	$[0, \pi]$...
$M_\star (M_\odot)$	1.05	i (deg)	$[0, \pi/2]$	$[0, \pi/2]$...
System: HD 74156 ^d					
λ (deg)	131.71	α (μas)	6.35	383.9	...
β (deg)	-12.86	a (AU)	0.276	3.47	...
μ_λ (mas/yr)	-28.19	T (d)	51.61	2300.0	...
μ_β (mas/yr)	-200.05	e	0.65	0.40	...
π (mas)	15.49	τ (JD)	2451981.4	2450849.0	...
V Magnitude	7.62	ω (deg)	183.7	240.0	...
Spectral Type	G0	$M_p \sin i (M_J)$	1.56	7.5	...
d (pc)	64.56	Ω (deg)	$[0, \pi]$	$[0, \pi]$...
$M_\star (M_\odot)$	1.05	i (deg)	$[0, \pi/2]$	$[0, \pi/2]$...
System: HD 37124					
λ (deg)	84.62	α (μas)	15.37	98.62	...

Table 7.1: (continued)

Stellar Parameters ^a	Central Star	Orbital elements ^b	Planet b	Planet c	Planet d
β (deg)	-2.17	a (AU)	0.54	2.95	...
μ_λ (mas/yr)	-96.14	T (d)	153.0	1942.0	...
μ_β (mas/yr)	-416.51	e	0.10	0.40	...
π (mas)	30.12	τ (JD)	2451227.0	2451828.0	...
V Magnitude	7.68	ω (deg)	97.0	265.0	...
Spectral Type	G4V	$M_p \sin i$ (M_J)	0.86	1.01	...
d (pc)	33.20	Ω (deg)	$[0, \pi]$	$[0, \pi]$...
M_\star (M_\odot)	0.91	i (deg)	$[0, \pi/2]$	$[0, \pi/2]$...

In order to tackle the issues discussed in the previous Sections, we ran simulations of SIM narrow angle astrometric campaigns dedicated to the observations of the 11 stars known to harbor multiple-planet systems, utilizing the observing scenario sketched in Section 7.2.1. In particular, we generated sets of 500 planetary systems on the celestial sphere. The values we utilized for the stellar parameters and orbital elements were taken from various online catalogs in September 2002, as summarized in Table 7.1.² The analysis carried out and results presented in this and the following Sections are based on a total of 990 000 simulated planetary systems.

Two orbital elements cannot be determined by radial velocity measurements, namely i and Ω . We simulate systems with random uniform distributions for the lines of nodes ($0^\circ \leq \Omega \leq 180^\circ$) and express detection probabilities as a function of the orbital inclination, constrained to vary in the range $1^\circ \leq i \leq 90^\circ$. Planet masses are scaled with the co-secant of the inclination angle.

An important point is the choice of the relative inclination angle between pairs of components in multiple systems. The relative inclination i_{rel} of two orbits is defined as the angle between the two orbital planes, and is given by the formula (see for example Kells et al. 1942):

$$\cos i_{\text{rel}} = \cos i_{\text{in}} \cos i_{\text{out}} + \sin i_{\text{in}} \sin i_{\text{out}} \cos(\Omega_{\text{out}} - \Omega_{\text{in}}), \quad (7.11)$$

²For an up-to-date list of extra-solar multiple-planet systems and their orbital elements as they are known at the time of writing see for example Fischer et al. (2003a)

where i_{in} and i_{out} , Ω_{in} and Ω_{out} are the inclinations and lines of nodes of the inner and outer planet, respectively. We choose the orbits of the multiple-planet systems shown in Table 7.1 to be perfectly coplanar, i.e. i and Ω are exactly identical for all the components in each systems. This choice has been adopted everywhere, unless otherwise noted.

There are three important questions related to the use of χ^2 statistics as a tool for multiple-planet detection that we aimed to answer:

- a) does detection probability depend on the shape and orientation of the orbits?³
- b) is detection of low signal-to-noise astrometric perturbations (the detection limit intrinsic to the χ^2 test is reached for $\alpha/\sigma_d \rightarrow 1$) influenced by the previous removal of larger astrometric signals?
- 3) what is the behavior of false detections (once all planetary perturbations have been detected and removed) as a function of a broad range of orbital arrangements and astrometric signals?

Figure 7.1 shows, for each planet in each of the 11 systems considered, the results of the χ^2 test expressed as a function of the orbital inclination i . For each given system, the test was applied to the residuals to a single-star model, to a model containing the previously detected companion(s), and finally after the removal of all the Keplerian motions. In each system, the dominant signature is always easily detectable, regardless of the inclination of the orbital plane. Even long-period planets such as 55 Cnc d, due to its large mass, are unambiguously discovered. When the companion producing the larger signal is removed, the remaining components, due to the usually large astrometric perturbation induced on its parent star (even for edge-on configurations), are also detected without ambiguities, independent of the value of i , with the exception of the inner planet around HD 38529, the innermost planet orbiting ν And, and the middle planet in the 55 Cnc system.⁴ For the first two objects, in fact, in the edge-on configuration, the amplitude of the astrometric perturbation is of order of σ_d , thus the χ^2 test fails to recognize their presence about sixty percent of the

³In previous works (Lattanzi et al. 2000; S02) it was found that, for the case of single planets, averaging over orbital eccentricity, the astrometric detection probability based on the χ^2 test of the null hypothesis that the star is single did not depend upon the apparent orientation of the orbit

⁴We recall that the astrometric signature $\alpha \propto T^{2/3}$, while the radial velocity amplitude $K \propto T^{-1/3}$, thus the *Hot Jupiters* on very short-period orbits, the first to be detected by spectroscopy, are most difficult to detect with the astrometric method

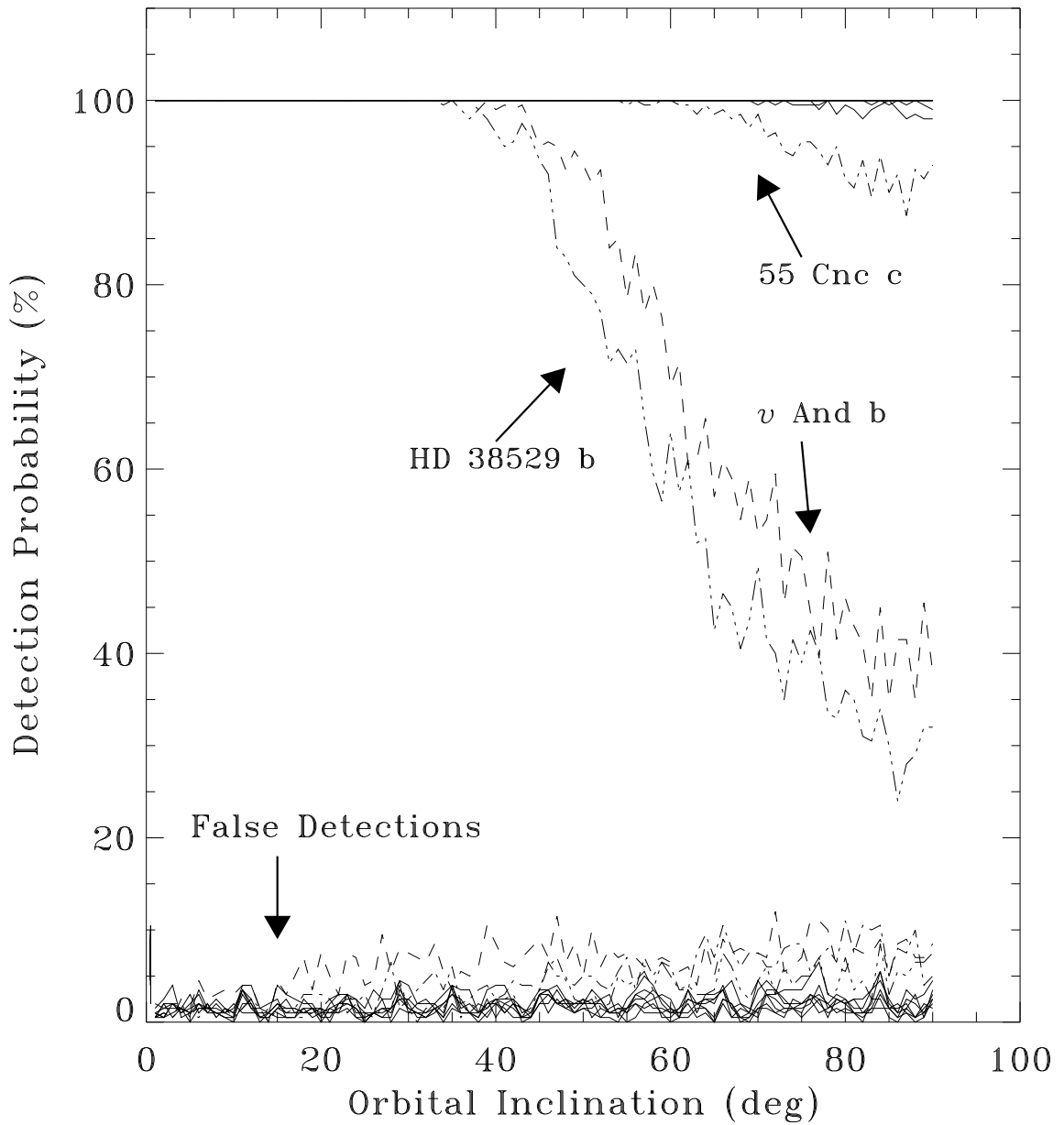


Figure 7.1 Probability of detection as a function of orbital inclination i , for each planet in each of the 11 multiple-planet systems considered in our study. The three planets HD 38529 b (dashed-dotted-dotted line), v And b (long-dashed line), and 55 Cnc c (dashed-dotted line) are the most difficult to detect. After the not accurate subtraction of their low-amplitude astrometric signatures, the corresponding false detection rates are up to a factor 2 larger than the expected 5%

time. 55 Cnc c has a minimum signature $\alpha \simeq 4 \mu\text{as}$, yet its detection probability in the edge-on configuration is a little below the 95% detection threshold due to the fact that its minimum mass also corresponds to the configuration in which only one dimension of the orbit is measurable by astrometry. As $i \rightarrow 0^\circ$, towards a face-on configuration, their projected masses increase, and in all cases detection probability reaches 100% for a value of $\sin i$ such that the correspondent astrometric signature $\alpha \simeq 2\sigma_d$. This result confirms what had been found in our previous works (Casertano et al. 1996; Casertano & Sozzetti 1999; Lattanzi et al. 2000; Sozzetti et al. 2001; S02). In particular, we find that, as long as the orbital period does not exceed the mission lifetime, detectability of astrometric perturbations close to the detection limit is not hampered by the presence of one or more companions producing larger signals. After the larger perturbations have been fitted and removed, a signal-to-noise ratio $\alpha/\sigma_d \simeq 2$ is sufficient for secure detection (at the 95% confidence level), just as if the planet was the only orbiting companion.

The last point addressed in Figure 7.1 concerns the fraction of false detections after all the planets have been discovered and removed. Due to the confidence level adopted for the χ^2 test, we expect $\sim 5\%$ of false positives if the subtraction of all planetary signatures has been successful. On the other hand, we may expect in principle that orbits with long or very short periods and producing low signal-to-noise ratios might not be accurately fitted and removed, with the result of larger spurious residuals, that could translate in a larger amount of false detections. As shown in Figure 7.1, the rate of false positives is roughly independent on the value of i , and comparable for all the systems investigated. Again, three exceptions are present, 55 Cnc c, HD 38529 b, and v And b. In these three cases, the signal to be fitted approaches the detection limit as we move towards $i = 90^\circ$. The quality of the fits when $\alpha \simeq \sigma_d$ is poor, and this degradation translates into a number of false detections up to a factor 2 larger than the expected 5%, with a more pronounced trend as we move close to edge-on orbits. Instead, whenever all the planets in a given system produce a signal $\alpha > 2\sigma_d$ (even in the minimum mass configuration), then the number of false detections drops even below the expected threshold. We find that the average false detection rate, including all systems, is $\overline{F_d} = 3.2\%$, well within the predicted 5% of false positives in case of satisfactory removal of all planetary perturbations.

7.3.1.2 Periodogram Analysis The χ^2 test only allows us to draw general conclusions on the need to reject or keep an a priori theoretical model describing the observations, but provides no clues to the actual nature of the residuals, if the assumed model is proven to be not consistent with the data. In order to provide a direct identification of the nature of the observation residuals and determine the true significance of planet detection/non-detection, a standard procedure is that of inspecting the data by means of a periodogram analysis, to search for evidence of the presence of a clear periodicity in the time-series.

At the end of each χ^2 test, we perform a periodogram analysis (utilizing the tools described in Section 7.2.2) to assess the presence or absence of further periodic signals. This test is applied to a set of observations that contain an a priori known set of planetary signatures, but nonetheless it has proven a useful exercise in order to gauge the ranges of applicability of this procedure to future, actual observations.

Table 7.2: Results from the periodogram analysis of the 11 planetary systems known to date, in the case of an average value of the orbital inclination angle ($i = 45^\circ$). The columns display, respectively, the name of the system, the type of fit performed (single-star, single- or multiple-planet), the value of the reduced chi-square χ_ν^2 of the fit, the highest peak z_p in the periodogram power spectrum, the value of the orbital period $T(z_p)$ corresponding to the peak in the spectrum, and the false-alarm probability $P(z_p)$ of the peak

System	Type of Fit	χ_ν^2	z_p	$T(z_p)$	$P(z_p)$
<i>v</i> And	Single Star	3096.55	50.6828	3.75855	0.0
	1 Planet	1736.20	48.5907	0.671169	0.0
	2 Planets	1.87563	14.6750	0.119567	6.35×10^{-5}
	3 Planets	1.14677	8.41723	0.220069	0.0326138
55 Cnc	Single Star	1856.12	65.3129	5.87275	0.0
	1 Planet	25.3619	51.3840	0.0401112	0.0
	2 Planets	4.13032	39.1092	0.121448	0.0
	3 Planets	0.791748	4.85446	0.0705180	0.690751
HD 38529	Single Star	1063.33	35.7711	3.49768	0.0
	1 Planet	1.46852	28.3746	0.0389847	1.37×10^{-9}
	2 Planets	0.974422	6.45905	0.0402565	0.209530

Table 7.2: (continued)

System	Type of Fit	χ_ν^2	z_p	$T(z_p)$	$P(z_p)$
Gliese 876	Single Star	583.995	57.6141	0.166749	0.0
	1 Planet	392.007	53.6403	0.0821299	0.0
	2 Planets	0.720508	7.41911	0.393050	0.0860501
HD 168443	Single Star	13919.0	54.8187	4.50731	0.0
	1 Planet	534.999	42.8020	0.157193	0.0
	2 Planets	0.943551	6.85225	0.109261	0.146701
HD 12661	Single Star	67.2261	28.1816	3.30105	1.23×10^{-7}
	1 Planet	481.436	44.0427	0.741820	0.0
	2 Planets	1.13029	6.83758	0.0402566	0.148699
HD 160691	Single Star	225.807	50.5789	1.65052	0.0
	1 Planet	1650.87	56.9019	3.27908	0.0
	2 Planets	0.857078	7.96351	0.397465	0.0508595
47 UMa	Single Star	688.689	42.7118	2.81892	0.0
	1 Planet	402.954	51.3840	4.95227	1.35×10^{-9}
	2 Planets	1.04254	4.81968	0.1009260	0.703383
HD 82943	SingleStar	29.2090	53.8883	1.23789	0.0
	1 Planet	36.8078	43.9404	0.618946	0.0
	2 Planets	1.01055	5.77669	0.0398152	0.372220
HD 74156	Single Star	224.126	48.2071	3.30105	0.0
	1 Planet	4.25179	36.1520	0.140470	0.0
	2 Planets	0.994640	5.25626	0.0330859	0.543543
HD 37124	Single Star	82.4841	57.8993	4.36463	0.0
	1 Planet	36.8113	39.9654	0.415679	0.0
	2 Planets	0.931258	5.95232	0.0394809	0.321418

Table 7.2 shows a set of results pertaining to simulations of the 11 planetary systems

assuming an average value of the common inclination angle ($i = 45^\circ$). The crucial points to be discussed are related to how well the period of the signal can be identified, and to how strong the signal must be with respect to the single-measurement precision, in order to give a peak z_p in the periodogram power allowing for a significant detection, i.e. a small value of the false-alarm probability. For the purpose of this analysis, we set a threshold $P(z_p) \leq 10^{-3}$, which implies, given the assumed number of independent frequencies discussed in Section 7.2.2, a value of $z_p \geq 12.0$ to ensure a significant detection of a periodic signal.

From inspection of Table 7.2, the first conclusion that can be drawn is that even in the case of an astrometric signal-to-noise ratio $\alpha/\sigma_d \simeq 1$, as long as the orbital period is shorter than the mission duration, a significant peak can be found in the spectrum. This is the case for example for HD 38529 b, that exhibits $\alpha/\sigma_d = 1.23$ (for $i = 45^\circ$), and while χ_ν^2 approaches 1 (in fact, from Figure 7.1 its presence goes undetected about 15% of the time), the false alarm probability is well below the threshold, and the actual peak in the spectrum matches the true orbital period to within $\sim 1\%$. A graphical interpretation of the results for this system is given in Figure 7.2.

Secondly, three main period ranges can be identified, over which the efficacy of the periodogram analysis is significantly different. First of all, the orbital period may happen to be short enough that the spectrum may peak at a value of T which departs significantly from the true one. This is for example the case of ν And b, for which (see Figure 7.1) the probability of detection is close to 100% (in fact, $\alpha/\sigma_d = 1.64$, at $i = 45^\circ$), but the period is more than a factor 3 shorter than that of HD 38529 b, and the periodogram analysis fails to recognize the correct value of T , identifying a significant peak in the spectrum at a period value which is about an order of magnitude off the true one. As shown in Figure 7.3, bottom-left panel, only the second highest peak is close to the actual value of the period of ν And b, but still about a factor 1.5 off. The failure of the periodogram analysis at very short periods can be dealt with at least in part in two ways. First of all, this problem may be corrected by increasing the number of observations. From the results in Table 7.2, in fact, we see how, in the case of randomly spaced data, it is possible to retrieve meaningful information on periods much shorter than the ‘average’ sampling rate in the case of evenly spaced data. For 24 two-dimensional observations distributed over 5 years, the average sampling rate

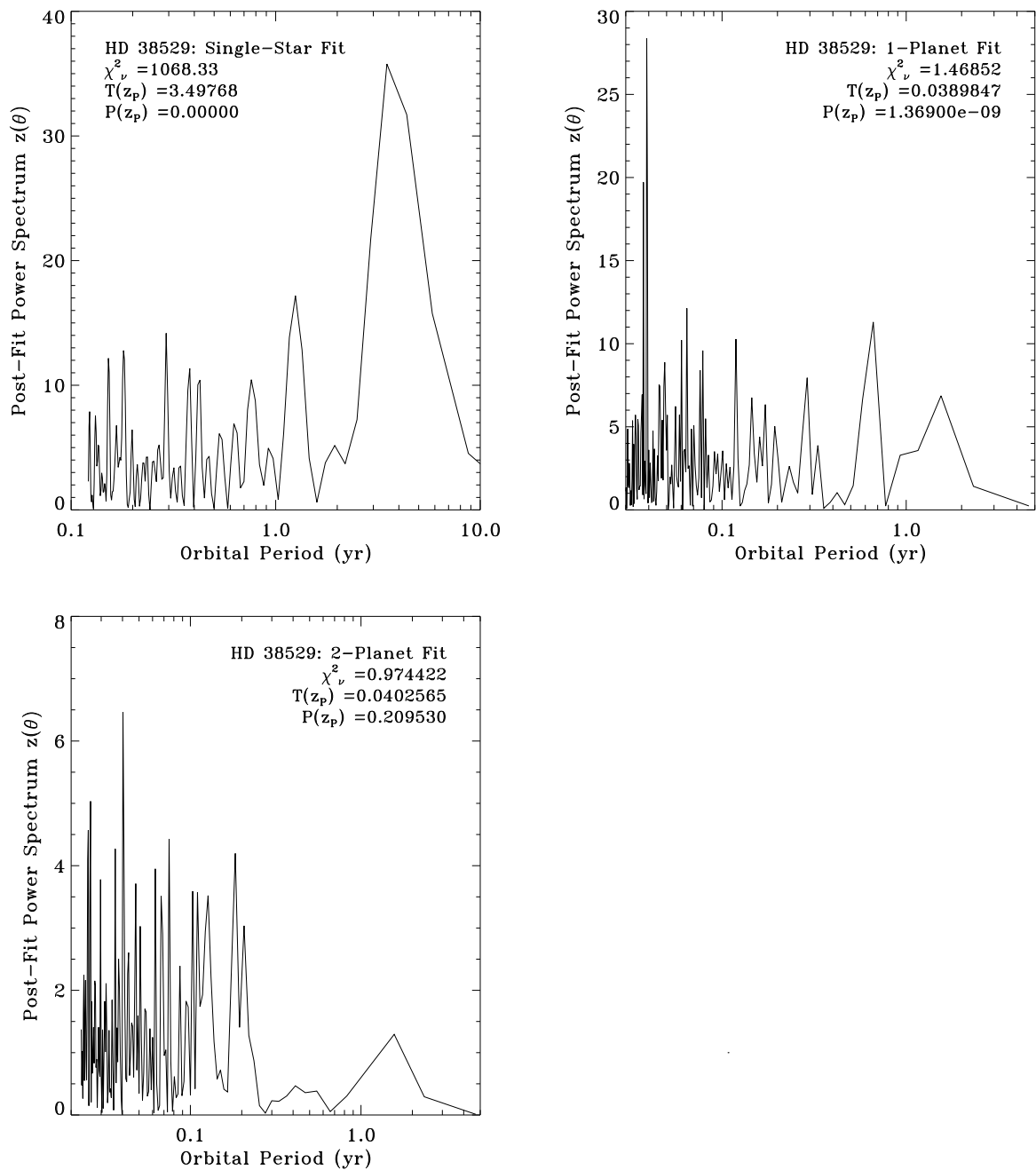


Figure 7.2 Periodogram analysis for the HD 38529 planetary system. In the upper left panel we show the periodicity search after the single-star fit: a long-period signal is clearly found with high significance, but due to the incomplete orbital sampling, its value is about a factor 2 shorter than the actual period of HD 38529 c. The upper right panel highlights how, after the removal of the signal with the larger amplitude, the period of HD 38529 b is still accurately identified, in spite of the very low astrometric signature induced by the inner planet of the system on its central star. The lower left panel present the results of the periodogram analysis after the dual Keplerian fit to the observations: no significant peaks are found

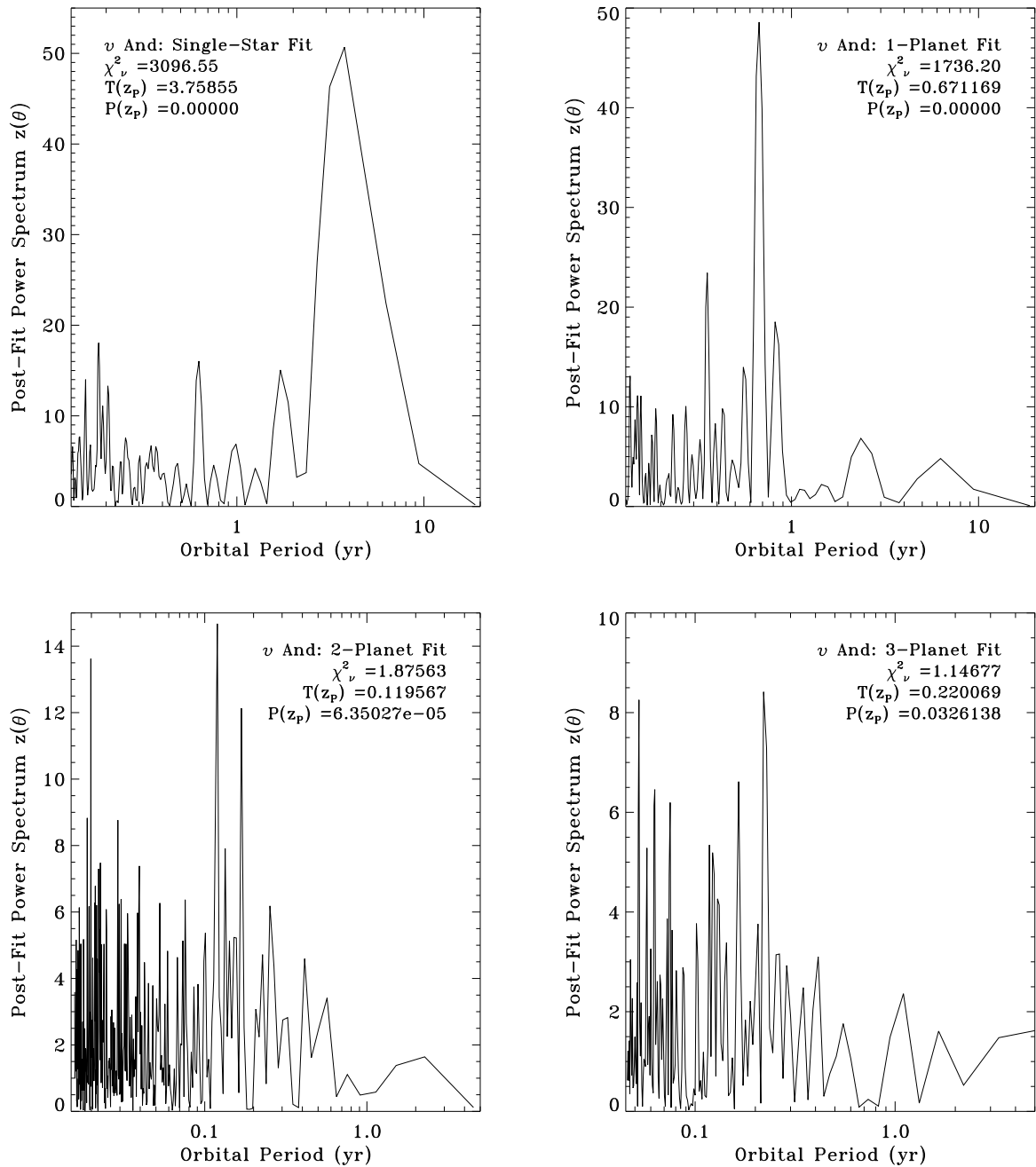


Figure 7.3 Same as Figure 7.2, but for the v And planetary system. The periodogram analysis correctly identifies the periods of the two outer planets (two upper panels), and rules out the presence of additional planets after subtraction of all planetary signatures (lower right panel). Due to very short period of the innermost planet, instead, after removal of the signatures of v And c and v And d the periodogram search identifies a significant peak in the spectrum which does not correspond to the true period of v And b (lower left panel)

would be ~ 0.2 yr, or 72 days. Due to the fact that *some* points are spaced much closer than that, the periodogram can effectively identify signals with periods as short as 15 days. Increasing the number of observations would obviously increase the ability to recover even shorter periods. Improvements in this direction can be obtained also by extending the range of test frequencies to values that are much greater than the average Nyquist frequency, and by over-sampling the spanned frequency range, in order to obtain information on frequency bins that are much smaller than the typically lowest independent frequency, that corresponds to the inverse of the timespan of the input data (i.e., the frequency such that the data can include one complete cycle). In our present analysis we have not quantified the effect of these different choices.

Furthermore, the results summarized in Table 7.2 tell us that well-sampled periods up to roughly the mission lifetime constitute ‘easy’ cases, for which the correct period can be identified with high confidence and accuracy (typically better than 7-8%), and this independently on the actual magnitude of the astrometric signature, as far as it lies above the single-measurement error. Figure 7.4 provides a graphical example of the results in Table 7.2 for the ‘easy’ case of HD 82943.

Finally, when $T > 5$ yr we enter a regime in which the classic periodogram is intrinsically doomed to fail. Increasing the number of observations (without increasing the mission length) or manipulating the frequency range and the way it is sampled does not improve the results. In fact, several authors (e.g., Black & Scargle 1982; Walker et al. 1995; Cumming et al. 1999) in the past highlighted that the periodogram power at periods exceeding the timespan of the data can be significantly reduced in the traditional periodogram formula. From the results in Table 7.2 we note how, in all the cases where the actual orbital period of the planet is greater than 5 years, the periodogram still identifies a significant periodic signal, but the peak systematically appears at a period of order of the total timespan of the data. Figure 7.5 provides a graphical representation of the data in Table 7.2 for the classic case of 55 Cnc, which harbors the planet with the longest period discovered so far. The situation is somewhat different from the spectroscopic case, where as T lengthens the radial velocity amplitude decreases, and indeed the peaks in the power spectrum relative to long period signals are significantly reduced. For astrometry, the amplitude of the signal increases with

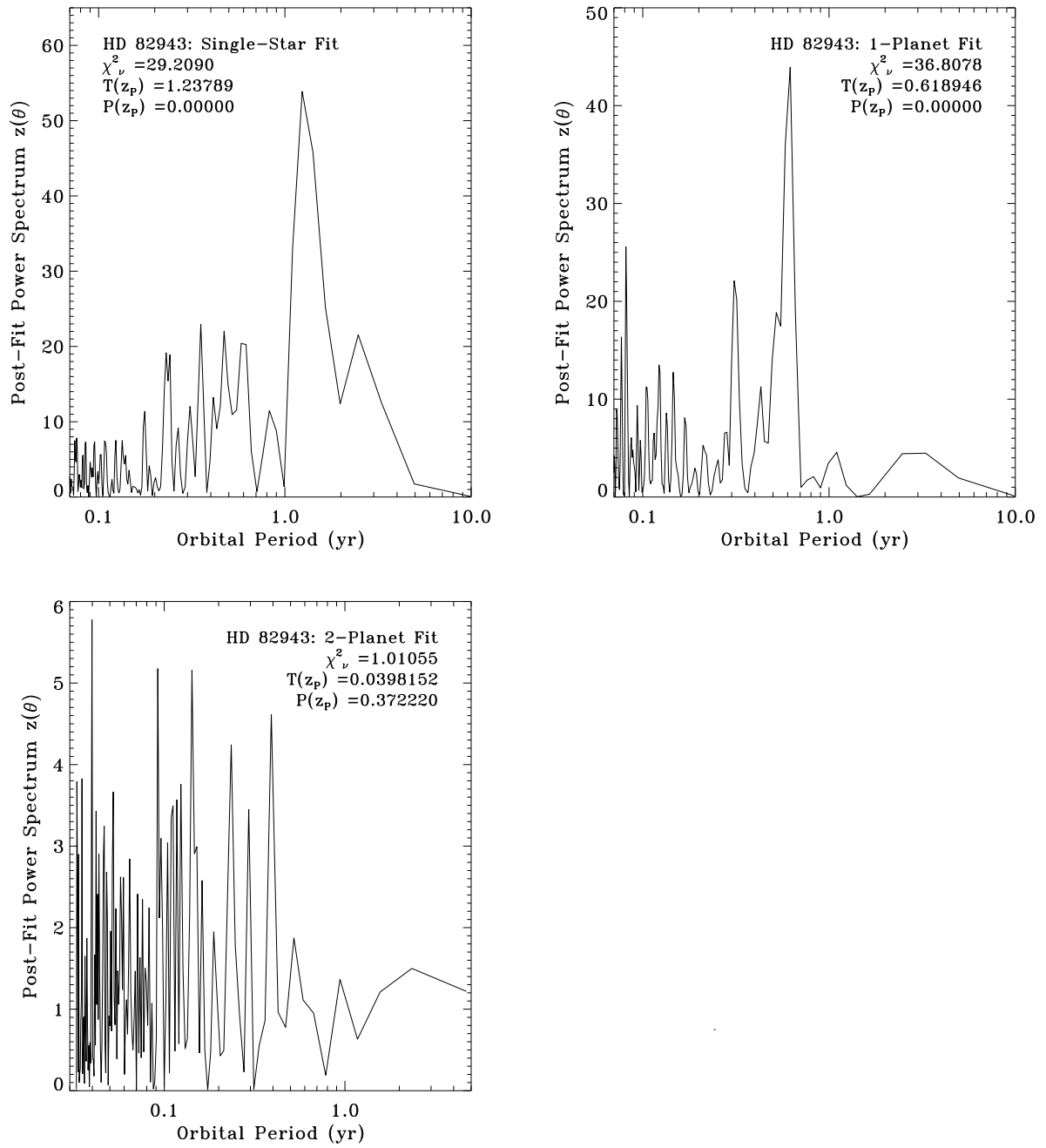


Figure 7.4 Same as Figure 7.2, but for the ‘easy’ case of the HD 82943 planetary system

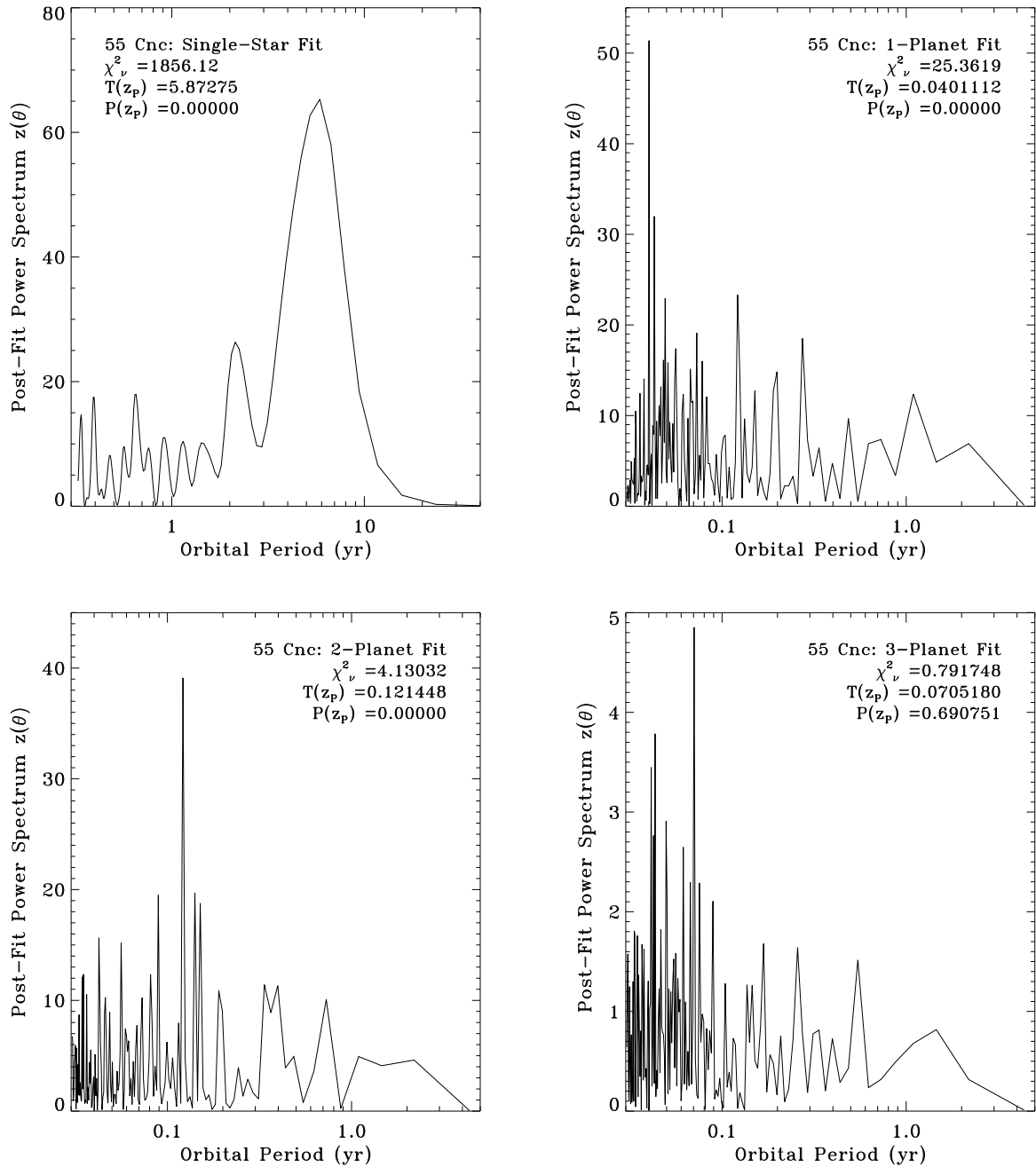


Figure 7.5 Same as Figure 7.2, but for the case of the 55 Cnc planetary system. The planet inducing the larger signature, 55 Cnc d, is identified immediately in the power spectrum (upper left panel), but, similarly to the case of HD 38529 c shown in Figure 7.2, the incomplete orbital sampling causes the periodogram analysis to identify an incorrect value for the orbital period of 55 Cnc d

increasing T , and in the sample of the presently known extra-solar planetary systems all companions are massive (as they are easier to detect by spectroscopy). The astrometric signal-to-noise ratio $\alpha/\sigma_d \gg 1$, and so, even if only a fraction of the orbit is sampled during the 5 years of simulated mission lifetime, the acceleration in the residuals is easily disentangled from the proper motion and a significant peak in the spectrum can also be identified. Nevertheless, the exact period cannot be recovered in a periodogram analysis. This systematic trend of a significant peak detected at $T \simeq L$ whenever the true period is greater than the timespan of the data is likely to become less evident for sufficiently small-mass planets (or, equivalently, sufficiently distant systems) on sufficiently long-period orbits. In fact, a reduction in the measured amplitude of long-period signals may occur either in the case of $\alpha/\sigma_d \rightarrow 1$ or when T is so long that secular effects such as proper motion begin overlapping efficiently to the astrometric signature. We have not investigated these issues here, as the main focus of this paper is on the actual characteristics of the multiple-planet systems discovered so far, and how they can be detected and measured with SIM.

7.3.1.3 Search for Periodicities when $T > L$ As we have seen, there exist regimes of orbital periods (shorter than the SIM mission lifetime) for which the Lomb-Scargle periodogram approach is robust, but others (comparable to or longer than the duration of the observations) for which the periodogram analysis fails to provide sensible results. One possible solution to overcome the ‘impasse’ was proposed in the recent past ([Walker et al. 1995](#); [Nelson & Angel 1998](#); [Cumming et al. 1999](#)). It consists of utilizing the zero point of the sinusoid in the fit as a free parameter, i.e. letting the mean of the data to float during the fit. This is contrary to what happens in the classic periodogram formula, in which the mean (taken as a proxy for the zero point) is subtracted from the data, and thus assumed to be perfectly known. When applied to radial velocity data, the floating mean periodogram approach has been shown to be successful at confirming existing companions and characterizing variations in the observation residuals due to long-period companions with orbits still awaiting phase closure (e.g., [Fischer et al. 2001](#)). We choose a different approach, with the aim of illustrating the potential of a strategy for period searches that tiles the classic periodogram approach to the Fourier analysis of periodic signals. When combined with the

standard χ^2 statistics, this multi-method approach to planet detection provides an operational framework that may also be applied more in general to datasets from other astrometric observatories such as the upcoming ESA Cornerstone Mission GAIA (Perryman et al. 2001).

From the theory of Fourier analysis we know that a periodic, but non-sinusoidal, motion can be represented by a series containing a sinusoidal term at the fundamental frequency (corresponding to the actual period of the motion) plus higher order harmonics at exact multiple integers of this frequency, which carry on the information about the magnitude of the distortion from a purely sinusoidal motion due to the eccentricity (see for example Monet 1983). In the tangent plane to the celestial sphere, for the j -th planet in a system, the two components of its projected orbital motion can then be written as:

$$\begin{aligned} x_{j,tan} &= \sum_{k=0}^{\infty} a_{k,j} \cos k\gamma_j t + \sum_{k=0}^{\infty} b_{k,j} \sin k\gamma_j t \\ y_{j,tan} &= \sum_{k=0}^{\infty} c_{k,j} \cos k\gamma_j t + \sum_{k=0}^{\infty} d_{k,j} \sin k\gamma_j t \end{aligned}$$

where $j = 1, \dots, n_p$, and $\gamma_j = 2\pi/T_j$. The series is quickly convergent except for large eccentricities. For moderately eccentric orbits, say $e \leq 0.5$, three terms (fundamental, first and second harmonic) are sufficient to cover more than 95% of the signal (Jensen & Udrych 1973; Konacki et al. 2002). For the purpose of our analysis, we have tested the ability of the above model to detect a significant long-period signal in the case of the five multiple systems (HD 37124, HD 38529, HD 74156, 55 Cnc, and 47 UMa) containing one planet on a moderately eccentric ($e \leq 0.40$), long-period orbit ($T > 5$ yr). We have limited the Fourier expansion to the second harmonic term ($k_{max} = 3$), and performed a linear fit (the unknowns being the parameters a_k, b_k, c_k, d_k , for $k = 0, \dots, k_{max}$) to the simulated SIM astrometric data relative to the systems described above, as a function of a large number of trial frequencies (4000) corresponding to the period range 0.01-20 yr. Under the assumption of coplanarity of the orbits, then in the case of 47 UMa the inner planet has a larger signature, thus the outer planet signal has been searched for utilizing a model in which the Fourier expansion is superposed to a fully Keplerian orbit for the inner planet. The results are summarized in Figure 7.6.

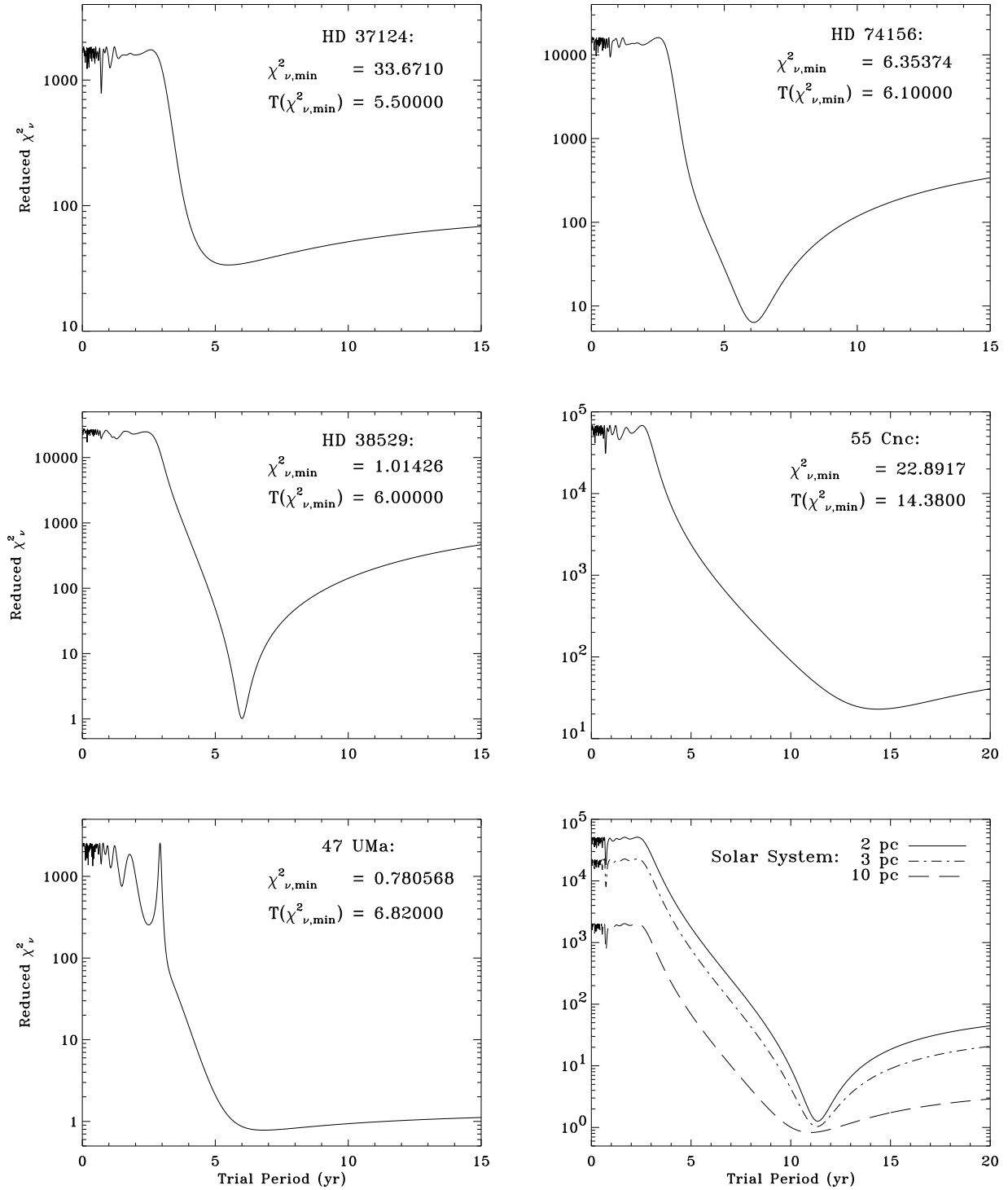


Figure 7.6 Reduced chi-square χ^2_{ν} as a function of a dense grid of trial periods for the five planetary systems harboring one planet with a period exceeding the timespan of SIM observations (two upper, two middle, and lower left panels). For comparison, the lower right panel shows the results of the same procedure applied to our own solar system, placed at increasing distance from the observer (details in the text)

The two upper, the two middle, and the lower left panels show the behavior of the reduced chi-square χ_ν^2 as a function of the dense grid of trial periods for the abovementioned systems, again setting an average value of the inclination $i = 45^\circ$. As opposed to the periodogram analysis, the Fourier series approach is capable of identifying the correct period of the outer planet, corresponding to the minimum of χ_ν^2 , to better than 4% in all the five cases. The periodicity with the larger amplitude can be correctly retrieved with high accuracy independently of the underlying presence of the second, inner companion, which is clearly evident from the fact that χ_ν^2 still departs significantly from unity even at its minimum. There are two exceptions, i.e. 47 UMa c, beyond which at present no other planetary companions have been discovered, and HD 38529 b, for which χ_ν^2 appears to be consistent with the outer planet being the only one in the system due to the very low signature induced by the inner planet. Nonetheless, as we have seen in the previous Section, the signal from the inner companion can still be identified in the periodogram power spectrum with high confidence, even in a case in which the χ^2 statistics approach is more sensitive to failure. These results underline the importance of utilizing a range of different tools for planet detection, which can be combined in order to improve significantly the efficiency with which planetary signatures can be revealed even at low values of the astrometric signal-to-noise ratio α/σ_d .

[!t]

Finally, we note how in Figure 7.6 the minima of χ_ν^2 for HD 37124 c, 55 Cnc d, and 47 UMa c are broader than those for HD 74156 c and HD 38529 d. This is primarily due to the combined effect of the magnitude of the astrometric signature induced on the parent star and the fraction of the orbit covered by the observations. For comparison, the lower right panel shows the results of a simulation in which the same fitting procedure was applied to our own solar system (nine independent, coplanar Keplerian orbits), placed at different distances from the observer. The dominant signature is the one associated with Jupiter, and its period is easily identified with an accuracy of 5-6%. As we move farther away from the observer, the value of the minimum of χ_ν^2 , which is initially located at $\chi_\nu^2(\min) = 1.26$, indicating the presence of a second underlying signal (from Saturn, the second heaviest planet in our system and the one producing the second largest signature), decreases, and eventually at 10 pc it is perfectly consistent with Jupiter being the only planet around the Sun. At the same time,

Table 7.3. Ranges of plausible starting guesses

Planet	Plausible χ_ν^2 Ranges	Plausible T Ranges
HD 37124 c	$28.62 \leq \chi_\nu^2 \leq 38.72$	$4.69 \leq T \leq 7.12$ yr
HD 74156 c	$5.40 \leq \chi_\nu^2 \leq 7.31$	$5.85 \leq T \leq 6.38$ yr
HD 38529 c	$1.17 \leq \chi_\nu^2 \leq 0.86$	$5.93 \leq T \leq 6.08$ yr
55 Cnc d	$19.46 \leq \chi_\nu^2 \leq 26.33$	$12.99 \leq T \leq 16.25$ yr
47 UMa c	$0.66 \leq \chi_\nu^2 \leq 0.90$	$5.91 \leq T \leq 9.22$ yr
Jupiter (2 pc)	$1.07 \leq \chi_\nu^2 \leq 1.45$	$11.11 \leq T \leq 11.61$ yr
Jupiter (3 pc)	$0.87 \leq \chi_\nu^2 \leq 1.18$	$10.98 \leq T \leq 11.66$ yr
Jupiter (10 pc)	$0.70 \leq \chi_\nu^2 \leq 0.95$	$10.16 \leq T \leq 12.07$ yr

Note. — Ranges of plausible starting guesses for the orbital period of the 5 planets with $T > 5$ yr in the presently known extrasolar multiple-planet systems. For reference, the same results are reported for Jupiter in simulations of the solar system as ‘seen’ by SIM at increasing distances (in pc) from the observer. The results are derived in the context of the Fourier analysis approach discussed in the text. Preliminary values of T are considered acceptable if the corresponding χ_ν^2 does not differ from the minimum $\chi_{\nu,\min}^2$ by more than $\pm 15\%$ of the latter value

while the presence of the second largest planet becomes undetectable, also the signature from Jupiter decreases and correspondingly, for the same fraction of the orbit covered by the observations, the slope of the χ_ν^2 curve at long periods becomes increasingly less steep.

In the perspective of the optimization of a global search strategy for the determination of the best configuration of starting values for the orbital parameters in the fully Keplerian fit *for newly discovered planetary mass objects*, a precise guess for the actual value of the orbital period is needed, in order to try to minimize the dimensions of the parametric space to be searched. Suppose in fact we select as plausible preliminary values of T those whose χ_ν^2 difference with the minimum $\chi_{\nu,\min}^2$ is less than 15% of the latter value, as done by Guirado et al. (1997) in their astrometric orbit determination of a low-mass companion around the star AB Doradus. This would mean that, for the cases shown in Figure 7.6, assuming no spectroscopic orbits are available, plausible starting guesses for the orbital period in a subsequent global least-squares fit would lie in the ranges reported in Table 7.3. As it is clear, whenever we have a configuration approaching a regime in which χ_ν^2 has a very broad minimum (HD 37124 c, 47 UMa c, 55 Cnc d, Jupiter at 10 pc), this corresponds to a range of plausible starting guesses for the period covering several years, and it is likely this would cause accurate orbit determination and mass measurements to become a more difficult task.

Clearly, the results shown in these Sections constitute only a very preliminary investigation of the potential of the approach to the problem of real-life detection of *newly discovered planetary systems* with a method that combines χ^2 statistics, periodogram and Fourier analysis of SIM astrometric observation residuals. Due to the illustrative purpose of our work, some important topics have been left aside, such as estimates of the degradation in SIM's ability to detect planets with low values of α/σ_d on long-period orbits due to significant correlation with the target's proper motion. Also, some relevant technical issues remain open, such as the possibility to not only provide robust estimates of the reliability of the adopted model, through additional statistical hypothesis testing (e.g., Bevington & Robinson 2003), but also assess the reliability of the estimates themselves, through further testing and placing statistical constraints on the post-fit observation residuals and their covariance matrices, in order to select the optimal least-squares solution (e.g., Bard 1974; Bernstein 1997). Nevertheless, within the limited scope of our study, we have been able to provide

quantitative examples which are useful for understanding that it will be very beneficial if a variety of numerical and statistical tools will be implemented to maximize the robustness of the method aimed at verifying the true significance and reliability of a detection.

7.3.2 Multiple-Planet Orbits Reconstruction

Once a reliable detection of a system of planets has been established, a number of other important issues must be addressed, all primarily related to how well it is possible to measure the orbital parameters and masses of each planet.

As soon as the number of planets in a system is greater than one, the parameter space to investigate becomes immediately very large. In this illustrative study, we have parameterized the ability of SIM to measure multiple-planet systems in terms of their astrometric signatures, orbital periods, eccentricities, and inclinations of the orbital planes. We have then investigated the potential of SIM to make meaningful coplanarity measurements by gauging how accurately the relative inclination of pairs of planetary orbits may be determined. Finally, we have quantified the improvement in the accuracy on the determination of orbital parameters and masses that maybe reached when both astrometric and spectroscopic data are available.

7.3.2.1 Accuracy in Orbit and Mass Determination The first relevant question to be addressed is: what is the impact on the accuracy in orbital parameters and mass determination when the number of planets in a system is larger than one, and the number of parameters to be fitted correspondingly increases?

Table 7.4 shows, for each planet in the 11 systems under consideration, the ratios of rms errors σ_m for the most relevant parameters (M_p , a , T , e , and i) derived from a multiple-planet fit to the same quantities σ_s obtained from a single-planet solution (in simulations where only one planet was generated around the observed parent star). The values are averaged over the inclination angle.

In general, for planets with periods $T \leq L$, the two-planet fit (or three-planet fit, as in the case of ν And and 55 Cnc) degrades the orbital elements and mass estimates by $\sim 30 - 40$

Table 7.4. Ratios of the rms errors for various parameters

Planet	$\sigma_m(M_p)/\sigma_s(M_p)$	$\sigma_m(a)/\sigma_s(a)$	$\sigma_m(T)/\sigma_s(T)$	$\sigma_m(e)/\sigma_s(e)$	$\sigma_m(i)/\sigma_s(i)$
<i>v</i> And b	2.42	2.32	1.56	0.98	1.36
<i>v</i> And c	1.42	1.35	1.59	1.40	1.35
<i>v</i> And d	1.35	1.37	1.54	1.52	1.35
55 Cnc b	1.39	1.39	1.49	1.35	1.23
55 Cnc c	1.48	1.48	1.40	1.14	1.18
55 Cnc d	1.00	0.76	0.83	1.53	1.71
47 UMa b	15.4	18.0	9.64	1.54	2.31
47 UMa c	1.04	1.09	1.12	3.69	2.71
Gliese 876 b	1.21	1.21	1.21	1.39	1.12
Gliese 876 c	1.22	1.23	1.55	1.14	1.12
HD 12661 b	1.15	1.15	1.24	1.15	1.12
HD 12661 c	1.19	1.21	1.37	1.33	1.10
HD 160691 b	1.54	1.54	1.86	1.38	1.32
HD 160691 c	2.09	2.07	2.00	1.78	1.66
HD 168443 b	1.13	1.15	1.21	1.13	1.09
HD 168443 c	0.46	0.47	0.86	0.97	1.09
HD 37124 b	1.18	1.17	1.27	1.16	1.11
HD 37124 c	0.28	0.48	1.00	0.84	0.86
HD 38529 b	1.19	1.19	1.19	1.04	1.07
HD 38529 c	0.86	0.85	0.78	0.55	0.87
HD 74156 b	1.08	1.08	1.29	1.06	1.06
HD 74156 c	0.59	0.71	0.94	0.68	0.66
HD 82943 b	2.87	2.08	1.69	3.23	1.77
HD 82943 c	2.50	1.81	1.95	2.05	1.70

Note. — Ratios of the rms errors σ_m for a given parameter (M_p , a , T , e , and i) derived from a multiple-planet fit (in simulations where the full planetary system was generated around the parent star) to the rms errors σ_s derived from a single-planet solution (in simulations where only one planet orbited the central star). The values are averaged over the inclination angle

% with respect to the single-planet fit, with typical fluctuations of order of 5 – 10 % among different parameters. From closer inspection of Table 7.4, some particularly interesting cases stand out.

First of all, there is a clear trend for larger values of the ratio σ_m/σ_s for a given parameter, as the magnitude of the astrometric signature decreases. For example, HD 82943 b and HD 82943 c, with signatures of only $65/\sin i \mu\text{as}$ and $22/\sin i \mu\text{as}$ respectively (see Table 7.1), have values of the rms errors typically about a factor 2 or more larger than the respective single-planet case, as opposed for example to the case of the Gliese 876 system, in which the two planets, producing larger signals, are measured together only about 20% worse than if they were the only orbiting bodies.

The second relevant feature arising from the results of Table 7.4 concerns those systems in which the orbit of the outer planet is not fully sampled during the 5 years of simulated SIM observation. In three such cases (HD 38529 c, HD 37124 c, and HD 168443 c), the ratios $\sigma_m/\sigma_s \leq 1$ for almost all parameters shown in Table 7.4. The reason for this is to be found in the intrinsic superiority of the model containing more than one planet, when it is applied to configurations where the outer planet has $T > L$ and produces a signature much larger than the inner one. In fact, the larger number of free parameters (with respect to the single-planet case) is compensated by the superior model, and the net result is that in the least squares solution a smaller fraction of the outer planet’s signal is identified as proper motion, with the consequence of a more precise determination of the outer planets’ orbital elements and masses as opposed to the single-planet solution (up to about a factor 2-3 better). This behavior is not very prominent for 55 Cnc d, due to its much longer period ($T \simeq 3L$), which translates in such poor sampling of the orbit that the larger signature is not enough for the orbital solution to improve significantly.

Finally, the case of the 47 UMa system stands out. Assuming coplanarity of the two planets’ orbits, then the astrometric signature of the outer one is smaller. The inner planet’s orbit is sampled completely only once during the timespan of SIM observations, and the outer planet’s period is 1.42 times longer. Even utilizing the spectroscopic orbital elements as starting guesses for the iterative least square procedure, the net result is that a significant portion of the inner planet’s signal is assigned to the outer one, and the accuracy in the

determination of semi-major axis, period, and mass is degraded by over an order of magnitude with respect to the single-planet solution. For what concerns the uncertainties on eccentricity and inclination angle, the degradation effects due to this particular configuration are only marginal. However, the orbital solution for the outer planet does not benefit from this redistribution of the inner planet’s signal, and its orbital parameters and mass are also more poorly determined than in the single-planet case.

In Figure 7.7 and 7.8 we provide a detailed visualization of the results on orbit reconstruction and planet mass determination for the three-planet system 55 Cnc and the two-planet system HD 12661, which are representative of the variety of configurations addressed in this study, i.e. well-sampled, well-spaced orbits, or poorly sampled due to either very short or very long periods, high values of the astrometric signal-to-noise ratio as well as values of α/σ_d approaching 1. In the two Figures, the fractional deviation of the measured from the true value for the five relevant parameters discussed above is plotted against the inclination angle, both in the case of single- and multiple-planet realizations. Four of the five parameters (M_p , a , e , and i) are primarily sensitive to the value of α/σ_d . The larger the astrometric signal-to-noise ratio, the more accurate their measured value, independently on the orbital period. So for example in the 55 Cnc system the outermost planet has these parameters best measured (even though only one third of its orbit is sampled), while the middle planet’s parameters are the least accurately determined. An important exception in this case is the orbital eccentricity of the innermost planet: its orbit is tidally circularized ($e = 0.02$), and although its astrometric signature is a factor 2 larger than the middle planet, its period is so short that the inadequate sampling causes the value of e to be more poorly constrained as compared to the one of the middle planet. On the contrary, the accuracy with which T itself is retrieved primarily depends on how well the orbit is sampled (center left panels in Figures 7.7 and 7.8). Thus, wider orbits have the period less accurately measured, while the accuracy on the determination of the other parameters is improved.

As the inclination i decreases, we move from a perfectly edge-on to almost face-on configuration, i.e. from a situation in which only one dimension is actually measured to one in which the SIM measurements provide full two-dimensional information. At the same time, the true mass inferred for each planet from the radial velocity data increases, therefore

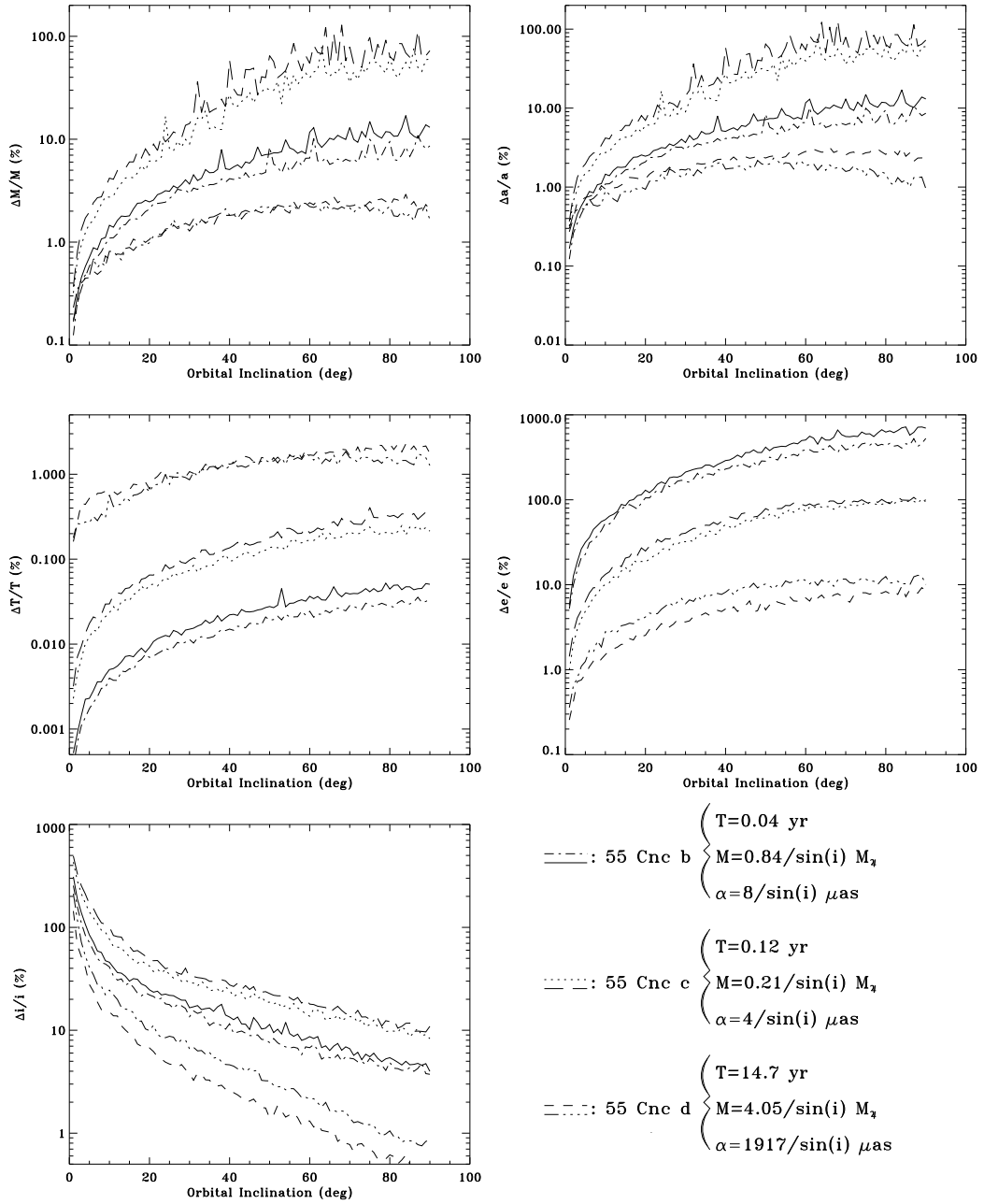


Figure 7.7 Fractional errors (%) for M_p , a , T , e , and i , as a function of the inclination of the orbital plane, in the case of the 55 Cnc planetary system. In each panel, the results for a given parameter are shown for all the system components, for the cases of a single-planet solution (dashed-dotted, dotted, and short-dashed lines for 55 Cnc b, 55 Cnc c, and 55 Cnc d, respectively) and a complete three-planet model (solid, long-dashed, and dashed-dotted-dotted lines for 55 Cnc b, 55 Cnc c, and 55 Cnc d, respectively)

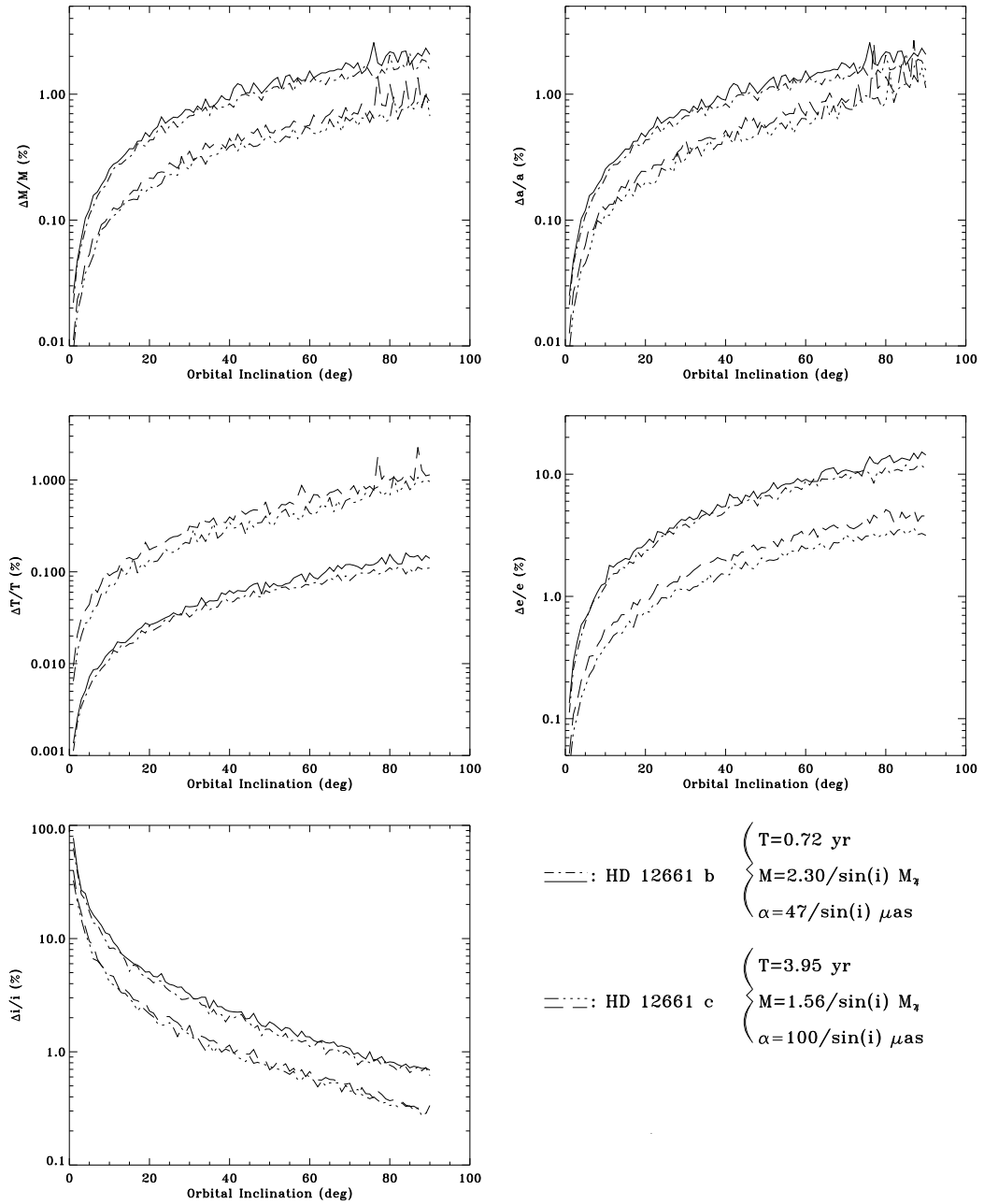


Figure 7.8 Same as Figure 7.7, but for the case of the HD 12661 planetary system. The dashed-dotted and dashed-dotted-dotted lines are relative to the single-planet solution for HD 12661 b and HD 12661 c, respectively. The solid and long-dashed lines are relative to the dual Keplerian fit for HD 12661 b and HD 12661 c, respectively

the astrometric signature is larger. These effects combined translate into increasingly more accurate measurements of the planet’s mass, semi-major axis, eccentricity, and period, as $i \rightarrow 0^\circ$. At the same time, the observations are less sensitive to the inclination itself, and its fractional measurement error increases (lower left panels in both Figure 7.7 and 7.8).

The present set of extra-solar planetary systems covers a relatively wide range of shapes and sizes of the orbits, and planetary masses. We can then attempt to generalize the results presented here to characterize the variety of configurations of potential planetary systems in the solar neighborhood for which SIM could provide accurate measurements, for the given template observing strategy outlined in Section 7.2.1. In the three-dimensional parameter space defined by astrometric signal-to-noise ratio α/σ_d , period T , and eccentricity e we have identified the loci for the measurement of a given orbital parameter or mass of a planet in a multiple system to a specified level of accuracy. Figure 7.9 shows iso-accuracy contours for M_p , a , T , e , i , and Ω (expressed in percentages of the true value) in the $e - T$ plane. The results are averaged over the inclination angle. The general indication is that the correlation between these two parameters is relatively limited. When the sampling is poor due to very short-period orbits, the degradation in accuracy is common to all parameters, and regardless of the orbital eccentricity. For well-sampled orbits, the parameters can be measured better, with varying degrees of improved accuracy. Again, the results are essentially insensitive to e . In fact, massive planets on relatively long-period orbits such as 55 Cnc d produce astrometric signals large enough that the fraction of the orbit covered by the observations still allows for accurate measurements of the orbital elements, regardless of the value of the eccentricity. An important exception is constituted by the accuracy on the eccentricity itself (central right panel), which appears to degrade for periods exceeding the 5-year SIM mission duration, unless $e \geq 0.1$.⁵ Finally, it must be noted how the accuracy in the determination of the orbital period (central left panel) shows a behavior opposite to that of the other parameters, in agreement with the fact that how well the periodicity of the astrometric signal can be measured depends upon the number of times an orbit is fully sampled. The same mostly

⁵When the orbital period is sufficiently long or the mass of the planet sufficiently low, instead, e is likely to play an important role in the degradation of the reachable accuracy on other parameters as well, as eccentric orbits not sampled in correspondence of the pericenter passage may not be properly measured by the fitting algorithms due to a lack of curvature sufficient to disentangle the periodic motion from the stellar proper motion

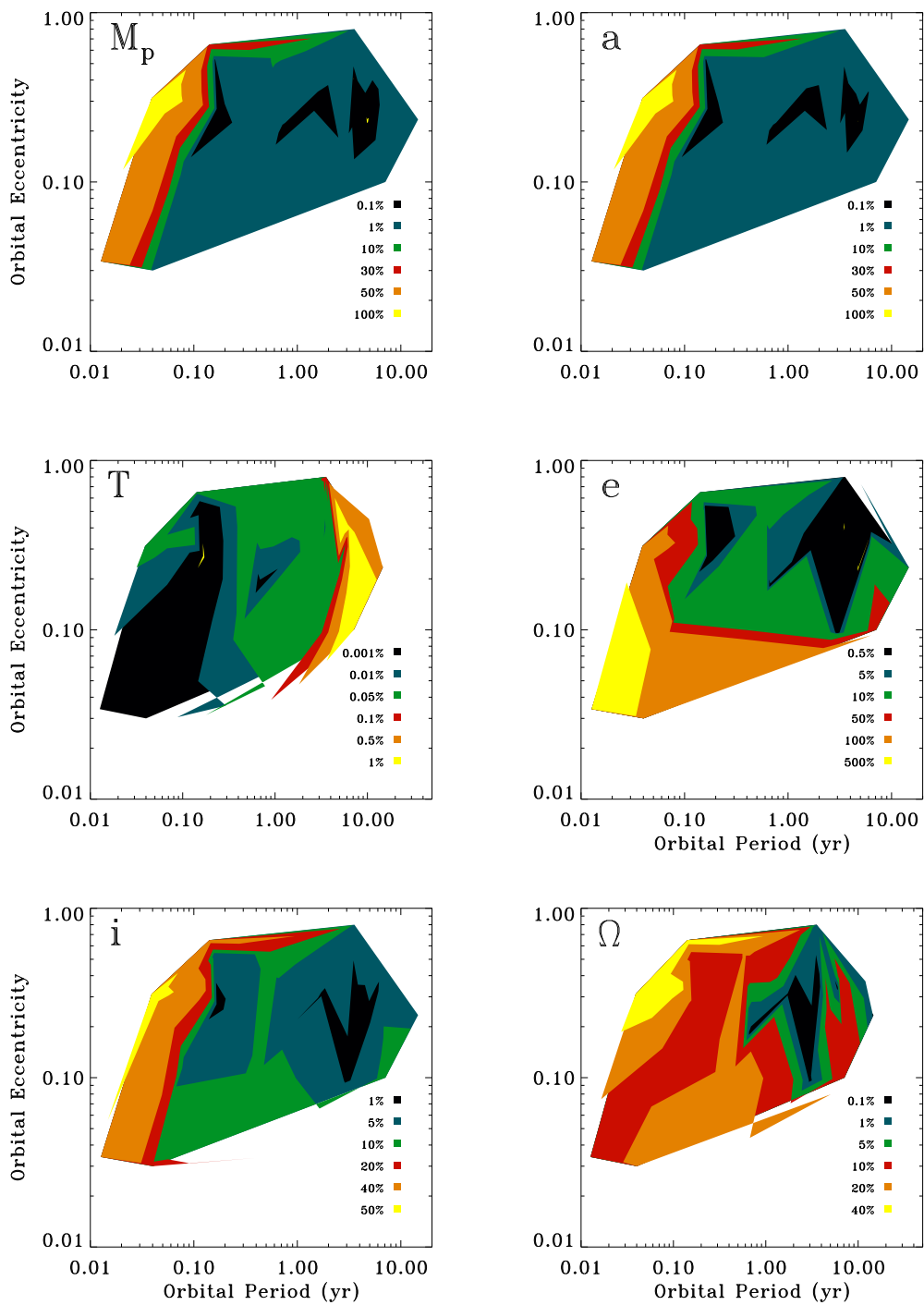


Figure 7.9 Iso-accuracy contours in the $e - T$ plane, for the most relevant orbital parameters and planet mass. The results in each panel have been obtained utilizing the 11 planetary systems known to-date. The contour regions are color-coded by the accuracy achieved in the determination of the given parameter, expressed as a fraction (%) of its true value

uncorrelated behavior is evident in the plane defined by signal-to-noise ratio and eccentricity.

Figure 7.10 shows the same results, but this time in the plane defined by α/σ_d and T . Here we appreciate a clear correlation between these two crucial parameters, as it is shown by the trend for lower accuracy on M_p , a , e , i , and Ω towards low values of α/σ_d and short periods, and for improved determination of orbital elements and masses for large values of α/σ_d and longer periods. Again, the orbital period itself behaves in an opposite fashion.

It is possible to provide an analytic representation for the dependence of the fractional errors on the estimated orbital elements and masses as a function of the three quantities α/σ_d , T , and e . In order to do so, we have performed a fit to the data (i.e., the fractional uncertainties σ_p on a given parameter, where the subscript p can be equal to M_p , a , T , e , i , or Ω) with a model of the form:

$$\sigma_p(\%) = \eta_0 \times (\alpha/\sigma_d)^{\eta_1} \times T^{\eta_2} \times e^{\eta_3} \quad (7.12)$$

The results are summarized in Table 7.5, and are averaged over the inclination angle. Again, similarly to what we saw in Figures 7.9 and 7.10, we realize how, for example, the fractional errors on M_p , a , and i are dominated by the behavior of α/σ_d and T , while the dependence on e in such cases is relatively weak. For σ_e , instead, the dependence on the eccentricity itself is much stronger. Finally, in the case of σ_T , the exponent of α/σ_d , that would have the fractional error on the orbital period decrease as the astrometric signal-to-noise ratio increases, is largely compensated by the opposite, and stronger, dependence on T itself, with the result that, as T increases, σ_T grows larger as well. It is important to stress the limits of applicability of such empirical multi-dimensional power-laws. In fact, these formulas do not include a variety of effects, such as the degradation induced by the increasingly poor sampling at very short or very long periods. Due to the former effect, for example, the best-fit formula for σ_T systematically underestimates the errors on the orbital period for $T < 0.1$ yr. In general, the agreement between the power-laws shown in Table 7.5 and the data is good when the values of σ_p are larger than 1%, while discrepancy factors of a few typically arise when the fractional errors on the parameters become very small. Finally, we expect the functional dependence of the fractional errors on α/σ_d , T , and e , as well as the values of the zero-points η_0 , to be somewhat different when a range of possible observing strategies and

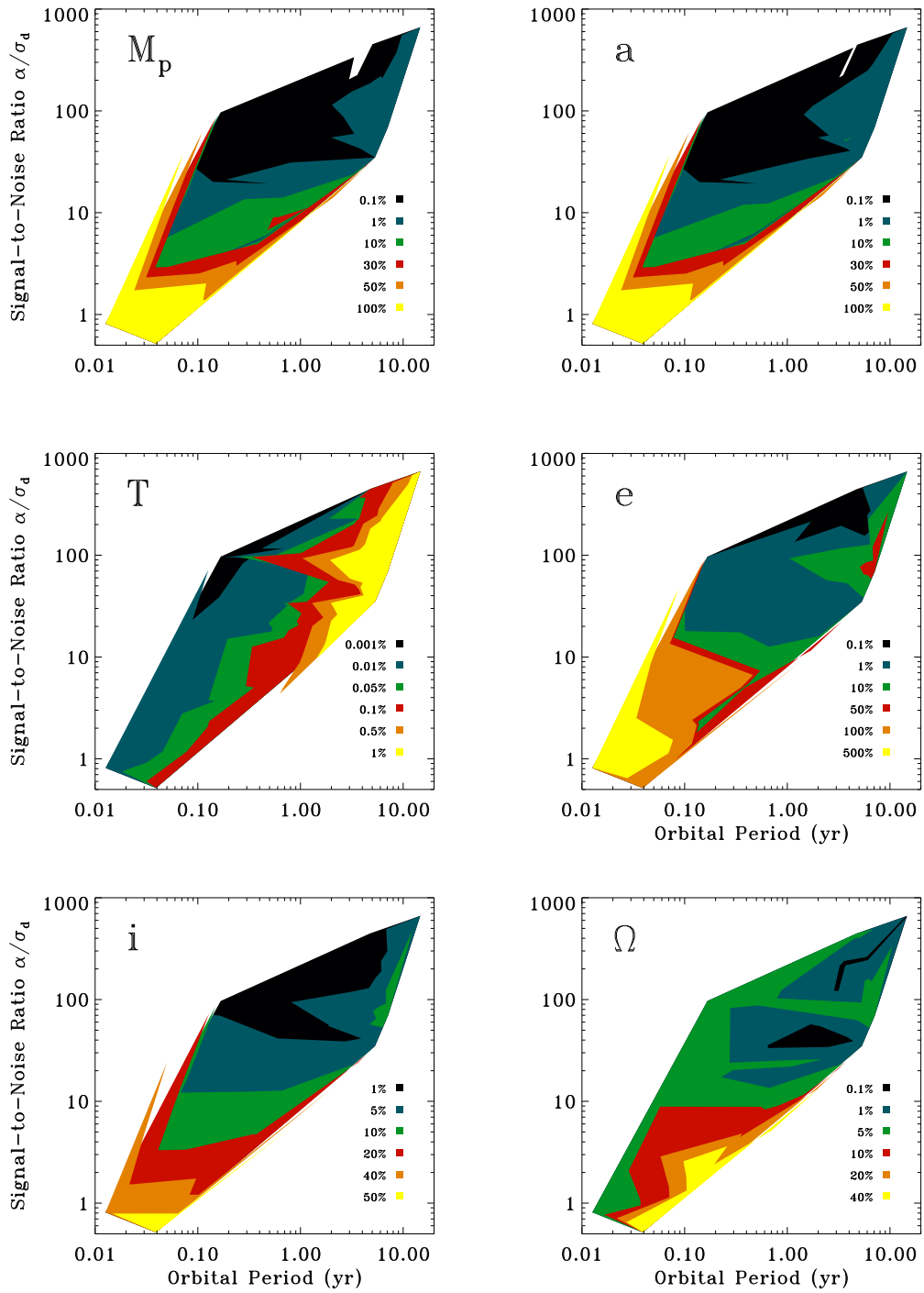


Figure 7.10 Same as Figure 7.9, but with the contour regions identified in the $\alpha/\sigma_d - T$ plane

Table 7.5. Power-law fit to fractional errors on various parameters

Parameter Error (%)	Best-Fit Power-Law
σ_{M_p}	$34.96 \times (\alpha/\sigma_d)^{-0.72} \times T^{-0.42} \times e^{0.35}$
σ_a	$34.08 \times (\alpha/\sigma_d)^{-0.73} \times T^{-0.43} \times e^{0.36}$
σ_T	$2.50 \times (\alpha/\sigma_d)^{-1.19} \times T^{2.65} \times e^{-0.12}$
σ_e	$23.39 \times (\alpha/\sigma_d)^{-0.87} \times T^{0.01} \times e^{-1.06}$
σ_i	$24.28 \times (\alpha/\sigma_d)^{-0.59} \times T^{-0.13} \times e^{0.08}$
σ_Ω	$67.85 \times (\alpha/\sigma_d)^{-0.43} \times T^{-0.06} \times e^{0.43}$

Note. — Results from a fit to the fractional errors on orbital elements and planet mass, assuming a three-dimensional power-law dependence on the three parameters α/σ_d , T , and e of the form: $\eta_0 \times (\alpha/\sigma_d)^{\eta_1} \times T^{\eta_2} \times e^{\eta_3}$. The results are averaged over the inclination angle

different values of the measurement errors were to be considered. In our exploratory work we have not investigated further such issues.

Taking into account the results reported in Tables 7.4 and 7.5 and those summarized in Figures 7.9 and 7.10, we can attempt to draw some general conclusions as for what concerns the ability of SIM to measure the most relevant parameters in multiple-planet systems: on average, 10% accuracy, or better, will be reached in the determination of the mass of planets in two or three-planet systems with components on periods not shorter than $T \simeq 0.1$ yr, and producing an astrometric signal-to-noise ratio $\alpha/\sigma_d \geq 5$. Similar accuracy will be attainable for systems containing massive planets with periods longer than the SIM mission duration (up to $T \simeq 3L$), which produce $\alpha/\sigma_d \geq 100$. The semi-major axis, orbital inclination, and lines of nodes will behave similarly, while the eccentricity will require $\alpha/\sigma_d \simeq 10$ for periods $T \leq L$, and accurate measurements will become increasingly more difficult to achieve for periods exceeding the mission lifetime. The orbital period will be recovered with typical accuracies of a fraction of a percent for $T \leq L$. Even for objects with $T \simeq 3L$ and producing $\alpha/\sigma_d \gg 1$, such as 55 Cnc d, 1% accuracy should be attainable.

7.3.2.2 Coplanarity Measurements As discussed in the Introduction, the increasing number of extra-solar planetary systems has motivated detailed theoretical studies on their

dynamical evolution and long-term stability. It is worth mentioning in detail the main results derived so far for some of the systems which have been the target of the larger theoretical efforts. For example, in the case of the ν And system, neglecting to first order the effects of the innermost planet on the overall stability of the system, Stepinski et al. (2000) come to the conclusion that dynamical stability requires the orbital inclination of the outer two companions to be greater than $i \sim 13^\circ$, otherwise the two objects would be too massive and gravitational interactions would disrupt the system. Furthermore, the system cannot be stable in the long term if relative inclinations are greater than 55° , 35° , and 10° , for $i \sim 64^\circ$, $i \sim 30^\circ$, and $i \sim 15^\circ$, respectively: then, the more massive the planets, the closer to coplanarity their orbits have to be, for the system not to be destabilized on a short time-scale. As for what concerns the strongly interacting two-planet system on short-period orbits around Gliese 876, Laughlin & Chambers (2001), Rivera & Lissauer (2001), and Goździewski et al. (2002) have found limits for dynamical stability on their relative inclinations that, similarly to the ν And case, are a strong function of the unknown inclination of the orbital planes (and thus unknown masses): the relative inclinations of stable systems can vary in the ranges of $\pm 15^\circ$ for $\sin i = 0.5$ up to $\pm 90^\circ$ for $\sin i = 1$. Finally, Laughlin et al. (2002) have studied extensively the 47 UMa system, and found that, somewhat surprisingly, the mutual inclination of the two long-period planets orbiting 47 UMa must be less than 45° for the system to be stable, but the results are essentially insensitive to the actual planet masses.

As the above results clearly suggest, dynamical limitations on the relative inclinations and masses of planetary companions in extra-solar multiple-planet systems cannot be stated very precisely. Such estimates suffer from large uncertainties due to the typically poorly constrained orbital inclinations and planet masses, and undetermined position angles of the lines of nodes. More accurate observational data to complement the one-dimensional radial velocity measurements are needed before the details of the long-term evolution of multiple-planet systems can be assessed with a high degree of confidence.

Figure 7.11 shows the estimated accuracy with which SIM would measure the coplanarity of the orbits of the present set of extra-solar planetary systems. After the multiple-planet fit, the estimated values of i and Ω for all components in each system were used to derive

their actual relative inclination (Eq. 7.11). In Figure 7.11, for each system, the relative inclination of each pair of planets is plotted against the (common) inclination of the orbital plane with respect to the plane of the sky. The corresponding error bars have been computed by propagating (Eq. 7.9) the formal expressions from the covariance matrix of the multiple-planet fit.

In order to establish coplanarity, we must measure $i_{\text{rel}} \simeq 0^\circ$. The first seven panels show how, as long as all components in a given system have minimum masses and orbital periods such that the astrometric signal-to-noise ratio is favorable ($\alpha/\sigma_d \simeq 10$ or greater) for any inclination of the orbital plane with respect to the plane of the sky, the quasi-coplanarity of each pair of planetary orbits can be assessed with high accuracy. Even in the case of two systems with one of the planets having period exceeding the timespan of the observations (HD 37124 and 47 UMa), the net result is that for such well-measured systems the relative inclination can be determined to be $i_{\text{rel}} \leq 3^\circ$, with relative uncertainties of a few degrees. The next seven panels of Figure 7.11 highlight instead how, when dealing with astrometric signatures approaching the detection limit ($\alpha/\sigma_d \rightarrow 1$), to make accurate coplanarity measurements will be a significantly more challenging task. In the specific cases shown, only towards quasi-face-on configurations, in which the signal from the smaller and/or shorter period planet becomes large enough (due to significantly larger projected mass), the results resemble those obtained in the favorable cases. Otherwise, the relative inclinations will typically be measured to be $i_{\text{rel}} \sim 10^\circ$ or greater, with uncertainties of additional tens of degrees. Finally, as the bottom right panel shows, for the two outer planets of the ν And system quasi-coplanarity can be reliably established, in agreement with the findings of Sozzetti et al. (2001).

It is worth mentioning another interesting feature arising from the results presented in Figure 7.11. Almost all panels show a more or less pronounced trend for increasing uncertainties in the determination of i_{rel} as we move away from the edge-on configuration, with a somewhat sharp change in behavior as $i \rightarrow 0^\circ$. The explanation is to be found in the details of the dependence of i_{rel} on i_{in} , i_{out} , and the difference $\Omega_{\text{out}} - \Omega_{\text{in}}$. In fact, as i decreases, the uncertainty in the position angle of the line of nodes grows, because of the increasing difficulty in its correct identification (Ω eventually becomes undefined at $i = 0^\circ$). However,

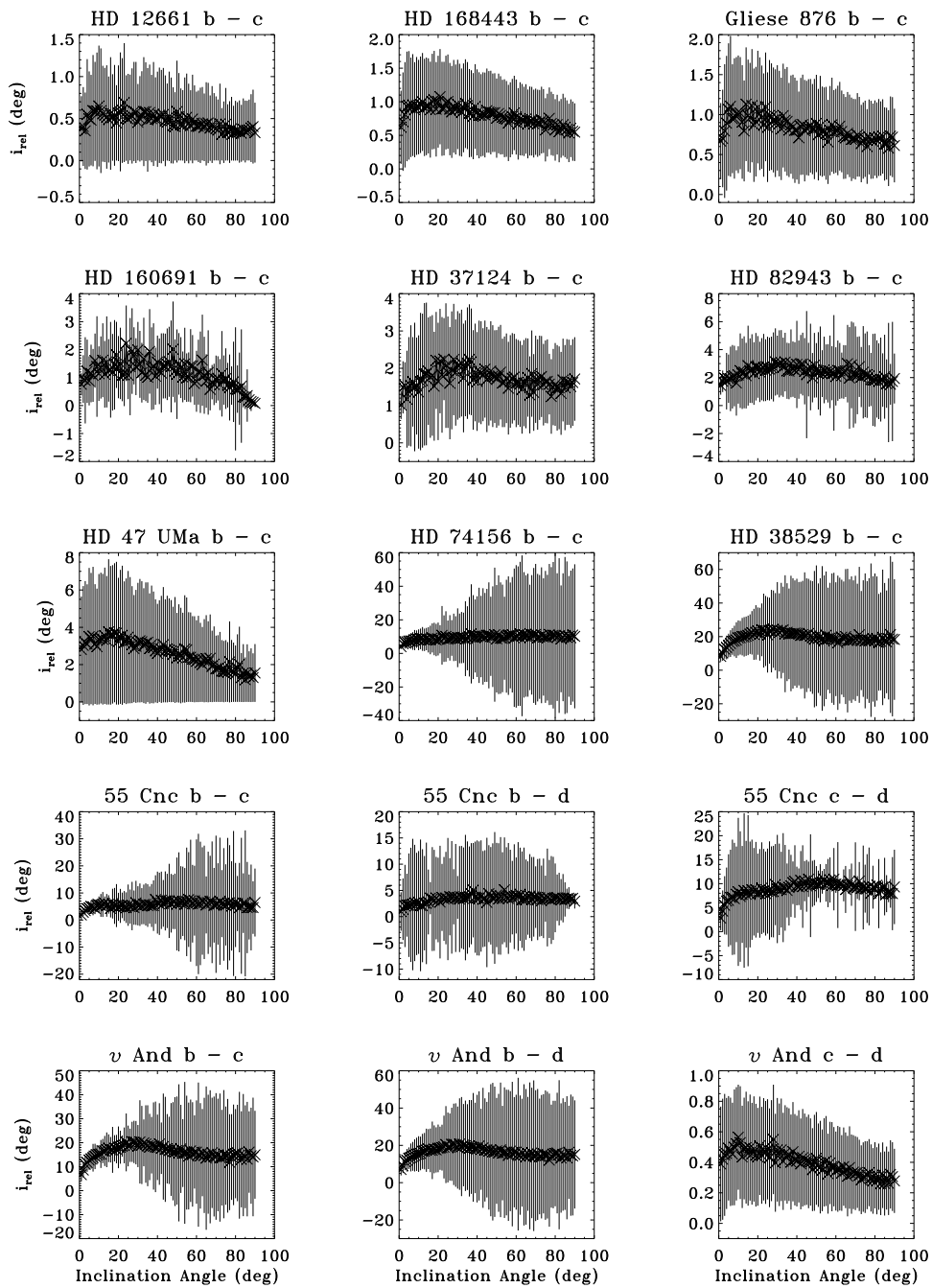


Figure 7.11 Relative inclination i_{rel} between pairs of planetary orbits as a function of the common inclination angle with respect to the line of sight, for the entire set of presently known multiple-planet systems. In each panel, the corresponding uncertainties are computed utilizing the formal expressions from the covariance matrix of the multiple Keplerian fit

the uncertainty in the value of i_{rel} defined in Eq. 7.11 increases correspondingly only up to the point in which, for sufficiently low values ($i \leq 5^\circ$) of the inclination angles, the second term $\sin i_{\text{in}} \sin i_{\text{out}} \cos(\Omega_{\text{out}} - \Omega_{\text{in}})$ of the right-hand side becomes essentially negligible with respect to the first term $\cos i_{\text{in}} \cos i_{\text{out}}$, irrespective of the fact that the uncertainty of the line of nodes keeps on growing. Thus, ultimately for quasi-face-on configurations an accurate knowledge of Ω_{in} and Ω_{out} is not required. In their recent work on extra-solar planetary system detection and measurement with GAIA, Sozzetti et al. (2001) do not consider orbital configurations of the ν And system with inclination angles less than 5 degrees. As a consequence, they come to the conclusion that when $i \rightarrow 0^\circ$ accurately estimating the coplanarity of the outer two planets of the ν And system would be difficult because of the increasing uncertainties on the measurement of Ω for the two planets. Here instead we have shown how the relative inclination becomes essentially insensitive to the retrieved values of Ω_{in} and Ω_{out} , as we approach a perfectly face-on configuration.

Finally, simulations of non-coplanar systems with $\Omega_{\text{in}} \neq \Omega_{\text{out}}$ and/or $i_{\text{in}} \neq i_{\text{out}}$ yielded similar results. Our findings help to reaffirm the importance of SIM high-precision position measurements in verifying the stability of multiple-planet system. Accurately determining the inclination angles and lines of nodes of multiple planetary orbits will allow in turn to derive meaningful mass and relative inclination angle estimates, which will be used to better constrain the results from theoretical studies on the long-term evolution of planetary systems.

7.3.2.3 Combining Radial Velocity and Astrometric Data In recent works, Eisner & Kulkarni (2001a, 2001b, 2002) have utilized a semi-analytical method to show how planet detection efficiency would benefit from the simultaneous availability of both astrometric *and* radial velocity measurements, especially as far as long-period, edge-on orbits are concerned. This combined approach has indeed proved very successful when dealing with real data. For example, utilizing both astrometric measurements from the Fine Guidance Sensor 3 on board the *Hubble Space Telescope* and ground-based precision radial velocity data, Benedict et al. (2001) have improved the accuracy on the mass estimates for the M dwarf binary Wolf 1062 by a factor 4 with respect to the same values obtained by Franz et al. (1998) using only *HST* astrometry. Very recently, the same combined method revealed itself an essential

ingredient in the spectacular determination of the first actual mass of an extra-solar planet, the outer component in the Gliese 876 system (Benedict et al. 2002).

Usually, a combined astrometric + spectroscopic orbit is obtained by modeling time-series of data from both techniques in a simultaneous least-squares solution, with a few additional constraints, the most important of which is the identity (Pourbaix & Jorissen 2000):

$$\frac{\alpha \sin i}{\pi_{\star}} = \frac{TK_1\sqrt{1-e^2}}{2\pi \times 4.7405}, \quad (7.13)$$

which relates quantities only derived from astrometry (inclination angle, astrometric signature, and stellar parallax on the left-hand side) to quantities derivable from both techniques or radial velocity alone (orbital period and eccentricity, and radial velocity semi-amplitude of the primary on right-hand side).

In our exploratory work, we have adopted a more limited approach. For each of the 11 planetary systems under study, we have utilized the orbital elements derived from spectroscopy (T , e , τ , and ω) as constraints in the sense that we have kept them fixed to their input values in the global least-squares iterative solution, and solved only for α , i , Ω . Figure 7.12 shows the estimated improvement that may be obtained in the determination of planet mass, semi-major axis, and inclination when SIM relative astrometry of the presently known planetary systems is “combined” (in the abovementioned sense) with spectroscopy, as opposed to the scenario in which all orbital elements are solved for in the least-squares minimization procedure. The three contour plots identify, in the plane defined by α/σ_d and T , regions of increasingly larger values of the ratio σ_G/σ_C between the estimated fractional uncertainties on M_p , a , and i in the case of ‘global’ orbital fits in which all parameters were adjusted and the same quantities as computed after the ‘constrained’ fits. The results are averaged over the inclination angle.

The general indication is that for well-sampled orbits, with large astrometric signatures the constrained fit does not improve significantly the final accuracy of the results. In such cases, typically $1 \leq \sigma_G/\sigma_C \leq 2$. The ability to recover accurate values of M_p , a , and i will be improved especially when the period is larger than the timespan of the observations (and the astrometric signal-to-noise ratio is very large), with typical values of $\sigma_G/\sigma_C \geq 6$ for a and M_p , while the inclination is less sensitive to the constrained solution. For low values

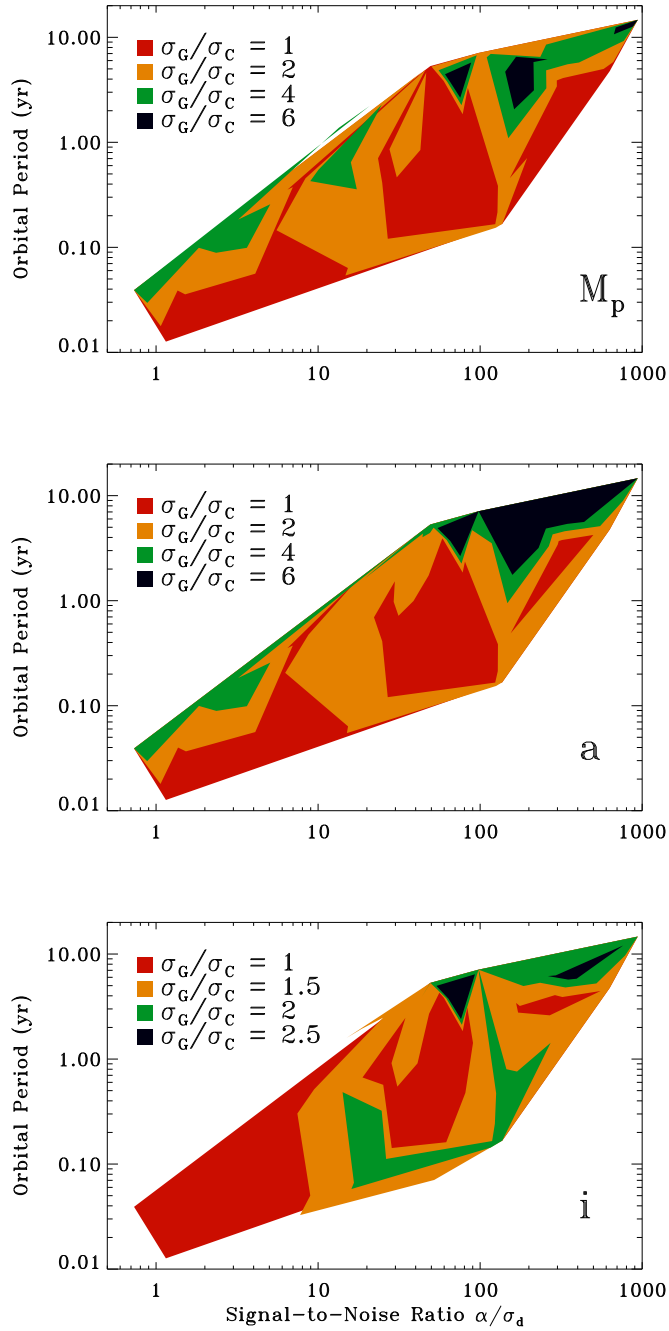


Figure 7.12 Contours identifying regions, in the $\alpha/\sigma_d - T$ plane, with equal values of the ratios σ_G/σ_C of the estimated fractional uncertainties on M_p , a , and i in the case of ‘global’ fits in which all parameters were adjusted to the same quantities as computed after the ‘constrained’ fits (as discussed in the text), for the set of presently known planetary systems. The results are averaged over the inclination angle (coplanar orbits are assumed). The contour regions are color-coded by the value of the ratio σ_G/σ_C for each parameter

of α/σ_d and short-period orbits the improvement on the fractional accuracy for the fitted parameters will be marginal.

In their work on multiple-planet system detection and measurement with GAIA, Sozzetti et al. (2001) suggested that, for systems with configurations very close to face-on, the accuracy of the inclination measurement will be substantially increased by combining radial velocity and astrometric data. On the other hand, although in their work they focused mainly on combining astrometry and radial velocity in the case of edge-on (single-planet) orbits, Eisner and Kulkarni (2002) argue that the short-period accuracy of astrometry + radial velocity should be approximately independent of orbital inclination. In Figure 7.13 and 7.14 we show the behavior of the ratios σ_G/σ_C for M_p (upper panels), a (central panels), and i (lower panels) as a function of the common inclination of the orbital plane for four representative systems (55 Cnc, 47 UMa, HD 12661, and HD 38529), whose characteristics allow us to provide quantitative answers to the above arguments. Although the predictions made by Sozzetti et al. (2001) and Eisner & Kulkarni (2002) are in general confirmed, when it comes to multiple-planet orbital fits some details become more subtle and complex. In fact, not only the average value of the ratios σ_G/σ_C (as shown in Figure 7.12), but also their behavior as a function of the orbital inclination depends on the ranges of periods and astrometric signatures we are dealing with. In the case of 55 Cnc d, for example, with a period $T \simeq 3L$, the accuracy on all fitted parameters benefits greatly from a constrained fit, which minimizes the residual covariance between the orbital solution and the solution for the parallax and the proper motion of the primary. The improvement in orbit reconstruction reaches its maximum for an almost face-on configuration. On the other hand, for 47 UMa c and HD 38529 c, with $T \simeq 1.4L$ and $T \simeq 1.2L$ respectively, σ_G/σ_C increases as $i \rightarrow 0^\circ$ only in the case of i itself, while the semi-major axis is almost insensitive to the inclination angle. In the range of periods $T < L$, again different parameters behave slightly differently, in these cases primarily due to the magnitude of α/σ_d . While the accuracy on orbital inclination is only marginally improved towards face-on configurations, the estimated semi-major axis (and in turn the derived planet mass) is more accurately retrieved in a constrained fit on an edge-on configuration, in which case astrometry loses completely the second dimension of

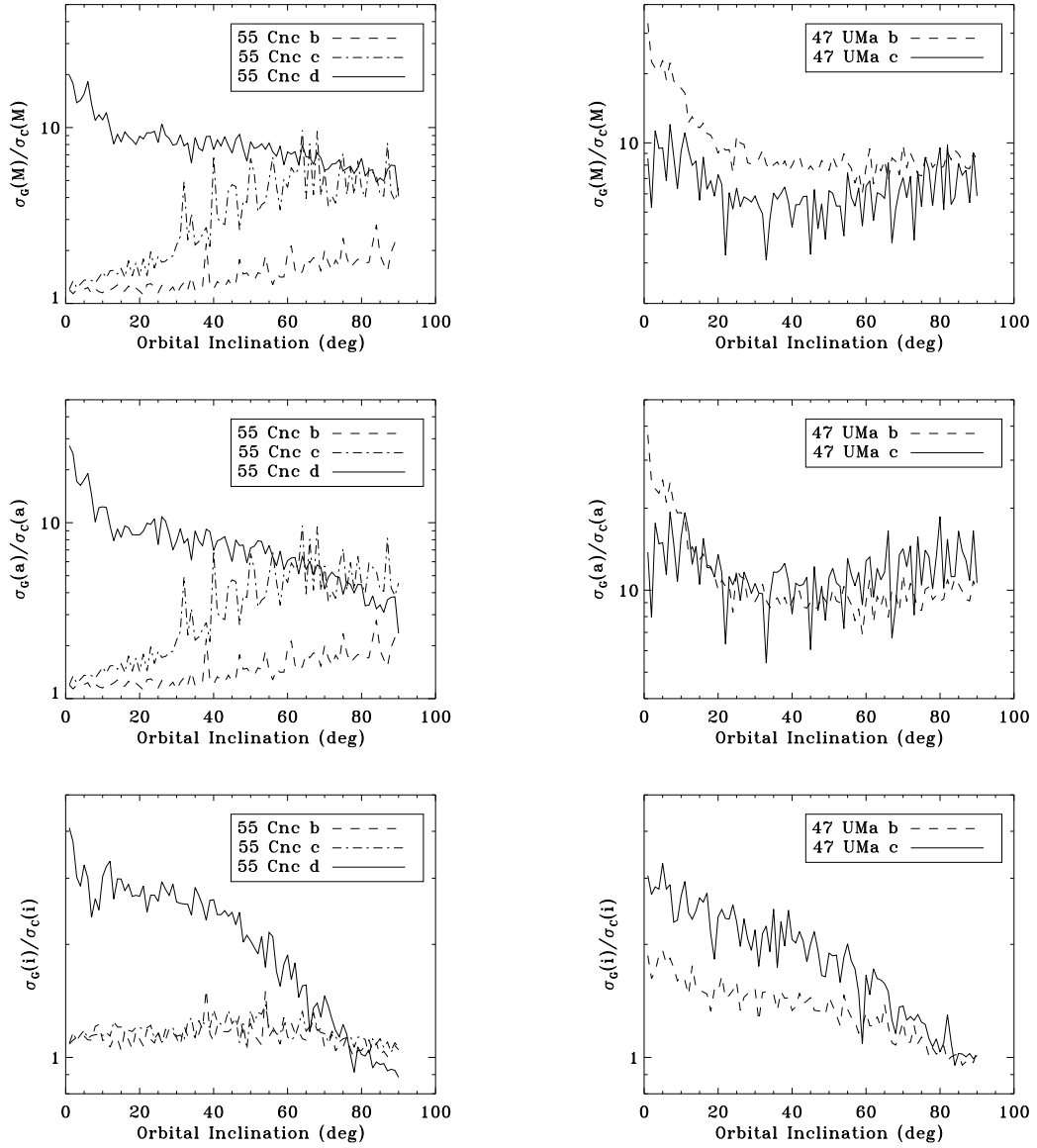


Figure 7.13 The behavior of the ratios σ_G/σ_C for M_p (upper panels), a (middle panels), and i (lower panels), expressed as a function of the common inclination angle, for the two representative multiple-planet systems 55 Cnc and 47 UMa

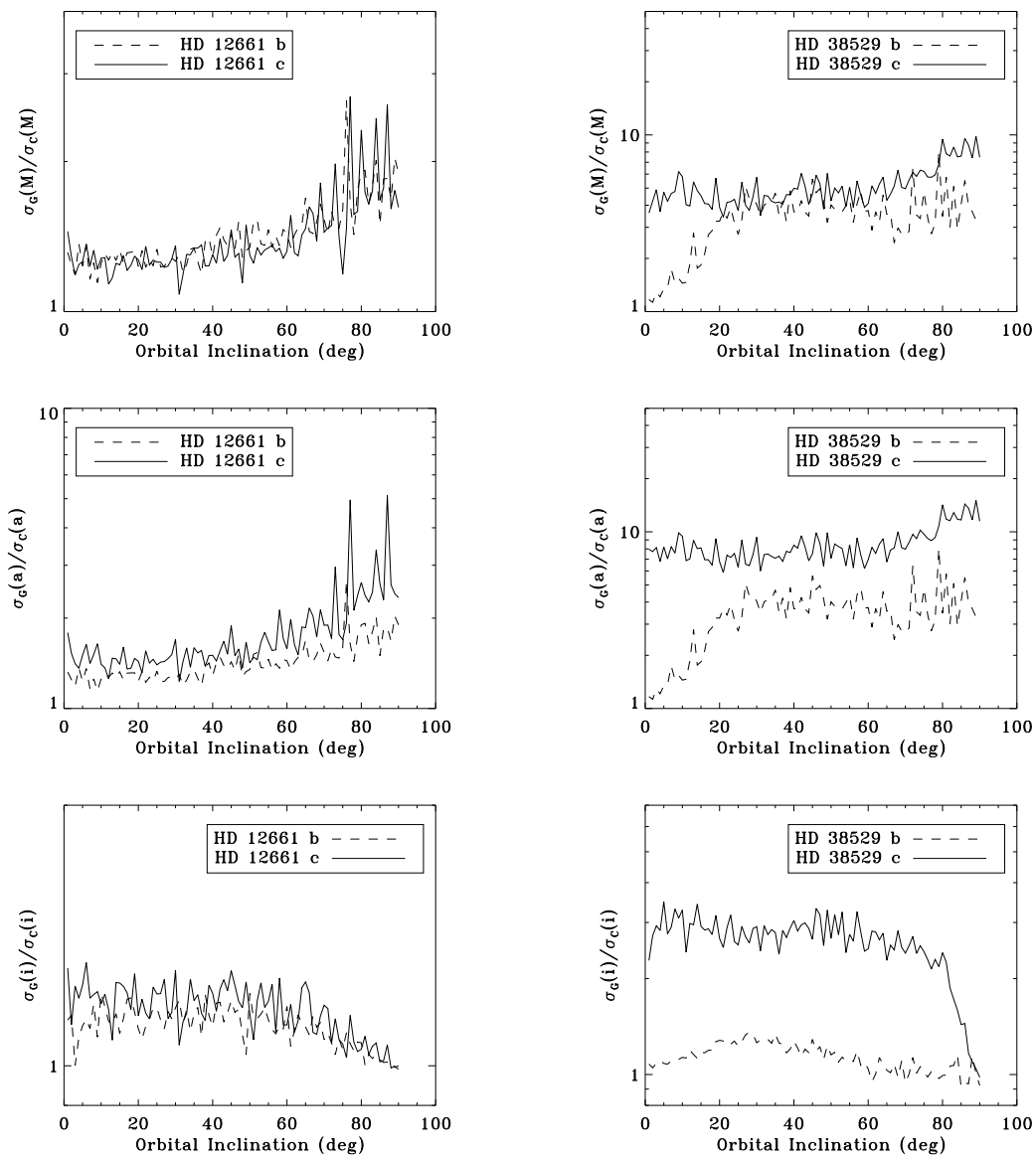


Figure 7.14 Same as Figure 7.13, but for the HD 12661 and HD 38529 planetary systems

the measurements. ⁶ For an accurate determination of the semi-major axis, the combination between astrometric and spectroscopic data will be effective particularly when $\alpha/\sigma_d \rightarrow 1$, as in the case of HD 38529 b or 55 Cnc c, while for example the results for the two planets in the HD 12661 system, both with large signatures, are only marginally improved by the constrained fit.

7.4 SUMMARY AND CONCLUSIONS

The properties of extra-solar giant planets detected by radial velocity surveys of nearby solar-type stars (Marcy et al. 2004a) seem to indicate that the Solar System configuration is just one of the many possible outcomes of disk evolution around young stars. Indeed, the strong coupling between the early evolutionary processes of a star and its disk can have a significant impact on planet formation time-scales and the final orbital configurations after the disk dissipates.

Over the next decade or so, a series of new instruments will come on line, which will provide data of great value to shed new light in the complex scenarios of the formation and evolution of planetary systems. Among indirect detection techniques, ground-based precision spectroscopy, the most successful technique so far, will be complemented by high-precision ground-based (Keck Interferometer, VLTI) and space-borne (SIM, GAIA) astrometry, and transit photometry from ground (e.g., OGLE III, STARE, STEPSS, Vulcan Camera Project) and in space (Corot, Kepler, Eddington). In the field of direct detection techniques, near- and far-infra-red diffraction-limited ground- and space-based imaging (ALMA, SIRTf, JWST) will pave the way to ambitious projects of coronagraphic/interferometric imaging from space (TPF, Darwin), with the long-term goal of directly imaging terrestrial planets in the Habitable Zone of nearby stars.

In this paper we have completed the analysis begun in our previous works (Casertano & Sozzetti 1999; S02), in order to connect and relate the basic capabilities of the Space

⁶A noticeable exception is constituted by 47 UMa b, that exhibits significant improvement in the accuracy with which its semi-major axis can be determined when the configuration is face-on. This behavior is due to the particular orbital arrangement of the system, with the longer period planet producing the smaller astrometric signal, under the assumption of coplanar orbits

Interferometry Mission (SIM) to the properties of extra-solar planetary systems. We have utilized detailed end-to-end numerical simulations of sample SIM narrow-angle astrometric observing campaigns (Section 7.2.1), an improved methodology for planet detection which combines χ^2 statistics, periodogram analysis, and Fourier series expansions (Sections 7.2.2), an upgraded analytical model that allows for multiple-planet orbital fits (Sections 7.2.3), and the set of presently known extra-solar planetary systems as templates. The experiments described in this paper have allowed us to quantify the limiting capability of SIM to discover systems of planets around solar-type stars in the solar neighborhood (Sections 7.3.1.1, 7.3.1.2, and 7.3.1.3), measure their orbital properties and masses (Sections 7.3.2.1 and 7.3.2.3), and accurately determine the coplanarity of multiple-planet orbits (Section 7.11). Our main results can be summarized as follows.

1. Additional planets in systems have little impact on SIM ability to detect each component in a system, in comparison to the single-planet configurations. The inaccurate fit and subtraction of orbits with astrometric signal-to-noise ratio $\alpha/\sigma_d \rightarrow 1$ can on the other hand increase the false detection rate by up to a factor 2. The periodogram analysis adds robustness to the detection method when $T \leq L$, by singling out periodicities even in the case of α/σ_d close to the χ^2 detection limit. For very short-period orbits, a more dense time-series of observations will be the obvious choice in order to overcome poor sampling. When $T \geq L$, the least squares technique combined with Fourier analysis can correctly identify periods as long as three times the timespan of the observations. This approach is arguably preferable, as opposed to the periodogram method, which needs modifications in the long-period regime.
2. Accurate measurements of multiple-planet orbits and determination of planet masses are only moderately affected by the presence of more than one object in a system, with typical degradation of 30-40% with respect to single-planet solutions. When $T \leq L$, it is possible to determine masses and orbital inclinations to better than 10% for systems with planets having periods as short as 0.1 yr, and for systems with components producing astrometric signals as low as $\sim 5 \sigma_d$, while $\alpha/\sigma_d \simeq 100$ is required in order to measure with similar accuracy objects with periods as long as three times the mission duration. Orbital eccentricity typically requires larger signals for the same accuracy level, and

its correct identification can become a non trivial task when $T \geq L$. The accuracy on estimated orbital elements improves significantly as we move towards face-on orbits, except for the inclination angle.

3. Accurate coplanarity measurements are possible for systems with all components producing $\alpha/\sigma_d \simeq 10$ or greater. In the case of truly coplanar systems, the relative inclination between pairs of planetary orbits is measured to be $i_{\text{rel}} \leq 3^\circ$, with uncertainties of a few degrees, for periods $0.1 \leq T \leq 15$ yr. In systems where at least one component has $\alpha/\sigma_d \rightarrow 1$, uncertainties on i_{rel} of order of $30^\circ - 40^\circ$, or larger, are likely to preclude a robust assessment of the system coplanarity.
4. Whenever feasible, an approach that combines astrometry and radial velocity will yield significantly more accurate estimates of planet masses and orbital elements. The uncertainties on orbital elements and masses can be reduced by up to an order of magnitude, especially in the case of long-period orbits in face-on configurations, and for low amplitude orbits seen edge-on. Well-sampled, well-measured orbits ($T \leq L$, $\alpha/\sigma_d \gg 1$) are only marginally affected by the combination of astrometric and radial velocity measurements.

Our results reaffirm the important role future high-precision space-borne astrometric missions promise to play in the realm of extra-solar planets. With its unprecedented astrometric precision, SIM will not only complement other on-going and planned spectroscopic, astrometric, and photometric surveys, but its position measurements will have a unique impact in the study of some important aspects of multiple-planet systems. By directly measuring the line of nodes and inclination angle for each component in a system, SIM will determine whether planetary orbits are coplanar with uncertainties of a few degrees. For instance, this will provide theory with the observational evidence needed to address the long-term evolution issue, and draw sensible conclusions on the chaotic and stable/unstable dynamical behavior of multiple-planet orbits. The same SIM measurements will also be instrumental to help confirm or rule out one of paradigms which form the basis for present-day theoretical models, i.e. that the sole conceivable environment for planet formation are flattened circumstellar disks around young pre-main sequence stars. If multiple-planet orbits are found to be coplanar, this will indicate that planetary systems indeed originate and evolve in a way

similar to our own (Lissauer 1993; Pollack et al. 1996). If large relative orbital inclinations were found, this would provide evidence that other systems are truly different from ours, and thus their present configurations should be explained in terms of either an early, chaotic phase of orbital evolution or formation by another mechanism such as disk instability (Boss 2000, 2001; Mayer et al. 2002).

ACKNOWLEDGMENTS

This project was partially funded by the Italian Space Agency under contract ASI-I/R/117/01 (to A. S. and M. G. L.). We thank an anonymous referee for a very careful reading of the paper and for illuminating comments that helped improve the original manuscript. A. S. is greatly indebted to the Smithsonian Astrophysical Observatory and its Computation Facility for kind hospitality and technical support during the completion of this work. This research has made use of the SIMBAD database, operated at CDS, Strasbourg, France.

8.0 SUMMARY AND FUTURE PROSPECTS

8.1 SUMMARY OF RESULTS

The work presented in this thesis has been motivated by the desire to improve our understanding of some crucial aspects of the properties of extrasolar planets, in connection with the predictions formulated by models of giant planet formation, evolution, and dynamical interaction. We have carried out a set of experiments aimed at providing answers to some outstanding questions in planetary science. We have conducted such studies utilizing a combination of spectroscopic, photometric, and astrometric planet-search techniques.

8.1.1 A Test of Planet Formation and Migration Models

We have found new statistical evidence for a correlation between the orbital periods P of extrasolar planets and the metallicity $[\text{Fe}/\text{H}]$ of the parent stars. The correlation is highlighted by a paucity of hot Jupiters with $P \lesssim 5$ days around metal-poor stars ($[\text{Fe}/\text{H}] \leq 0.0$). If real, the P - $[\text{Fe}/\text{H}]$ correlation might be due to an inverse dependence of orbital migration rates on the metal-content of the protoplanetary disk. Alternatively, the effect could be related to longer time-scales for planet formation around metal-poor stars, and thus reduced migration efficiency before disk dispersal. The small-number statistics at the metal-poor end of the sample of planet-host stars, however, does not allow to draw clear-cut conclusions. It is thus crucial to enlarge the sample-size of metal-poor stars screened for planets.

We are undertaking a Doppler survey of 200 field metal-poor stars ($-2.0 \leq [\text{Fe}/\text{H}] \leq -0.6$) with the Keck telescope. The data collected will ultimately allow us to not only confirm or

rule out the evidence of the P -[Fe/H] correlations, thus improving our understanding of the migration-related issues described above, but by determining on firm statistical grounds the frequency of giant planets f_p around metal-poor stars, for a wide range of orbital periods, we will be able to provide crucial constraints on the proposed models of giant planet formation. If f_p keeps on decreasing for increasingly more metal-poor stars, this will strongly argue in favor of the core accretion model, while the confirmation of a flat dependence of f_p on [Fe/H] in the metal-poor regime would favor the disk instability model. After two years of observations, our main result is the evidence for a lack of close-in planets ($P \lesssim 1$ month), which further supports our statistical findings. However, $\sim 7\%$ of the stars in our sample show evidence for long-period orbital motion. We will thus continue to monitor the variable objects in our sample to understand which are previously unrecognized spectroscopic binaries, and which are long-period planets.

8.1.2 A Test of Evolutionary Models of Irradiated Giant Planets

We have measured the spectroscopic orbit of the transiting planet TrES-1, the first discovered by a wide-field transit survey. The combined analysis of the photometric and radial-velocity datasets has allowed us to derive estimates of the planetary radius and mass. We have carried out a detailed spectroscopic determination of the chemical abundances of the relatively bright ($V = 11.79$) parent star, based on high-resolution spectra obtained with the Keck and Hobby-Eberly telescopes. This has allowed us to refine the estimates of the stellar atmospheric parameters (T_{eff} , $\log g$, [Fe/H]), and age, and to obtain more accurate values of the stellar mass and radius, by comparison with theoretical stellar evolution models. Then, a new analysis of the transit photometry of TrES-1 provided significantly improved values of the planetary mass and radius, which very closely agree with the predictions of theoretical evolutionary models of irradiated giant planets.

8.1.3 A Test of Models of Dynamical Interactions in Multiple-Planet Systems

We have carried out detailed end-to-end numerical simulations of sample narrow-angle astrometric observing campaigns with the Space Interferometry Mission (*SIM*) and the sub-

sequent data analysis process, utilizing the set of extrasolar planetary systems discovered so far by radial velocity surveys as templates. We have provided meaningful estimates of the limiting capabilities of *SIM* for the detection and measurement of multiple-planet systems around solar-type stars in the solar neighborhood. In particular, we have shown how, for well-sampled, well-measured systems, *SIM* will be capable of measuring relative inclination angles between pairs of planetary orbits with uncertainties of a few degrees. Our results reaffirm the fundamental role of μ as astrometry as a tool to confirm or rule out the various mechanisms of dynamical interactions proposed to explain the large eccentricities of planets in multiple systems.

In the next Sections we first describe a number of follow-up observations of the transiting planet system TrES-1. We then conclude by highlighting several important additional tests of planet formation and evolution that can be carried out with a variety of techniques, both from the ground and in space, in the near future.

8.2 FURTHER STUDIES OF THE TRANSITING PLANET SYSTEM TRES-1

TrES-1 is only the second transiting planet orbiting a star bright enough to allow for a variety of follow-up analyses similar to those conducted for HD 209458b (see, e.g., [Charbonneau 2004](#) and references therein).

I present here four studies to further characterize the transiting planet TrES-1 and its parent star, which have been already undertaken, are underway, or will be carried out in the near future. These are: 1) *Spitzer Space Telescope* infrared observations of the secondary eclipse, to directly detect for the first time a planet orbiting another star, and to constrain thermal emission models of close-in giant planets; 2) *Hubble Space Telescope (HST)* visible wavelength observations of the primary eclipse, to derive an accurate estimate of the planet's diameter by resolving the uncertainty concerning the diameter of the parent star; 3) detailed abundance analysis of the host star, to establish the presence or absence of chemical abundance anomalies with respect to the sample of stars with planets, and to place TrES-1

in the context of Galactic chemical evolution by comparison with disk or halo stars of similar metal content; 4) an accurate, direct distance measurement for the system, to derive improved constraints on the parent star’s radius, and thus further reduce the uncertainties on the estimate of the planetary radius, to help discriminate between models of irradiated giant planet interiors with and without rocky cores.

8.2.1 Detection of Thermal Emission

At infrared wavelengths the ratio of the planet-to-star flux is more favorable than in visible light, especially for hot Jupiters on orbital periods of a few days, which are exposed to intense insolation. Longward of $3 \mu\text{m}$, the planetary thermal emission is significant. A successful detection of the secondary eclipse of a transiting planet, i.e. the flux decrement due to the passage of the planet behind the star, would be particularly valuable for several reasons. First, it would constitute the first direct detection of (i.e. the observation of photons emitted by) a planet orbiting another star. Second, the measured depth of the eclipse ΔF_{II} yields, under the assumption of blackbody emission, an estimate of the effective temperature T_p of the planet. Under the further assumption of thermal equilibrium and isotropic emission, observations of the secondary eclipse in the infrared allow to estimate the wavelength-integrated, phase-integrated Bond albedo A of the planet, i.e. a proxy for the ratio of energy reflected by the planet to the amount received. This can be obtained by solving for A the equation:

$$T_p \simeq T_{\text{eq}} = T_{\star}(R_{\star}/2a)^{1/2}[f(1 - A)]^{1/4}, \quad (8.1)$$

where T_{eq} is the equilibrium temperature, R_{\star} and T_{\star} are the stellar radius and effective temperature, a the orbital distance, and the factor $f = 1$ if the planetary emission is isotropic. An estimate of ΔF_{II} , T_p , and A for a transiting planet would provide the first direct observational constraints for atmospheric models of hot Jupiters. Finally, the detection of the secondary eclipse would place constraints on the orbital eccentricity in addition to those provided by the radial velocity observations described in Chapter 5. A non-zero value of e could produce a measurable shift in the separation of the times of center of primary (t_1)

and secondary t_{II}) eclipse away from $1/2$ period. The approximate formula for the offset is (Kallrath & Milone 1999):

$$\frac{\pi}{2P} \left(t_{\text{II}} - t_{\text{I}} - \frac{P}{2} \right) \simeq e \cos \omega, \quad (8.2)$$

where P is the orbital period and ω is the longitude of periastron.

D. Charbonneau (PI), L. E. Allen, R. Alonso, T. M. Brown, R. L. Gilliland, D. W. Latham, G. Mandushev, S. T. Megeath, F. T. O'Donovan, A. Sozzetti, and G. Torres observed the newly discovered transiting planet TrES-1 during the time of secondary eclipse with the Infrared Array Camera (IRAC) on the *Spitzer Space Telescope* for 5.6 hours spanning UT 30-31 October 2004. We obtained 1518 images in two bandpasses at $4.5 \mu\text{m}$ and $8.0 \mu\text{m}$, with a cadence of 13.2 sec and an effective integration time of 10.4 sec. In both bands of our observations, we detected a flux decrement with a timing, amplitude, and duration as predicted by published parameters of the system (see Chapter 6; [Sozzetti et al. 2004b](#)). The signal detected in the *Spitzer*/IRAC infrared photometric time series ([Charbonneau et al. 2005](#)), together with a similar detection by Deming et al. ([2005b](#)) who presented *Spitzer*/MIPS $24 \mu\text{m}$ photometry spanning a time of secondary eclipse of the HD 209458 transiting planet system, represents the first direct detection of light emitted by a planet orbiting a star other than the Sun. The observed eclipse depths (in units of the relative flux) are 0.00066 ± 0.00013 at $4.5 \mu\text{m}$, and 0.00225 ± 0.00036 at $8.0 \mu\text{m}$. These estimates provide the first observational constraints on models of the thermal emission of hot Jupiters. Under the assumptions described above, we estimate an effective temperature $T_p = 1060 \pm 50$ K, and we find a Bond albedo $A = 0.31 \pm 0.14$. The low value found for A implies that the planet likely absorbs the majority of stellar radiation incident upon it. The fact that the planet's atmosphere appears relatively clear is a conclusion of significant impact to atmospheric models of these objects. We also compare our data to a previously published model of the planetary thermal emission ([Sudarsky et al. 2003](#)), which predicts prominent spectral features in our observational bands due to water and carbon monoxide. This model adequately reproduces the observed planet-to-star flux ratio at $8.0 \mu\text{m}$, however it significantly over-predicts the ratio at $4.5 \mu\text{m}$. We also present an estimate of the timing of the secondary eclipse, which we use to place a strong constraint on the expression $e \cos \omega$.

As discussed in Chapter 2, Bodenheimer et al. (2001, 2003) and Laughlin et al. (2005a) have proposed that the tidal dissipation of a non zero eccentricity, produced by the perturbative effects of a distant companion, could generate an internal energy source sufficient to increase significantly the planetary radius. Our accurate estimate of R_p for TrES-1 described in Chapter 6 already provided good agreement with theoretical models that do not require any additional source of energy in the planet interior. The resulting upper limit on e derived here is sufficiently small that we conclude that tidal dissipation is unlikely to provide a significant source of energy interior to the planet.

8.2.2 An *HST* Light-Curve

Shortly after discovery of the transiting planet TrES-1, T. M. Brown (PI), R. Alonso, J. A. Belmonte, D. Charbonneau, H.-J. Deeg, E. W. Dunham, R. L. Gilliland, D. W. Latham, G. Mandushev, F. T. O'Donovan, and A. Sozzetti proposed for Director's Discretionary time on the *Hubble Space Telescope* (*HST*) to observe the planet during transits and obtain very precise time-series photometry of the transit in visible wavelengths with the Advanced Camera for Surveys (ACS). The Cycle 13 GO/DD Proposal has been awarded 15 *HST* orbits, and observations are underway.

The greatest uncertainty in the estimated radius of TrES-1 arises from uncertainty in the radius of the parent star. Ground-based efforts to obtain precise time series photometry of transiting planets are limited to a precision of ~ 2 mmag and a cadence of ~ 10 minutes (Charbonneau 2003, and references therein). With data of this quality, there is a strong degeneracy between R_p , R_s , and the orbital inclination i . At the lowest level of approximation, the two basic transit observables, depth d and duration l , depend mostly on the ratio R_p/R_s and on the transit chord length, thus on R_s and i . Then, by increasing the planetary and stellar radii in tandem to preserve their ratio, the same transit depth can be produced, and reducing the orbital inclination preserves the chord length across the star to match the observed transit duration. In this case, there are more unknowns than observables, and a family of curves with different values of R_p , R_s , and i can fit the data equally well. This degeneracy can be removed by taking into account additional, more subtle features of the

light curve. The duration w of the planet's ingress and egress depends upon R_p but is also proportional to $\sec \psi$, where ψ is the angle between the planet's line of motion and the local normal to the stellar limb. Thus, w depends upon R_p , R_s , and i . Finally, the curvature C of the light curve between second and third contacts depends upon the stellar limb darkening parameter u and upon i and R_s . Thus, if d , l , w , and C can be measured with adequate precision, one may estimate each of the 4 independent system parameters R_s , R_p , i , and u (Brown et al. 2001). The above estimates are still subject to the uncertainty in the independent estimate of the stellar mass, M_s , but the effect is small since the uncertainty in the radius is only weakly dependent upon that of the mass, i.e. $\Delta R_p/R_p \simeq 0.3 \Delta M_s/M_s$ (Charbonneau 2004).

An ultra-precise light curve is however needed to resolve the uncertainty concerning the radius of the parent star, which can only be obtained from space. We will observe TrES-1 during three visits with *HST*/ACS, to disperse the large number of photons over as many pixels as possible (to retain a high observing efficiency and mitigate flat-fielding effects). With a time-series cadence of 2.1 min and an actual exposure time of 95 sec, the light curve we will obtain will be stunning (although the host star TrES-1, at $V = 11.79$ is ~ 4 mag fainter than the one of the first transiting planet observed by Brown et al. (2001) with *HST*), with some 330 exposures in total over the three, five-orbits visits with each exposure at a S/N of 7,150, and a projected typical photometric precision of $\sim 10^{-4}$ mag.

This study, complementary to that undertaken with *Spitzer*/IRAC, will allow us to put the planetary radius on firmer grounds, thus further refining the observational constraints on the planet's composition and evolutionary history (e.g., Burrows et al. 2000, 2004; Baraffe et al. 2003; Chabrier et al. 2004; Guillot 2005, and references therein). Furthermore, the data collected will also be useful for other, more challenging investigations. For example, the sharp ingress/egress light-curve transitions displayed by TrES-1 lend themselves to accurate timing measurements, with uncertainties of a few sec. Then, sensitive tests for gravitational perturbations caused by moons of the transiting planet, or by other yet undetected planets of the same star, might be conducted. We will also search for small distortions of the light curve measured by *HST*/ACS, such as would be caused by planetary rings, or by Earth-sized moons.

8.2.3 Placing the Host Star in Context

Following up on the determination of the Fe and Li abundances for TrES-1 described in Chapter 6 and utilized by Sozzetti et al. (2004b) to improve on the planetary radius determination, A. Sozzetti, D. Yong, B. W. Carney, D. W. Latham, G. Torres, and J. B. Laird have re-analyzed the Keck and HET high-resolution spectra and undertaken a detailed chemical abundance analysis of the host star (Sozzetti et al. 2005), which includes elemental abundances of both refractories (e.g., α -elements such as Si, Mg, Ca, Ti, and iron-group elements such as Cr, Ni, and Co) as well as volatiles (e.g., CNO, S, and Zn). The twin goal of our study is a) to search for possible chemical abundance anomalies between TrES-1 and the sample of stars with planets and b) to put TrES-1 in the context of Galactic chemical evolution.

First, as discussed in Chapter 2, analyses of over a dozen other elements have been carried out in the recent past (Santos et al. 2000; Gonzalez et al. 2001; Bodaghee et al. 2003; Ecuivillon et al. 2004a, b), and the general evidence is that the abundance distributions in stars with planets are the extension of the observed behavior with $[\text{Fe}/\text{H}]$, a result quantified by trends of decreasing $[X/\text{Fe}]$ with decreasing $[\text{Fe}/\text{H}]$. How do chemical abundances of TrES-1 compare with sample of planet hosts? As highlighted in Chapter 2, wide-field transit surveys typically target stars that are a few hundred pc away from the Sun, a sample with little or no distance overlap with that of solar-neighborhood stars ($D < 50 - 100$ pc) targeted by Doppler surveys. Then, one could in principle expect that large-scale metallicity trend should also be taken into account, such as the evidence for a mild radial metallicity gradient of ~ -0.09 dex/kpc in the disk of the Milky Way presented by Nordström et al. (2004). On the other hand, based on the distance estimate of ~ 150 pc to TrES-1 inferred by Sozzetti et al. (2004b), one could *a priori* expect that no significant anomalies should be found.

Second, Galactic kinematics is a useful observational discrimination for various populations of objects in the Milky Way Galaxy. A few recent studies (Gonzalez et al. 2001; Barbieri & Gratton 2002; Santos et al. 2003) have highlighted a strong similarity between the kinematics of stars with planets and that of control samples of stars without known planets. How do the kinematic properties of TrES-1 compare with those of stars with planets?

Is the star a likely member of the thin or the thick disk?

Our study will pioneer those that will be carried out to better characterize the parent stars of all transiting planets that will likely be found in the coming years by the large number of ongoing and planned wide-field, ground-based photometric surveys (for a review see for example [Horne 2004](#) and [Charbonneau 2004](#)).

8.2.4 Taking the Distance to the System

The effective temperature, radius, and mass of the parent star of TrES-1 are known with uncertainties in the range 1%-6%, and its metallicity is derived within a few hundredths of a dex, as described in Chapter 6 ([Sozzetti et al. 2004b](#). See also [Laughlin et al. 2005a](#)). However, it is remarkable how, in spite of several well-known stellar parameters, no direct estimate of the distance D to the system is available, and this prevents the determination of an absolute luminosity M_v . In absence of a light curve of sufficient quality, initial constraints on R_s and M_s are placed by fitting stellar evolution models to the observed T_{eff} , $[\text{Fe}/\text{H}]$, M_v , and D . For TrES-1, the first two of the latter quantities are the only reliable metrics that can be used in the comparison with theoretical isochrones.

An accurate parallax measurement, combined with a mmag precision estimate of V to deliver a reliable value of M_v , would imply further useful constraints on R_s and M_s . Thus, TrES-1 is an attractive target for either ground- or space-based high-precision astrometric observatories that will come online in the near future. In the near term, the most promising results can be obtained from the ground by performing narrow-angle astrometric measurements of TrES-1 with either Keck-I ([van Belle et al. 1998](#)) or VLTI ([Glindemann et al. 2003](#)). The star is relatively bright ($K = 9.8$), and it has several neighbors of similar brightness within a radius of ~ 1 arcmin. Upon availability of suitable reference objects sufficiently nearby, it will be possible to fully exploit the atmospheric limit to narrow-angle astrometry for interferometers operated in phase-referencing mode (e.g., [Lane & Colavita 2003](#)).

If the actual distance to TrES-1 is ~ 150 pc, as inferred by [Sozzetti et al. \(2004b\)](#) and by [Laughlin et al. \(2005a\)](#), then the projected single-measurement astrometric precision of 20-30 μas achievable with Keck-I and VLTI would allow to deliver a distance estimate with

an uncertainty of $< 0.1\%$. The consequently very accurate estimate for M_c would allow to improve the estimates of R_s and M_s , by comparison with theoretical evolutionary tracks. Finally, the refined value of R_p will help to further improve the comparison with the theory of irradiated giant planet interiors, to discriminate between models with or without core.

8.3 FUTURE TESTS OF PLANET FORMATION AND EVOLUTION

The set of key questions in the science of planetary systems at the end of Chapter 2 can be addressed and answered in the coming years thanks to the combined effort of 1) refined theoretical models of planet formation and evolution with a strong predictive power and 2) ground-based as well space-borne observatories with improved precision/resolution capable of surveying large samples of stars of all spectral types and ages and of better characterizing the properties of extrasolar planets and their host stars. I outline below some of the important contributions various observational techniques will be able to provide, in connection with the predictions from theory.

8.3.1 Discriminating Between Planet-Formation Models

As discussed in Chapter 2, the competing giant-planet formation models make very different predictions regarding formation time-scales, planet mass ranges, and planet frequency as a function of host star characteristics. For example, the core accretion mechanism requires at least a few Myr to grow a solid core massive enough to accrete a gaseous envelope (Polack et al. 1996; Alibert et al. 2004). In contrast, the disk instability mechanism leads to Jupiter-mass clumps, which can survive and give rise to actual proto-planets, within a few thousand years (Boss 2004a; Mayer et al. 2004). Core accretion is likely to be enhanced in metal-rich stars, as increased surface densities of solids can shorten the overall time-scales for giant planet formation by this mechanism (Ida & Lin 2004b; Kornet et al. 2005), while disk instability is remarkably insensitive to the primordial metallicity of the protoplanetary disk (Boss 2002). These predictions could be tested on firm statistical grounds by extending planet surveys to large samples of PMS objects and field metal-poor stars, respectively. A

better understanding of the dependence of migration processes on environment (see Chapters 3 and 4) could also be achieved by surveying a large enough sample of metal-poor stars.

Pre-main-sequence and metal-poor stars are difficult targets for Doppler surveys, due to intrinsic faintness, chromospheric activity, rotation, and weakness of spectral lines.

Transit surveys are not suited for observations of metal-poor stars, due to the fact that they are rare. YSOs have large intrinsic photometric variability, in addition to the presence of nebulosity and disks, which prevents this technique from being effective.

The weak spectral features of metal-poor stars do not constitute an obstacle to high-precision astrometric measurements, the limiting factors being faintness and distance. The full sample of ~ 1500 relatively bright ($m_v < 13$), nearby ($D \lesssim 200$ pc), field metal-poor stars presently known could be screened for giant planets on wide orbits by *SIM* and *Gaia*, thus complementing the shorter-period ground-based spectroscopic observations (Sozzetti et al. 2005). This would allow for improved understanding of the behavior of the probability of planet formation in the low-metallicity regime, by direct comparison between large samples of metal-poor and metal-rich stars, in turn putting stringent constraints on the proposed planet formation models. Disproving or confirming the existence of the P -[Fe/H] correlation would also help to understand whether metallicity plays a significant role in the migration process of giant planets, or if this simply reflects a reduced migration efficiency in the low-metallicity regime due to increased giant planet formation time-scales.

Starspots and circumstellar disks can also be an obstacle to high-precision astrometric observations. However, pollution from this type of astrophysical noise is not nearly as severe as it is for the other two techniques (e.g., Sozzetti 2005, and references therein). The crucial exploration of the initial conditions for planet formation in the circumstellar disk as a function of age and composition can be carried out by means of an high-precision astrometric survey of PMS stars. At least a few hundred relatively bright ($m_v < 13 - 14$) PMS stars in a dozen of nearby ($D < 200$ pc) star-forming regions could be screened for planets orbiting at 1-5 AU by *SIM* and *Gaia*. Indeed, one of the Key Science Projects ¹ awarded observing time

¹C. A. Beichman et al. 2002, "The Search for Young Planetary Systems and the Evolution of Young Stars", http://planetquest.jpl.nasa.gov/Navigator/ao_support/beichman.pdf

with *SIM* consists of an astrometric planet survey of 200 young stellar objects, in the age range 1-100 Myr. The possibility to determine the epoch of giant planet formation in the protoplanetary disk would provide the definitive observational test to distinguish between the proposed theoretical models. These data would uniquely complement near- and mid-infrared imaging surveys (e.g., [Burrows 2005](#), and references therein) for direct detection of young, bright, wide-separation ($a > 30 - 100$ AU) giant planets.

8.3.2 Structural and Evolutionary Properties of Giant Planets

The key to unlocking a planet's chemical, structural, and evolutionary properties is the direct detection of its light. Detailed predictions for the internal and atmospheric properties, thermal profiles, emergent and reflected spectra, and their temporal evolution, for both irradiated and isolated giant planets have recently been proposed (e.g., [Seager & Sasselov 2000](#); [Barman et al. 2001](#); [Burrows et al. 2000, 2003](#); [Sudarsky et al. 2000, 2003](#); [Chabrier et al. 2004](#); [Burrows 2005](#), and references therein). For example, in terms of atmospheric and chemical composition of giant planets, the predominant elements predicted are H_2 , He, H_2O , Na, K, CO, and CH_4 . Furthermore, atmospheres of close-in Jupiters should be mostly clear, with correspondingly low albedos.

However, the study of the spectral signatures and light curves of extrasolar giant planets, and their inversion to obtain planetary parameters, is complicated by several factors, such as their dependence on M_p , rotation, and meteorology, age, orbital distance, and stellar type of the parent star, and the overall viewing geometry of the star-planet system as seen from Earth. In many cases, predictions can vary with wavelength and orbital distance by factors 2 to 10 (!).

The major observational problem is to detect the planet flux in presence of the overwhelming glare of the star, as already briefly discussed in [Chapter 2](#). The typical projected star-planet separations (assuming nearby systems within a few tens of pc) range from a few milli-arcsec for hot Jupiters to ~ 1 arcsec for objects orbiting within a few tens of AUs. In this regime, the predicted planet/star contrast ratio in the visible ranges between $10^{-5} - 10^{-6}$ and $\sim 10^{-10}$, respectively. Although the situation improves by 1 to 2 orders of magnitude at

near- and mid-infrared wavelengths ($4\ \mu\text{m} \lesssim \lambda \lesssim 10\ \mu\text{m}$), this still constitutes a challenging task for imaging instruments.

Given the wide range of planet/star contrast ratios and spectral diagnostics, a variety of technological solutions to directly detect extrasolar planets are being actively studied (see [Burrows 2005](#), and references therein). From the ground, imaging systems for both operational 8-10 meter-class telescopes (VLT, Keck, LBT, and their interferometric modes, Gemini, Subaru) as well as proposed giant-sized telescopes (GMT, GSMT, OWL) are being gauged in terms of their capabilities to attain a specific star/planet contrast ratio at a certain λ , and for a given angular separation from the central star. Successful detections will ultimately be obtained by the combined use of several technologies, including adaptive optics, accurate wavefront sensing, apodizing and coronagraphic masks, and interferometric nulling. From space, both monolithic- (*Corot*, *Kepler*, *MOST*, *ECLIPSE*, *JWST*, TPF-C) and diluted-aperture (*EPIC*, TPF-I/Darwin) observatories, operating at visible as well as infrared wavelengths, utilizing either coronagraphic or interferometric nulling options to suppress the starlight, hold the promise for directly detecting and characterizing extrasolar giant planets. When this will not be feasible, particularly for hot Jupiters orbiting too close to the parent star, the planetary flux could still be measured directly by means of other techniques, such as ultra-high-precision spectrophotometry of the summed optical or near-infrared light to disentangle the planetary component. This method has warranted the first direct detection of planetary flux in the case of the two transiting planet systems TrES-1 ([Charbonneau et al. 2005](#)) and HD 209458b ([Deming et al. 2005b](#)), as we have described in the previous section and in Chapter 2.

Finally, the planet/star flux ratio is given by $f = p(R_p/a)^2\Phi(\alpha)$, with a the instantaneous orbital distance, p the wavelength-dependent geometric albedo, and $\Phi(\alpha)$ the phase function (itself a function of λ), with α the star-planet-Earth angle. This last quantity depends on the orbital geometry as $\cos\alpha = \sin(\theta + \omega)\sin i\sin\Omega - \cos\Omega\cos(\theta + \omega)$, with $\theta = 90^\circ - \alpha$. As a result, depending on the eccentricity and orientation, f could vary dramatically (or not at all) as a function of time. For directly detected extrasolar giant planets which induce large perturbations in the stellar motion (particularly those at separations $\gtrsim 0.5$ AU), high-precision astrometry with *SIM* and *Gaia* could provide important information to improve

in the interpretation of the light-curves.

8.3.3 Statistical Properties and Correlations

Planet properties (orbital elements distributions, masses) and frequencies are likely to depend upon the characteristics of the parent stars (spectral type, age, metallicity, binarity/multiplicity). It is thus desirable to be able to provide as large a database as possible of stars screened for planets.

The size of the stellar database being observed by Doppler surveys is of order of a few thousand objects (as discussed in Chapter 2). The two major contributions from this technique in the near future will be the long time-span of the observations, which will soon permit to provide estimates of giant planet frequency out to Jupiter-like orbital radii (> 5 AU), and ongoing efforts (Fischer et al. 2005) to search for hot Jupiters orbiting a completely new sample of a few thousand objects, to better constrain the frequency of hot Jupiters around solar-type stars. However, it is unlikely the number of objects in the Doppler surveys will grow by an order of magnitude within the next decade. Furthermore, the Doppler technique is unsuited to look for planets around stars covering a very wide range of spectral types and ages.

Transit surveys globally observe hundreds of thousands of objects, of all spectral types. The *Corot* (Baglin et al. 2002) and *Kepler* (Borucki et al. 2003) missions will provide enough high-quality photometric data on transiting planets to fully characterize the mass function of close-in planets, down to the terrestrial planet regime. However, they are strongly limited in the regime of orbital periods that can be probed and by the stringent requisites on favorable orbital alignment.

The size of the stellar sample screened for planets by an all-sky astrometric survey such as *Gaia* (Lattanzi et al. 2000; Sozzetti et al. 2001) could be of order of a few hundred thousand relatively bright ($m_v < 13$) stars of spectral type F-G-K out to ~ 150 pc (not counting the majority of M dwarfs). The statistical value of such a sample is better understood when one considers that, depending on actual giant planet frequencies as a function of spectral type and orbital distance, of order of a few thousand planets could be detected and measured.

This number is comparable to the present-day *size* of the target list of Doppler surveys, and it would constitute at least a ten-fold improvement in the number of stars with planets.

8.3.4 The Hunt for Other Earths

The holy grail in extra-solar planet science is clearly the direct detection characterization of Earth-sized, habitable planets, with atmospheres where bio-markers (e.g., Lovelock 1965; Ford et al. 2001b; Des Marais et al. 2002; Selsis et al. 2002; Seager & Ford 2005) might be found that could give clues on the possible presence of life forms.

Space-borne transit photometry carried out with *Corot* and *Kepler* has the potential to be the first technique to make such a detection. It may even provide an estimate for the frequency of terrestrial planets as a function of orbital radius out to 1 AU.

However, a typical target in the *Kepler* field is of order of a few hundred pc away from the Sun. Thus, *Kepler* is unlikely to provide relevant targets to a follow-up mission with the goal of imaging terrestrial planets, such as the coronagraphic or interferometric configuration of the Terrestrial Planet Finder (Beichman et al. 2002), and Darwin (Fridlund 2000).

Radial-velocity measurements at the 1 m/s precision level (e.g., Santos et al. 2004b) hold the promise to uncover close-in rocky planets, down to a few M_{\oplus} . However, the radial-velocity signal induced by a 1 M_{\oplus} planet orbiting a 1 M_{\odot} star at 1 AU is $\simeq 9$ cm/s. It is not inconceivable that spectrographs stable at the cm/s could be built in the future. However, the typical m/s atmospheric jitter of *inactive* stars like our Sun probably constitutes a very severe obstacle to the ability of Doppler spectroscopy to provide the first terrestrial planet targets for TPF/Darwin.

Astrometry of all nearby stars within 10-20 pc from the Sun at the μ as level (with *SIM* and *Gaia* in space, and possibly with Keck-I and VLTI from the ground) is thus an essential ingredient in order to be able to provide Darwin/TPF with a) systems containing *bona fide* terrestrial planets (Ford & Tremaine 2003; Sozzetti et al. 2002; Marcy et al. 2005); and b) a comprehensive database of objects with and without giant planets orbiting out to a few AU from which to choose additional targets based on the presence or absence of Jupiter signposts (Sozzetti et al. 2004a). Another *SIM* Key Science Project ² involves a survey of

²G. W. Marcy et al. 2002, "Discovery of Planetary Systems", <http://planetquest.jpl.nasa.gov/>

250 of the nearest stars ($D < 20$ pc), with the main goal of detecting and characterizing terrestrial ($1-5 M_{\oplus}$) planets, and thus return a reconnaissance database for TPF.

BIBLIOGRAPHY

- Adachi, I., Hayashi, C., & Nakazawa, K. 1976, *Prog. Theor. Phys.*, 56, 1756
- Adams, F. C., Hollenbach, D., Laughlin, G., & Gorti, U. 2004, *ApJ*, 611, 360
- Agol, E., Steffen, J., Sari, R., & Clarkson, W., *MNRAS*, 359, 567
- Alard, C. 2000, *A&AS*, 144, 363
- Alibert Y., Mordasini C., & Benz W., 2004, *A&A*, 417, L25
- Alibert, Y., Mordasini, C., Benz, W., & Winisdoerffer, C. 2005, *A&A*, 434, 343
- Allard, F., Hauschildt, P. H., Alexander, D. R., & Starrfield, S. 1997, *ARA&A*, 35, 137
- Allard, F., Baraffe, I., Chabrier, G., Barman, T. S., & Hauschildt, P. H. 2004, in *Scientific Frontiers in Research on Extrasolar Planets*, D. Deming & S. Seager eds., *ASP Conf. Ser.*, 294, 483
- Alonso, A., Arribas, S., & Martinez-Roger, C. 1996, *A&A*, 313, 873
- Alonso, R., Deeg, H.J., Brown, T.M., & Belmonte, J.A. 2004a, *AN*, 325, 594
- Alonso, R., et al. 2004b, *ApJ*, 613, L153
- Armitage P. J., Livio M., Lubow S. H., & Pringle J. E., 2002, *MNRAS*, 334, 248
- Artymowicz, P. 1993, *ApJ*, 419, 166
- Artymowicz, P., & Lubow, S. H. 1994, *ApJ*, 421, 651
- Artymowicz, P. 2001, *BAAS*, 33, #10.01
- Asghari, N., et al. 2004, *A&A*, 426, 353
- Asplund, M. 2003, to appear in *IAU Highlights of Astronomy*, ed. E. Engvold, Vol. 13, in press
- Atobe, K., Ida, S., & Ito, T. 2004, *Icarus*, 168, 223

- Auvergne, M., et al. 2003, Proc. SPIE, 4854, 170
- Baglin, A., et al. 2002, in *Radial and Nonradial Pulsations as Probes of Stellar Physics*, eds. C. Aerts, T. R. Bedding, & J. Christensen-Dalsgaard, ASP Conf. Ser., 259, 626
- Bally, J., Testi, L., Sargent, A., & Carlstrom, J. 1998, AJ, 116, 854
- Baraffe, I., Chabrier, G., Barman, T., Allard, F., & Hauschildt, P. H. 2003, A&A, 402, 701
- Baraffe, I., Selsis, F., Chabrier, G., Barman, T., Allard, F., Hauschildt, P. H., & Lammer, H. 2004, A&A, 419, L16
- Barbieri, M., & Gratton, R. G. 2002, A&A, 384, 879
- Barbieri, M., Marzari, F., & Scholl, H. 2002, A&A, 396, 219
- Bard, Y. 1974, *Nonlinear Parameter Estimation*, New York: Academic Press
- Barman, T. S., Hauschildt, P. H., Schweitzer, A., Stancil, P. C., Baron, E., & Allard, F. 2002, ApJ, 569, L51
- Barnes, R., & Quinn, T. 2001, ApJ, 550, 884
- Barnes, R., & Quinn, T. 2004, ApJ, 611, 494
- Barnes, R., & Raymond, S. N. 2004, ApJ, 617, 569
- Barrow, J. D., & Tipler, F. J. 1986, *The Anthropic Cosmological Principle* (Oxford University Press)
- Basri, G., & Marcy, G. W. 1997, in *Star Formation, Near and Far*, S. Holt & L. G. Mundy eds., AIP Conf. Proc., 393, , 228
- Bastian, T. S., Dulk, G. A., & Leblanc, Y. 2000, ApJ, 545, 1058
- Bate, M. R., Lubow, S. H., Ogilvie, G. I., & Miller, K. A. 2003, MNRAS, 341, 213
- Beaugé, C., Ferraz-Mello, S., & Michtchenko, T. A. 2003, ApJ, 593, 1124
- Beaugé, C., & Michtchenko, T. A. 2003, MNRAS, 341, 760
- Beaugé, C., Ferraz-Mello, S., & Michtchenko, T. A. 2004, MNRAS, submitted (astro-ph/0404166)
- Beckwith, S. V. W., & Sargent, A. I. 1996, Nature, 383, 139
- Beer, M. E., King, A. R., Livio, M., & Pringle, J. E. 2004, MNRAS, 354, 763
- Beichman, C. A., Coulter, D. R., Lindensmith, C., & Lawson, P. R. 2002, in *Future Research Direction and Visions for Astronomy*, ed. A. M. Dressler, Proc. SPIE, 4835, 115

- Benedict, G. F., et al. 2001, *AJ*, 121, 1607
- Benedict, G. F., et al. 2002, *ApJ*, 581, L115
- Benedict, G. F., et al. 2003a, *BAAS*, 35, #07.10
- Benedict, G. F., et al. 2003b, *BAAS*, 35, #67.05
- Benedict, G. F., et al. 2004, *BAAS*, 36, #42.02
- Bernstein, H.-H. 1997, *Proc. ESA Symp.*, Hipparcos - Venice '97, ESA SP-402, 705
- Bevington, P. R., & Robinson, D. K. 2003, *Data reduction and Error Analysis for the Physical Sciences - 3rd ed.*, Boston: McGraw-Hill
- Black, D. C., & Scargle, J. D. 1982, *ApJ*, 263, 854
- Bodaghee, A., Santos, N. C., Israelian, G., & Mayor, M. 2003, *A&A*, 404, 715
- Bodenheimer, P., & Pollack, J. B. 1986, *Icarus*, 67, 391
- Bodenheimer, P., Hubickyj, O., & Lissauer, J. J. 2000, *Icarus*, 143, 2
- Bodenheimer, P., Lin, D. N. C., & Mardling, R. A. 2001, *ApJ*, 548, 466
- Bodenheimer, P., Laughlin, G., & Lin, D. N. C. 2003, *ApJ*, 592, 555
- Boesgaard, A. M., & King, J. R. 2002, *ApJ*, 565, 587
- Bois, E., Rambaux, N., Kiseleva-Eggleton, L., & Pilat-Lohinger, E. 2004, in *Extrasolar Planets: Today and Tomorrow*, J.-P. Beaulieu, A. Lecavelier des Etangs and C. Terquem Eds., *ASP Conf. Ser.*, 321, 349
- Bond I., et al., 2004, *ApJ*, 606, L155
- Bonfils, X., et al. 2004, in *Extrasolar Planets: Today and Tomorrow*, J.-P. Beaulieu, A. Lecavelier des Etangs and C. Terquem Eds., *ASP Conf. Ser.*, 321, 101
- Booth, A. J., et al. 1999, in *Working on the Fringe: Optical and IR Interferometry from Ground and Space*, ed. S. Unwin & R. Stachnik, *ASP Conf. Series*, 194, 256
- Borucki, W. J., et al. 2003, in *Future EUV/UV and Visible Space Astrophysics Missions and Instrumentation*, eds. J. C. Blades & O. H. W. Siegmund, *Proc. SPIE*, 4854, 129
- Boss A. P., 1997, *Science*, 276, 1836
- Boss, A. P. 1998, *Nature*, 393, 141
- Boss, A. P. 2000, *ApJ*, 536, L101

- Boss A. P., 2001, ApJ, 563, 367
- Boss, A. P., 2002, ApJ, 567, L149
- Boss, A. P. 2003, ApJ, 599, 577
- Boss, A. P. 2004a, ApJ, 610, 456
- Boss, A. P. 2004b, in ISSI Workshop on Planetary Systems and Planets in Systems, eds. S. Udry, W. Benz, & R. von Steiger, Space Science Reviews, in press
- Bouchy, F., Pont, F., Santos, N. C., Melo, C., Mayor, M., Queloz, D., & Udry, S. 2004, A&A, 421, L13
- Briceño, C., et al. 2001, Science, 291, 93
- Brown, T. M., Charbonneau, D., Gilliland, R. L., Noyes, R. W., & Burrows, A. 2001, ApJ, 552, 699
- Brown, T. M., Libbrecht, K. G., & Charbonneau, D. 2002, PASP, 114, 826
- Brown, T. M. 2003, ApJ, 593, L125
- Brown, T.M., Alonso, R., Belmonte, J.-A., & Charbonneau, D. 2004, in preparation
- Bryden, G., Chen, X., Lin, D. N. C., Nelson, R. P., & Papaloizou, J. C. B. 1999, ApJ, 514, 344
- Bryden, G., Rózyczka, M., Lin, D. N. C., & Bodenheimer, P. 2000, ApJ, 540, 1091
- Burrows, A., & Lunine, J.I. 1995, Nature, 378, 333
- Burrows, A., Marley, M., Hubbard, W.B., Lunine, J.I., Guillot, T., Saumon, D., Freedman, R., Sudarsky, D., & Sharp, C. 1997, ApJ, 491, 856
- Burrows, A., Guillot, T., Hubbard, W. B., Marley, M. S., Saumon, D., Lunine, J. I., & Sudarsky, D. 2000, ApJ, 534, L97
- Burrows, A., Sudarsky, D., & Hubbard, W.B. 2003, ApJ, 594, 545
- Burrows, A., Hubeny, I., Hubbard, W. B., Sudarsky, D., & Fortney, J. J. 2004, ApJ, 610, L53
- Burrows, A. 2005, Nature, 433, 261
- Butler, R. P., Marcy, G. W., Williams, E., McCarthy, C., Dosanjuh, P., & Vogt, S. S. 1996, PASP, 108, 500
- Butler, R. P., et al. 1999, ApJ, 526, 916

- Butler, R. P., Tinney, C. G., Marcy, G. W., Jones, H. R. A., Penny, A. J., & Apps, K. 2001, *ApJ*, 555, 410
- Butler, R. P., Marcy, G. W., Vogt, S. S., Fischer, D. A., Henry, G. W., Laughlin G., & Wright, J. 2003, *ApJ*, 582, 455
- Butler, R. P., Vogt, S. S., Marcy, G. W., Fischer, D. A., Wright, J. T., Henry, G. W., Laughlin, G., & Lissauer, J. J. 2004, *ApJ*, 617, 580
- Cameron, A. G. W. 1978, *Moon Planets*, 18, 5
- Carney, B. W., Latham, D. W., Laird, J. B., & Aguilar, L. A., 1994, *AJ*, 107, 2240
- Carney, B. W., et al., 2001, *AJ*, 122, 3419
- Casertano, S., Lattanzi, M. G., Perryman, M. A. C., & Spagna, A. 1996, *Ap&SS*, 241, 89
- Casertano, S., & Sozzetti, A. 1999, in *Working on the Fringe: Optical and IR Interferometry from Ground and Space*, ed. S. Unwin & R. Stachnik, *ASP Conf. Series* 194, 171
- Chabrier, G., Barman, T., Baraffe, I., Allard, F., & Hauschildt, P. H. 2004, *ApJ*, 603, L53
- Charbonneau, D., Noyes, R. W., Korzennik, S. G., Nisenson, P., Jha, S., Vogt, S. S., & Kibrick, R. I. 1999, *ApJ*, 522, L145
- Charbonneau, D., Brown, T. M., Latham, D. W., & Mayor, M. 2000, *ApJ*, 529, L45
- Charbonneau, D., Brown, T. M., Noyes, R. W., & Gilliland, R. L. 2002, *ApJ*, 568, 377
- Charbonneau, D. 2003, in *ISSI Workshop on Planetary Systems and Planets in Systems*, eds. S. Udry, W. Benz, and R. von Steiger, *Space Science Reviews*, in press (astro-ph/0302216)
- Charbonneau, D. 2004, in *Scientific Frontiers in Research on Extrasolar Planets*, D. Deming & S. Seager eds., *ASP Conf. Ser.*, 294, 449
- Charbonneau, D., Brown, T.M., Dunham, E.W., Latham, D.W., Looper, D., & Mandushev, G. 2004, *AIP Conf. Proc: The Search for Other Worlds*, eds. S.S. Holt & D. Deming, 151
- Charbonneau, D., et al. 2005, *ApJ*, 626, 523
- Chiang, E. I., Tabachnik, S., & Tremaine, S. 2001, *AJ*, 122, 1607
- Chiang, E. I., & Murray, N. 2002, *ApJ*, 576, 473
- Chiang, E.I., Fischer, D. A., & Thommes, E. 2002, *ApJ*, 564, L105
- Chmielewski, Y. 2000, *A&A*, 353, 666
- Claret, A. 2000, *A&A*, 363, 1081

- Cochran, W. D., & Hatzes, A. P. 1996, *Ap&SS*, 241, 43
- Cochran, W. D., Hatzes, A. P., & Paulson, D. B. 2002, *AJ*, 124, 565
- Cochran W., et al., 2004, *ApJ*, 611, L133
- Cody, A. M., & Sasselov, D. D. 2002, *ApJ*, 569, 451
- Colavita, M. M., et al. 1999, *ApJ*, 510, 505
- Collier Cameron, A., Horne, K., Penny, A., & Leigh, C. 2002, *MNRAS*, 330, 187
- Coradini, A., Magni, G., & Federico, C. 1981, *A&A*, 98, 173
- Correia, A. C. M., Udry, S., Mayor, M., Laskar, J., Naef, D., Pepe, F., Queloz, D., & Santos, N. C. 2005, *A&A*, accepted (astro-ph/0411512)
- Cumming, A., Marcy, G. W., & Butler, R. P. 1999, *ApJ*, 526, 890
- Cumming A., Marcy G. W., Butler R. P., & Vogt S. S., 2004, in *Scientific Frontiers in Research on Extrasolar Planets*, D. Deming & S. Seager eds., ASP Conf. Ser., 294, 27
- Cumming, A. 2004, *MNRAS*, 354, 1165
- Cuntz, M., Saar, S. H., & Musielak, Z. E. 2000, *ApJ*, 533, L151
- Cuntz, M., Von Bloh, W., Bounama, C., & Franck, S. 2003, *Icarus*, 162, 215
- Currie, T. 2005, *ApJ*, in press (astro-ph/0409730)
- Cuzzi, J. N., Dobrovolskis, A. R., & Champney, J. M. 1993, *Icarus*, 106, 102
- D'Angelo, G., Henning, T., & Kley, W. 2002, *A&A*, 385, 647
- D'Angelo, G., Kley, W., & Henning, T., 2003, *ApJ*, 386, 540
- Danner, R., & Unwin, S. 1999, *SIM: Taking the Measure of the Universe*, NASA/JPL
- David, E.-M., Quintana, E. V., Fatuzzo, M., & Adams, F. C. 2003, *PASP*, 115, 825
- Delfosse, X., Forveille, T., Mayor, M., Perrier, C., Naef, D., & Queloz, D. 1998, *A&A*, 338, L67
- Deliyannis, C. P., Cunha, K., King, J. R., & Boesgaard, A. M. 2000, *AJ*, 119, 2437
- Del Popolo, A., Gambera, M., & Ercan, N. 2001, *MNRAS*, 325, 1402
- Del Popolo, A., & Ekşi, K. Y. 2002, *MNRAS*, 332, 485
- Del Popolo, A., Yeşilyurt, S., & Ercan, E. N. 2003, *MNRAS*, 339, 556

- Deming, D., Brown, T. M., Charbonneau, D., Harrington, J., & Richardson, L. J. 2005, *ApJ*, 622, 1149
- Deming, D., Seager, S., Richardson, L. J., & Harrington, J. 2005, *Nature*, 434, 740
- Des Marais, D. J., et al. 2002, *Astrobiology*, 2, 153
- Dobbs-Dixon, I., Lin, D. N. C., & Mardling, R. A. 2004, *ApJ*, 610, 464
- Drake, F. D. 1962, *Intelligent Life in Space* (New York: MacMillan)
- Dunham, E. W., Mandushev, G., Taylor, B., & Oetiker, B. 2004, *PASP*, 116, 1072
- Duncan, D. K., et al. 1991, *ApJS*, 76, 383
- Durisen, R., Cai, K., Meija, A., & Pickett, M., 2005, *Icarus*, 173, 417
- Dvorak, R. 1986, *A&A*, 167, 379
- Dvorak, R., Pilat-Lohinger, E., Funk, B., & Freistetter, F. 2003a, *A&A*, 398, L1
- Dvorak, R., Pilat-Lohinger, E., Funk, B., & Freistetter, F. 2003b, *A&A*, 410, L13
- Dvorak, R., Pilat-Lohinger, E., Bois, E., Funk, B., Freistetter, F., & Kiseleva-Eggleton, L. 2004, in *The Environment and Evolution of Double and Multiple Stars*, Proc. IAU Coll. 191, C. Allen & C. Scarfe eds, *Revista Mexicana de Astronomía y Astrofísica (Serie de Conferencias)*, 21, 222
- Ecuivillon, A., Israelian, G., Santos, N. C., Mayor, M., García López, R. J., & Randich, S. 2004a, *A&A*, 418, 703
- Ecuivillon, A., Israelian, G., Santos, N. C., Mayor, M., Villar, V., & Bihain, G. 2004b, *A&A*, 426, 619
- Edgar, R., & Artymowicz, P. 2004, *MNRAS*, 354, 769
- Eggenberger, P., Charbonnel, C., Talon, S., Meynet, G., Maeder, A., Carrier, F., & Bourban, G. 2004a, *A&A*, 417, 235
- Eggenberger A., Udry, S., & Mayor M., 2004b, *A&A*, 417, 353
- Eisner, J. A., & Kulkarni, S. R. 2001a, *ApJ*, 550, 871
- Eisner, J. A., & Kulkarni, S. R. 2001b, *ApJ*, 561, 1107
- Eisner, J. A., & Kulkarni, S. R. 2002, *ApJ*, 574, 426
- Endl, M., Kürster, M., Els, S., Hatzes, A. P., Cochran, W. D., Dennerl, K., & Döbereiner, S. 2002, *A&A*, 392, 671

- Endl, M., Cochran, W. D., Tull, R. G., & MacQueen, P. J. 2003, *AJ*, 126, 3099
- Endl, M., et al. 2004, *ApJ*, 611, 1121
- Érdi, B., Dvorak, R., Sándor, Zs., Pilat-Lohinger, E., & Funk, B. 2004, *MNRAS*, 351, 1043
- Farrell, W. M., Desch, M. D., & Zarka, P. 1999, *JGR*, 104, 14025
- Farrell, W. M., Desch, M. D., & Lazio, T. J., Bastian, T., Zarka, P. 2004, in *Scientific Frontiers in Research on Extrasolar Planets*, D. Deming and S. Seager eds., *ASP Conf. Ser.*, 294, 151
- Ferraz-Mello, S., Beaugé, C., & Michtchenko, T. A. 2004, *CeMDA*, 87, 99
- Ferraz-Mello, S., Michtchenko, T. A., & Beaugé, C. 2005, *ApJ*, 621, 473
- Fischer, D. A., Marcy, G. W., Butler, R. P., Vogt, S. S., Frink, S., & Apps, K. 2001, *ApJ*, 551, 1107
- Fischer, D. A., Marcy, G. W., Butler, R. P., Vogt, S. S., Walp, B., & Apps, K. 2002a, *PASP*, 114, 529
- Fischer, D. A., Marcy, G. W., Butler, R. P., Laughlin, G., & Vogt, S. S. 2002b, *ApJ*, 564, 1028
- Fischer, D. A., et al. 2003a, *ApJ*, 586, 1394
- Fischer, D., Valenti, J. A., & Marcy, G. W., 2003b, in *proc. IAU Symp. 219: Stars as Suns: Activity, Evolution, and Planets*, A. K. Dupree ed., *ASP*, 29
- Fischer, D. A., et al. 2005, *ApJ*, 620, 481
- Ford, E. B., Rasio, F. A., & Sills A. 1999, *ApJ*, 514, 411
- Ford, E.B., Kozinsky, B., & Rasio, F.A. 2000, *ApJ*, 535, 385
- Ford, E. B., Havlickova, M., & Rasio, F. A. 2001, *Icarus*, 150, 303
- Ford, E. B., Seager, S., & Turner, E. L. 2001, *Nature*, 412, 885
- Ford, E. B., & Tremaine, S. 2003, *PASP*, 115, 1171
- Ford, E. B., Lystad, V., & Rasio, F. 2005, *Nature*, 434, 873
- Fortney, J.J., & Hubbard, W.B. 2004, *ApJ*, 608, 1039
- Franz, O. G., et al. 1998, *AJ*, 116, 1432
- Fridlund, C. V. M. 2000, in *Darwin and astronomy - the infrared space interferometer*, *ESA-SP 451*, 11

- Frink, S., Mitchell, D. S., Quirrenbach, A., Fischer, D. A., Marcy, G. W., & Butler, R. P. 2002, *ApJ*, 576, 478
- Fuhrmann, K., Pfeiffer, M. J., & Bernkopf, J. 1997, *A&A*, 326, 1081
- Fuhrmann, K., Pfeiffer, M. J., & Bernkopf, J. 1998, *A&A*, 336, 942
- Gammie, C. F. 2001, *ApJ*, 553, 174
- Garaud, P., & Lin, D. N. C. 2004, *ApJ*, 608, 1050
- García López, R. J., & Pérez de Taoro, M. R. 1998, *A&A*, 334, 599
- Gatewood, G. D. 1996, *BAAS*, 28, 885
- Gatewood, G. D., Han, I., & Black, D. C. 2001, *ApJ*, 548, L61
- Gaudi, B. S., et al. 2002, *ApJ*, 566, 463
- Gaudi, B. S., Seager, S., & Mallén-Ornelas, G. 2005, *ApJ*, 623, 472
- Gilliland, R. L., & Baliunas, S. L. 1987, *ApJ*, 314, 766
- Gilliland, R. L., et al. 2000, *ApJ*, 545, L47
- Giménez, A. 2000, *A&A*, 356, 213
- Girardi, L., Bressan, A., Bertelli, G., & Chiosi, C. 2000, *A&AS*, 141, 371
- Gladman, B. 1993, *Icarus*, 106, 247
- Glindemann, A., et al. 2003, *Ap&SS*, 286, 35
- Goldreich, P., & Soter, S 1966, *Icarus*, 5, 375
- Goldreich, P., & Ward, W. R. 1973, *ApJ*, 183, 1051
- Goldreich, P., & Tremaine S., 1979, *ApJ*, 233, 857
- Goldreich, P., & Tremaine, S 1980, *ApJ*, 241, 425
- Goldreich, P. & Sari, R. 2003, *ApJ*, 585, 1024
- Goldreich, P., Lithwick, Y., & Sari, R. 2004, *ARA&A*, 42, 549
- Gonzalez G., 1997, *MNRAS*, 285, 403
- Gonzalez, G. 1998a, *A&A*, 334, 221
- Gonzalez G., 1998b, in *Brown Dwarfs and Extrasolar Planets*, R. Rebolo, E.L. Martin & M.R. Zapatero Osorio eds., *ASP Conf. Ser.*, 134, 431

- Gonzalez, G., & Vanture, A. D. 1998, *A&A*, 339, L29
- Gonzalez, G., & Laws, C. 2000, *AJ*, 119, 390
- Gonzalez G., Laws C., Tyagi S., & Reddy B. E., 2001, *AJ*, 121, 432
- Gonzalez G., 2003, *RvMP*, 75, 101
- Goodman, J., & Pindor, B. 2000, *Icarus*, 148, 537
- Goździewski, K., & Maciejewski, A. J. 2001, *ApJ*, 563, L81
- Goździewski, K., Bois, E., & Maciejewski, A. J. 2002, *MNRAS*, 332, 839
- Goździewski, K. 2002, *A&A*, 393, 997
- Goździewski, K. 2003a, *A&A*, 398, 315
- Goździewski, K. 2003b, *A&A*, 398, 1151
- Goździewski, K., & Maciejewski, A. J. 2003, *ApJ*, 586, L153
- Goździewski, K., Konacki, M., & Maciejewski, A. J. 2003, *ApJ*, 594, 1019
- Goździewski, K., Konacki, M., & Maciejewski, A. J. 2005, *ApJ*, 622, 1136
- Goździewski, K., & Konacki, M. 2004, *ApJ*, 610, 1093
- Gratton, R., et al. 2004, in *Scientific Frontiers in Research on Extrasolar Planets*, D. Deming and S. Seager eds., *ASP Conf. Ser.*, 294, 47
- Green, R. 1985, *Spherical Astronomy*, Cambridge University Press
- Grießmeier, J.-M., et al. 2004, *A&A*, 425, 753
- Gu, P.-G., Lin, D. N. C., & Bodenheimer, P. H. 2003, *ApJ*, 588, 509
- Gu, P.-G., Bodenheimer, P. H., & Lin, D. N. C. 2004, *ApJ*, 608, 1076
- Guillot, T., Burrows, A., Hubbard, W.B., Lunine, J. I., & Saumon, D. 1996, *ApJ*, 459, L35
- Guillot, T., Gautier, D., & Hubbard, W. B. 1997, *Icarus*, 130, 534
- Guillot, T. 1999, *Science*, 286, 72
- Guillot, T., & Showman A. P. 2002, *A&A*, 385, 156
- Guillot, T. 2005, *Annual Review of Earth and Planetary Sciences*, 33, 493
- Guirado, J. C., et al. 1997, *ApJ*, 490, 835

- Haisch, K. E., Lada, E. A., & Lada, C. J. 2001, *ApJ*, 553, L153
- Halbwachs, J. L., Arenou, F., Mayor, M., Udry, S., & Queloz, D. 2000, *A&A*, 355, 581
- Halbwachs, J. L., Mayor, M., & Udry, S. 2005, *A&A*, 431, 1129
- Han, I., Black, D. C., & Gatewood, G. D. 2001, *ApJ*, 548, L57
- Hatzes, A. P., et al. 2003, *ApJ*, 599, 1383
- Hayashi, C. 1981, *Prog. Theor. Phys. Suppl.*, 70, 35
- Hayashi, C., Nakazawa, K., & Nakagawa, Y. 1985, in *Protostars and Planets II*, ed D. C. Black & M. S. Matthews (Tucson: University of Arizona Press), 1100
- Heacox, W. D. 1999, *ApJ*, 526, 928
- Heintz, W. D. 1978, *Double Stars*, Boston D. Reidel Publishing Company
- Heiter, U., & Luck, R. E. 2003, *AJ*, 126, 2015
- Henry, T. J., Soderblom, D. R., Donahue, R. A., & Baliunas, S. L. 1996, *AJ*, 111, 439
- Henry, G., Marcy, G. W., Butler, R. P., & Vogt, S. S. 2000, *ApJ*, 529, L41
- Heppenheimer, T. A. 1973, *Icarus*, 22, 436
- Heppenheimer, T. A. 1978, *A&A*, 65, 421
- Hershey, J. L., & Lippincott, S. L. 1982, *AJ*, 87, 840
- Holman, M., Touma, J., & Tremaine, S. 1997, *Nature*, 386, 254
- Holman, M. J., & Wiegert, P. A. 1999, *AJ*, 117, 621
- Holman, M. J., & Murray, N. W. 2005, *Science*, 307, 1288
- Horne, J. H., & Baliunas, S. L. 1986, *ApJ*, 302, 757
- Horne, K. 2004, *ASP Conf. Ser. 294: Scientific Frontiers in Research on Extrasolar Planets*, eds. D. Deming & S. Seager, 361
- Hubbard, W.B., Fortney, J.F., Lunine, J.I., Burrows, A., Sudarsky, D., & Pinto, P.A. 2001, *ApJ*, 560, 413
- Hubbard, W. B., Burrows, A., & Lunine, J. I. 2002, *ARA&A*, 40, 103
- Ida, S., & Lin, D. N. C., 2004a, *ApJ*, 604, 388
- Ida, S., & Lin, D. N. C., 2004b, *ApJ*, 616, 567

- Ida S., & Lin D. N. C., 2005, *ApJ*, 626, 1045
- Ikoma, M., Emori, H., & Nakazawa, K. 2001, *ApJ*, 553, 999
- Innanen, K. A., Zheng, J.Q., Mikkola, S., & Valtonen, M. J. 1993, *AJ*, 113, 1915
- Irion, R. 2004, *Science*, 305, 1382
- Israelian G., Santos N. C., Mayor M., & Rebolo R., 2001, *Nature*, 411, 163
- Israelian, G., Santos, N. C., Mayor, M., & Rebolo, R. 2003, *A&A*, 405, 753
- Israelian, G., Santos, N. C., Mayor, M., & Rebolo, R. 2004, *A&A*, 414, 601
- Ivanov, P. B., Papaloizou, J. C. B., & Polnarev, A. G. 1999, *MNRAS*, 307, 791
- Jang-Condell, H., & Sasselov, D. D. 2004, *ApJ*, 608, 497
- Jenkins, J. M. & Doyle, L. R. 2003, *ApJ*, 595, 429
- Jensen, O. G., & Ulrych, T. 1973, *AJ*, 78, 1104
- Ji, J., Li, G., & Liu, L. 2002, *ApJ*, 572, 1041
- Ji, J., Kinoshita, H., Liu, L., & Li, G. 2003, *ApJ*, 585, L139
- Jiang, I., & Ip, W. 2001, *A&A*, 367, 943
- Jones, B. W., Sleep, P. N., & Chambers, J. E. 2001, *A&A*, 366, 254
- Jones, B. W., & Sleep, P. N. 2002, *A&A*, 393, 1015
- Jones, B. W., & Sleep, P. N. 2004, in *Scientific Frontiers in Research on Extrasolar Planets*, ed. D. Deming and S. Seager, ASP Conf. Series, 294, 225
- Jones, H. R. A., Butler, R. P., Marcy, G. W., Tinney, C. G., Penny, A. J., McCarthy, C., & Carter, B. D. 2002, *MNRAS*, 337, 1170
- Jones H., 2003, in *IAU Symp. 219: Stars as Suns: Activity, Evolution, and Planets*, A. K. Dupree ed., ASP Conf. Ser. in press
- Jones, H. R. A., Butler, R. P., Tinney, C. G., Marcy, G. W., Penny, A. J., McCarthy, C., & Carter, B. D. 2003, *MNRAS*, 341, 948
- Jorissen, A., Mayor, M., & Udry, S. 2001, *A&A*, 379, 992
- Kant, I. 1755, *Allgemeine Naturgeschichte und Theorie des Himmels*, ed. Königsberg & Leipzig
- Kasting, J. F., Whitmire, D. P., & Reynolds, R. T. 1993, *Icarus*, 101, 108

- Kells, L. M., Kern, W. F., & Bland, J. R. 1942, *Spherical Trigonometry with Naval and Military Applications*, New York: McGraw-Hill
- Kenworthy, M. A. & Hinz, P. M. 2003, *PASP*, 115, 322
- Kinoshita, H., & Nakai, H. 2001, *PASJ*, 53, L25
- Kiseleva-Eggleton, L., Bois, E., Rambaux, N., & Dvorak, R. 2002, *ApJ*, 578, L145
- Kley, W. 1999, *MNRAS*, 303, 696
- Kley, W. 2000a, *MNRAS*, 313, L47
- Kley, W., & Burkert, A. 2000, in *Disks, Planetesimals, and Planets*, ed. F. Garzón, C. Eiroa, D. de Winter, & T. J. Mahoney, *ASP Conf. Ser.*, 219, 189
- Kley, W. 2000b, in *Birth and Evolution of Binary Stars*, *Proc. IAU Symp.* 200, ed. B. Reipurth & H. Zinnecker, 211
- Kley, W. 2001, in *The Formation of Binary Stars*, *Proc. IAU Symp.* 200, ed. H. Zinnecker & R. D. Mathieu, 511
- Kley, W., D'Angelo, G., & Henning, T. 2001, *ApJ*, 547, 457
- Kley, W., Peitz, J., & Bryden, G. 2004, *A&A*, 414, 735
- Kokubo, E., & Ida, S. 2002, *ApJ*, 581, 666
- Konacki, M., Maciejewski, A. J., & Wolszczan, A. 2002, *ApJ*, 567, 566
- Konacki, M., Torres, G., Jha, S., & Sasselov, D. D. 2003, *Nature*, 421, 507
- Konacki, M., et al. 2004, *ApJ*, 609, L37
- Konacki, M., Torres, G., Sasselov, D. D., & Jha, S. 2005, *ApJ*, 624, 372
- Konacki, M. 2005, *ApJ*, accepted, 626, 431
- Kornet, K., Stepinski, T. F., & Różyczka, M. 2001, *A&A*, 417, 151
- Kornet, K., Różyczka, M., & Stepinski, T. F. 2004, *A&A*, 378, 180
- Kornet, K., Bodenheimer, P., Różyczka, M., & Stepinski, T. F. 2005, *A&A*, 430, 1133
- Korzennik, S. G., et al. 1998, in *Cool Stars, Stellar Systems, and the Sun*, *ASP Conf. Ser.*, 154, 1876
- Kozai, Y. 1962, *AJ*, 67, 591
- Krymowski, Y., & Mazeh, T. 1999, *MNRAS*, 304, 720

- Kuchner, M. J., & Lecar, M. 2002, *ApJ*, 574, L87
- Kuchner, M. J. 2004, *ApJ*, 612, 1147
- Kuiper, G. P. 1951, *Proc. Natl. Acad. Sci. U.S.A.* 37, 1
- Kürster, M., et al. 2003, *A&A*, 403, 1077
- Kürster, M., & Endl, M. 2004, in *Extrasolar Planets: Today and Tomorrow*, J.-P. Beaulieu, A. Lecavelier des Etangs and C. Terquem Eds., *ASP Conf. Ser.*, 321, 84
- Kurucz, R. L. 1993, *ATLAS9 Stellar Atmosphere Programs and 2 km/s Grid CDROM*, Vol. 13, Smithsonian Astrophysical Observatory
- Lammer, H., Selsis, F., Ribas, I., Guinan, E. F., Bauer, S. J., & Weiss, W. W. 2003, *ApJ*, 598, L121
- Landolt, A. U. 1992, *AJ*, 104, 340
- Lane, B. F., & Colavita, M. M. 2003, *AJ*, 125, 1623
- Laskar, J. 1994, *A&A*, 287, L9
- Latham, D. W. 1985, *IAU Colloq. 88: Stellar Radial Velocities*, eds. A. Philip & D. Latham, 21
- Latham, D. W. 1992, *ASP Conf. Ser. 32: IAU Colloq. 135: Complementary Approaches to Double and Multiple Star Research*, eds. H. McAlister & W. Hartkopf, 110
- Latham, D. W. 2000, in *Disks, Planetesimals, and Planets*, F. Garzón, C. Eiroa, D. de Winter, and T. J. Mahoney eds, *ASP Conf. Ser.*, 219, 596
- Latham, D. W., et al., 2002, *AJ*, 124, 1144
- Latham, D. W. 2004, *ASP Conf. Ser. 294: Scientific Frontiers in Research on Extrasolar Planets*, eds. D. Deming & S. Seager, 409
- Lattanzi, M. G., Spagna, A., Sozzetti, A., & Casertano, S. 2000, *MNRAS*, 317, 211
- Laughlin, G., & Bodenheimer, P. 1994, *ApJ*, 346, 335
- Laughlin G., & Adams F. C., 1997, *ApJ*, 491, L51
- Laughlin, G., & Adams, F. C. 1999, *ApJ*, 526, 881
- Laughlin G., 2000, *ApJ*, 545, 1064
- Laughlin, G., & Chambers, J. E. 2001, *ApJ*, 551, L109
- Laughlin, G., Chambers, J. E., & Fischer, D. A. 2002, *ApJ*, 579, 455

- Laughlin, G., Bodenheimer, P., & Adams, F. C. 2004a, ApJ, 612, L73
- Laughlin, G., Steinacker, A., & Adams, F. C. 2004b, ApJ, 608, 489
- Laughlin, G., Wolf, A., Vanmunster, T., Bodenheimer, P., Fischer, D., Marcy, G. W., Butler, R. P., & Vogt, S. S. 2005a, ApJ, 621, 1072
- Laughlin, G., Butler, R. P., Fischer, D. A., Marcy, G. W., Vogt, S. S., & Wolf, A. S. 2005b, ApJ, 622, 1182
- Laws, C., & Gonzalez, G. 2001, ApJ, 553, 405
- Laws C., Gonzalez G., Walker K. M., Tyagi S., Dodsworth J., Snider K., & Suntzeff N. B., 2003, AJ, 125, 2664
- Lazio, T. J. W., Farrell, W. M., Dietrick, J., Greenlees, E., Hogan, E., Jones, C., & Hennig, L. A. 2004, ApJ, 612, 511
- Lee J.-W., & Carney, B. W. 2002, AJ, 124, 1511
- Lecar, M., & Sasselov, D. D. 2003, ApJ, 596, L99
- Lecavelier des Etangs, A., Vidal-Madjar, A., McConnell, J. C., & Hébrard, G. 2004, A&A, 418, L1
- Lee, M. H., & Peale, S. J. 2002, ApJ, 567, 596
- Lee, M.H., & Peale, S. J. 2003, ApJ, 592, 1201
- Lee, M.H. 2004, ApJ, 611, 517
- Lee, M. H., & Peale, S. J. 2004, in Scientific Frontiers in Research on Extrasolar Planets, ed. D. Deming and S. Seager, ASP Conf. Series, 294, 197
- Leigh, C., Collier Cameron, A., Horne, K., Penny, A., & James, D. 2003a, MNRAS, 344, 1271
- Leigh, C., Collier Cameron, A., Udry, S., Donati, J., Horne, K., James, D., & Penny, A. 2003b, MNRAS, 346, L16
- Lin, D. N. C., & Papaloizou, J. C. B. 1979, MNRAS, 188, 191
- Lin, D. N. C., & Papaloizou, J. C. B. 1986, ApJ, 307, 395
- Lin, D. N. C., & Papaloizou, J. C. B. 1986, ApJ, 309, 846
- Lin, D. N. C., & Papaloizou, J. C. B. 1993, in Protostars and Planets III, ed E. H. Levy & J. I. Lunine (Tucson: University of Arizona Press), 749
- Lin, D. N. C., & Papaloizou, J. C. B. 1996, ARA&A, 34, 703

- Lin, D. N. C., & Ida, S. 1997, *ApJ*, 477, 781
- Lin, D. N. C., Papaloizou, J. C. B., Terquem, C., Bryden, G., & Ida, S. 2000, in *Protostars and Planets IV*, eds. V. Mannings, A. P. Boss, & S. S. Russell (Tucson: University of Arizona Press), 1111
- Lineweaver, C. H., & Grether, D. 2002, *Astrobiology*, 2, 325
- Lineweaver, C. H., & Grether, D. 2003, *ApJ*, 598, 1350
- Lippincott, S. L. 1960a, *AJ*, 65, 349
- Lippincott, S. L. 1960b, *AJ*, 65, 445
- Lissauer, J. J. 1987, *Icarus*, 69, 249
- Lissauer J. J., 1993, *ARA&A*, 31, 129
- Lissauer, J. J., & Rivera, E. J. 2001, *ApJ*, 554, 1141
- Livio, M., & Pringle, J. E., 2003, *MNRAS*, 346, L42
- Lomb, N. R. 1976, *Ap&SS*, 39, 447
- Lovelock, J. 1965, *Nature*, 207, 568
- Lufkin, G., Quinn, T., Wadsley, J., Stadel, J., & Governato, F. 2004, *MNRAS*, 347, 421
- Lubow, S. H., Seibert, M., & Artymowicz, P. 1999, *ApJ*, 526, 1001
- Lucas, P. W. & Roche, P. F. 2002, *MNRAS*, 336, 637
- Mandell, A. M., Ge, J., & Murray, N. 2004, *AJ*, 127, 1147
- Mandushev, G., et al. 2005, *ApJ*, 621, 1061
- Mardling, R. A., & Lin, D. N. C. 2002, *ApJ*, 573, 829
- Marcy, G. W., & Benitz, K. J. 1989, *ApJ*, 344, 441
- Marcy, G. W., & Butler, R. P. 1998, *ARA&A*, 36, 57
- Marcy G. W., Butler R. P., & Fischer D., et al. 2001a, *ApJ*, 556, 296
- Marcy G. W., Butler R. P., & Vogt S. S., et al. 2001b, *ApJ*, 555, 418
- Marcy, G. W., Butler, R. P., Fischer, D. A., Laughlin, G., Vogt, S. S., Henry, G. W., & Pourbaix, D. 2002b, *ApJ*, 581, 1375

- Marcy, G. W., Butler, R. P., Fischer, D. A., & Vogt, S. S. 2004a, in *Scientific Frontiers in Research on Extrasolar Planets*, ed. D. Deming and S. Seager, ASP Conf. Series, 294, 1
- Marcy, G. W., Butler, R. P., Fischer, D. A., & Vogt, S. S. 2004b, in *Extrasolar Planets: Today and Tomorrow*, J.-P. Beaulieu, A. Lecavelier des Etangs and C. Terquem Eds., ASP Conf. Ser., 321, 3
- Marcy, G. W., Fischer, D. A., McCarthy, C., & Ford, E. B. 2005, in *Astrometry in the Age of the Next Generation of Large Telescopes*, eds. P. K. Seidelmann & A. K. B. Monet, ASP Conf. Ser., in press
- Mariotti, J. M., et al. 1998, *Proc. SPIE 3350, Astronomical Interferometry*, Ed. R. D. Reasenberg, p. 800
- Marley, M. S., Gelino, C., Stephens, D., Lunine, J. I., & Freedman, R. 1999, *ApJ*, 513, 879
- Martell, S., & Laughlin, G. 2002, *ApJ*, 577, L45
- Martínez-Roger, C., Arribas, S., & Alonso, A. 1992, *Mem. Soc. Astr. Italiana*, 63, 263
- Marzari, F., & Scholl, H. 2000, *ApJ*, 543, 328
- Marzari, F., Weidenschilling, S., Barbieri, M., & Granata, V. 2005, *ApJ*, 618, 502
- Masset, F., & Snellgrove, M. 2001, *MNRAS*, 320, L55
- Masset, F. S., & Papaloizou, J. C. B. 2003, *ApJ*, 588, 494
- Mayer, L., Quinn, T., Wadsley, J., & Stadel, J. 2002, *Science*, 298, 1756
- Mayer, L., Quinn, T., Wadsley, J., & Stadel J., 2004, *ApJ*, 609, 1045
- Mayer L., Quinn T., Wadsley J., & Stadel J., 2005, *MNRAS*, submitted (astro-ph/0405502)
- Mayor, M., & Queloz, D. 1995, *Nature*, 378, 355
- Mayor, M., Queloz, D., & Udry, S. 1998a, in *Brown Dwarfs and Extrasolar Planets*, ed. R. Rebolo, E. L. Martin, & M. R. Zapatero-Osorio, ASP Conf. Ser., 134, 140
- Mayor, T., Udry, S., & Queloz, D. 1998b, in *Tenth Cambridge Workshop on Cool Stars, Stellar Systems, and the Sun*, ed. R. Donahue & J. Bookbinder, ASP Conf. Ser. 154, 77
- Mayor, M., & Udry, S. 2000, in *Disks, Planetesimals, and Planets*, ASP Conf. Proc., 219, 441
- Mayor, M., et al. 2001, ESO Press Release 07/01
- Mazeh, T., Latham, D. W., & Stefanik, R. P. 1996, *ApJ*, 466, 415
- Mazeh, T., Krymolowski, Y., & Rosenfeld, G. 1997, *ApJ*, 477, L103

- Mazeh, T., Goldberg, D., & Latham, D. W. 1998, *ApJ*, 501, L199
- Mazeh, T. 1999, *Physics Reports*, 311, 317
- Mazeh, T., Zucker, S., dalla Torre, A., & van Leeuwen, F. 1999, *ApJ*, 522, L149
- Mazeh, T., et al. 2000, *ApJ*, 532, L55
- Mazeh, T., & Zucker, S. 2001, in *The Formation of Binary Stars*, Proc. IAU Symp. 200, ed. H. Zinnecker and R. D. Mathieu, 519
- Mazeh, T., & Zucker, S. 2002, in *JENAM 2001: Astronomy with Large Telescopes from Ground and Space*, ed. R. E. Schielicke, *Reviews in Modern Astronomy*, 15, 133
- Mazeh T., & Zucker S., 2003, *ApJ*, 590, L115
- McArthur, B. E., et al. 2004, *ApJ*, 614, L81
- McGrath, M. A., et al. 2002, *ApJ*, 564, L27
- McGrath, M. A., et al. 2004, in *Scientific Frontiers in Research on Extrasolar Planets*, ed. D. Deming and S. Seager, *ASP Conf. Series*, 294, 145
- Mejía, A. C., Durisen, R. H., Pickett, M. K., & Cai, K. 2005, *ApJ*, 619, 1098
- Menou, C., & Tabachnik, S. 2003, *ApJ*, 583, 473
- Michtchenko, T. A., & Malhotra, R. 2004, *Icarus*, 168, 237
- Miralda-Escudé, J. 2002, *ApJ*, 564, 1019
- Mitchell, D. S., Frink, S., Quirrenbach, A., Fischer, D. A., Marcy, G. W., & Butler, R. P. 2003, *BAAS*, 35, #17.03
- Mizuno, H. 1980, *Prog. Theor. Phys.*, 64, 544
- Monet, D. G. 1983, in *Current Techniques in Double and Multiple Star Research*, ed. R. S. Harrington and O. G. Franz, *IAU Coll.*, 62, 286
- Monet, D. G., et al. 2003, *AJ*, 125, 984
- Montalbán, J., & Rebolo, R. 2002, *A&A*, 386, 1039
- Montes, D., Ramsey, L. W., & Welty, A. D. 1999, *ApJS*, 123, 283
- Moriwaki, K., & Nakagawa, Y. 2004, *ApJ*, 609, 1065
- Moutou, C., Coustenis, A., Schneider, J., St Gilles, R., Mayor, M., Queloz, D., & Kaufer, A. 2001, *A&A*, 371, 260

- Moutou, C., Coustenis, A., Schneider, J., Queloz, D., & Mayor, M. 2003, *A&A*, 405, 341
- Moutou, C., Pont, F., Bouchy, F., & Mayor, M. 2004, *A&A*, 424, L31
- Mugrauer M., Neuhäuser R., Mazeh T., Alves J., & Guenther E. W., 2004a, *A&A*, 425, 249
- Mugrauer M., Neuhäuser R., Mazeh T., Guenther E. W., & Fernández M., 2004b, *AN*, 325, 718
- Murray, N., Hansen, B., Holman, M., & Tremaine, S. 1998, *Science*, 279, 69
- Murray, N., Paskowitz, M., & Holman, M. 2002, *ApJ*, 565, 608
- Murray, N., & Chaboyer, B. 2002, *ApJ*, 566, 442
- Musielak, Z. E., Cuntz, M., Marshall, E. A., & Stuit, T. D. 2005, *A&A*, 434, 355
- Naef, D., et al. 2001, *A&A*, 375, L27
- Naef, D., Mayor, M., Beuzit, J. L., Perrier, C., Queloz, D., Sivan, J. P., & Udry, S. 2004, in *XIII Cambridge Workshop on cool stars, stellar systems, and the Sun*, ESA-SP, 560, in press
- Nagasawa, M., Lin, D. N. C., & Ida, S. 2003, *ApJ*, 586, 1374
- Nakagawa, Y., Nakazawa, K., & Hayashi, C. 1981, *Icarus*, 45, 517
- Nakagawa, Y., Sekiya, M., & Hayashi, C. 1986, *Icarus*, 67, 375
- Nakano, T. 1987, *MNRAS*, 224, 107
- Narayan R., Cumming A., & Lin D. N. C., 2004, *ApJ*, 620, 1002
- Nelson, A. F., & Angel, J. R. P. 1998, *ApJ*, 500, 940
- Nelson, A.F., 2000, *ApJ*, 537, L65
- Nelson, R. P., Papaloizou, J. C. B., Masset, F., & Kley, W. 2000, *MNRAS*, 318, 18
- Nelson, R. P., & Papaloizou, J. C. B. 2002, *MNRAS*, 333, L26
- Nelson, A.F., 2003, *MNRAS*, 345, 233
- Nelson, R. P., & Papaloizou, J. C. B. 2003, *MNRAS*, 339, 993
- Nelson, R. P., & Papaloizou, J. C. B. 2004, *MNRAS*, 350, 849
- Neuforge-Verheecke, C., & Magain, P. 1997, *A&A*, 328, 261
- Noble, M., Musielak, Z. E., & Cuntz, M. 2002, *ApJ*, 572, 1024

- Nordström B., et al., 2004, *A&A*, 418, 989
- Novak, G. S., Lai, D., & Lin, D. N. C. 2004, in *Scientific Frontiers in Research on Extrasolar Planets*, ed. D. Deming and S. Seager, ASP Conf. Series, 294, 177
- Noyes, R. W., Hartmann, L. W., Baliunas, S. L., Duncan, D. K., & Vaughan, A. H. 1984, *ApJ*, 279, 763
- Ogilvie, G. I., & Lubow, S. H. 2003, *ApJ*, 587, 398
- Ogilvie, G. I., & Lin, D. N. C. 2004, *ApJ*, 610, 477
- Oppenheimer B. R., Kulkarni S. R., & Stauffer J. R., 2000, in *Protostars and Planets IV*, ed V. Mannings, A. P. Boss & S. S. Russell (Tucson: University of Arizona Press), 1313
- Pace, G., & Pasquini, L. 2004, *A&A*, 426, 1021
- Papaloizou J., & Lin D. N. C., 1984, *ApJ*, 285, 818
- Papaloizou, J. C. B., & Terquem, C. 1999, *ApJ*, 521, 823
- Papaloizou, J. C. B., & Larwood, J. D. 2000, *MNRAS*, 315, 823
- Papaloizou, J. C. B., & Terquem, C. 2001, *MNRAS*, 325, 221
- Papaloizou, J. C. B., Nelson, R. P., & Masset, F. 2001, *A&A*, 366, 263
- Papaloizou, J. C. B., & Nelson, R. P. 2003, *MNRAS*, 339, 983
- Papaloizou, J. C. B., Nelson, R. P., & Snellgrove, M. D. 2004, *MNRAS*, 350, 829
- Patience, J., et al. 2002, *ApJ*, 581, 654
- Pätzold, M., & Rauer, H. 2002, *ApJ*, 568, L117
- Pätzold, M., Carone, L., & Rauer, H. 2004, *A&A*, 427, 1075
- Paulson, D. B., Saar, S. H. Cochran, W. D., & Hatzes, A. P. 2002, *AJ*, 124, 572
- Pepe, F., et al., 2004, *A&A*, 423, 385
- Perrier, C., Sivan, J.-P., Naef, D., Beuzit, J. L., Mayor, M., Queloz, D., & Udry, S. 2003, *A&A*, 410, 1039
- Perryman M. A. C. et al., 1996, *A&A*, 310, L21
- Perryman, M. A. C., et al. 2001, *A&A*, 369, 339
- Pickett, B. K., Mejía, A. C., Durisen, R. H., Cassen, P. M., Berry, D. K., & Link, R. P. 2003, *ApJ*, 590, 1060

- Pilat-Lohinger, E., & Dvorak, R. 2002, *Celestial Mechanics and Dynamical Astronomy*, 82, 143
- Pilat-Lohinger, E., Funk, B., & Dvorak, R. 2003, *A&A*, 400, 1085
- Pilat-Lohinger, E., Dvorak, R., Bois, E., & Funk, B. 2004, in *Extrasolar Planets: Today and Tomorrow*, J.-P. Beaulieu, A. Lecavelier des Etangs and C. Terquem Eds., *ASP Conf. Ser.*, 321, 410
- Pinsonneault, M. H., DePoy, D. L., & Coffee, M. 2001, *ApJ*, 556, L59
- Pollack, J. B., Hubickyj, O., Bodenheimer, P., Lissauer, J. J., Podolack, M., & Greenzweig, Y. 1996, *Icarus*, 124, 62
- Pont, F., Bouchy, F., Queloz, D., Santos, N. C, Melo, C., Mayor, M., & Udry, S. 2004, *A&A*, 426, L15
- Pourbaix, D., & Jorissen, A. 2000, *A&AS*, 145, 161
- Pourbaix, D. 2001, *A&A*, 369, L22
- Pourbaix, D., & Arenou, F. 2001, *A&A*, 372, 935
- Press, W. H., & Rybicki, G. B. 1989, *ApJ*, 338, 277
- Press W. H., Teukolsky S. A., Vetterling V. T., & Flannery B. P., 1992, *Numerical Recipes in FORTRAN: the Art of Scientific Computing*, Cambridge University Press
- Queloz D., et al., 2000a, *A&A*, 354, 99
- Queloz, D., et al. 2000b, *A&A*, 359, L13
- Quintana, E. V., Lissauer, J. J., Chambers, J. E., & Duncan, M. J. 2002, *ApJ*, 576, 982
- Rafikov, R. R. 2004, *AJ*, 128, 1348
- Rafikov, R. R. 2005, *ApJ*, 621, L69
- Ramírez, I., & Meléndez, J. 2004, *ApJ*, 609, 417
- Rasio, F. A., & Ford, E. B. 1996, *Science*, 274, 954
- Raymond, S. N., & Barnes, R. 2004, *ApJ*, 619, 549
- Raymond, S. N., Quinn, T., & Lunine, J. I. 2004, *Icarus*, 168, 1
- Reddy, B. E., Lambert, D. L., Laws, C., Gonzalez, G., & Covey, K. 2002, *MNRAS*, 335, 1005
- Reid I. N., 2002, *PASP*, 114, 306

- Rice, W. K. M., & Armitage, P. J. 2003, ApJ, 598, L55
- Rice W. K. M., Armitage P. J., Bate M. R., & Bonnell I. A. 2003, MNRAS, 339, 1025
- Rice W. K. M., Armitage P. J., Bonnell I. A., Bate M. R., Jeffers S. V., & Vine S. G., 2003, MNRAS, 346, L36
- Rice W. K. M., Armitage P. J., Bate M. R., & Bonnell I. A. 2003, MNRAS, 338, 227
- Richardson, L. J., Deming, D., Wiedemann, G., Goukenleuque, C., Steyert, D., Harrington, J., & Esposito, L. W. 2003, ApJ, 584, 1053
- Richardson, L. J., Deming, D., & Seager, S. 2003, ApJ, 597, 581
- Rivera, E. J., & Lissauer, J. J. 2000, ApJ, 530, 454
- Rivera, E. J., & Lissauer, J. J. 2001, ApJ, 558, 392
- Rivera, E. J., & Haghighipour N. 2004, in Scientific Frontiers in Research on Extrasolar Planets, ed. D. Deming and S. Seager, ASP Conf. Series, 294, 205
- Ryan, S. G., 1989 AJ, 98, 1693
- Ryan, S. 2000, MNRAS, 316, L35
- Saar, S. H., Butler, R. P., & Marcy, G. W. 1998, ApJ, 498, L153
- Saar, S. H., & Cuntz, M. 2001, MNRAS, 325, 55
- Sadakane, K., Ohkubo, M., Takeda, Y., Sato, B., Kambe, E., & Aoki, W. 2002, PASJ, 54, 911
- Safronov, V. S. 1969, Evolution of the Protoplanetary Cloud and Formation of the Earth and the Planets (NASA Tech. Trans. F-677; Moscow: Nauka Press)
- Santos, N. C., Israelian, G., & Mayor, M. 2000, A&A, 363, 228
- Santos, N. C., Israelian, G., & Mayor, M. 2001, A&A, 373, 1019
- Santos, N. C., García López, R. J., Israelian, G., Mayor, M., Rebolo, R., García-Gil, A., Pérez de Taoro, M. R, & Randich, S. 2002, A&A, 386, 1028
- Santos N. C., Israelian G., Mayor M., Rebolo R., & Udry S., 2003, A&A, 398, 363
- Santos, N. C., Israelian, G., & Mayor, M. 2004a, A&A, 415, 1153
- Santos, N. C., et al. 2004b, A&A, 426, L19
- Santos, N. C., et al. 2004c, A&A, 427, 1085

- Sasselov, D. D., & Lecar, M. 2000, *ApJ*, 528, 995
- Sasselov, D. D. 2003, *ApJ*, 596, 1327
- Sato, B., et al. 2003, *ApJ*, 597, L157
- Saumon, D., Hubbard, W. B., Burrows, A., Guillot, T., Lunine, J. I., & Chabrier, G. 1996, *ApJ*, 460, 993
- Scargle, J. D. 1982, *ApJ*, 263, 835
- Schäfer, C., Speith, R., Hipp, M., & Kley, W. 2004, *A&A*, 418, 325
- Schneider, J., & et al. 1998, in *Origins*, ed. C. E. Woodward, J. M. Shull, & H. A. Thronson, Jr., *ASP Conf. Ser.*, 148, 298
- Schultz, A. B., et al. 2004, in *Scientific Frontiers in Research on Extrasolar Planets*, ed. D. Deming & S. Seager *ASP Conf. Ser.*, 294, 479
- Schwarzenberg-Czerny, A. 1996, *ApJ*, 460, L107
- Seager, S., & Sasselov, D.D. 1998, *ApJ*, 502, L157
- Seager, S., & Sasselov, D.D. 2000, *ApJ*, 537, 916
- Seager, S. & Mallén-Ornelas, G. 2003, *ApJ*, 585, 1038
- Seager, S., & Ford, E. B. 2005, in *Astrophysics of life*, eds. M. Livio, I. N. Reid, & W. B. Sparks, *STScI Symposium Series*, 16, 67 (Cambridge, UK: Cambridge University Press)
- Sekiya, M. 1983, *Prog. Theor. Phys.*, 69, 1116
- Sekiya, M. 1998, *Icarus*, 133, 298
- Sekiya, M., & Takeda, H. 2003, *Earth, Planets and Space*, 55, 263
- Selsis, F., Despois, D., & Parisot, J.-P. 2002, *A&A*, 388, 985
- Setiawan, J., et al. 2003, *A&A*, 398, L19
- Shakura, N. I., & Sunyaev, R. A. 1973, *A&A*, 24, 337
- Shkolnik, E., Walker, G. A. H., & Bohlender, D. A. 2003a, *ApJ*, 597, 1092
- Shkolnik, E., Walker, G. A. H., Bohlender, D. A., Gu, P.-G., & Kürster, M. 2005, *ApJ*, 622, 1075
- Showman, A. P., & Guillot, T. 2002, *A&A*, 385, 166

- Sigurdsson, S., Richer, H. B., Hansen, B. M., Stairs, I. H., & Thorsett, S. E. 2003, *Science*, 301, 193
- Smith, V. V., Cunha, K., & Lazzaro, D. 2001, *AJ*, 121, 3207
- Snedden, C. A. 1973, Ph.D. Thesis, The University of Texas at Austin
- Snellen, I. A. G. 2004, *MNRAS*, 353, L1
- Snellgrove, M. D., Papaloizou, J. C. B., & Nelson, R. P. 2001, *A&A*, 374, 1092
- Snodgrass, C., Horne, K., & Tsapras, Y. 2004, *MNRAS*, 351, 967
- Sozzetti, A., Casertano, S., Lattanzi, M. G., & Spagna, A., 2001, *A&A*, 373, L21
- Sozzetti, A., Casertano, S., Brown, R. A., & Lattanzi, M. G., 2002, *PASP*, 114, 1173 (S02)
- Sozzetti, A., Casertano, S., Brown, R. A., & Lattanzi, M. G., 2003a, *PASP*, 115, 1072
- Sozzetti, A., Casertano, S., Lattanzi, M. G., & Spagna, A. 2003b, in *Towards Other Earths: DARWIN/TPF and the Search for Extrasolar Terrestrial Planets*, M. Fridlund, & T. Henning eds., ESA SP-539, 605
- Sozzetti, A., 2004, *MNRAS*, 354, 1194
- Sozzetti, A., et al., 2004a, in *XIXth IAP Symposium - Extrasolar Planets: Today and Tomorrow*, J.-P. Beaulieu, A. Lecavelier des Etangs and C. Terquem eds., ASP Conf. Ser., 321, 107
- Sozzetti, A., et al., 2004b, *ApJ*, 616, L167
- Sozzetti, A., Latham, D. W., Torres, G., Stefanik, R. P., Boss, A. P., Carney, B. W., & Laird, J. B. 2004c, *BAAS*, 36, 62.01
- Sozzetti, A., Latham, D. W., Torres, G., Stefanik, R. P., Boss, A. P., Carney, B. W., & Laird, J. B. 2005, in *Gaia: The Three-Dimensional Universe*, ESA-SP, 576, 309
- Sozzetti, A. 2005, *PASP*, in press (astro-ph/0507115)
- Sozzetti, A., Yong, D., Latham, D. W., Torres, G., Carney, B. W., & Laird, J. B. 2005, *AJ*, submitted
- Stevens, I. R. 2005, *MNRAS*, 356, 1053
- Stepinski, T. F., & Black, D. C. 2000, *A&A*, 356, 903
- Stepinski, T. F., Malhotra, R., & Black, D.C. 2000, *ApJ*, 545, 1044
- Stepinski, T. F., & Black, D. C. 2001, *A&A*, 371, 250

- Struve, O. 1952, *The Observatory*, 72, 199
- Sussman, G. J., & Wisdom, J. 1992, *Science*, 257, 56
- Sudarsky, D., Burrows, A., & Pinto, P. 2000, *ApJ*, 538, 885
- Sudarsky, D., Burrows, A., & Hubeny, I. 2003, *ApJ*, 588, 1121
- Tabachnik, S., & Tremaine, S. 2002, *MNRAS*, 335, 151
- Takeda, Y., et al. 2001, *PASJ*, 53, 1211
- Takeuchi, T., Velusamy, T., & Lin, D. N. C. 2005, *ApJ*, 618, 987
- Tanaka, H., Takeuchi, T., & Ward, W. R. 2002, *ApJ*, 565, 1257
- Tanaka, H., & Ward, W. R. 2004, *ApJ*, 602, 388
- Tanga, P., Weidenschilling, S. J., Michel, P., & Richardson, D. C. 2004, *A&A*, 427, 1105
- Tanigawa, T., & Watanabe, S. 2002, *ApJ*, 580, 506
- Terquem, C., Papaloizou, J. C. B., & Nelson, R. P. 2000, *Space Science Reviews*, 92, 323
- Terquem, C., & Papaloizou, J.C.B. 2002, *MNRAS*, 332, 39
- Terquem, C. 2003, in *Planetary Systems and Planets in Systems*, eds. S. Udry, W. Benz and R. von Steiger (ISSI Space Sciences Series, 19, reprinted from *Space Science Reviews* - Kluwer)
- Terquem, C. 2003, *MNRAS*, 341, 1157
- Thébaud, P., Marzari, F., & Scholl, H. 2002, *A&A*, 384, 594
- Thébaud, P., Marzari, F., Scholl, H., Turrini, D., & Barbieri, M. 2004, *A&A*, 427, 1097
- Thommes, E. W., & Lissauer, J. J. 2003, *ApJ*, 597, 566
- Throop, H. B., Bally, J., Esposito, L. W., & McCaughrean, M. J. 2001, *Science*, 292, 1686
- Tinney, C. G., Butler, R. P., Marcy, G. W., Jones, H. R. A., Penny, A. J., McCarthy, C., & Carter, B. D. 2002, *ApJ*, 571, 528
- Toomre, A. 1964, *ApJ*, 139, 1217
- Torres, G., Konacki, M., Sasselov, D. D., & Jha, S., 2004a, *ApJ*, 609, 1071
- Torres, G., Konacki, M., Sasselov, D. D., & Jha, S. 2004b, *ApJ*, 614, 979
- Torres, G., Konacki, M., Sasselov, D. D., & Jha, S. 2005, *ApJ*, 619, 558

- Tremaine, S., & Zakamska, N. L. 2004, in *The Search for Other Worlds: XIV Astrophysics Conference*, AIP Conf. Proc., 713, 243
- Trilling, D. E., Benz, W., Guillot, T., Lunine, J. I., Hubbard, W. B., & Burrows, A. 1998, *ApJ*, 500, 428
- Trilling D. E., Lunine J. I., & Benz W., 2002, *A&A*, 394, 241
- Tull, R. G. 1998, in *Optical Astronomical Instrumentation*, S. D'Odorico ed., Proc. SPIE, 3355, 387
- Udalski, A., et al. 2002a, *Acta Astronomica*, 52, 1
- Udalski, A., Zebrun, K., Szymanski, M., Kubiak, M., Soszynski, I., Szewczyk, O., Wyrzykowski, L., & Pietrzynski, G. 2002b, *Acta Astronomica*, 52, 115
- Udalski, A., Pietrzynski, G., Szymanski, M., Kubiak, M., Zebrun, K., Soszynski, I., Szewczyk, O., & Wyrzykowski, L. 2003, *Acta Astronomica*, 53, 133
- Udry, S., Mayor, M., Naef, D., Pepe, F., Queloz, D., Santos, N. C., & Burnet, M. 2002, *A&A*, 390, 267
- Udry S., Mayor M., & Santos N. C., 2003, *A&A*, 407, 369
- Udry, S., Eggenberger, A., Mayor, M., Mazeh, T., & Zucker, S. 2004, in *The Environment and Evolution of Double and Multiple Stars*, Proc. IAU Coll. 191, C. Allen & C. Scarfe eds, *Revista Mexicana de Astronomía y Astrofísica (Serie de Conferencias)*, 21, 207
- Valenti, J. A., Butler, R. P., & Marcy, G. W. 1995, *PASP*, 107, 966
- van Belle, G. T., Boden, A. F., Colavita, M. M., Shao, M., Vasisht, G., & Wallace, J. K. 1998, in *Astronomical Interferometry*, ed. R. D. Reasenberg, Proc. SPIE, 3350, 362
- van de Kamp, P. 1963, *AJ*, 68, 515
- van de Kamp, P. 1969, *AJ*, 74, 238
- van de Kamp, P. 1969, *AJ*, 74, 757
- van de Kamp, P. 1975, *AJ*, 80, 658
- van de Kamp, P. 1982, *Vistas in Astronomy*, 26, 141
- Vauclair, S. 2004, *ApJ*, 605, 874
- Veras, D., & Armitage, P. J. 2004, *MNRAS*, 347, 613
- Vidal-Madjar, A., Lecavelier des Etangs, A., Désert, J.-M., Ballester, G. E., Ferlet, R., Hébrard, G., & Mayor, M. 2003, *Nature*, 422, 143

- Vidal-Madjar, A., et al. 2004, ApJ, 604, L69
- Vogt, S. S., et al. 1994, in Instrumentation in Astronomy VIII, D. L. Crawford & E. R. Craine eds., Proc. SPIE , 2198, 362
- Vogt, S. S., Butler, R. P., Marcy, G. W., Fischer, D. A., Pourbaix, D., Apps, K., & Laughlin, G. 2002, ApJ, 568, 352
- Walker, G. A. H., Walker, A. R., Irwin, A. W., Larson, A. M., Yang, S. L. S., & Richardson, D. C. 1995, Icarus, 116, 359
- Walker, G. A. H., et al. 2003, PASP, 115, 1023
- Ward, W. R. 1986, Icarus, 67, 164
- Ward, W. R., & Hourigan, K. 1989, ApJ, 347, 490
- Ward W. R., 1997, ApJ, 482, L211
- Ward, W.R. & Hahn, J.M. 1998, AJ, 116, 489
- Ward, W.R. & Hahn, J.M. 2000, in Protostars and Planets IV, eds. V. Mannings, A.P. Boss, & S.S. Russell (Tucson: University of Arizona Press), 1135
- Weidenschilling, S. J. 1977, Ap&SS, 51, 153
- Weidenschilling, S. J. 1980, Icarus, 44, 172
- Weidenschilling, S. J., & Cuzzi, J. N. 1993, in Protostars and Planets III, ed E. H. Levy & J. I. Lunine (Tucson: University of Arizona Press), 1031
- Weidenschilling, S. J. 1995, Icarus, 116, 433
- Weidenschilling, S. J., & Marzari, F. 1996, Nature, 384, 619
- Weidenschilling, S. J. 2003, Icarus, 165, 438
- Weldrake, D. T. F, Sackett, P. D, Freeman, K. C, & Bridges, T. J. 2005, ApJ, 620, 1043
- Wetherill, G. W. 1990, in Annual Reviews of Earth and Planetary Sciences, (Palo Alto, CA: Annual Reviews, Inc.), 18, 205
- Whitmire, D. P., Matese, J. J., Criswell, L., & Mikkola, S. 1998, Icarus, 132, 196
- Wiedemann, G., Deming, D., & Bjoraker, G. 2001, ApJ, 546, 1068
- Wilson, J. C., Kirkpatrick, J. D., Gizis, J. E., Skrutskie, M. F., Monet, D. G., & Houck, J. R. 2001, AJ, 122, 1989
- Winglee, R. M., Dulk, G. A., & Bastian, T. S. 1986, ApJ, 309, L59

- Winn, J. N., et al. 2004, PASJ, 56, 655
- Winters, W. F., B. albus, S. A., & Hawley, J. F. 2003, MNRAS, 340, 519
- Wolszczan, A., & Frail, D. A. 1992, Nature, 355, 145
- Wu, Y., & Murray, N. 2003, ApJ, 589, 605
- Wu, Y. 2004, in Scientific Frontiers in Research on Extrasolar Planets, ed. D. Deming & S. Seager ASP Conf. Ser., 294, 213
- Wuchterl, G. 1997, in Science with the VLT Interferometer, ed. F. Paresce (Berlin, Springer & Verlag) , 64
- Wurm, G., Blum, J., & Colwell, J. E. 2001, Icarus, 151, 318
- Yamoto, F., & Sekiya, M. 2004, Icarus, 170, 180
- Yelle, R. V. 2004, Icarus, 170, 167
- Yi, S., Kim, Y. -C., & Demarque, P. 2003, ApJS, 144, 259
- Yong, D., Lambert, D. L., Allende Prieto, C., & Paulson, D. B. 2004, ApJ, 603, 697
- Youdin, A. N., & Shu, F. H. 2002, ApJ, 580, 494
- Youdin, A. N., & Chiang, E. I. 2004, ApJ, 601, 1109
- Youdin, A. N., & Goodman, J. 2005, ApJ, 620, 459
- Yu, Q., & Tremaine, S. 2001, AJ, 121, 1736
- Zakamska, N. L., & Tremaine, S. 2004, AJ, 128, 869
- Zarka, P., Treumann, R. A., Ryabov, B. P., & Ryabov, V. B. 2001, Ap&SS, 277, 293
- Zhou, J., & Sun, Y. 2003, ApJ, 598, 1290
- Zucker, S., & Mazeh, T. 2000, ApJ, 531, L67
- Zucker, S., & Mazeh, T. 2001a, ApJ, 562, 1038
- Zucker, S., & Mazeh, T. 2001b, ApJ, 562, 549
- Zucker S., & Mazeh T., 2002, ApJ, 568, L113
- Zucker, S., Mazeh, T., Santos, N. C., Udry, S., & Mayor, M. 2004, A&A, 426, 695